12-16-2020

The Role of Pyroptosis and Associated Inflammasomes during Experimental Cytomegalovirus Retinitis

Jessica Carter
Georgia State University

THE ROLE OF PYROPTOSIS AND ASSOCIATED INFLAMMASOMES DURING EXPERIMENTAL CYTOMEGALOVIRUS RETINITIS

by

JESSICA J. CARTER

Under the Direction of Richard D. Dix, PhD

ABSTRACT

Human cytomegalovirus (HCMV) is a species-specific β-herpesvirus that establishes a lifelong latent infection in ~80% of the world's population and can cause severe opportunistic diseases in immunosuppressed patients including those with AIDS. Of these, AIDS-related HCMV retinitis is a significant ophthalmological problem worldwide. Although the clinical features of AIDS-related HCMV retinitis are well established, the virologic and immunologic events that take place during onset and development of this sight-threatening retinal disease remain poorly understood. Toward this end, an established animal model of murine cytomegalovirus (MCMV) retinitis in mice with retrovirus-induced immunodeficiency (MAIDS) that mimics AIDS-related HCMV retinitis was used in the present investigation to test the central

hypothesis that pyroptosis, as a programmed cell death pathway of innate immunity, and associated inflammasomes contribute to the onset and development of full-thickness retinal necrosis during MAIDS-related MCMV retinitis. Our findings show (i) intraocular MCMV infection stimulates key pyroptosis-associated transcripts and proteins within the eyes of retinitis-susceptible MAIDS mice but not within the eyes of retinitis-resistant mice; (ii) a deficiency in key pyroptosis-associated molecules and inflammasomes in MAIDS mice results in an atypical histopathologic pattern of retinal disease within MCMV-infected eyes characterized by preservation of the neurosensory retina without full-thickness retinal necrosis but with proliferation of the retinal pigmented epithelium; (iii) MCMV-infected eyes of corticosteroid-immunosuppressed mice display stimulation of key pyroptosis-associated molecules and inflammasomes similar to that observed for MCMV-infected eyes of mice with MAIDS; (iv) MCMV infection of IC-21 macrophages and mouse embryo fibroblasts grown in culture stimulates key pyroptosis-associated transcripts in a cell-type specific manner; and (v) increased susceptibility to MCMV retinitis during the progression of MAIDS is associated with robust upregulation of a surprisingly large number of immune response genes that operate within several immune response pathways. Taken together, these results suggest that pyroptosis and associated inflammasomes play a significant role during the pathogenesis of full-thickness retinal necrosis within MCMV-infected eyes during MAIDS. These findings add new knowledge to our understanding of the contributions of programmed cell death pathways of innate immunity towards the pathogenesis of AIDS-related HCMV retinitis and may extend to other AIDS-related opportunistic virus infections.

INDEX WORDS: Cytomegalovirus retinitis, Human cytomegalovirus (HCMV), HIV/AIDS, Inflammasomes, Murine cytomegalovirus (MCMV), Murine AIDS (MAIDS), Pyroptosis

THE ROLE OF PYROPTOSIS AND ASSOCIATED INFLAMMASOMES DURING EXPERIMENTAL CYTOMEGALOVIRUS RETINITIS

by

JESSICA J. CARTER

A Dissertation Submitted in Partial Fulfillment of the Requirements for the Degree of

Doctor of Philosophy

in the College of Arts and Sciences

Georgia State University

2020

THE ROLE OF PYROPTOSIS AND ASSOCIATED INFLAMMASOMES DURING EXPERIMENTAL CYTOMEGALOVIRUS RETINITIS

by

JESSICA J. CARTER

Committee Chair: Richard D. Dix

Committee: Julia K. Hilliard

Yuan Liu

Homayon Ghiasi

Electronic Version Approved:

Office of Graduate Studies

College of Arts and Sciences

Georgia State University

December 2020

DEDICATION

This dissertation is dedicated to all those who have supported me and believed in me. To my family, for always being there for me. To my mom, Irene, for never doubting I can achieve anything. To my sister, Lora, for always being honest with me and helping to keep things in perspective. To my sister, Eva, for reminding me how it is important to take of yourself above all else. You will always be my role model. To my twin sister, Jennifer, for all the numerous and different types of support given; but most importantly, for finally teaching me what "rhetoric" means (it only took five years).

To my significant other, James, thank you for not giving up on me. Through it all you have stood by my side and supported me. You believed in me when I was unable to believe in myself. I could not have done this without you.

To my oldest friend, Sarah MacDonald, for making sure I never got an ego and making sure I know that earning a Ph.D. does not mean anything if you do not know what side of a blow-up mattress to sleep on.

To all the friends I made at GSU, thank you for being there for it all. Through the laughs, through the tears, you were there the whole way. You have made a lasting impression on my life. I am better because I got to know each of you.

Finally, to my previous mentors, Dr. Rebekah Ward, Dr. Philip Gibson, and Dr. Robert Powers for helping redefine how I viewed myself and help shaping my educational goals. Through your guidance, I was able to find confidence in myself and discover my potential, which led me here.

ACKNOWLEDGEMENTS

I would first like to start by extending my fullest and deepest gratitude to my PI and mentor, Dr. Richard D. Dix, for his unwavering belief in me and his unyielding support. Through his constant pushing me to reach beyond my self-imposing limits, he allowed me to see the potential I have, not only as a researcher, but throughout other aspects of my life. A sincere appreciation is also extended to my committee members Dr. Julia Hilliard, Dr. Yuan Liu, and Dr. Homayon Ghiasi for expanding my knowledge, providing me guidance, and opening my mind to different ways of thinking.

To all the members of the Emory Eye Center, I am beyond grateful for the acceptance and inclusion in the weekly seminars. Through the insightful discussions, I learned so much, and I believe my own research to be better for it. I would especially like to thank Dr. Michael Iuvone, Dr. Jeffery Boatright, Dr. Hans Grossniklaus, and Dr. John Nickerson for supporting and renewing my involvement in the Emory Eye Center T32 Vision Training Grant and Micah Chrenek for his willingness to provide constant technical assistance and training.

Lastly, I would like to acknowledge the members of the Ocular Virology and Immunology Laboratory. Their constant camaraderie, help, and support made all the difference during my time with this lab. Without them, I am not sure I would have made it as far as I have. Thank you all.

"No man is an island" —John Donne

TABLE OF CONTENTS

LIST OF TABLES

LIST OF FIGURES

1 INTRODUCTION

Human cytomegalovirus (HCMV) is a species-specific β-herpesvirus that establishes lifelong infection in approximately 80% of the world's population [1]. Although usually asymptomatic in immunocompetent individuals, infection with HCMV is often asymptomatic and can cause severe morbidity in at-risk immunocompromised populations. Specifically, AIDS-related HCMV retinitis is a sight-threatening manifestation of this virus that remains a significant ophthalmological problem since access to combination antiretroviral therapy (cART) is not readily available worldwide and several individuals who do have access fail to adhere or respond to treatment [2, 3]. Understanding the pathogenesis of this disease is essential to developing new and effective treatments for its prevention. Although the clinical features of AIDS-related HCMV retinitis are well established, the direct mechanisms by which HCMV infection results in severe retinal damage is still unknown. To investigate these direct mechanisms, our lab uses a well-established, reproducible, clinically relevant mouse model with retroviral-induced immunosuppression (MAIDS) that results in susceptibility to experimental murine cytomegalovirus (MCMV) retinitis, which mimics the pathophysiology seen during AIDS-related HCMV retinitis [1, 4, 5]. Using this model, we have previously found that several inflammasomes and pyroptosis markers are significantly stimulated in the eyes of mice during experimental MAIDS-related MCMV retinitis [6]. However, the impact and effect this inflammatory form of programmed cell death has on the onset and progression of MAIDS-related MCMV retinitis has yet to be explored.

1.1 Herpesviruses

As obligate intracellular organisms, viruses have adapted several basic structures necessary for replication inside the cells of living host, and the differences in these essential

structures differ between the various classes of viruses. All viruses have genetic material that is either single-stranded (ss) or double-stranded (ds) DNA or RNA and is packaged in a protein capsid, forming the nucleocapsid. The virus may have an envelope surrounding the nucleocapsid, which is derived from the host cell, depending on the virus' evolution for infection. Filling the space between the envelope and the capsid is an area known as the tegument. The tegument contains viral proteins that are indispensable for early infection and are released into the host cell once the virus has gained entry. Entry into the host cell is typically mediated on the surface of the virus (either the nucleocapsid or the envelope) by glycoproteins that recognize and bind to specific receptors on the host cell. The target host cells, morphological features, mode of replication, and pathological consequence of the host organism differ significantly among different types of viruses, and so the classification of these viruses are phylogenetically organized based on the similarities of the viruses to each other, and how they are thought to have evolved [7].

Herpesvirales is one of several orders of viruses characterized as enveloped dsDNA viruses composed of an icosahedral capsid with a T=16 symmetry, whose target host is animals. CMV is further classified into the family *Herpesviridae* due to its preferred infection of amniotes (birds, reptiles, and mammals). Members of this family replicate and partially assemble within the nucleus and can establish latency in their host, which often results in reoccurring lytic infections that destroy the infected host cell [7, 8]. Herpesviruses are extremely widespread among humans, as at least 90% of adults have been infected and therefore maintain a latent form of at least one of several herpesviruses. There are nine known human herpesviruses (HHV) to date referred to as HHV-1 through HHV-8, with HHV-6B being recognized as distinctly

different from HHV-6A (Table 1.1)**.** These nine human viruses are further classified into subfamilies based on where they form latency in the host cell [7].

Table 1.1: Human Herpesviruses in the Family Herpesviridae

Type	Synonym	Subfamily	Primary Target Cell	Pathophysiology
HHV-1	Herpes simplex virus-1 (HSV-1)	α	Mucoepithelial	Oral and/or genital herpes (predominantly orofacial), as well as other herpes simplex infections
HHV-2	Herpes simplex virus-2 (HSV-2)	α	Mucoepithelial	Oral and/or genital herpes (predominantly genital), as well as other herpes simplex infections
HHV-3	Varicella zoster virus (VZV)	α	Mucoepithelial	Chickenpox and shingles
HHV-4	Epstein-Barr virus (EBV), lymphocryptovirus	γ	B cells and epithelial cells	Infectious mononucleosis, Burkitt's lymphoma, CNS lymphoma in AIDS patients, post-transplant lymphoproliferative syndrome (PTLD), nasopharyngeal carcinoma, HIV-associated hairy leukoplakia
HHV-5	Cytomegalovirus (CMV)	β	Monocyte, lymphocyte, and epithelial cells	Infectious mononucleosis-like syndrome, retinitis, etc.
HHV-6	Roseolovirus, Herpes lymphotropic virus	β	T cells	*Sixth disease* (roseola infantum or *exanthem subitum*)
HHV-7	Roseolovirus	β	T cells	*Sixth disease* (roseola infantum or *exanthem subitum*)
HHV-8	Kaposi's sarcoma-associated herpes virus (KSHV), a type of rhadinovirus	γ	Lymphocyte and other cells	Kaposi's sarcoma, primary effusion lymphoma, some types of multicentric Castleman's disease

Adapted from [9]

Alphaherpesvirinae. The α-herpesviruses (HHV-1 through HHV-3) infect several host species and are known to replicate and spread more quickly than the other subfamilies of herpesviruses. These viruses initially infect epithelial cells via direct contact and quickly disseminate to the neurons to establish latency. The *Simplexvirus and Varicellovirus* genera of the α-herpesviruses infect humans and establish latency in the sensory nerve ganglia. Most known of the *Simplexvirus* genus are herpes simplex type 1 (HSV-1) and HSV-2, which manifest in the form of orofacial lesions, genital lesions, keratoconjunctivitis, and encephalitis. The *Varicellovirus* genus contains the varicella-zoster virus (VZV), which is responsible for the development of chickenpox in young children and reoccurs as shingles later in life [7].

Betaherpesvirinae. The β-herpesviruses are classified based on their tendency to establish latency in lymphoid cells of hematopoietic origin. These viruses also tend to replicate more slowly than the other herpesviruses and have strict specificity of the host in which they can replicate. The human herpesviruses that comprise this subfamily include HHV-6 and HHV-7, which are part of the *Roseolavirus* genus, form latency in CD4+ T cells, and are responsible for roseola [10, 11]. Also included in this subfamily is the genus *Cytomegalovirus,* which includes HHV-5, or HCMV, and form latency in monocytes and bone marrow cells. HCMV is responsible for various congenital infections, as well as several infections spanning multiple organs in immunocompromised individuals [7].

Gammaherpesvirinae. The γ-herpesviruses establish latency within lymphoid tissues of mammalian hosts. These viruses vary in their rate of replication—which is generally in B or T lymphocytes—and contain the human herpesviruses HHV-4 and HHV-8. HHV-4, known as Epstein-Barr virus (EBV), is part of the *Lymphocryptovirus* genus and is responsible for infectious mononucleosis. HHV-8 is part of the *Rhadinovirus* genus and is commonly referred to as Kaposi's sarcoma-associated herpesvirus (KSHV) [7].

1.2 Cytomegalovirus

1.2.1 *CMV Structure*

Because herpesviruses share similar morphological features with other membranes in the same order, it makes sense that they share similar virion structures and protein functions. A notable difference of CMV is their 200-230 nm diameter, making them slightly larger than all other herpesviruses. This size includes their envelope, which is entrenched with virus-encoded glycoproteins. HCMV is thought to derive its envelope from the host endoplasmic reticulum (ER), the ER-Golgi intermediate compartment, or endosomes [12-14]. The envelopes of HCMV

are coated with several glycoproteins, which form complexes that are important for HCMV replication. One of these complexes consists of a glycoprotein B (gB) trimer, while another complex is composed of gH and gL, which form the heterodimer gH:gL. Both complexes are required for viral entry into the host cell. Another complex, gM:gH, is vital for virion maturation [15].

Beneath the envelope is a thick tegument, which contains most of the proteins encoded by the genome. The tegument is composed of at least 32 known viral proteins as well as several host proteins [16] and even host RNA [17]. These tegument proteins are involved in all steps of viral replication, including entry into the host cell, in which the virion transactivator (VTA) tegument phosphorylated protein (pp)71 quickly translocates to the nucleus and recruits host cell machinery to initiate gene transcription [12]. Tegument proteins are also involved with egress from the host cell, where other phosphorylated proteins can interact with the immune system of the host.

The tegument encloses a 130 nm, icosahedral nucleocapsid of 162 capsomeres with a T=16 symmetry. The genome of CMV is contained in a core of linear dsDNA and encodes at least 66 known tegument proteins (reviewed in [12], and as shown in Figure 1.1 from [18]). Four of these virally encoded proteins form the HCMV capsid. These proteins—the major capsid protein (MCP), triplex subunits 1 (TRI1), TRI2, and smallest capsid protein (SCP)—are essential for the growth of the virus. As the name suggests, MCP comprises the bulk of the capsid and contains a specific pore made of the portal protein (PORT), which facilitates the packaging and release of the virion genome [12].

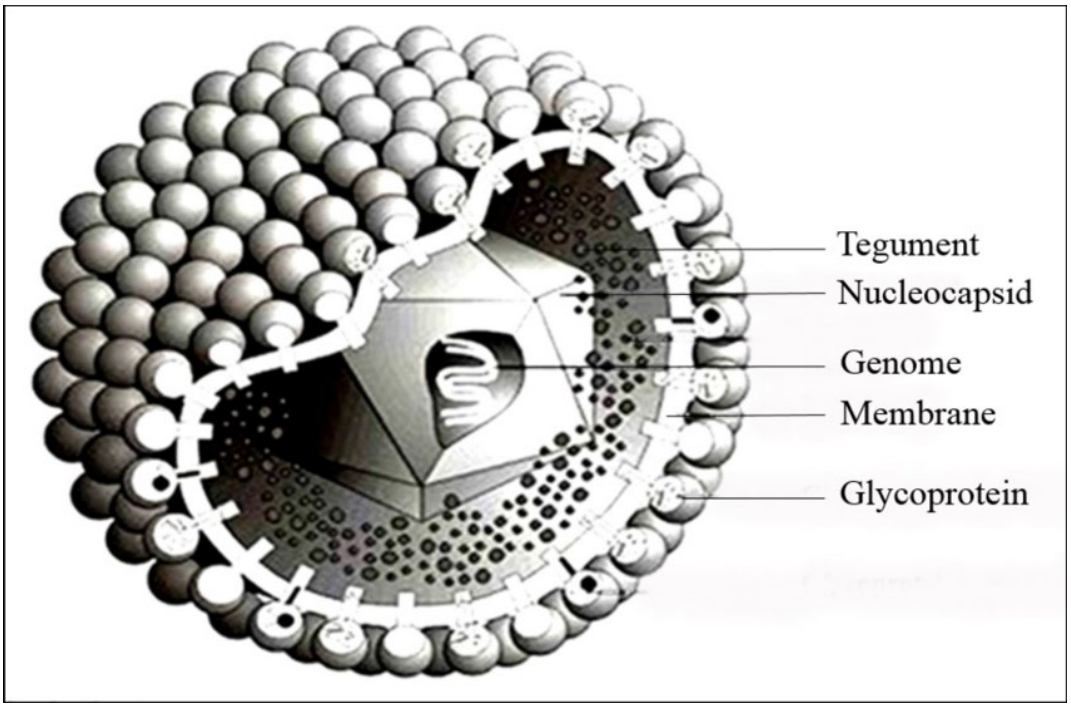

Figure 1.1. Cytomegalovirus virion structure
Representation of the cytomegalovirus virion structure, modified from [18].

The HCMV genome consists of linear dsDNA that is divided into two regions, the unique long (U_L) and the unique short (U_S) regions. The ends of these regions are flanked by terminal inverted repeat sequences and contain internal redundancy sequences [7] (depicted in Figure 1.2). The HCMV genome is roughly 236 kb long, and the genes are numbered according to their U_L or U_S loci. Additionally, the HCMV genome contains about 200 open reading frames (ORFs) and can encode at least 167 proteins [19], including structural and nonstructural proteins, tegument proteins, and glycoproteins.

The genome of the Smith strain of MCMV differs somewhat from HCMV in that it contains only one long segment of DNA (U_L) and lacks internal repeat sequences [20, 21]. The MCMV genome is also approximately 230 kb long and can encode for roughly 170 gene products [22]. Despite species-specificity of each, the genomic structures of MCMV and HCMV

are comparable to one other [20-23]. The sequences of these two CMV strains overlap one another by about 180 kbps of DNA and contain about 78 homologous ORFs [22].

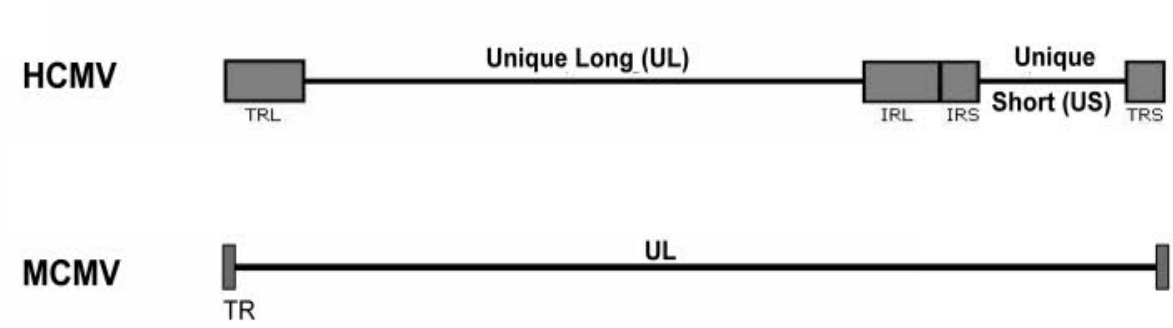

Figure 1.2. HCMV and MCMV genomic structures.

Comparison of the HCMV and MCMV genome modified from [24]. TR: terminal repeat, TRL: terminal repeat long, TRS: terminal repeat short, IRL: internal repeat long, IRS: internal repeat short.

1.2.2 CMV Replication

HCMV and MCMV replication and assembly occur in the nucleus of the host cell, and both viruses undergo a temporal, step-wise viral gene expression and replication cascade [12]. The interaction of glycoproteins on the envelope of the virus with a complementary host receptor, such as heparin sulfate, mediates attachment and adsorption. Immediately after attachment and adsorption, entry into the permissive host cell results from receptor-mediated endocytosis (endothelial and epithelial cells) or fusion (fibroblasts) of the viral envelop with the host membrane [25]. Viral tegument proteins are then released into the cell, and some are believed to be transported to the nucleus of the host cell alongside nucleocapsids via interactions with the host microtubule machinery. The nucleocapsid interacts with nuclear pores where it injects viral DNA into the nucleus [7], allowing for the commencement of transcription [26-28]. The transcription and subsequent translation of viral genes follow a specific sequence, starting with immediate early (IE), also known as α genes. Proteins translated from IE transcripts

dysregulate cellular functions to allow for viral production. Following transcription of IE genes, the transcription of early (E), or β, genes, drive viral DNA synthesis and the expression of late (L), or γ, genes. The L genes encode for most of the tegument and glycoproteins. The transcription of L genes allows for the assembly of progeny virions, which then egress from the cell via exocytosis [12] as outlined in Figure 1.3.

CMV can infect epithelial cells, endothelial cells, fibroblasts, and myeloid cells. The characteristics of CMV infection of several cell types have been widely studied and can differ with the species of CMV as well as the infected cell type. Viral IE genes immediately begin transcription once the genome enters the nucleus, and this transcription peaks between 8-12 hours post-infection (hpi) and begins the transcription of E genes, which continues until approximately 24 hpi [12, 29]. At this point, the expression of L gene transcription can be seen in HCMV infected fibroblasts [30-33], while MCMV IE gene transcription occurs between 1-4 hpi in fibroblasts, and as early as 1 hpi in macrophages [32]. The E genes for MCMV are detected at about 2 hpi and are seen until about 16 hpi in fibroblasts [33], at the point in which MCMV L gene expression begins and can continue for at least 36 hours [30]. The transcription of these L genes encodes for most of the viral tegument and glycoproteins, which are involved in capsid assembly, virion maturation, and egress from the host cell.

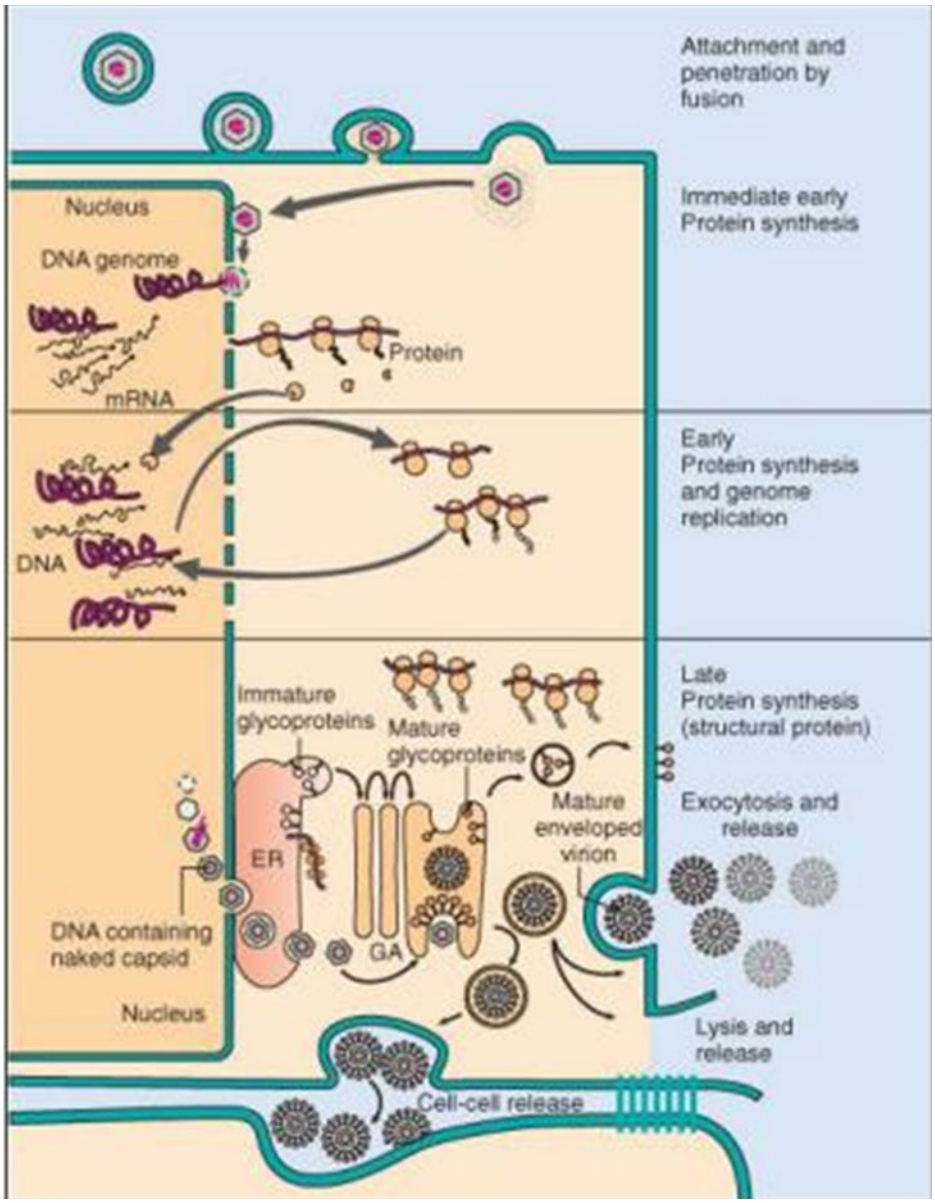

Figure 1.3. Lifecycle of HCMV and MCMV within a host cell.

Depiction of the viral replication of MCMV or HCMV within a host cell. Virion attachment and adsorption is followed by entry via fusion into the host cell. The nucelocapsid is shuttled to the nucleus followed by IE, and E gene expression. Genome replication is then followed by L gene expression, capsid assembly, maturation of virion and ultimately envelopment and egress as the virion is released from the cell. Figure from [34].

1.3 HCMV Clinical Disease

1.3.1 HCMV Infection in Immunocompetent Hosts

HCMV infects about 80% of adults in developed countries [1] and passes through direct contact with bodily fluids, such as saliva, urine, and breast milk. HCMV can be sexually transmitted and contracted during organ transplants, blood transfusions, and pregnancy. Following acute infection, most immunocompetent individuals do not show any symptoms, although occasionally a mild mononucleosis specific for HCMV, has been associated with primary infection in immunologically normal persons [35]. Although rare, immunocompetent individuals may develop severe diseases, such as myocarditis [36, 37], pneumonia [38-40], hepatitis [41-43], encephalitis [44-47], and retinitis [48]. Primary HCMV infection that occurs during the first trimester of pregnancy can cross the placenta causing congenital HCMV disease [12]. Infected infants may develop neurological inclusion disease [49], which could result in manifestations, including microcephaly, the enlargement of ventricles, or cerebral atrophy. Later in life, those infected could experience neurological ailments, such as hearing or vision loss or even mental retardation [50].

1.3.2 HCMV Infection in Immunocompromised Hosts

HCMV alters the host defenses by either altering the signaling of the recognition receptors, weakening the cytokine and interferon activation and suppressing cell death of infected cells, thus allowing the virus to survive in the cell and reproduce effectively [12]. In healthy individuals, the primary infection is systemic and asymptomatic [1], and the adaptive T cell immunity helps to maintain low viral levels [12]. Regardless of the immune response to the primary infection, the virus remains latent in the lymphocytes throughout the infected individual's life. Competent immune systems typically suppress reactivation of the virus, but in

those who are immunocompromised, HCMV becomes an opportunistic infection, and individuals exhibit a variety of diseases that are dependent on the cause of their immunosuppression. Recipients of organ transplants or bone marrow transplants are at a high risk of developing colitis or life-threatening HCMV pneumonitis. Additionally, infection of the transplanted organ by HCMV can also contribute to the rejection of the organ by the recipient due to reactivation and uncontrolled viral replication in the latent virus [51]. Those who are immunosuppressed by HIV-1 infections are particularly susceptible to sight-threatening retinitis caused by HCMV directly infecting the retinal tissues [1].

1.4 HIV and AIDS

1.4.1 HIV-1 Replication and Tropism

HIV-1 has a roughly spherical structure with a 120 nm diameter and is a member of the *Retroviridae* family, meaning that it is an ssRNA virus that changes the genome of the host cell. Upon entry into the cytoplasm, HIV-1 uses its own viral reverse transcriptase to produce DNA from its RNA genome. The retroviral DNA is then inserted into the host's genome by a viral enzyme, integrase, and is transcribed and translated along with the cell's own genes. The genome encodes for *gag, pol,* and *env* regions that are translated as one polypeptide chain cleaved by viral-specific proteases. Gag proteins are major components of the capsids, while Pol proteins are responsible for viral DNA synthesis and the integration of the viral genome into the host genome. The Env proteins are essential for entry of the virions in the host cell, and although there are a few copies of these proteins contained within the viral envelope, the enveloped nucleocapsid of HIV-1 is composed mostly of lipids obtained from the plasma membrane of the host during the budding process. The Env proteins present on the envelope consist of a cap made of three molecules of glycoprotein (gp)120, in addition to a stem formed by a trimer of gp41

molecules, which anchor this structure to the viral envelope (Figure 1.4). This protein complex is what allows the virus to attach to the target host receptors, leading to the fusion of the viral envelope with the host cell membrane and allowing for entry into the cell. HIV-1 is further classified into the genus *Lentivirus,* which consist of retroviruses that result in deadly diseases following long incubation periods. *Lentivirus* has a wide range of susceptible hosts that are distributed worldwide. There are five serogroups of known *Lentivirus,* which are classified based on the type of host in which they are associated. Primate specific *Lentivirus,* including HIV-1, are distinguished, in part, by their use of CD4 as a receptor for viral entry [52, 53].

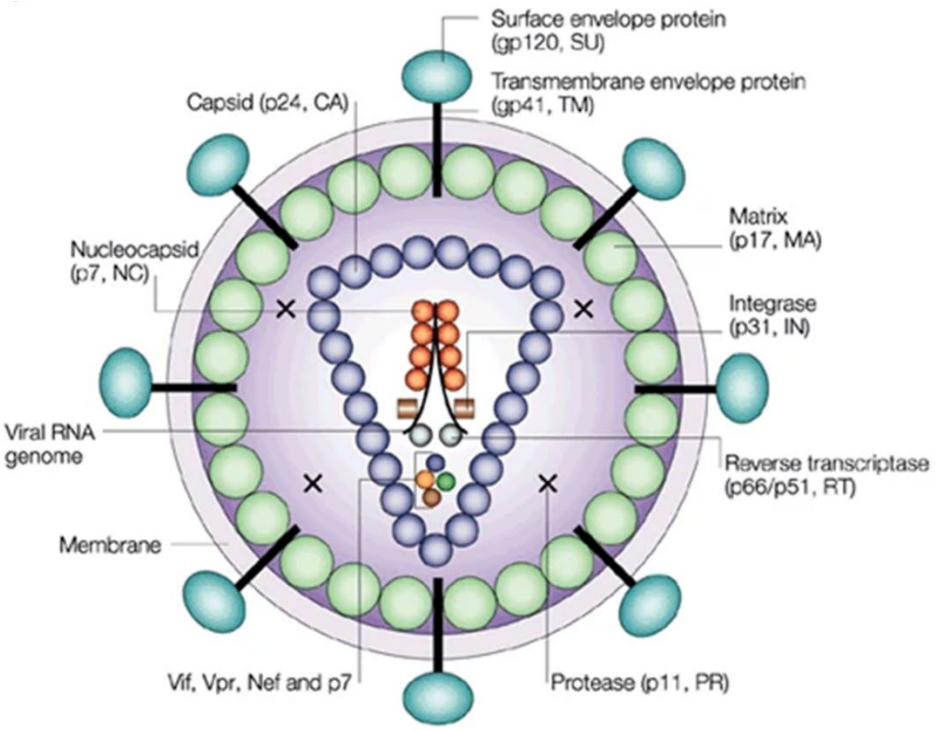

Figure 1.4. HIV-1 virion structure.
Schematic representation of the HIV-1 virion structure. Modified from [54].

Macrophages, dendritic cells, and CD4+ T cells are the primary targets of HIV-1 due to the presence of CD4 on the surface of these cells [52, 53]. In addition to gp120 interacting with

the CD4 molecule on the host cell membrane, HIV-1 also interacts with host cell-specific chemokine co-receptors, depending on the strain of HIV-1. Macrophage-tropic (M-tropic) HIV-1 are strains of HIV-1 that do not undergo multiple cell fusions, resulting in multinucleated cells known as syncytia. They use the β-chemokine receptor, CCR5, for entry into host cells. T-tropic strains of HIV-1 can form syncytia and use the α-chemokine receptor, CXCR4, for entry into host cells. There are dual-tropic HIV-1 strains that can use both CXCR4 and CCR5 as co-receptors for viral entry into host cells. Following binding of the viral Env proteins to the specific host receptors and co-receptors, the cell membranes are brought close together, allowing for a fusion of the membranes and the injection of HIV-1 RNA and enzymes into the host cell, where the virus begins to incorporate its genome into the host's genome [52, 53]. Following transcription, the gp41 and gp120 glycoproteins are again anchored to the host's plasma membrane, where the forming virion is then able to bud from the cell as an immature virion. The Gag polyproteins are then cleaved into the matrix, capsid, and nucleocapsid proteins that assemble to produce a mature HIV virion, which is able to infect another cell (Figure 1.5) [55].

HIV-1 is capable of infecting cells by two distinct mechanisms. The first is cell-free spread in which a mature virion enters the blood after recently budding from a host cell and encounters another permissible cell in which it enters [56]. The other method of HIV-1 dissemination is direct transmission from one cell to another, aptly named cell-to-cell spread. This direct transmission is either mediated by a virologic synapse [57, 58] or from the help of antigen-presenting cells [59]. Cell-to-cell spread is generally more efficient at dissemination of the virus within the body than a cell-free spread [60]. Importantly, infection of a host cell by HIV-1 results in the destruction of the infected immune cell or obliteration of their immune function.

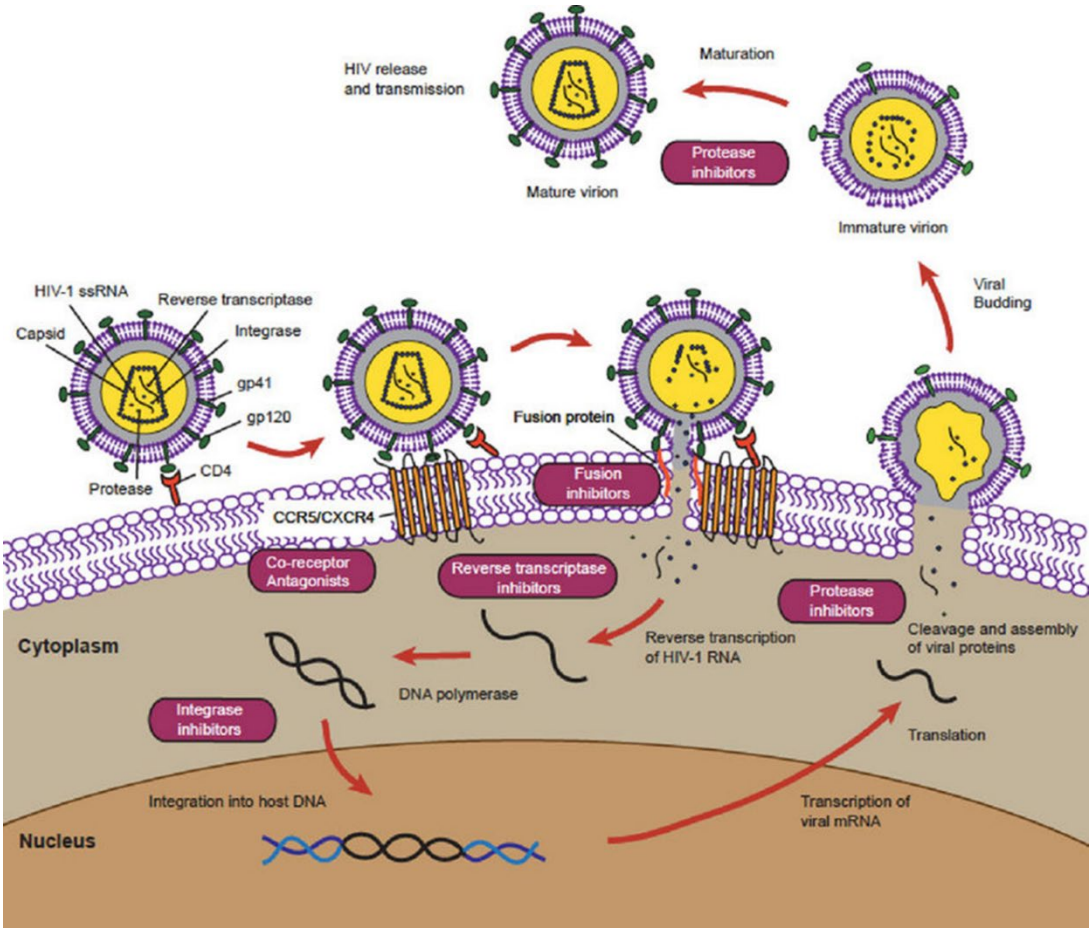

Figure 1.5. Steps in HIV-1 replication cycle.

HIV-1 replication begins by fusion of the HIV-1 virion to the host cell via recognition of the CD4 host receptor. The capsid containing the viral genome enters the cell, is disintegrated, and the viral reverse transcriptase transcribes the viral RNA into DNA. The viral DNA is then transported to the nucleus where it is integrated into the host DNA by the viral protein integrase. The host then transcribes the viral genome along with its own DNA, making more copies of virus as well as new HIV proteins. The new viral RNA and HIV proteins move to the cell surface forming a new, immature HIV virus. Once released from the cell the viral protein, protease, cleaves newly synthesized polyproteins to create a mature infectious virus. Image from [61].

Each HIV-1 virion contains two RNA genomes, and recombination between these two genomes can occur [62, 63]. This recombination event happens multiple times during each replication cycle, which rapidly shuffles the genetic information transmitted to the progeny virus [63]. This viral recombination is thought to be a natural repair mechanism against damage to the

RNA genome [64]. However, the genetic variability is also compounded with a very rapid replication cycle with a high mutation rate, resulting in generations that contain multiple variants in a single day. Additionally, a single cell may also be infected by different strains of HIV-1, which can result in the progeny being a hybrid of the two strains. The resulting genetic variability is likely a contributing factor to the difficulties faced by the host's immune defenses against infection, as well as targets for therapy [65].

1.4.2 Pathophysiology of HIV/AIDS

HIV-1 was first discovered in the early 1980s [53] and, since its discovery, has reached a global pandemic in which just under 40 million people worldwide are currently infected, with about 1.8 million new infections a year. Those infected with HIV-1 shed the virus in bodily fluids and secretions, such as blood, semen, saliva, urine, or breast milk, and transmission occurs with direct exchange of the fluids [52, 53]. Infection with HIV-1 can be broken down into three main stages: acute infection, clinical latency, and AIDS.

Acute Infection. Acute HIV-1 infection occurs during the initial period after contracting HIV-1, and many individuals exhibit influenza-like symptoms—including fever, headache, tiredness, throat inflammation, and larger tender lymph nodes—2-4 weeks following viral exposure. Vomiting, diarrhea, and other gastrointestinal symptoms may also occur. Approximately 20-50% of individuals may experience a maculopapular rash occurring on the trunk of the body. Due to their non-specificity, these symptoms are not often recognized as signs of HIV-1 infection and are even often misdiagnosed as a more common infectious disease [66].

Chronic latency. Following the initial symptoms is a stage of asymptomatic infection referred to as chronic latency. Without treatment, this stage lasts an average of eight years but can prolong for over 20 years. Although there are typically little to no symptoms seen

in the early years of this disease, fever, weight loss, muscle pains, gastrointestinal issues, and persistent generalized lymphadenopathy are often seen in infected individuals [67] as the infection progresses to AIDS.

Acquired immunodeficiency symptoms. Without treatment, HIV-1 infection can progress to AIDS approximately ten years following initial infection. The clinical definition of AIDS is a CD4+ T cell count below 200 cells/μL of peripheral blood, which is a dramatic reduction from the normal range of between 1,000 and 1,500 cell/μL of peripheral blood [67]. HIV-induced cell lysis, as well as the killing of infected cells by cytotoxic CD8+ T cells, accounts for much of the CD4+ T cell loss following the acute stage of infection. As HIV-1 infection progresses through the chronic stages of infection, the regenerative capacity of the thymus is slowly destroyed by HIV-1 infection resulting in a gradual loss of the CD4+ T cells. At this point, individuals start to present with conditions such as pneumocystis pneumonia, cachexia, esophageal candidiasis, and recurrent respiratory tract infections [67]. As the CD4+ T cells count continues to drop, infected individuals begin to become more susceptible to a myriad of opportunistic infections (as depicted in Figure 1.6). Susceptibility to HCMV diseases, including HCMV retinitis, generally occurs when the CD4+ T cell count reaches levels below 50 cells/μL of peripheral blood.

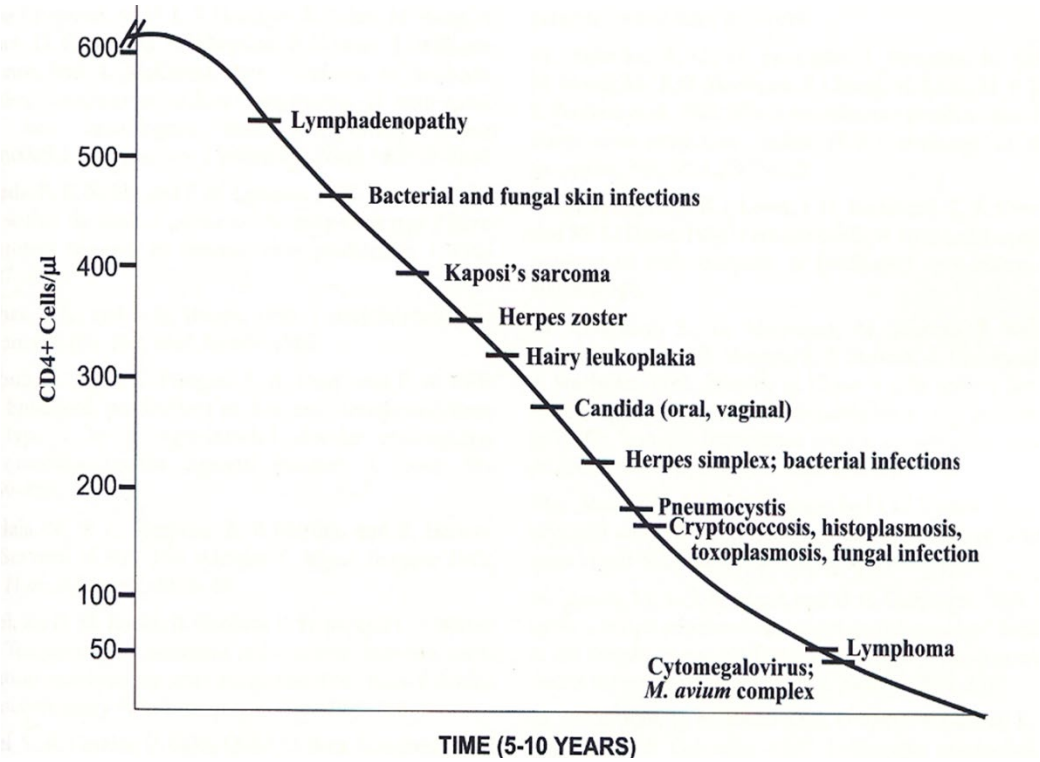

Figure 1.6. Opportunistic infections with depleting CD4+ T cell counts.
During the progression of AIDS, the CD4+ T cell count depletes, rendering afflicted individuals vulnerable to diseases by a number of opportunistic infections [68].

1.5 AIDS-related HCMV Retinitis

AIDS patients are particularly susceptible to sight-threatening retinitis caused by HCMV directly infecting the retinal tissues. Factors that contribute to retinal tissue destruction are virus-induced cytopathology and inflammation mediated by neutrophils and activated macrophages. Before the availability of cART, 46% of patients with AIDS experienced vision loss and blindness caused by HCMV retinitis [69-71]. Although treatment with cART has lowered the number of new cases of HCMV retinitis, AIDS-related HCMV retinitis remains a significant ophthalmological problem as access to cART is not readily available worldwide and several of the individuals who do have access fail to adhere or respond to treatment [12, 72, 73]. Although vaccination is one of the more effective methods for controlling other infectious diseases,

attempts at creating an effective vaccine against HCMV have so far been unsuccessful [74, 75]. HCMV replication can generally be controlled by lifelong administration of antiviral drugs, such as ganciclovir (GCV), yet these drugs may cause harmful side-effects, do not eradicate the virus, and only slows the progression of ocular damage associated with HCMV infection [76-78]. HCMV-related disease, therefore, remains a severe ophthalmological problem worldwide.

1.5.1 Anatomy of the Eye

The human eye is a complex organ that reacts to light and facilitates vision with the use of a complex visual system. The eye sits in a protective socket, known as the orbit, and is attached to the six extraocular muscles that are responsible for moving the eye. These muscles are attached to the white part of the eye, known as the sclera, which is a strong layer of tissue that helps maintain the integrity of the organ [79, 80]. Although the anatomy of the eye has an intricate design and is comprised of multiple layers, the basic anatomy can be separated into two distinct segments. The anterior segment is the outer portion of the eye and is composed of the cornea, the anterior side of the uveal tract (consisting of the iris and ciliary body), and the crystalline lens, which are the components necessary to focus incoming light. Behind the cornea is the anterior chamber that is filled with a fluid known as the aqueous humor. This fluid produced by the eye, bathes the crystalline lens, and helps maintain proper ocular pressure in the eye [79]. Between the lens and the back of the eye lies the vitreous cavity, which comprises a majority of the posterior segment of the eye. This cavity is filled with a jelly-like substance consisting of hyaluronic acid, collagen, water, proteins, and regulatory cytokines [81]. Also, a part of the posterior segment is the posterior side of the uveal tract (the choroid), the retinal pigment epithelium, and the neurosensory retina. Information that is processed by the retina

travels to the brain through the optic nerve and allows us to process the information received by the eye [79] (Figure 1.7).

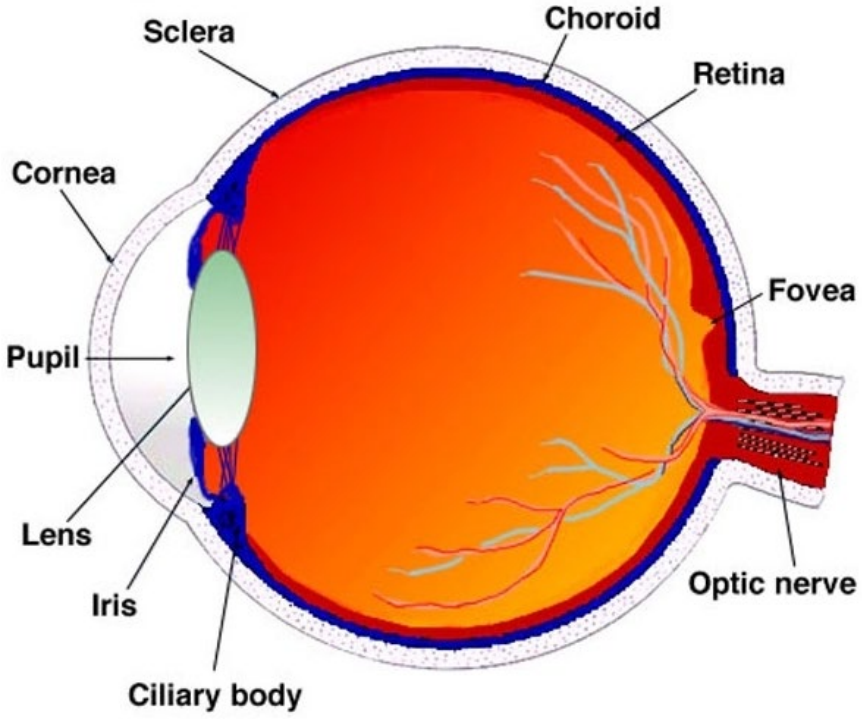

Figure 1.7. Schematic of the human eye.
Depiction of a sagittal section of the adult human eye [82].

1.5.2 The Neurosensory Retina and RPE

Light first enters the front of the eye through the cornea, where the lens focuses it towards the back of the eye and onto the retina. The retina itself is composed of several layers that consist of specific cells: the inner limiting membrane, the nerve fiber layer, the ganglion cell layer, the inner plexiform layer, the inner nuclear layer, the outer plexiform layer, the outer nuclear layer, the external limiting membrane, the photoreceptor layer, and the retinal pigment epithelium (RPE) (Figure 1.8). The inner limiting membrane is the layer closest to the vitreous cavity, while the RPE is more posterior and lies just next to the choroid. The cells that compose these layers have a specialized function that aid in the processing of information received by the

retina. The ganglion cell layer is composed of the nuclei of ganglion cells that run their axons throughout the nerve fiber layer. The ganglion cells receive signals from amacrine cells and bipolar cells whose nuclei are within the inner nuclear layer but whose synapses extend into the inner plexiform layer. Horizontal cell nuclei also compose the inner nuclear layer, and their dendrites extend into the outer plexiform layer where they can interact with photoreceptors. The nuclei of these photoreceptors comprise the outer nuclear layer, and the inner and outer segments of photoreceptors span the external limiting membrane and towards the RPE [80, 83, 84].

The photoreceptors contain proteins that can absorb photons and convert them into signals to neurons within the retina. There are three main types of photoreceptors in human eyes: rods, cones, and intrinsically photosensitive retinal ganglion cells. While the rods and cones are notorious for their role in sight, the function of intrinsically photosensitive retinal ganglion cells is thought to hone more of a regulatory role important for vision, by supporting circadian rhythms and pupillary reflexes [85]. The human retina contains about 120 million rod cells dispersed throughout the retina, that are extremely sensitive to light and are the sole cell type responsible for vision processing at low light levels. The six million cone cells of the human retina are concentrated in the fovea and require a more significant amount of light to produce a signal than the rods. Three different kinds of cone cells respond to light of different wavelengths: short, medium, or long, referred to as S-cone, M-cone, and L-cones, respectively. The response of these three distinct signals is perceived as color. In order to process the vast amount of information fed to the retina, the outer segments of the photoreceptors are shed continuously and replaced with help from the RPE layer of cells (reviewed in [86]).

The RPE cells are polarized epithelial cells that reside between the retina and choroid and provide several functions essential for the survival of the neurosensory retina. Some of these

functions include transporting nutrients to the retina, regulating homeostasis, scavenging free radicals and reactive oxygen species, and phagocytosis of the rod outer segments following normal circadian shedding [87]. The RPE cells are connected by tight junctions forming a physical barrier between the retina and choroid, referred to as the blood-retinal-barrier [86, 88]. This barrier prevents the passage of drugs and other large substances from penetrating the eye, therefore contributing to the immune privilege of the eye [89].

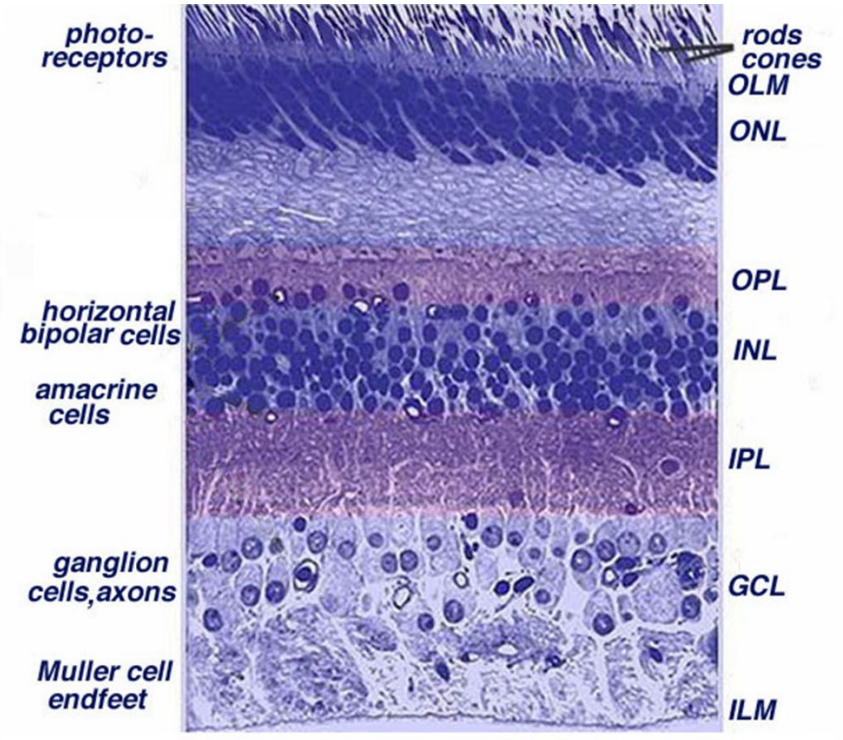

Figure 1.8. Light micrograph of the human retina.

Light focused from the cornea and the crystalline lens and hits the retina starting at the inner limiting membrane (ILM) and transverses the retina until it reaches the rods and cones, directly past the outer limiting membrane (OLM), also referred to as the external limiting membrane (ELM). Adapted from [90]

1.5.3 Ocular Immune Privilege

Ocular immune privilege essentially means that the eye does not generate a typical inflammatory immune response to an unknown antigen [91-93]. Therefore, the passage of nutrients delivered to the retina must be tightly regulated and is delivered by two major blood

supply routes supplied from either the choroid to the photoreceptors via the choriocapillaris or in conjunction with the optic nerve [83]. The physical barrier alone is not all that is necessary for the establishment and maintenance of ocular immune privilege. Another essential feature is the establishment of a microenvironment that drives the immune cells of the eye into anti-inflammatory phenotypes, therefore providing some protection from the damaging effects of inflammation. One such example is the production of immunoregulatory molecules, such as the anti-inflammatory molecules, transforming growth factor-β2, somatostatin, and alpha-melanocyte-stimulating hormone by the aqueous humor and neurosensory retina, which work to inhibit T cell activation [94]. Due to the tight regulation in maintaining this microenvironment, it is no surprise that the neurosensory retina contains its own, specialized glial cells, to help maintain the integrity of the retina.

Microglial cells are resident, macrophage-like cells, that are distributed throughout the inner and outer plexiform, the ganglion cell, and the nerve fiber layers of the retina [95]. The functions of microglial include antigen presentation and phagocytosis during the onset of retinal injury or infection [96]. Müller cells are macroglial cells that span the entire thickness of the retina and aid in many functions, including regulating glucose metabolism, maintaining ion balance through ion channels and transmembrane transporters, and mitigating oxidative stress. Müller cells are also capable of releasing pro-inflammatory cytokines following retinal insult or injury. Müller cells then act in tandem with microglial to phagocytize foreign substances or damaged cells and can alter the retinal blood flow, allowing for the infiltration of leukocytes into the retina [97].

1.5.4 Pathogenesis of AIDS-Related MCMV Retinitis

During AIDS-related MCMV retinitis, the ocular immune privilege of the eye fails, leaving the eye vulnerable to high levels of HCMV replication and subsequent inflammatory response, which included the infiltration of activated macrophages and neutrophils [98, 99]. HCMV enters the eye through the hematogenous spread of infected monocytes that enter the retinal vasculature and is then capable of penetrating and replicating in all layers of the retina and the contiguous RPE. [73]. The presence of active viral replication can be confirmed by the appearance of conspicuous cytomegalic cells, which are characterized as giant cells with eosinophilic type A intranuclear or "owl eye" inclusions. HCMV replication destroys all layers of the retina, resulting in a distinctive full-thickness retinal necrosis. Ultimately, a thin white membrane replaces the areas of retinal destruction, which can be clinically observed, and may be accompanied by hemorrhaging. Fundus photographs depicting the differences in a healthy retina and a retina with advanced AIDS-related HCMV retinitis are seen in Figure 1.9. Left untreated, these areas with irreversible lesion of retinal destruction are capable of merging and may consume the whole retina within six months [100].

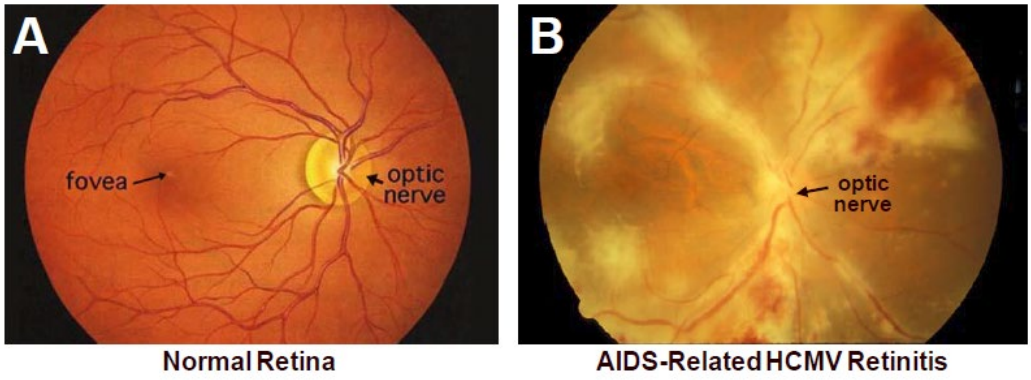

Figure 1.9. Fundus of the human retina during AIDS-related HCMV retinitis

Fundus photograph of a normal human retina (A), from [90], and a retina during AIDS-related HCMV retinitis (B). Present are white areas of retinal necrosis and red areas of associated hemorrhaging, from Drs. Dix and Cousins, Bascom Palmer Eye Institute, Miami, FL.

1.6 Animal Models of MCMV Retinitis

A murine model of experimental CMV retinitis is valuable to study the mechanisms responsible for the retinal destruction involved in the pathogenesis of AIDS-related HCMV retinitis. As CMV is a species-specific virus, HCMV is unable to establish a productive infection in animal models [101], but MCMV offers a viable substitute to explore the pathophysiology of CMV retinitis [12]. As with humans, MCMV infection of mice is generally not as productive in immunologically normal mice, and these mice are often resistant to developing MCMV retinitis [4, 102-104]. However, if the mice are immunosuppressed and injected with a high enough titer of MCMV into the subretinal space (Figure 1.10), MCMV retinitis typically manifests with frequencies higher than 75% [1, 105, 106], although exact frequencies depend on the strain of mouse used [4, 105-109]. Two methods of immunosuppression are successful in establishing susceptibility to MCMV retinitis: corticosteroid-induced immunosuppression [105, 106, 109] and the administration of a mixture of mouse-specific retroviruses (LP-BM5) [110, 111], which results in the established of immunosuppression that confers susceptibility to MCMV retinitis in C57BL/6 mice 8-12 weeks following the onset of immunosuppression [5, 112, 113].

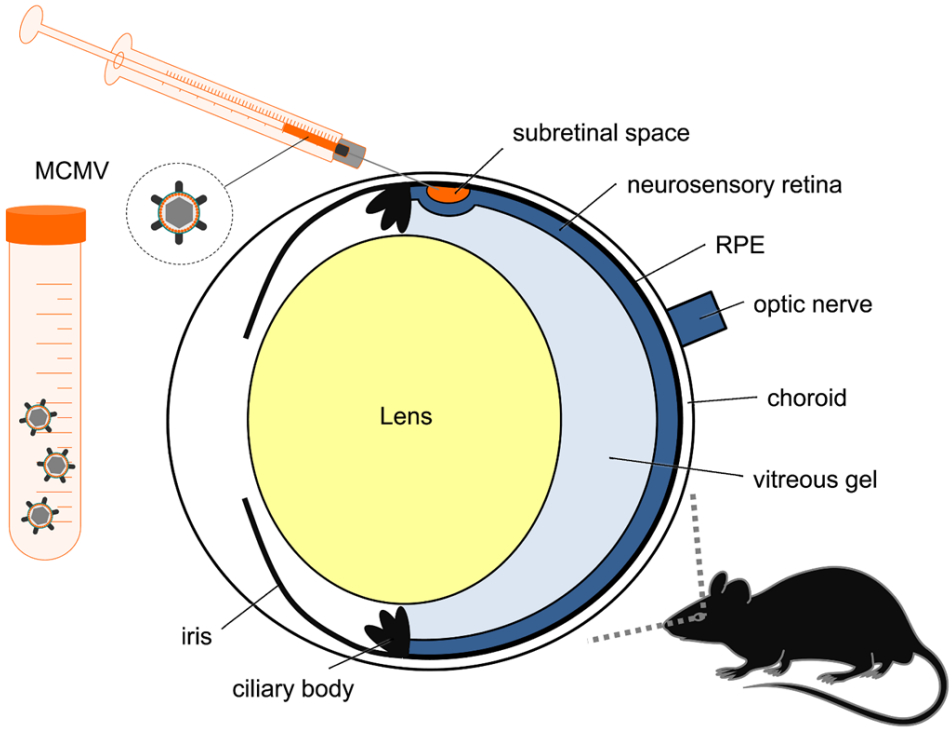

Figure 1.10. Schematic mouse eye depicting site of subretinal injection.

Representation of the subretinal injection site for MCMV by 1 30-gauge needle. A 2-uL volume in injected into the subretinal space, followed by an air bubble to prevent back flow. Figure from [114].

1.6.1 Corticosteroid-Induced Immunosuppression

Corticosteroid-induced immunosuppression results in a rapid, acute decline in the immune system, which develops over several days resulting in dysfunction of several types of immune cell populations [115, 116]. Specifically, corticosteroid-induced immunosuppression results in a rapid loss of macrophages within days of immunosuppression [115], and the number and function of CD4+ and CD8+ T cells are also dramatically reduced. This model, therefore, results in a dampened immune response by suppressing inflammatory cytokines expressions, such as IFN-γ, TNF-α, IL-2, and IL-1β [116].

1.6.2 Murine Acquired Immunodeficiency Syndrome (MAIDS)

Retroviral-induced immunosuppression (MAIDS) is established by intraperitoneal injection of murine leukemia viruses (MuLV) and designated as lymphoproliferative bone marrow 5 (LP-BM5) [111]. The induction of MAIDS is dependent on the infected strain of mice. For instance, BALB/c mice are more resistant to MAIDS development than C57BL/6 and take over a year to progress to late-stage MAIDS [5, 117]. The MAIDS model of immunosuppression differs in many ways from that of corticosteroid-induced immunosuppression. One of the more prominent differences is the timing it takes to establish immune suppression. MAIDS have a slow and progressive development, which goes through distinct phases of immune cell dysfunction over several weeks. Also different is the presence and functionality of the immune cell populations throughout the course of infection. For instance, macrophage populations show a dramatic difference between the two models of immunosuppression. In MAIDS mice, macrophage populations decrease and change their phenotypic function towards the later stages of the disease, which is in direct contrast to the rapid loss of macrophage numbers within days following corticosteroid-induced immunosuppression [115]. Additionally, MAIDS results in an unusual proliferation of B and T cells [118], which are rendered dysfunctional by the retrovirus [5, 110, 119]. Furthermore, natural killer cells [120] and neutrophils [118] are also dysfunctional during the progression of MAIDS development.

1.7 MAIDS-related MCMV Retinitis

The use of subretinal MCMV infection in susceptible MAIDS mice is a combination unique to our laboratory [1, 4]. The MAIDS model is a suitable model for this study because species-specific retroviruses cause both MAIDS and AIDS, and mice with MAIDS share many immunopathologic features with AIDS patients. These similarities include a characteristic

progressive development of chronic generalized lymphadenopathy, a polyclonal B cell activation, and a shift in the levels of Th1 and Th2 CD4+ T-cells with an eventual diminishment in CD4+ T cell and CD8+ T cell counts and functions [112, 119, 121-123]. Healthy mice and mice with MAIDS-4 duration (MAIDS-4) or less are resistant to the development of MCMV retinitis. However, due to the decline in T cell functionality [123, 124], mice subjected to MAIDS for a duration of eight weeks (MAIDS-8) become susceptible to the development of MCMV retinitis with full susceptibility (80-100%) by MAIDS of ten-week duration (MAIDS-10) [4], as depicted in Figure 1.11. MAIDS-10 mice will then develop retinitis 10 days post subretinal MCMV injection and exhibit histopathological features similar to that seen in AIDS-related HCMV retinitis, which include full-thickness retinal necrosis, the presence of cytomegalic cells, and transition zones between areas of the normal and diseased retina [4, 125] as depicted in Figure 1.12. Since both MAIDS-4 and MAIDS-10 mice harbor equivalent amounts of infectious MCMV but MCMV-infected eyes of MAIDS-4 mice fail to develop retinal necrosis [1], the viral infection alone is not sufficient for the onset and progression of retinitis.

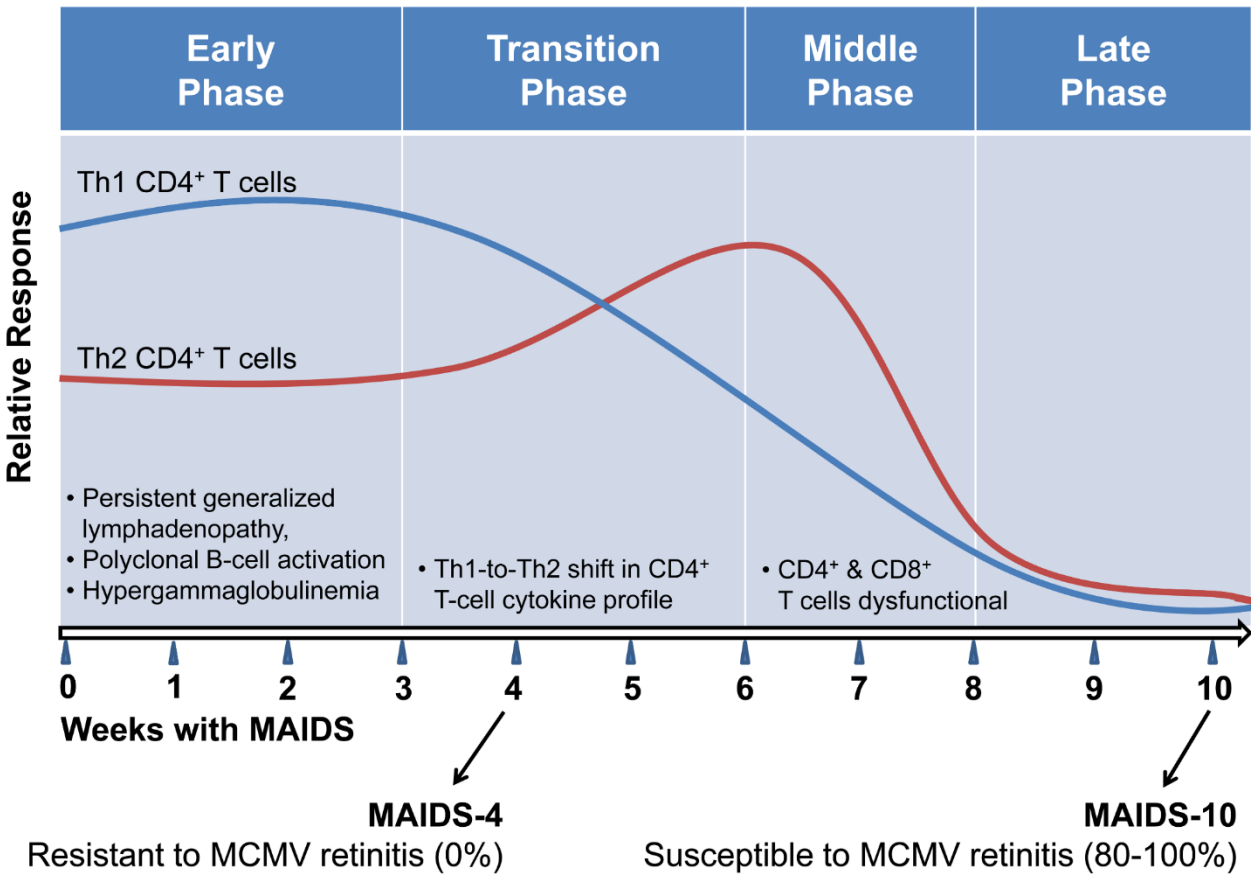

Figure 1.11. Progression of MAIDS.

The MAIDS model shares many features similar to the development of AIDS. During the first few weeks following MAIDS induction, mice experience chronic generalized lymphadenopathy, a polyclonal B-cell activation, and hypergammaglobulinemia. The progression of MAIDS then results in a shift in the levels of Th1 and Th2 CD4+ T-cells. Healthy mice and mice with a MAIDS duration of 4 weeks (MAIDS-4) are resistant to retinitis development. However, as MAIDS progresses and results in the diminishment in CD4+ T-cell and CD8+ T-cell counts and functions, mice become susceptible to MCMV retinitis. From [114].

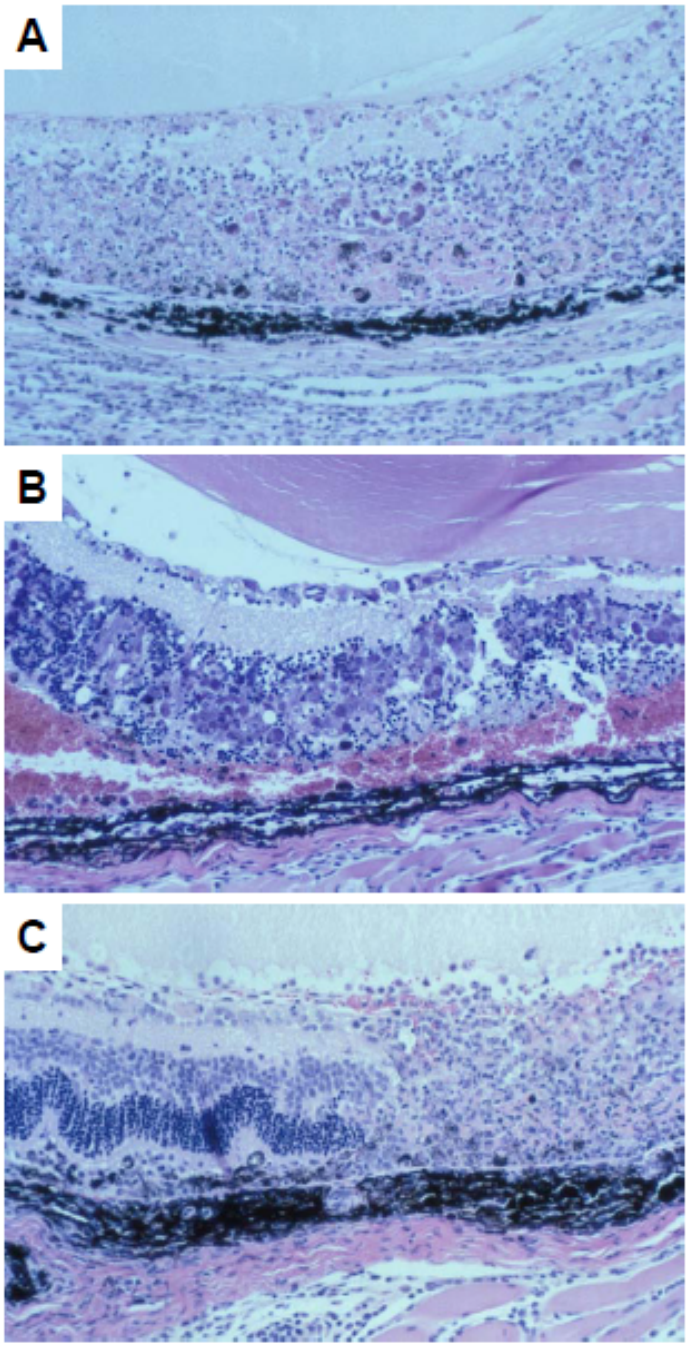

Figure 1.12. Histopathology of experimental MAIDS-related MCMV retinitis.

Hematoxalin and eosin (H&E)-stained cross-sections of eyes during retinitis development 8 days following subretinal MCMV infection. (A) full-thickness retinal necrosis, (B) section showing the presence of cytomegalic cells, and (C) transition zones between intact retina (with areas of retinal folding) and full-thickness retinitis. Photomicrographs from [4], original magnification 200×.

1.7.1 MAIDS-related MCMV Retinitis

Over the last several years, our lab has extensively studied several mechanisms that may be involved in the pathogenesis of MAIDS-related MCMV retinitis. Briefly, we have found that the expression of anti-inflammatory cytokines, interleukin (IL)-4 and IL-10, are upregulated during the onset and progression of experimental MCMV retinitis and may mediate the inflammatory response following MCMV infection. However, it has been demonstrated that the systemic deletion of either of these cytokines is insufficient to improve the developed retinitis [126]. Interestingly, the pro-inflammatory cytokine, IL-17, which is constitutively expressed intraocularly, is downregulated by MCMV during MAIDS-related MCMV retinitis. It is thought that this downregulation of IL-17 is mediated through the stimulation of the suppressor of cytokine signaling (SOCS)1 and SOCS3, which are both stimulated during the pathogenesis of MAIDS-related MCMV retinitis [127]. Although tumor necrosis factor alpha (TNF-α) is considerably upregulated following ocular MCMV infection of MAIDS-10 mice, this cytokine may be playing a dual role mediating either apoptosis or the anti-apoptotic pathway as the receptors for TNF-α, TNFR1 and TNFR2 are also stimulated following MCMV infection and diverge towards either pathway [6].

A major area of focus of our lab, the pathogenesis of experimental MAIDS-related MCMV retinitis, is the involvement of multiple cell death pathways. In addition to the stimulation of TNF-α, TNFR1, and TNFR2 being stimulated during experimental MCMV retinitis, activated caspase-3 and activated caspase-8 are also upregulated. Interestingly, however, neither apoptosome-related molecules, cytochrome c, apoptotic protease activating factor 1 (Apaf-1), nor caspase-9 are stimulated in MCMV-infected eyes, and histopathology has suggested that apoptosis-related cell death only constitutes about 8% of the dead cells during

retinitis. RIPK1 and MLKL molecules related to the inflammatory cell death pathway, necroptosis, are stimulated during MAIDS-related MCMV retinitis, suggesting the involvement of this mode of cell death may be associated with the retinal destruction seen in this model. Additionally, pyroptosis-associated molecules—caspase-1, caspase-11, IL-1β, and IL-18—and several inflammasome components are also stimulated during MAIDS-related MCMV retinitis. This suggests that multiple cell death pathways may operate simultaneously following ocular infection of MCMV in MAIDS-10 mice [6].

1.8 MAIDS-related MCMV Retinitis and the Stimulation of Cell Death Pathways

1.8.1 Apoptosis

Due to the discovery that MCMV-infected eyes of MAIDS-4 and MAIDS-10 mice harbor equivalent amounts of infectious MCMV despite MAIDS-4 mice being resistant to the development of retinal necrosis, it was concluded that virus alone is not sufficient for the onset and progression of retinal destruction in MCMV-infected eyes of MAIDS-10 mice [103]. It was therefore hypothesized that other mechanisms must be responsible for the retinal necrosis seen following MCMV infection. Bigger et al. [128] first detected apoptotic cells by TUNEL assay in retinal tissues of MCMV-infected eyes from immunocompetent BALB/c mice and methylprednisolone acetate-immunosuppressed BALB/c mice. As a result of this work, apoptosis, a programmed form of cell death, was considered the predominant mechanism of retinal pathology of AIDS-related HCMV retinitis, and its involvement in MCMV-infected eyes of MAIDS mice was investigated.

Apoptosis is often initiated by TNF-α. TNF-α is a proinflammatory cytokine that induces diverse cellular responses by binding to the receptors TNFR1 and TNFR2. Binding of TNF-α to its receptor results in the cleavage and activation of caspase-3 and caspase-8, leading to

apoptosis and cell death [129, 130]. TNF-α was shown to be ocularly expressed during AIDS-related HCMV retinitis [131], suggesting the infiltrating macrophages were a source of TNF-α [98]. Using the MAIDS model for MCMV retinitis, it was shown that key TNF-α-induced apoptotic molecules, TNF-α, TNFR1, TNFR2, caspase-8, and caspase-3 are not upregulated in MCMV-infected eyes of MAIDS-4 mice resistant to retinitis when compared to the media-injected contralateral control eye but that these molecules are highly stimulated in MCMV-infected eyes of MAIDS-10 mice that are susceptible to retinitis. This stimulation showed a peak of mRNA for all molecules occurring at day 6 post-infection before the development of severe retinal destruction seen at day 10 post-infection. The production of TNF-α was detected in several cell types, including infiltrating macrophages and neutrophils, as well as resident Müller cells and microglia. Using knock-out (KO) mice, it was shown that mice deficient in TNF-α, TNFR1, and TNFR2 showed a reduction in the frequency of retinitis in MCMV-infected MAIDS-10 mice when compared to MCMV-infected eyes of wild-type (WT) MAIDS-10 mice, suggesting that TNF-α and its receptors are important for the development of retinitis in this model. However, neither of these KO mice exhibited a change in the ocular levels of infectious MCMV, indicating that these molecules are not responsible for controlling the viral levels of MCMV, and also strengthening the idea that it is not solely the level of infectious virus that is responsible for the retinitis. This work suggests that TNF-α-induced apoptosis could be contributing to the retinal destruction seen during MAIDS-related MCMV retinitis [6].

Apoptosis is not limited to being induced by one signaling pathway and can be stimulated by several signaling proteins with specific death receptors (Figure 1.13) [132]. To help determine if apoptosis induced by stimuli other than TNF-α plays a role in the pathogenesis of MAIDS-related MCMV retinitis, other apoptotic pathways were investigated. TNF-related apoptosis-

inducing ligand (TRAIL) induces apoptosis via a caspase-8-dependent pathway after binding to death receptors (DR) 4 or DR5 (TRAIL-R) [133, 134]. Additionally, FasL can induce apoptosis via a caspase-independent pathway after binding to the Fas receptor [133, 135-137]. Similar to what was seen for TNF-α, mRNA for TRAIL, TRAIL-R (DR5), Fas, and FasL were all upregulated in MCMV-infected eyes of MAIDS-10 mice, but not MAIDS-4, when compared to media-injected control eyes, with a peak stimulation at day 6 post-infection. This indicated that apoptosis initiated through other pathways might also be stimulated during the pathogenesis of MAIDS-related MCMV retinitis. Surprisingly, however, mRNA for caspase-9, cytochrome c, and Apaf-1 were not upregulated in MCMV-infected eyes of MAIDS-4 or MAIDS-10 mice. These molecules are known to participate in apoptosis induced by the apoptosome [138, 139], and the absence of their stimulation suggests no significant role for the mitochondrion-associated mechanism of apoptosis during MAIDS-related MCMV retinitis. It is possible that the MCMV gene m38.5, which encodes vIBO, might be inhibiting apoptosis at the mitochondrial level [140]. To further elucidate the involvement of apoptosis in the retinal destruction, a study was done to detect the number and localization of TUNEL-positive cells in the MCMV-infected retina. Following MCMV infection of MAIDS-10 mice, sparse TUNEL-positive cells were detected at day 3 post-infection, and a substantial increase was seen at day 6 post-infection, with a distribution showing localization within the RPE layer as well as the neurosensory retina. At day 10 post-infection, the TUNEL-positive cells displayed a diffuse distribution within the retina. However, quantification revealed that only ~8% of retinal cells were found to be TUNEL positive after MCMV infection, suggesting that although apoptosis may contribute to retinal tissue destruction, its pathogenic contribution was relatively minimal [6].

Although mRNA for the ligands and receptors of the Fas and TRAIL-related apoptosis pathway, as well as mRNA for caspase-3 and caspase-8, were increased in MCMV-infected eyes, other molecules associated with apoptosis, including cytochrome c and Apaf-1, were not upregulated in MCMV-infected eyes when compared to the media-injected, contralateral control eyes. This may explain why apoptosis appears to only contribute minimally to the retinal damage seen during MAIDS-related MCMV retinitis. It has been shown that TNF-α- induced apoptosis is expressed at elevated levels within the eyes of patients with AIDS-related HCMV retinitis [98, 131], and TNF-α and its respective receptors were found to be upregulated in MCMV-infected eyes of MAIDS-10 mice. Since apoptosis may only contribute minimally to the retinal damage, it is also possible that the increase in TNF-α seen in MCMV-infected eyes could be related to that of another cell death pathway induced by TNF-α, such as necroptosis.

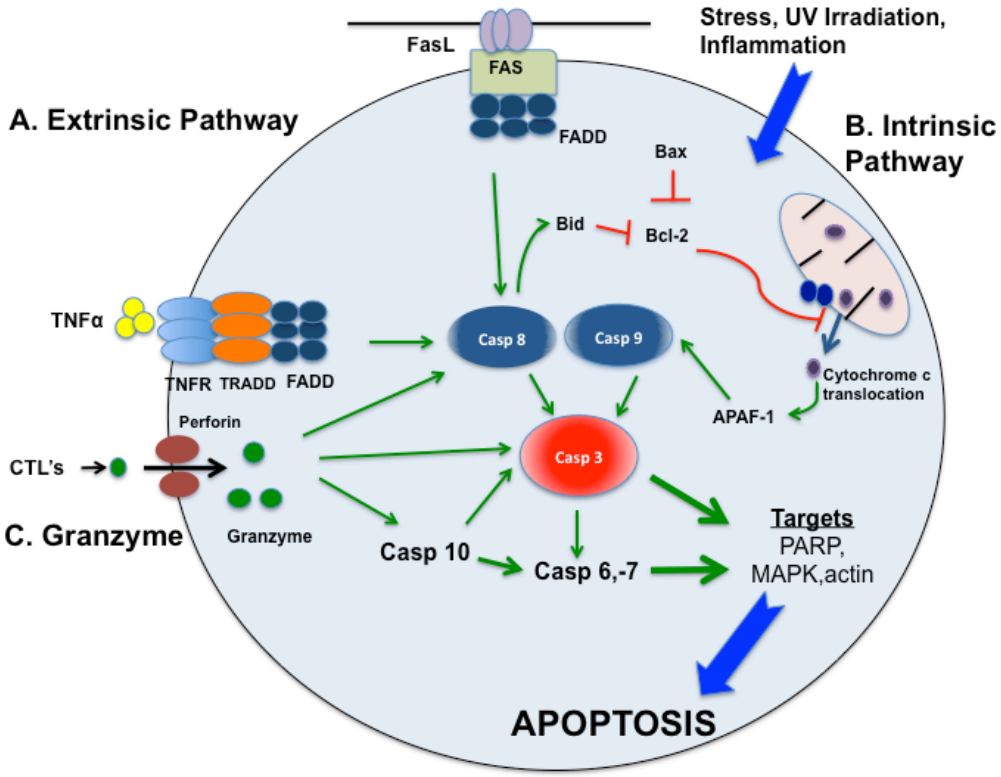

Figure 1.13. Apoptosis cell death signaling pathway.

The apoptosis pathway is a form of cell death that can be induced through either the extrinsic pathway, the intrinsic pathway, or the granzyme pathway. Induction through either of these pathways result in the activation of either caspase-8 or caspase-9 which both results in the activation of caspase-3, which leads to apoptotic death of the cell. Apoptosis results in mitochondrial membrane permeabilization, chromatin condensation, and DNA fragmentation. This results in smaller cells and apoptotic bodies that are phagocytized. Figure from [141].

1.8.2 Necroptosis

Necroptosis is a form of TNF-α induced programmed cell death that results in membrane and organelle swelling followed by cell lysis [17-19]. Necroptosis is induced when apoptosis is inhibited by blocking caspase-8 activity, such as by uncleaved caspase-8/cellular FLICE inhibitory protein (cFLIP) heterodimer formation [20]. Unlike apoptosis, necroptosis cell lysis results in the release of damage-associated-molecular patterns (DAMPs) that trigger a highly inflammatory response [21]. The necroptotic pathway is caspase-independent and initiated when ligand binding induces the recruitment of adaptor proteins Fas-associated protein with death

domain (FADD), tumor necrosis factor receptor type 1-associated death domain (TRADD) or TIR-domain-containing adapter-inducing interferon-β (TRIF) associated with various accessory proteins, in addition to receptor-interacting serine/threonine-protein kinase 1 (RIPK1), forming a death complex. The upregulation of the de-ubiquitinating enzyme CYLD or the cellular inhibitor of apoptosis protein 1 (cIAP1) causes RIPK1 to dissociate from the initial death complex and form a second death complex associated with caspase-8. When caspase-8 is inactivated, either directly by a pathogen or during anti-apoptosis signaling, RIPK1 recruits another receptor-interacting serine/threonine-protein kinase, RIPK3, through its RIP homotypic interaction motif (RHIM) domain. Both proteins are phosphorylated and form the necrosome [22, 23]. Subsequently, the formation of the necrosome recruits mixed-lineage kinase-like domain (MLKL) protein, and it too is phosphorylated. Activated MLKL forms an oligomer complex that associates with the cell membrane and forms a pore, resulting in cell lysis and the release of pro-inflammatory molecules (shown in Figure 1.14) [24].

To determine if necroptosis plays a role in the pathogenesis of MCMV retinitis, MCMV-infected eyes of MAIDS-4 and MAIDS-10 mice were compared to media-injected contralateral control eyes for the upregulation of crucial necroptosis molecules, RIPK1 and RIPK3. RIPK1 was found upregulated in MCMV-infected eyes of MAIDS-10 mice with a peak at day 6 post-infection but not in MCMV-infected eyes of mice with MAIDS-4. RIPK3, however, was not significantly upregulated in MCMV-infected eyes with either MAIDS-4 or MAIDS-10 duration [7]. The stimulation of RIPK1, but not RIPK3, following MCMV infection suggests that necroptosis may be playing a role in MAIDS-related MCMV retinitis, in a manner independent of RIPK3.

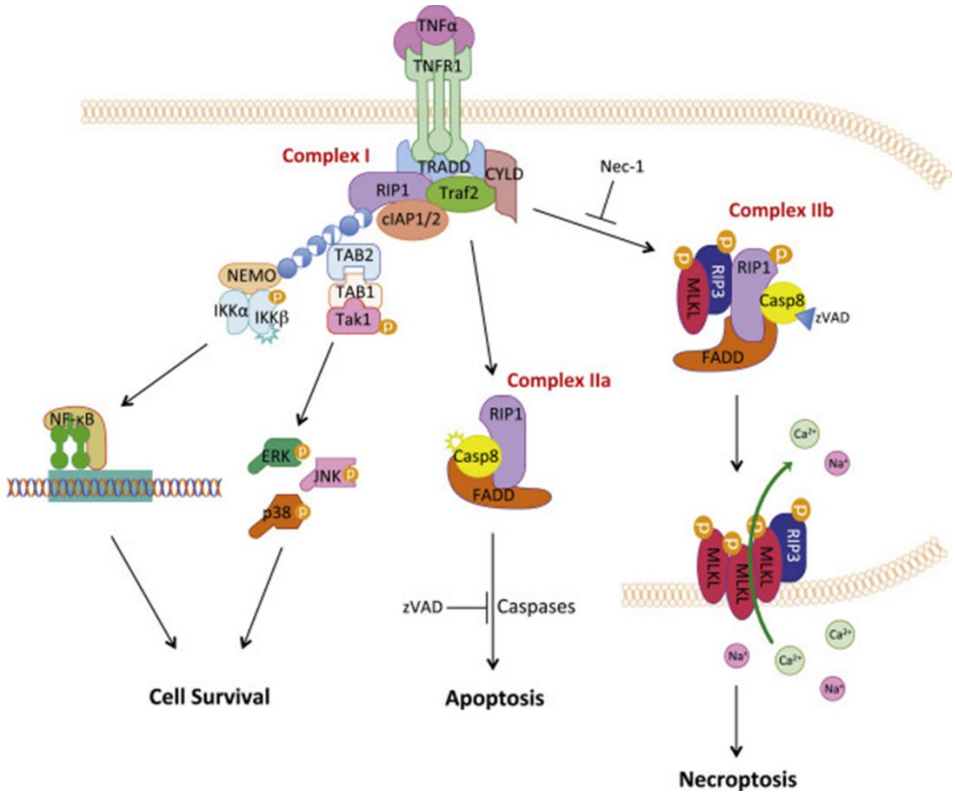

Figure 1.14. Necroptosis cell death signaling pathway.

TNFR1 can mediate either cell survival, apoptosis, or necroptosis pathways. Binding of TNFR1 with TNFα leads to the formation of complex I which consists of TRADD, TRAF2, RIP1, and cIAP1. Left: Polyubiquitination of RIP1 by cIAP1, leads to the recruitment of IKK complex and TAK1, activating the NF-κB and MAPK survival pathways. Middle: If cIAP1 does not polyubiquitinate RIP1, then RIP1, associates with FADD and caspase-8 to form cytosolic complex IIa which induces apoptosis. Right: If caspase-8 activity is inhibited, RIP1 interacts with RIP3 and MLKL to form complex Iib. RIP3 and MLKL are phosphorylated and translocate to the plasma membrane, mediating membrane permeabilization and resulting in cell death via necroptosis. Figure from [142].

1.8.3 Pyroptosis

In addition to the TNF-α-induced cell death pathways, there are other programmed cell death pathways that do not rely on TNF-α, such as pyroptosis. Pyroptosis is a highly inflammatory form of programmed cell death [143] that can be induced by both pathogen-associated molecular patterns (PAMPs) and DAMPs. During pyroptosis, there is a net increase of osmotic pressure, cell swelling, and lysis, followed by a mass release of cellular contents, including active IL-1β and IL-18 [144]. Alternatively, the noncanonical pathway involves the

activation of caspase-11 (murine), which can also cleave gasdermin D (GSDMD) and is thought to function independently of inflammasomes [145]. In addition to the upregulation of several apoptosis-and necroptosis-related molecules, it was shown that MCMV-infected eyes of MAIDS-10 mice highly upregulates mRNA expression of caspase-1, IL-1β, and IL-18, collectively peaking 6 days following subretinal MCMV infection, but no upregulation was seen in MCMV-infected eyes of MAIDS-4 mice [6]. Similar trends were seen for the upregulation of mRNA for several inflammasomes in the MCMV-infected eyes of MAIDS-10 mice but not those of MAIDS-4. Additionally, it was seen that the protein levels of cleaved caspase-11 were also significantly elevated at 6 days following MCMV infection [100]. Taken together, these results suggest that both the canonical and noncanonical pathways of pyroptosis may be playing a role in the pathogenesis of MAIDS-related MCMV retinitis.

1.9 Pyroptosis Pathway and Inflammasomes

1.9.1 Canonical Pyroptosis Pathway

The canonical pathway of pyroptosis occurs with the initiation and assembly of an inflammasome complex. The inflammasome is a multiprotein oligomer responsible for the activation of inflammatory responses by promoting the maturation and secretion of pro-inflammatory cytokines IL-1β and IL-18. Once active, the inflammasome binds to pro-caspase-1 either homotypically via its own caspase-activation and recruitment domain (CARD), or via the CARD of the adaptor protein, associated speck-like protein containing CARD (ASC), which it binds to during inflammasome formation. The clustering of many p45 pro-caspase-1 molecules together induces their autocatalytic cleavage allowing caspase-1 to then assemble into its active form consisting of two heterodimers each with a p20 and p10 subunit. Once active, caspase-1 then cleaves and activates pro-IL-1β and pro-IL-18 to induce interferon (IFN)-γ secretion

and natural killer cell activation [146]. Caspase-1 also cleaves the cytoplasmic protein, GSDMD, which localizes to the membrane where it is responsible for forming pores. These pores result in a net increase in osmotic pressure, water influx, swelling, and osmotic lysis, allowing for the release of IL-1β and IL-18 (Figure 1.15) [144].

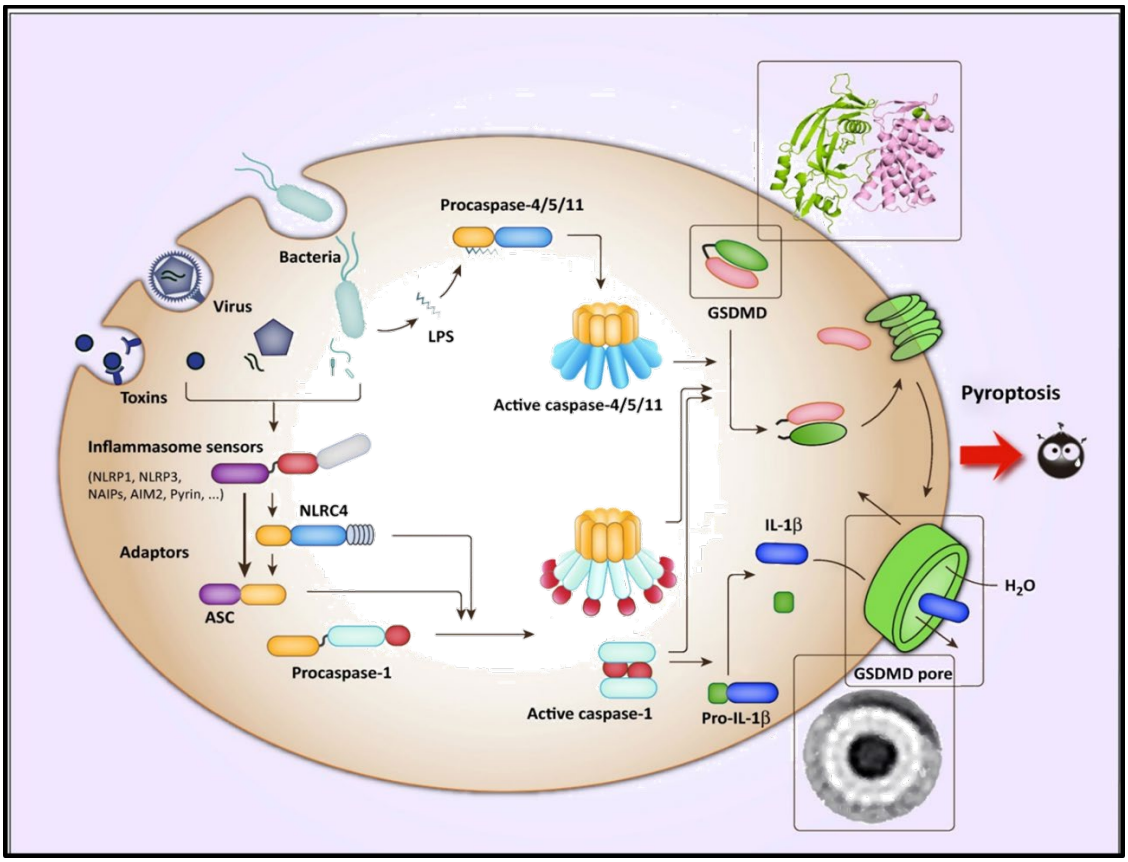

Figure 1.15. Pyroptosis cell death signaling pathway.

The canonical pyroptosis pathway results after intracellular danger signals initiate the assembly of an inflammasome, which then recruits and activates procaspase-1. Active caspase-1 is then able to cleave pro-inflammatory cytokines IL-1β and IL-18 as well as the cytosolic protein GSDMD which forms holes in the plasma membrane resulting in the release of cellular contents. GSDMD can also be cleaved by caspase-11 through the noncanonical pyroptosis pathway. Figure from [147].

Caspase-1. Caspase-1 is an evolutionarily conserved protease that, like other caspases, is produced as a biologically inactive zymogen that requires cleavage by other caspase-members, or themselves, to become active (reviewed in [148]). The structure of caspase-1 contains two heterodimers of cleaved subunits, p20 and p10, and is also composed of a catalytic domain [149] as well as a CARD domain. The CARD domain can interact with CARD domains on other proteins, such as the ASC-adapter protein associated with activated inflammasomes or directly with the CARD domain of the inflammasome [150, 151]. This interaction results in the self-cleavage of caspase-1 resulting in its activation. Cleaved caspase-1 is then able to cleave and activate the pro-inflammatory cytokines IL-1β and IL-18 [152].

IL-1β. IL-1β is a pro-inflammatory, fever producing cytokine, which is a member of the IL-1 family. The IL-1 family includes several cytokines that are either pro-inflammatory agonists— IL-1α, IL-1β, IL-18, IL-33, IL-36α, IL-36β, IL-36γ—or IL-1R antagonist (IL-1Ra)—IL-36Ra, IL-37, and IL-38—that exert anti-inflammatory activities. Many of these cytokines play a critical role in response to pathogens [153]. Pro-IL-1β is produced by activated macrophages as a biologically inactive protein that must be cleaved to become activated. Because IL-1β invokes a potent inflammatory response, its secretion is tightly regulated. The transcription of the inactive precursor is induced by activation of toll-like receptor (TLR) activation, TNF, or IL-1 receptor activation by cleaved IL-1β. In order for this mature form to be secreted and engage in the stimulation of these receptors, a second signal is needed in the form of inflammasome activation. The formation of the inflammasome then results in the activation of caspase-1, which results in the proteolytic processing of IL-1β. Cleavage of IL-1β by activated caspase-1 allows for IL-1β to fulfill its functions as part of the inflammatory response, as well as cellular activities, such as cell proliferation and differentiation. Caspase-1 is not the only

protease that can cleave pro-IL-1β, as neutrophil serine proteases proteinase 3 and elastase, and the mast cell-derived serine protease, chymase, also have this ability [154, 155].

IL-18. IL-18 is a pro-inflammatory cytokine notorious for the induction of IFN-γ production from Th1 cells, non-polarized T cells, natural killer cells, natural killer T cells, B cells, dendritic cells, and macrophages in the presence of IL-12. IL-18 also display other functions, including the induction of IL-2 production, the facilitation of the expression of IL-2 receptor on Th1 cells, and the activation of natural killer cells. In conjunction with IL-3, IL-18 is able to facilitate the production of IL-4 and IL-33 from mast cells and basophils (reviewed in [156]). Murine IL-18 proteins consist of 192 amino acids, and the homology of this sequence to IL-1β results in its classification as a member of the IL-1 family [157, 158]. Like IL-1β, IL-18 is produced as a biologically inactive precursor, pro-IL-18, which requires proteolytic processing to become active via caspase-1 [159].

Gasdermin D. GSDMD is the best-understood member belonging to the gasdermin family, and its role in pyroptosis has been well characterized [160]. The GSDMD protein consists of two domains, the N-terminal and C-terminal, with a cleavage site at D276 between the two domains. This cleavage site is mainly targeted by caspase-1 following inflammasome activation, while caspase-11 is also able to cleave GSDMD independent of canonical inflammasome activation [161]. Recently, however, it has been shown that caspase-8 is also capable of cleaving GSDMD, but the drive to cleave GSDMD by this caspase-is weaker than caspase-1, and thus it is thought that cleavage by caspase-8 is more of a backup measure in situations where the other caspases are unable to cleave GSDMD [162]. Additionally, both the neutrophil specific elastase [163] and cathepsin G [164] were shown to be sufficient in cleaving GSDMD at a site upstream of that cleaved by the caspases. Once cleaved, the two domains of

GSDMD serve different functions. The C-domain (p20) functions as an intrinsic inhibitor of the molecule while the N-terminal domain translocates to the plasma membrane where it oligomerizes and inserts itself into the membrane, forming a pore. It is the development of this pore that results in the loss of osmotic homeostasis, cell swelling, and mass release of inflammatory cytokines, including IL-1β and IL-18 [165-168]. Interestingly, it has been shown that cleavage of GSDMD by caspase-3 at D88 in the N-terminal domain can decrease the induction of pyroptosis by inhibiting oligomerization and pore formation [169, 170] that could be used as regulatory mechanisms against unwarranted cell death.

1.9.2 Inflammasomes

Characteristic of the canonical pathway of pyroptosis is the activation of inflammasomes. Inflammasomes are high-molecular-weight, multi-protein complexes that are found in the cytosol of immune cells and regulate the activation of inflammatory responses [171]. There are multiple types of inflammasomes, and each of their distinct assemblies is determined by a unique pattern-recognition receptor (PPR) in response to specific PAMPs or danger signals present in the host's cytosol. Once activated by the inflammatory ligand, the central domain of the inflammasome undergoes oligomerization, resulting in the recruitment of adaptor proteins, such as ASC, to the effector and variable N-terminal domain, which is composed of a pyrin domain (PYD) and a CARD domain. The CARD domain, on either the inflammasome or ASC binds and activates pro-caspase-1 to initiate an inflammatory response [172]. There are several types of inflammasome proteins known to date, including the nucleotide-binding oligomerization domain (NOD), leucine-rich repeat (LRR)-containing protein (NLR) family members, NLRP3, NLRP1b, and NLRC4, as well as the protein absent in melanoma 2 (AIM2) (Figure 1.16) [161].

NLRP3. NLRP3 is the more well-characterized inflammasome of the NLR subset of inflammasomes. Like all members of the NLR family, NLRP3 has a three-domain structure: An N-terminal homotypic interaction domain that contains CARD and PYD, a central NOD-like domain crucial for activation, and a series LRRs on the C-terminal which are presumed to be responsible for the recognition of NLR ligands. NLRP3 is known to respond to a variety of stimuli: particulate matter, such as uric acid crystals [173], silica and asbestos [174], extracellular ATP [175], toxins [176], and several viral [177], bacterial [178, 179], fungal [180] and protozoal [181] pathogens. Due to the diversity of these stimuli, a cellular event common to all these stimuli has been suggested to be the inducer for NLRP3. Possible triggers include potassium efflux [182], mitochondrial dysfunction [183], or reactive oxygen species [184], but no unified mechanism has yet to be determined.

NLRP1b. Although not as well characterized as NLRP3, NLRP1 was the first NLR shown to form an inflammasome complex [171]. Unique to NLRP1 is the presence of a function-to-find domain (FIIND) motif, which is flanked by the CARD domain at its C-terminal end, and aids in the recruitment of ASC. Although human NLRP1 contains a PYD, this is missing in murine paralogues, such as NLRP1b. While information is available on the involvement of NLRP1b with the lethal toxin of *B. anthracis* [185], much is still unknown regarding NLRP1b and other possible stimuli.

NLRC4. Unlike the other NLR family members, NLRC4 contains only a CARD domain that can interact with the CARD domain of caspase-1 resulting in direct activation of caspase-1 by NLRC4. Whereas the association with the adapter protein ASC enhances this activation of caspase-1, unlike the other inflammasomes, this interaction is not necessary for caspase-1 activation by NLRC4 [186]. NLRC4 can interact with different neuronal apoptosis

inhibitory protein (NAIP) members, and the combination of the different NAIPs may determine ligand specificity [187]. The NLRC4 inflammasome is often associated with bacterial infections [188-192], but the involvement of NLRC4 in non-alcoholic steatohepatitis supports the notion that stimuli other than bacteria can induce the activation of the NLRC4 inflammasome [193].

AIM2. AIM2 is independent of the NLR protein family, contains an N-terminal PYD domain and a C- hematopoietic interferon-inducible nuclear antigens with 200 amino acid repeats (HIN-200) domain [194], and senses and binds foreign cytoplasmic double-stranded DNA [195]. The PYD domain interacts with other PYD domains, such as that on the ASC protein, via highly specific, homotypical PYD-PYD interactions [196, 197]. As seen with NLRP3, the AIM2 inflammasome requires an initial pro-inflammatory signal to promote the expression of its substrates. For NLRP3, this priming is mostly mediated by NF-κB transcriptional activation, but for AIM2, this signal is type I interferon induction, a response typical of viral infections [198], including MCMV [195].

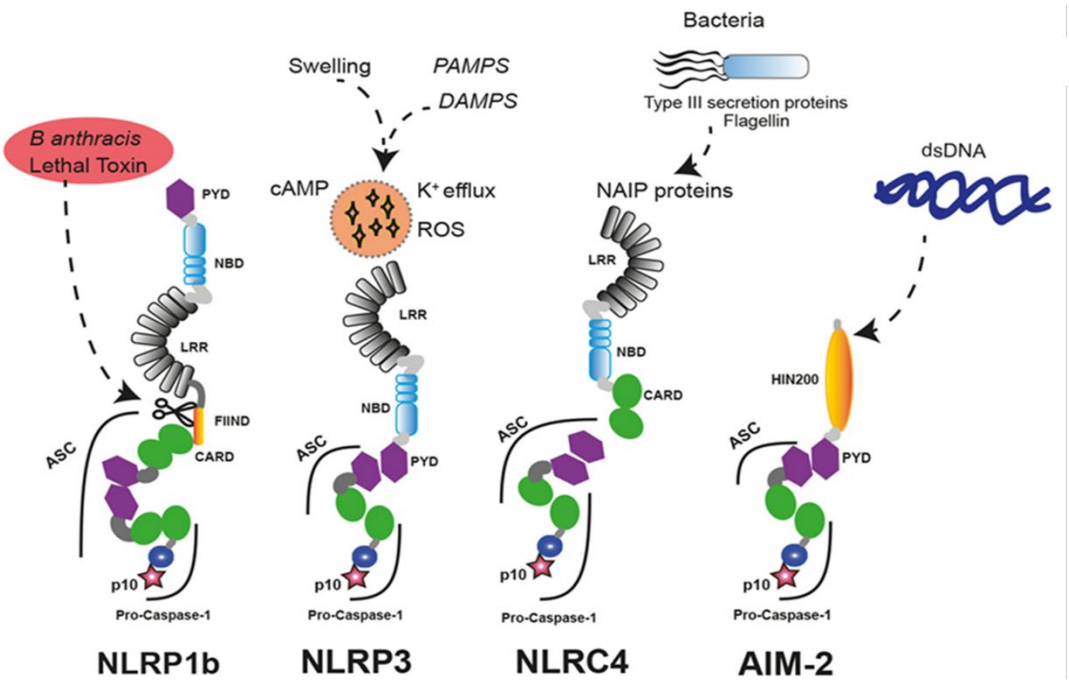

Figure 1.16. Inflammasomes sensors and potential activators.

Inflammasomes are multiprotein complexes that are activated in response to intracellular danger signals. Once activated, the inflammasome recruits and binds pro-caspase-1 through either a caspase-activation and recruitment domain (CARD) or a pyrin domain (PYD), and may also contain an adaptor proteins like the apoptosis speck-like protein with a CARD domain (ASC). The NLR subset of inflammasomes contain a central nucleotide-binding domain (NBD) as well a C-terminal leucine-rich repeat (LRR) domain. Unique to NLRP1b (far left) is the presence of a function-to-find domain (FIIND) presumably for the inflammasome activation. The AIM2 inflammasome (right) contains a C-terminal hematopoietic interferon (IFN)-inducible nuclear protein with 200-amino acid repeat (HIN-200) domain. Modified from [199]

1.9.3 Noncanonical Inflammasome Pyroptosis Pathway

In addition to the canonical pyroptosis pathway that is dependent on the activation of either NLRP3, NLRP1b, NLRC4, or AIM2 inflammasomes to recruit and activate caspase-1, there is also the noncanonical pathway mediated by caspase-11. In 2011, it was discovered that caspase-11 could trigger the maturation of IL-1β and subsequent pyroptosis in lipopolysaccharide (LPS)-primed mouse macrophages in an NLRP3-ASC-caspase-1 inflammasome-dependent pathway [200]. Additionally, the human homologs of caspase-11, caspase-4/5, were shown to have the ability to bind to intracellular LPS [188] directly, and the

caspase-4/5/11-LPS complex has since been referred to as the noncanonical inflammasome. Although activated caspase-11 can induce pyroptosis by cleaving GSDMD [165, 166], it is unable to promote the maturation of pro-IL-1β and pro-IL-18 by direct interaction and must do so through the stimulation of the NLRP3-ASC-caspase-1 noncanonical pathway [201]. Although much focus has been centered on the presence of lipopolysaccharide (LPS) to stimulate caspase-11, saturated fatty acids [202] and lipid peroxidation [203] have been shown to trigger caspase-11 mediated pyroptosis *in vitro,* suggesting that LPS is not the only ligand needed for caspase-11 induction of pyroptosis. Studies have suggested that caspase-11 does have a role in the murine host defenses against *Aspergillus fumigatus* [204] and may have a role in the murine host defenses against influenza A viruses [177, 205, 206], the rabies virus [207], and MCMV [6].

1.9.4 Pyroptosis and Inflammasomes in Ocular Disease

The stimulation of pyroptosis-associated molecules is not limited to MAIDS-related MCMV retinitis and has been associated with the pathogenesis of several other ocular diseases and ailments. Of note are the recent discoveries centered on the extent to which inflammasomes and/or pyroptosis plays a role in several ocular disorders. Age-related macular degeneration (AMD) is a sight-threatening, progressive disorder of the retina that specifically targets and damages the macula, the part of the retina responsible for sharp, central vision. Recently, elevated levels of the NLRP3 inflammasome, IL-1β, and IL-18 expression were found in AMD macular lesions [208]. The destructive effects of AMD can also be seen by resultant RPE thinning or depigmentation, which can lead to RPE atrophy and death of photoreceptors. The NLRP3 inflammasome was found to be upregulated in the RPE during the pathogenesis of advanced AMD following RPE atrophy [209]. Inhibition of the NLRP3 inflammasome components prevented RPE degeneration in a model of AMD [210], providing evidence for

NLRP3-driven pyroptosis in the pathophysiology of AMD. Analysis of photoreceptor cell death in a model of retinal degeneration showed an upregulation of NLRP3, caspase-1, IL-1β, and IL-18 in cone photoreceptors but not rod photoreceptors [211], suggesting that the overall induction of pyroptosis in the retina may be unique to specific cell populations or influenced by the mechanism leading to cell death.

Additionally, an association between pyroptosis and oxidative stress has been established, which is one factor that leads to the formation of cataracts. Human lens epithelium cells that were treated with H_2O_2 showed in a significant increase of caspase-1 and IL-1β mRNA and protein expression when compared to the control cells. This involvement was ablated by the addition of a caspase-1 inhibitor, implicating the role of these molecules in cataract formation [212]. Another ocular disease manifestation of oxidative stress is the formation of proliferating fibrovascular tissue on the cornea of the eye, known as pterygium. NLRP3, caspase-1, IL-1β, and IL-18 were all expressed in human pterygium samples, as well as an experimental cell model of pterygium, suggesting the involvement of this pathway in the process of pterygium formation and progression [213]. Additionally, an experimental model of ocular hypertension, brought on by mechanical stress and hypoxia, demonstrated the activation of the NLRP1, NLRP3, and AIM2 inflammasome complexes, as well as caspase-1 activation and subsequent IL-1β release and formation of GSDMD pores. These results thus provide evidence for inflammasome-driven pyroptosis in retinas damaged by ocular hypertension [214].

Pyroptosis induction has also been demonstrated in experimental models of diabetic-related diseases. One study looking at diabetic retinopathy determined that exogenous addition of a high level of glucose resulted in increased expression of NLRP3, NLRP1, caspase-1, and IL-1β. Furthermore, the downregulation of host miR-590-3p boosted pyroptosis by targeting

NLRP1 and activating the NOX4 signaling pathway [215]. Another study investigated the association of pyroptosis in diabetic corneal endothelial keratopathy. Their studies demonstrated that the long noncoding RNA KCNQ1OT1, associated with diabetic complications, was triggered in diabetic human and rat corneal endothelium, while the expression of miR-214 was downregulated. Further investigation revealed that KCNQ1OT1 may bind miR-214 to regulate the expression of caspase-1. Additionally, pyroptosis was promoted with the suppression of miR-214 and suppressed with the silencing of KCNQ1OT1. Therefore, their results suggest that KCNQ1OT1-mediated pyroptosis is induced by high glucose via targeting of miR-214 [216]. Taken together, these results emphasize the involvement of pyroptosis in ocular complications of diabetes and provide potential targets responsible for this induction.

The overwhelming association of pyroptosis-associated molecules with ocular disease underscores the importance of understanding the mechanisms behind pyroptosis induction in the ocular microenvironment. The advancement of this knowledge is critical for the development of treatment strategies that may help prevent the onset of ocular disease rather than in response to symptoms of this damage. Investigating the role of pyroptosis in the retinal destruction seen during MAIDS-related MCMV retinitis will not only expand the knowledge of the pathogenesis of this disease but will also provide valuable insight into the advancement of ocular research.

1.10 Goals of this Dissertation

We have previously shown that the NLRP3, NLRP1b, NLRC4, and AIM2 inflammasome mRNA is stimulated in MCMV-infected eyes MAIDS-10 mice but not in MCMV-infected eyes of MAIDS-4 mice [93] as shown in Figure 1.17. Additionally, canonical pyroptosis-associated mRNA (caspase-1, IL-1β, and IL-18) are also stimulated in MCMV-infected eyes of MAIDS-10

but not in MAIDS-4 mice [6] (Figure 1.18), while the activated, cleaved, noncanonical caspase-11 proteins were also expressed in MCMV-infected eyes of MAIDS-10 mice [93] (Figure 1.19).

To advance our understanding of the ocular expression of inflammasome-driven pyroptosis in MAIDS-related MCMV retinitis, this study focused on the role that MCMV has on the induction of pyroptosis and explored the extent to which pyroptosis effects retinal damage during MCMV-retinitis. One important focus is on the degree that MCMV infection results in the stimulation of GSDMD. As GSDMD is considered the executioner of pyroptosis, it is imperative to determine the involvement of GSDMD in the pathogenesis of MAIDS-related MCMV retinitis prior to attempting to attribute the associated retinal destruction with the induction of pyroptosis. If pyroptosis is directly responsible for the destruction seen during MAIDS-related MCMV retinitis, then pyroptosis-associated molecules are not likely to be stimulated in MCMV-infected eyes of mice that are not susceptible to the development of MCMV retinitis. Furthermore, the expression of these pyroptosis-associated molecules would likely have to be stimulated in other models of immunosuppression that confer susceptibility to the development of MCMV retinitis. Ultimately, if the inflammasome and pyroptosis-associated molecules are necessary for the onset and progression of retinal destruction seen during MAIDS-related MCMV retinitis, then the loss or suppression of these genes should ultimately spare the retina from destruction following ocular infection of MCMV.

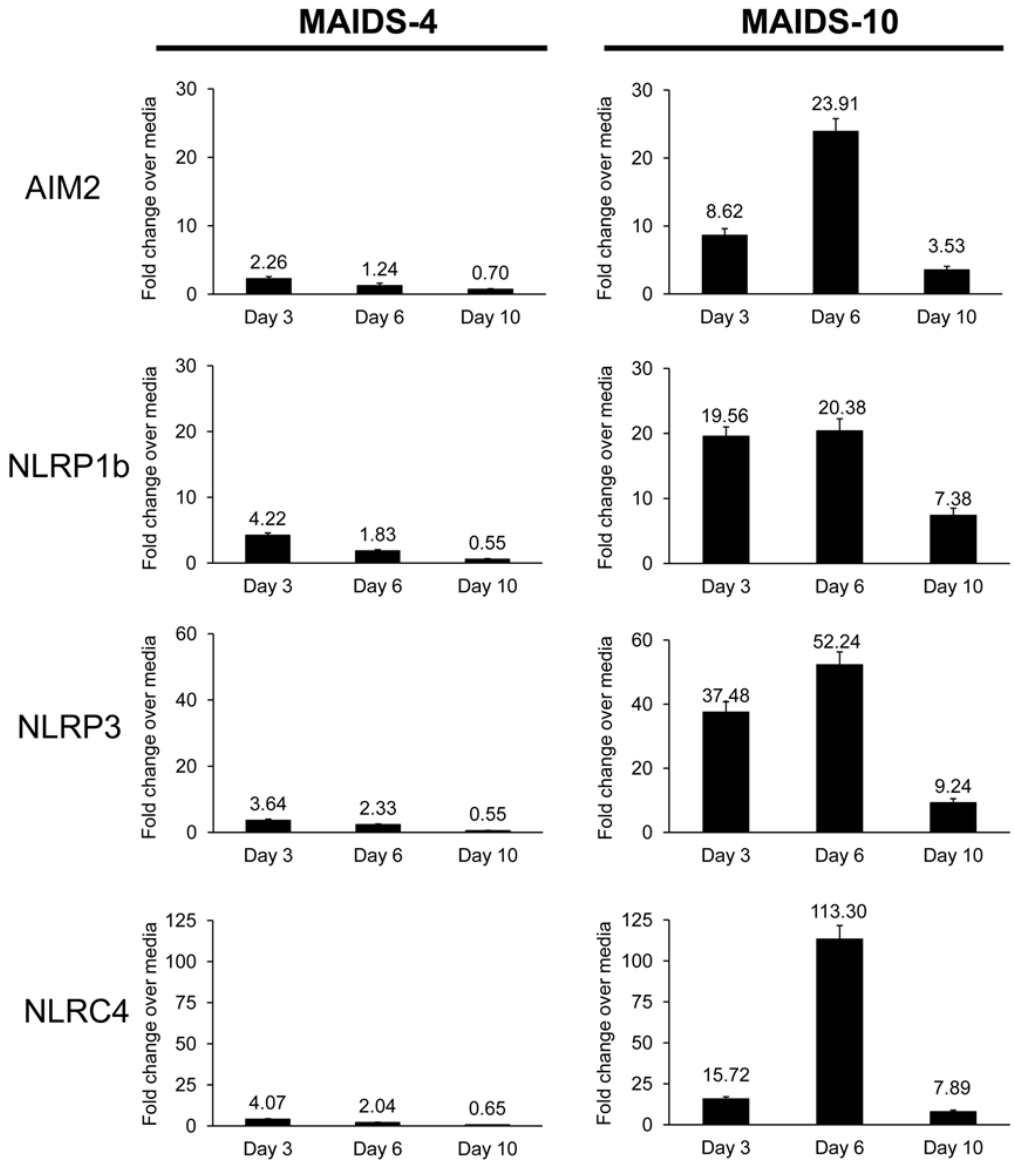

Figure 1.17. Intraocular inflammasome mRNA are highly stimulated in the MCMV-infected eyes of retinitis-susceptible MAIDS-10 mice, but not retinitis-resistant MAIDS-4 mice.

C57BL/6 mice with MAIDS-4 or MAIDS-10 were subretinally injected with 10^4 PFU of MCMV (left eye) or media (right eyes) and assessed for AIM2, NLRP1b, NLRP3, and NLRC4 inflammasome mRNA at 3, 6, and 10 days post-infection and depicted as a fold-change of MCMV infected eyes compared with media-injected control eyes. Adapted from [100]

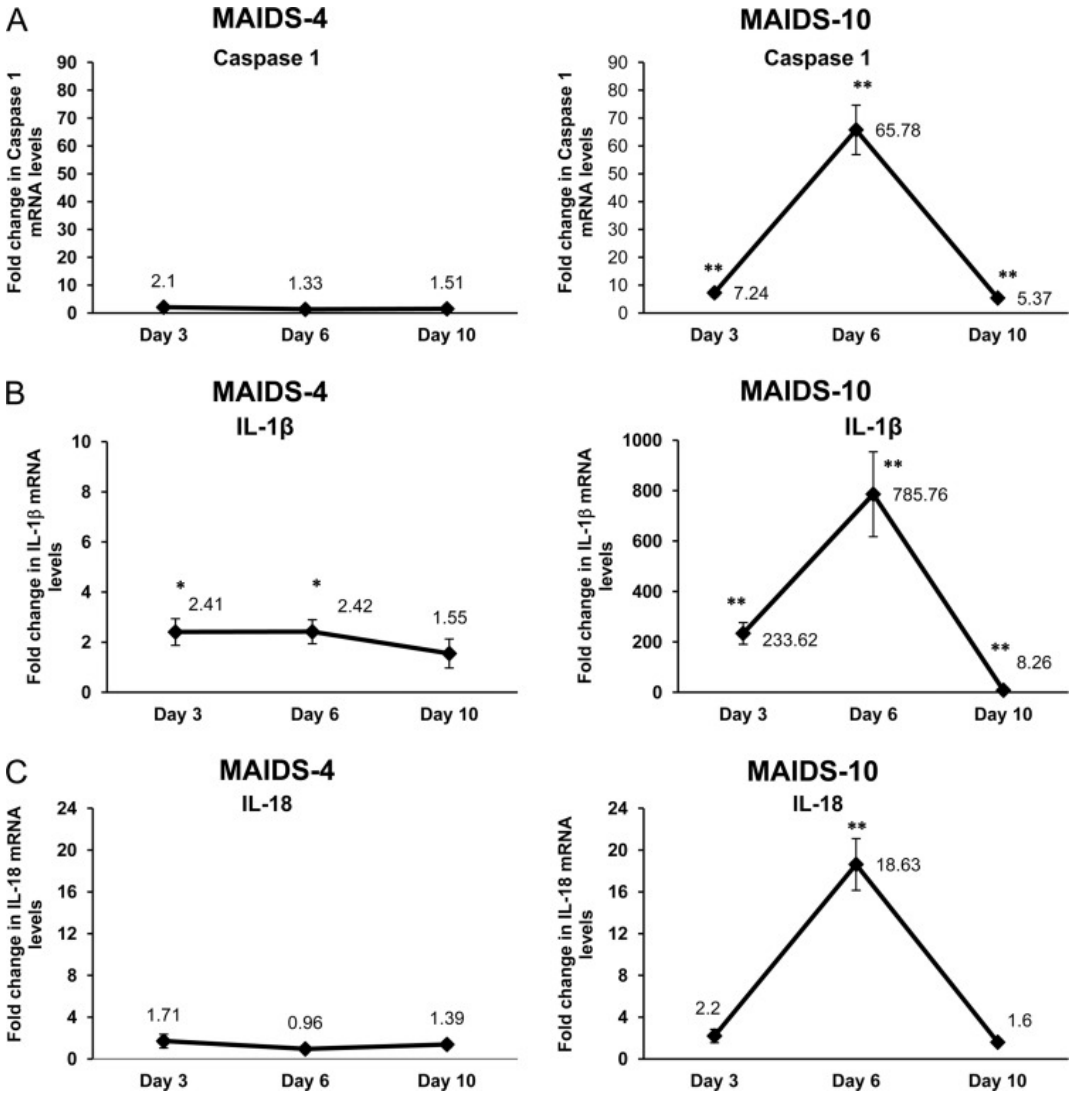

Figure 1.18. Intraocular pyroptosis-associated mRNA is highly stimulated in the MCMV-infected eyes of retinitis-susceptible MAIDS-10 mice, but not retinitis-resistant MAIDS-4 mice.

MCMV-infected eyes collected from groups of MAIDS-4 mice and MAIDS-10 mice at 3, 6, and 10 days after subretinal MCMV injection compared with mock-infected eyes. Levels (fold-change) of caspase-1 mRNA (A), IL-1β mRNA (B), and IL-18 mRNA (C) were determined by quantitative RT-PCR assay. Bars indicate standard errors (*, $P < 0.05$; **, $P < 0.001$). From [6]

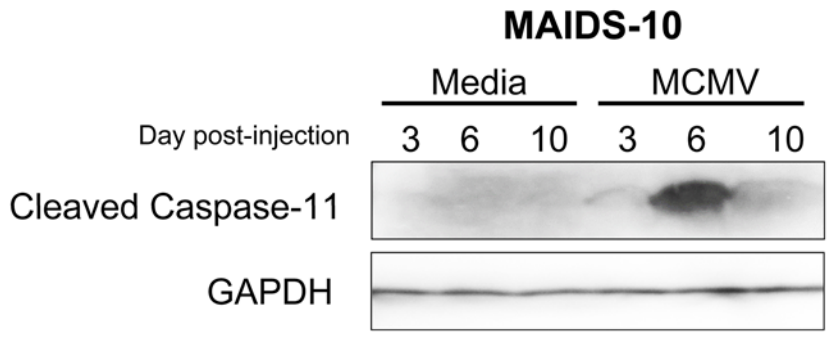

Figure 1.19. Figure 1.19: Intraocular cleaved caspase-11 protein is clearly abundant at day 6 post-infection in MCMV infected eyes of MAIDS-10 mice.

C57BL/6 mice with MAIDS-10 were subretinally injected with 10^4 PFU of MCMV (left eye) or media (right eyes) and assessed by western blot for cleaved caspase-11 protein at 3, 6, and 10 days post-infection. Adapted from [100]

Also, as whole eyes are being evaluated for the appearance of molecules connected with retinal destruction, it is possible that the stimulation of pyroptosis-associated molecules within the eye results from a multitude of stimuli following MCMV infection and may not be actually stimulated in the cells directly infected with MCMV. Therefore, it is crucial to determine whether or not CMV is capable of directly stimulating pyroptosis-associated molecules in infected cells and elucidating whether or not this stimulation requires viral replication.

As we have previously demonstrated that multiple facets of the immune response to infection are stimulated following subretinal injection of MCMV retinitis in MAIDS-10 mice [205], a multitude of factors may be interplaying with one another to contribute to the retinal destruction seen during MCMV retinitis. This, therefore, begs the question: What other factors are stimulated following MCMV infection of MAIDS-10 mice that may be contributing to the pathogenesis of MAIDS-related MCMV retinitis?

The central hypothesis that pyroptosis-associated molecules and associated inflammasomes contribute to the onset and progression of retinal damage during MAIDS-related MCMV retinitis was investigated by the use of three specific aims.

Specific Aim 1 will test the hypothesis that pyroptosis and associated inflammasomes are stimulated by MCMV during immunosuppression, contributing to the onset and development of MCMV retinitis. Pyroptosis-associated molecules, caspase-1, IL-1β, and IL-18, and inflammasomes NLRP3, NLRP1b, NLRC4, and AIM2 mRNA was significantly upregulated during experimental MAIDS-related MCMV retinitis but not in MAIDS-4 mice resistant to the development of MCMV retinitis [6] (Figure 1.18). As GSDMD is considered the executioner of pyroptosis, due to its ability to form pores resulting in the change in osmotic pressure and mass release of pro-inflammatory cytokines, we further support the notion that pyroptosis may be present during the onset of retinal destruction by determining whether GSDMD is stimulated following MCMV retinitis in MAIDS-10 mice. If pyroptosis is directly responsible for the destruction seen during MAIDS-related MCMV retinitis, then pyroptosis-associated molecules are not likely to be stimulated in MCMV-infected eyes of mice that are not susceptible to the development of MCMV retinitis. To deem the necessity of these pyroptosis-related molecules and associated inflammasomes for the development of CMV retinitis, we measured the frequency of retinitis in mice lacking one of the following genes: caspase-1, GSDMD, IL-18, IL-1R1, NLRP3, NLRP1b, and AIM2. If pyroptosis-related molecules and associated inflammasomes do play a role in the development of MCMV retinitis in mice with MAIDS, the expression of these pyroptosis-associated molecules would likely have to be stimulated in other models of immunosuppression that confer susceptibility to the development of MCMV retinitis, such as corticosteroid-induced immune suppression. Through the completion of these experiments, we will determine whether pyroptosis-related molecules and associated inflammasomes play a role in the development of MCMV retinitis is mice with immunosuppression.

Specific Aim 2 will test the hypothesis that MCMV replication directly stimulates pyroptosis in infected cells. Pyroptosis-related molecules were significantly upregulated in whole eyes infected with MCMV during experimental MAIDS-related MCMV retinitis [6] (Figure 1.18). As pyroptosis can be signaled by both PAMPs and DAMPs, it is uncertain if the stimulation of these pyroptosis-associated molecules during the pathogenesis of MAIDS-related MCMV retinitis is in direct response to MCMV replication in the cells or brought on indirectly by the host response to viral infection. To determine whether pyroptosis is directly stimulated by infection of cells by CMV, the stimulation of pyroptosis-associated molecules in response to MCMV replication was measured in IC-21 mouse macrophages and mouse embryonic fibroblasts (MEFs). HCMV-induced stimulation of pyroptosis-related molecules was measured in HCMV-infected ARPE-19 cells and MRC-5 fibroblasts. To determine the viral mechanisms responsible for any observed stimulation in infected cells, monolayers were infected with UV-inactived CMV. UV treatment damages the CMV genome preventing viral replication but allows for attachment and adsorption of the viral to host cells and the subsequent release of tegument proteins.

Specific Aim 3 will test the hypothesis that other immune response genes or pathways are stimulated during the pathogenesis of MAIDS-related MCMV retinitis.

Previous studies by us has demonstrated the involvement of several cell death pathways and cytokine signaling during MAIDS-related MCMV-retinitis. To determine what other factors might be involved during the onset and development of retinitis we looked at the stimulation of multiple additional immune response pathways between MAIDS-4 and MAIDS-10 mice. If pertinent, these findings could help shape the future focus of our investigation on the mechanisms underlying the pathogenesis of MAIDS-related MCMV retinitis.

2 MATERIALS AND METHODS

2.1 Cell Lines and Stocks

C57BL/6 MEF cells obtained from ATCC (Manassas, VA, No. SCRC-1002) were grown in Dulbecco's modified eagle medium (DMEM) supplemented with 15% fetal bovine serum (FBS), 4 mM L-glutamine, 1% penicillin/streptomycin, 0.1 mg/mL gentamicin, and 1.5 g/L sodium bicarbonate and maintained according to ATCC recommendations. These cells were used for titration of MCMV stocks and in some experiments.

IC-21 mouse macrophages (ATCC, Manassas, VA, No. TIB-186) were maintained according to ATCC recommendations and sustained in RPMI-1640 medium supplemented with 10% FBS, 1% penicillin/streptomycin, and 0.1 mg/mL gentamicin. This cell line was transformed with a simian virus 40 (SV40) [217] and is commonly used in cell culture studies with MCMV infection [32, 218-221].

MRC-5 (human fetal lung fibroblast obtained from ATCC, Manassas, VA, No. CCL-171) cells were cultured according to ATCC recommendations and in DMEM supplemented with 10% FBS, 4 mM L-glutamine, 1% penicillin/streptomycin, 0.1 mg/mL gentamicin, and 1.5 g/L sodium bicarbonate.

Human retinal pigmented epithelial cells, ARPE-19 (ATCC, Manassas, VA, No. CRL-2302), were grown in DMEM: F12 containing 10% FBS, 1% penicillin/streptomycin, and 0.1 mg/mL gentamicin and cultured as recommended by ATCC.

SC-1 fibroblasts (ATCC, Manassas, VA, No. CRL-1404) and SC-1/MuLV LP-BM5 cells [106] provided by the AIDS Research and Reference Reagent Program, Division of AIDS, NIAID, NIH (Germantown, MD) and were maintained in DMEM containing 10% FBS, 24 mM

L-glutamine, 1% penicillin/streptomycin, and 0.1 mg/mL gentamicin. These cell lines were used for propagation of the mouse retrovirus mixture used to induce MAIDS.

2.2 Viral Stocks

Propagation of CMV. MCMV (Smith) stocks were propagated via passage through salivary glands of adult female BALB/c mice (Harlan Laboratories, USA) as previously described [4, 222, 223]. The use of these BALB/c mice was conducted with the approval of the Georgia State University Institutional Animal Care and Use Committee (IACUC) and in compliance with the Association for Research in Vision and Ophthalmology (ARVO) statement for Use of Animals in Ophthalmic and Vision Research. The Towne strain of HCMV was propagated through (MRC-5) cells acquired from the American Type Culture Collection (ATCC, Manassas, VA, No. CCL-171). Stocks of viruses were centrifuged to remove cellular debris and frozen in liquid nitrogen. Viral titers for the MCMV and HCMV stocks were quantified by standard plaque assay in C57BL/6 MEFs and MRC-5, respectively.

Propagation of mouse retrovirus mixture for MAIDS induction. Stocks of murine retrovirus (LP-BM5 murine leukemia virus [MuLV]) were prepared in SC-1 fibroblasts and SC-1/MuLV LP-BM5 cells [106] provided by the AIDS Research and Reference Reagent Program, Division of AIDS, NIAID, NIH (Germantown, MD). To prepare each stock, the two cell lines were seeded in a 1:1 ratio and maintained for six days. The cells were then scraped into a complete SC-1 medium and stored at -80°C. Aliquots of stocks were thawed and clarified by centrifugation prior to each use.

UV-inactivation of MCMV. For experiments utilizing UV-inactivation of the virus, a portion of MCMV from the same stock of each experiment was exposed to DNA-damaging UV light (UVi-MCMV) [224]. UV-inactivation was achieved by placing approximately 1 mL of the

virus stock in an uncovered dish on ice approximately 5-cm from the UV light for three hours [99]. Aliquots of UVi-MCMV were titered to ensure complete inactivation.

2.3 Animals

Adult female BALB/c mice, used for MCMV propagation, were purchased from Harlan Laboratories (Indianapolis, IN, USA). Wild-type female C57BL/6 mice used for experiments were purchased from Jackson Laboratory (Bar Harbor, ME, USA). All mice were housed in the Georgia State University vivarium with 12-hr light/dark cycles with unrestricted access to standard diet and water. All animal procedures were conducted in compliance with Georgia State University IACUC protocols and with the ARVO statement for Use of Animals in Ophthalmic and Vision Research.

Induction of MAIDS. MAIDS was induced in WT C57BL/6 mice and in various groups of knockout mice (B6.129S6-*Nlrp3* ^{tm1Bhk}/J, B6.129S6-*Nlrp1b* ^{tm1Bhk}/J, and B6.129P2-Aim2$^{Gt(CSG445)\ Byg}$/J, B6N.129S2-Casp 1^{tm1Flv}/J, B6.129S7-Il1r1^{tm1Imx}/J, B6.129P2-Il18^{tm1Aki}/J, and C57BL/6J-Gsdmd^{em1Vnce}/J) by intraperitoneal injection of 1.0 ml of inoculum containing approximately 5×10^3 infectious LP-BM5 murine leukemia retrovirus. The retrovirus mixture was allowed to progress to MAIDS-4 or to MAIDS-10.

Corticosteroid-induced Immunosuppression. For the corticosteroid-induced immunosuppression experiments, corticosteroid-induced immunosuppression was established in adult female C57BL/6 mice, as previously described [109, 225, 226] via intramuscular injection of methylprednisolone acetate (2mg/mouse, ~40 mg/kg) every three days starting two days prior to MCMV infection. All mice were age matched to groups of female adult mice, immunosuppressed for MAIDS.

Subretinal MCMV Injections. Prior to subretinal injections of MCMV, all groups of mice eyes were first dilated with atropine and tropicamide eye drops. Mice were then anesthetized by intramuscular injection of 0.1 mL xylazine (1.72 mg/mL) and 0.1 mL acepromazine (0.28 mg/mL), followed by intraperitoneal injection of 0.1–0.2 mL ketamine (8.58 mg/mL). Once mice were confirmed to be under deep anesthesia, both eyes were injected with 2 µL of DMEM containing approximately 10^4 plaque-forming units (PFU) of MCMV. Three, six, or ten days following infection, mice were anesthetized with isoflurane, euthanized, and whole eyes were harvested. The eyes were either frozen in liquid nitrogen for protein analysis and quantification of ocular MCMV or stored in a 10% buffered formalin solution for histology.

2.4 Quantification of Infectious MCMV

Infectious MCMV was quantified in each eye by individually homogenizing the MCMV-infected eyes in a 2 mL Tenbroeck tissue grinder (Wheaton, Millville, NJ) with 1 mL phosphate-buffered saline (PBS). The virus was clarified from the tissue by centrifugation. The resultant aliquots underwent a freeze-thaw cycle and were then serially diluted and inoculated onto monolayers of ~90% confluency MEFs in duplicate. After a 1-hour incubation at 37°C, infected wells were then overlaid with 2% methylcellulose in DMEM and incubated for another six days. Individual plaques were counted with an inverted light microscope, and MCMV titers for whole eyes were reported as PFU/mL/eye.

2.5 Histology

The frequency of retinitis in all mice (n = >3) was measured after euthanizing and harvesting eyes ten days post-MCMV infection. Harvested eyes were stored at 4°C for at least five days in a 10% buffered formalin solution. After fixation, eyes were then embedded in paraffin, cut into 5-µm-thick transverse sections, and stained with hematoxylin and eosin by the

Pathology Department of the Emory Eye Center. Every sixth section of each eye was evaluated under light microscopy for the presence or absence of retinitis

2.6 Western Blot Analysis

MCMV-infected eyes frozen in liquid nitrogen were thawed and homogenized in PBS containing a protease inhibitor cocktail (Sigma, St. Louis, MO). Samples were subjected to sodium dodecyl sulfate (SDS) polyacrylamide gel electrophoresis (SDS-PAGE) and transferred to a 0.2-μm-pore polyvinylidene fluoride membrane blocked in 5% bovine serum albumin. Target proteins were completed using rabbit anti-mouse IL-1β antibody (1:250) (Abcam, Toronto, ON), rabbit anti-mouse IL-18 antibody (1:250) (Abcam), rabbit anti-mouse GSDMD (1:500) (Abcam), rabbit anti-mouse caspase-1 (1:500) (Abcam), rabbit anti-mouse caspase-11 (1:500) (Abcam), rabbit anti-mouse RIPK1 (1:500), rabbit anti-mouse RIPK3 (1:500), rabbit anti-mouse MLKL (1:500), rabbit anti-mouse TNFα (1:1000), rabbit anti-mouse beclin-1 (1:1000), rabbit anti-mouse LC3B (1:1000), rabbit anti-mouse GAPDH antibody (1:1,000) (Abcam), or rabbit anti-mouse β-actin antibody (1:1,000) (Abcam) as primary antibodies. Goat anti-rabbit IgG antibody (heavy plus light chains [H+L]) conjugated with horseradish peroxidase (Thermo Scientific, Pittsburgh, PA) was chosen as a secondary antibody (1:5,000). Probed nitrocellulose membranes (Bio-Rad, Hercules, CA) were treated with Clarity Western ECL Substrate (Biorad) and exposed to HyBlot film (Denville, Holliston, MA) for band detection.

2.7 Immunofluorescence Staining

Immunofluorescence (IF) staining was performed in MEFs grown in 24-well dishes infected with 0.5 mL per well of either MCMV (multiplicity of infection (MOI) = 3 PFU/cell), UVi-MCMV from the same stock, or control medium. At 6 and 24 hpi, wells were fixed in ice-cold methanol, blocked in 5% bovine serum albumin, and probed for rabbit-anti-mouse caspase-1, IL-

1β, IL-18, gasdermin D primary antibodies (Santa Cruz Biotechnology, Inc., Dallas, TX). Goat-anti-rabbit IgG Fab' fragment antibody conjugated with FITC (green) (Jackson ImmunoResearch, West Grove, PA) was used as the secondary antibody. Cell nuclei were counterstained with 4', 6-diamidino-2-phenylindole (DAPI) in Vectashield® mounting solution (Vector Laboratories, Burlingame, CA). Cells were then observed using a Keyence microscope.

2.8 RNA Extraction and Real-Time RT PCR

RNA extraction from tissue samples. Whole MCMV-infected eyes and mock infected eyes were collected at the indicated time points following subretinal injection and stored at 4°C in RNAlater solution (Ambion, Austin, TX). Following collection at all time points, eyes were then individually homogenized in 1mL of TRIzol® reagent (Invitrogen Life Technologies, Carlsbad, CA) using a 2-ml Ten Broeck tissue grinder (Wheaton, Millville, NJ). Total RNA was extracted in chloroform and purified using the PureLink® RNA Mini Kit according to the manufacturer's instructions (Ambion/ThermoFisher). RNA concentrations were determined using a Nanodrop™ 2000 spectrophotometer (Thermo Scientific, Pittsburgh, PA) and normalized for each sample.

RNA extraction from cell monolayers. Monolayers of cells were harvested at indicated time points in TRIzol® reagent (Ambion/ThermoFisher Scientific, Waltham, MA, USA) at indicated time points. Total RNA was extracted with chloroform and purified over PureLink® RNA Mini Kit spin cartridge filters according to the manufacturer's instructions (Ambion/ThermoFisher). RNA concentrations were determined using a Nanodrop 2000 spectrophotometer (Thermo Scientific, Pittsburgh, PA) and normalized for each sample.

Real-Time Reverse Transcriptase Polymerase Chain Reaction (RT-PCR). The RNA for all sample types was then reverse-transcribed into cDNA using SuperScript™ III First-Strand

Synthesis Kit reagents according to the manufacturer's instructions (Invitrogen/ThermoFisher). Detection and quantification of target gene expression were performed via real-time RT-PCR using Applied Biosystems 7500 Fast Real-Time PCR System hardware and software in conjunction with Power SYBR Green Master Mix (Applied Biosystems, Foster City, CA). Mouse-specific primers for caspase-1, caspase-11, IL-1β, IL-18, GSDMD, NLRP3, NLRP1b, NLRC4, AIM2, and GAPDH were obtained from QIAgen (Valencia, CA). Samples were run under the following thermocycling parameters: 10 min at 95°C followed by 40 cycles consisting of 15 seconds at 94°C, 31 seconds at 55°C, and 35 seconds at 70°C. Cycles to the threshold (CT) for each target gene were determined, and the ΔCT value for each sample was normalized by subtracting the CT value of their own endogenous housekeeping gene (GAPDH) from the CT value of the target gene. The ΔCT values of each target gene mRNA of MCMV-infected eyes were compared with mock infected control eyes by the 2-ΔΔCt method to determine the change in gene expression, yielding a relative fold-change in mRNA expression for each group. Data points represent mean fold-changes ± standard deviations (SD) of at least duplicate experimental repeats.

2.9 NanoString Analysis

Whole MCMV-infected eyes and mock infected eyes were collected at indicated time points and stored at 4°C in RNAlater solution (Ambion, Austin, TX). Eyes were then homogenized in 1 mL of TRIzol® reagent (Invitrogen Life Technologies, Carlsbad, CA) using a 2-ml Ten Broeck tissue grinder (Wheaton, Millville, NJ). Total RNA was extracted in chloroform and purified using the PureLink® RNA Mini Kit according to the manufacturer's instructions (Ambion/ThermoFisher). The extracted RNA from each group and respective time points were pooled together, and the RNA concentrations were determined using a Nanodrop

2000 spectrophotometer (Thermo Scientific, Pittsburgh, PA). Approximately 100 ng of the purified total RNA was hybridized to a reporter and capture probe prior to being added to the NanoString panels for analysis of raw RNA counts. The nCounter® murine immunology panel designed by NanoString Technology (Nanostring, Seattle, WA, USA) was used to analyze the expression of 561 genes, including several internal references and housekeeping genes. A custom-made panel including 30 genes of interest and 3 housekeeping genes was also loaded to explore the expression of RNA associated with several genes not specific to the murine nCounter® Immunology Panel. All data were analyzed using the NanoString nSolver™ 4.0 software (Nanostring, Seattle, WA, USA).

2.10 Statistical Analyses

All statistical analyses were performed with a significance level (α) set to 0.05. P-values of < 0.05 were considered statistically significant and were denoted by asterisks in figures where appropriate: * $p<0.05$, ** $p<0.01$, and *** $p<0.001$. Statistical tests were performed as appropriate for each study as specified below.

Statistical analysis for *in vivo* studies. All quantitative data obtained from real-time RT-PCR were performed with a significance level (α) set to 0.05 so that p-values of <0.05 were considered statistically significant and expressed as means ± SD. At least two independent experiments were performed for each study. Statistical analysis was performed by comparing MCMV-infected eyes with mock infected control eyes by paired, two-tailed Student's *t*-test.

Statistical analysis for *in vitro* studies. Statistical analysis was performed using GraphPad Prism® v8.2.1 software with a significance level (α) set to 0.05, so that p-values of <0.05 were considered statistically significant. Experimental groups were compared with

respective control groups at the same time points using a two-way analysis of variance (ANOVA) with Bonferroni posthoc analysis.

Statistical analysis for ocular titers. All quantitative data obtained for ocular titers were performed with a significance level (α) set to 0.05 so that p-values of <0.05 were considered statistically significant and expressed as means ± SD. At least two independent experiments were performed for each study. Statistical analysis was performed by comparing MCMV-infected eyes of WT MAIDS-10 mice to each knockout MAIDS-10 mouse by unpaired, two-tailed Student's *t*-test.

Statistical analysis for NanoString studies. Two independent experiments were performed for each study and ran independently through the NanoString software. Any p-values obtained were done on fold-changes of raw RNA counts as determined by the NanoString nSolver™ software and performed with a significance level (α) set to 0.05 so that p-values of <0.05 were considered statistically significant. Statistical analysis was performed by comparing MCMV-infected eyes with mock infected control eyes by unpaired, two-tailed Student *t*-test, and values were expressed as means ± SD.

3 SPECIFIC AIM 1

Specific Aim 1: Test the Hypothesis That Pyroptosis and Associated Inflammasomes are Stimulated by MCMV during Immunosuppression, Contributing to the Onset and Development of MCMV Retinitis

3.1 GSDMD and Caspase-11 Expression during MAIDS-related MCMV Retinitis

Expression and translation of GSDMD during MAIDS-related MCMV retinitis. We reported previously that MCMV-infected eyes of MAIDS-10 mice show high stimulation of mRNA expression of pyroptosis-associated molecules, caspase-1, IL-1β, and IL-18, collectively peaking 6 days following subretinal MCMV inoculation. To further confirm a role for pyroptosis in the pathogenesis of MAIDS-related MCMV retinitis, we assessed whether protein and/or mRNA of the pore-forming molecule, GSDMD, increased following ocular MCMV infection in MAIDS-10 mice. We found that MCMV-infected eyes of MAIDS-10 mice showed upregulation of both GSDMD mRNA transcripts (Fig. 3.1A) and protein (Fig. 3.1B). However, unlike caspase-1, IL-1β, and IL-18 mRNA transcripts that showed a peak upregulation at 6 days post-infection, GSDMD mRNA appeared to be consistently upregulated days 3, 6, and 10 following MCMV inoculation. Protein levels for full-length GSDMD were robustly increased in MCMV-infected eyes when compared to the media control eyes at all days post-infection while a substantial stimulation of cleaved GSDMD protein was seen at 10 days post-infection.

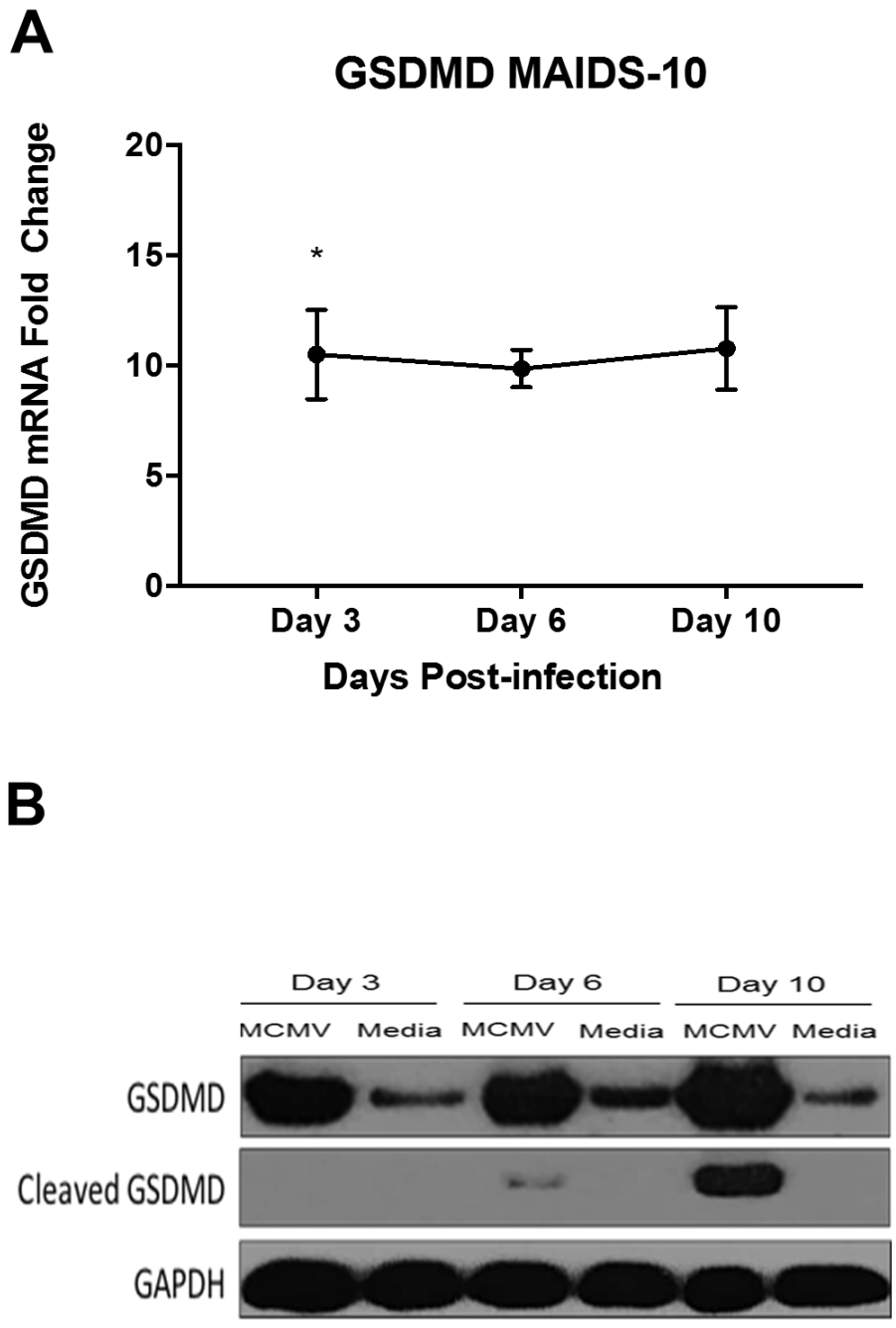

Figure 3.1. Intraocular GSDMD mRNA and protein expression were highly expressed in the MCMV infected eyes of retinitis-susceptible MAIDS-10 mice.

Whole eyes were collected at 3, 6, and 10 days following subretinal injection of MCMV (left eyes) or media control (right eyes) from groups (n=3-5) of MAIDS-10 mice. Homogenized eyes were assessed for GSDMD mRNA (A) or protein expression, with GAPDH used as a loading control. *$p<0.05$, MCMV groups compared with media group at the same time point.

Expression and translation of caspase-11 during MAIDS-related MCMV retinitis.

We previously saw that protein levels of cleaved caspase-11 was also significantly stimulated at 6 days following MCMV injection of MAIDS-10 mice [6]. Since we have not previously characterized the expression of caspase-11 mRNA, we assessed whether this was also stimulated during the onset and progression of MAIDS-related MCMV retinitis. Like GSDMD, mRNA levels of caspase-11 (Fig. 3.2A) were also stimulated in MCMV-infected eyes of MAIDS-10 consistently at days 3, 6, and 10, following ocular MCMV infection. Assessing levels of the zymogen version of caspase-11 revealed that procaspase-11 protein was also stimulated at days 3 and 6 post-MCMV infection (Fig.3.2B). The locus of caspase-11 has been shown to encode two polypeptides of 43 and 38 kDa [227] in which the p20 cleavage product of procaspase-11 appears to be derived from the 43 kDa species [228]. Interestingly, at day 3 post-infection, the 43 kDa band of procaspase-11 was highly expressed, while the 38 kDa band was more highly expressed at day 6 post-infection. Taken together, these results suggest that MCMV stimulates both GSDMD and caspase-11 mRNA and protein following ocular infection of MCMV in MAIDS-10 mice.

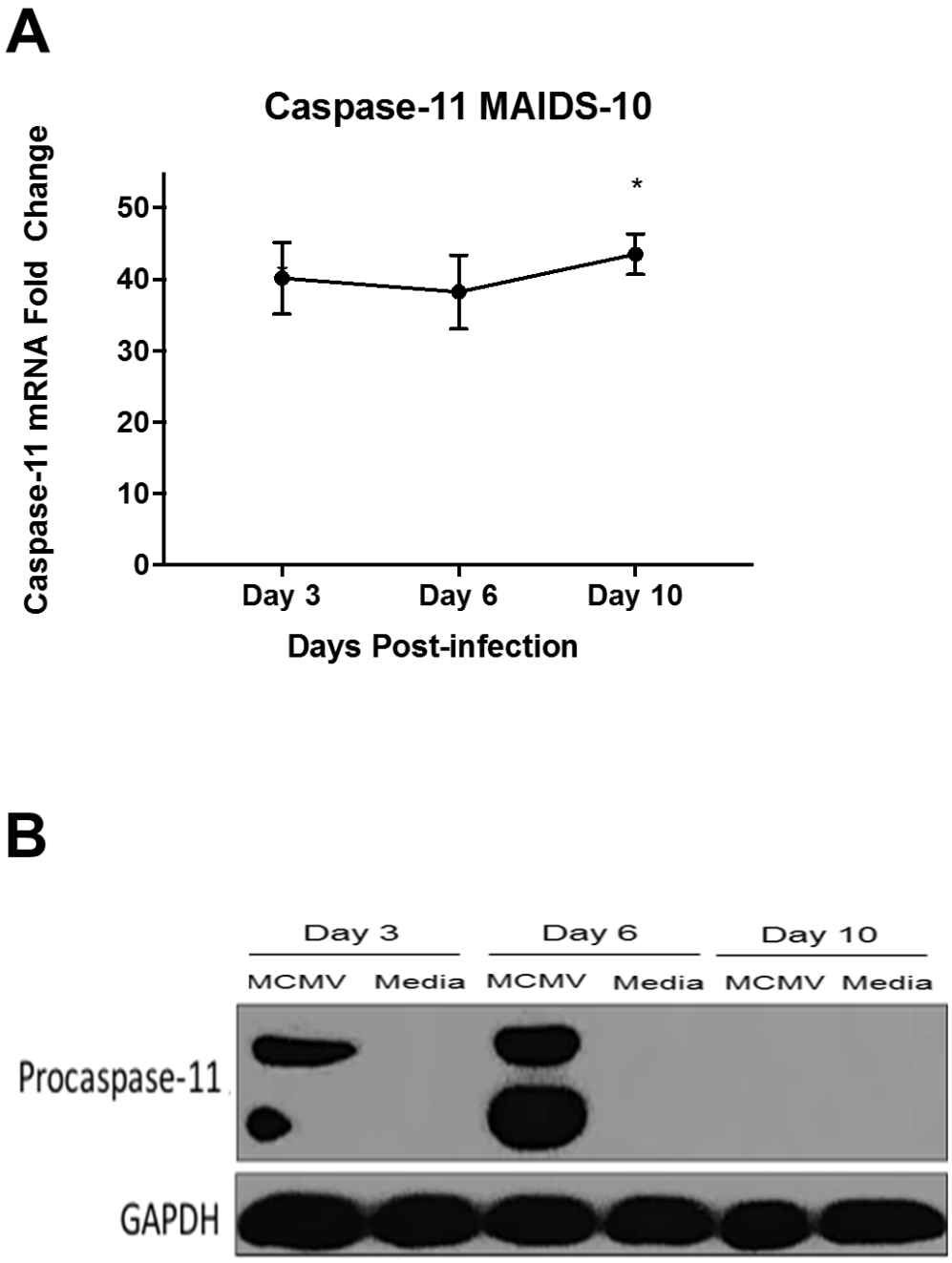

Figure 3.2. Intraocular caspase-11 mRNA and protein expression were highly stimulated in the MCMV infected eyes of retinitis-susceptible MAIDS-10 mice.

Whole eyes were collected at 3, 6, and 10 days following subretinal injection of MCMV (left eyes) or media control (right eyes) from groups (n=3-5) of MAIDS-10 mice. Homogenized eyes were assessed for caspase-11 mRNA (A) or protein expression, with GAPDH used as a loading control. *$p<0.05$, MCMV groups compared with media group at the same time point.

3.2 GSDMD and Caspase-11 Expression Following MCMV Infection in MAIDS-4 Mice

Expression and translation of GSDMD following MCMV infection of retinitis resistant MAIDS-4 mice. We reported previously that MCMV-infected eyes of MAIDS-10 but not MAIDS-4 mice showed mRNA expression of pyroptosis-associated molecules, caspase-1, IL-1β, and IL-18. To determine if GSDMD expression follows this pattern, we assessed whether the mRNA and/or protein of GSDMD was expressed following ocular infection of MCMV in retinitis resistant MAIDS-4 mice. Interestingly, expression of GSDMD during MCMV infection of MAIDS-4 eyes showed a substantial increase in fold-change of mRNA when compared to the mock infected control eyes at each time point during viral infection (Fig.3.3A). The pattern of mRNA production of GSDMD at MAIDS-4 was different from that at MAIDS-10 (Fig. 3.3B). MAIDS-4 mice showed a peak in mRNA production at day 6 post-infection that reached the relative level seen in MAIDS-10 infected eyes. Both at days 3 and 10 post-infection, however, there was less GSDMD transcript production than the corresponding days of MAIDS-10 MCMV-infected eyes. The pattern of protein expression for full-length GSDMD protein was similar at MAIDS-4 as it was at MAIDS-10, in which the protein was stimulated in MCMV-infected eyes at all days post-infection with higher expression at day 6 post-infection (Fig. 3.3C). Interestingly, cleaved GSDMD protein was expressed only at day 6 post-infection in MCMV-infected eyes of mice with MAIDS-4 while MAIDS-10 mice showed expression only at day 10 post-infection, which correlates with the presence of retinitis.

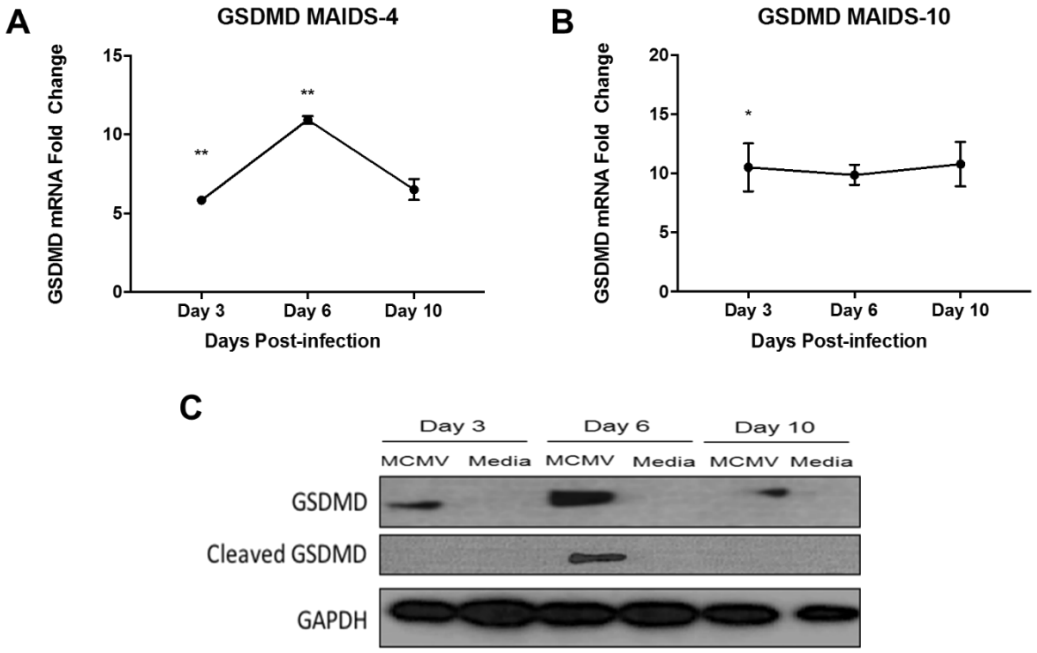

Figure 3.3. Intraocular GSDMD mRNA and protein were stimulated in MCMV infected eyes of both retinitis susceptible MAIDS-10 mice and retinitis-resistant MAIDS-4 mice.

Whole eyes were collected at 3, 6, and 10 days post-infection (dpi) and from MCMV infected eyes and media control eyes from groups (n=3-5) of MAIDS-4 and MAIDS-10 mice. Homogenized eyes were assessed for GSDMD mRNA from the MAIDS-4 mice (A) and the MAIDS-10 mice (B). Western blot analysis (C) was performed to assess ocular GSDMD protein expression in MAIDS-4 mice with GAPDH used as a loading control. *$p<0.05$ and **$p<0.01$, MCMV groups compared with media control at the same time points.

Expression and translation of caspase-11 following MCMV infection of retinitis resistant MAIDS-4 mice. We previously saw that protein levels of cleaved caspase-11 were also significantly stimulated at 6 days following MCMV injection of MAIDS-10 mice [6]. Since we had not previously characterized the expression of caspase-11 mRNA during MAIDS-4, we assessed whether caspase-11 mRNA was also stimulated in MAIDS-4 mice resistant to MCMV retinitis. Like GSDMD, mRNA levels of caspase-11 was stimulated in MCMV-infected eyes of both MAIDS-4 (Fig. 3.4A) and MAIDS-10 (Fig. 3.4B) mice. mRNA expression in MAIDS-4 mice, however, exhibited an initially high upregulation at day 3 post-infection which resulted in

an almost linear decrease in production continuing through 6- and 10-days post-infection. Similar to the protein levels seen at MAIDS-10, procaspase-11 protein levels showed a stimulation at day 6 post-infection in MCMV-infected eyes of MAIDS-4 mice, which decreased by day 10 post-infection, whereas media-injected eyes did not stimulate caspase-11 protein production at any days post-infection (Fig. 3.4C). However, unlike MCMV-infected eyes of MAIDS-10 mice, procaspase-11 protein was not expressed 3 days post-infection in MCMV-infected eyes of MAIDS-4 mice. Taken together, these results suggest that MCMV stimulates both GSDMD and caspase-11 following ocular infection in both retinitis susceptible MAIDS-10 mice and retinitis resistant MAIDS-4 mice.

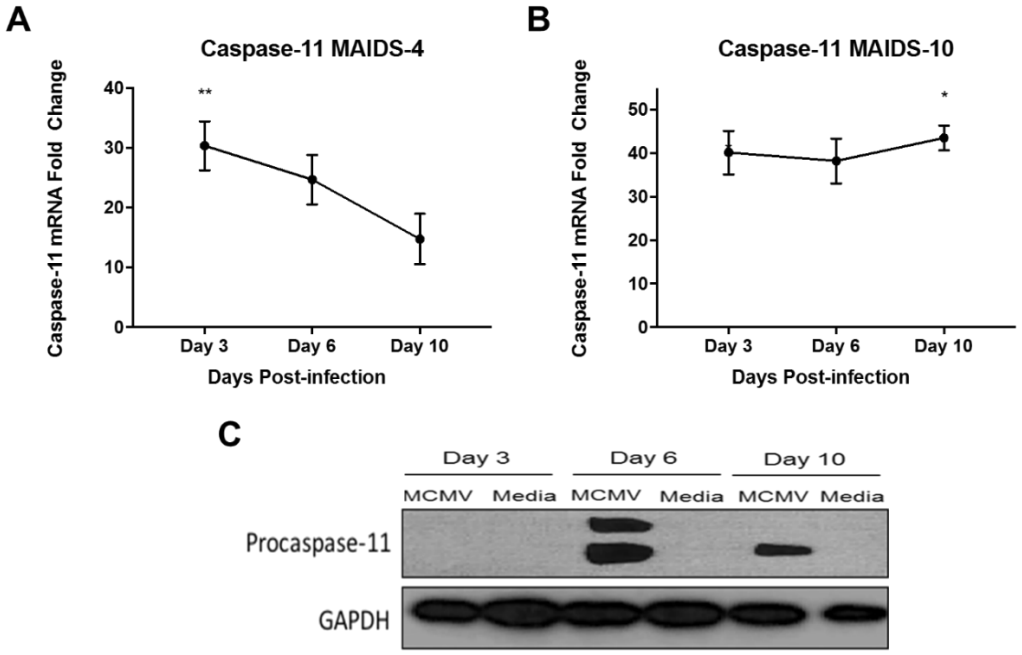

Figure 3.4. Intraocular caspase-11 mRNA and protein were stimulated in MCMV infected eyes of both retinitis susceptible MAIDS-10 mice and retinitis-resistant MAIDS-4 mice.

Whole eyes were collected at 3, 6, and 10 days post-infection (dpi) and from MCMV infected eyes and media control eyes from groups (n=3-5) of MAIDS-4 and MAIDS-10 mice. Homogenized eyes were assessed for caspase-11 mRNA from the MAIDS-4 mice (A) and the MAIDS-10 mice (B). Western blot analysis (C) was performed to assess ocular procaspase-11 protein expression in MAIDS-4 mice with GAPDH used as a loading control. *$p<0.05$ and **$p<0.01$, MCMV groups compared with media control at the same time points.

3.3 Effect of the Loss of the Pyroptosis Pathway or Associated Inflammasomes on the Development of MAIDS-related MCMV Retinitis

3.3.1 The Loss of the Pyroptosis Pathway and MAIDS-related MCMV Retinitis

We have previously reported that mRNA for caspase-1, IL-1β, and IL-18 are stimulated during the onset and development of MAIDS-related MCMV retinitis [6]. To continue our investigations on the involvement of pyroptosis-associated proteins in the retinal destruction seen during this disease, we employed several mice knocked-out of either caspase-1, GSDMD, IL-1R1, or IL-18 to determine the necessity of these proteins in the development of retinitis.

MCMV-infected eyes of caspase-1 KO mice with MAIDS, GSDMD KO mice with MAIDS, IL-1R1 KO mice with MAIDS, and IL-18 KO mice MAIDS show patterns of protein synthesis that are relatively similar to those of MCMV-infected eyes of wildtype mice with MAIDS. We next embarked on a comprehensive investigation of MCMV retinitis pathogenesis using mice with MAIDS that were deficient in one of four pyroptosis-associated genes to define with greater precision the contribution of pyroptosis toward the onset and progression of MAIDS-related MCMV retinitis. This investigation included a gene deficiency in the production of either caspase-1, GSDMD, IL-1R1, or IL-18. All caspase-1 KO mice**,** GSDMD KO mice, IL-1R1 KO mice, and IL-18 KO mice infected with the immunosuppressive murine retrovirus mixture (LP-BM5 MuLV) developed MAIDS as assessed by their development of a number of MAIDS-related physical and immunologic characteristics (data not shown) described by us previously [100].

Prior to assessing possible virologic, pathogenic, and histopathologic differences during the development of MCMV retinitis among MAIDS mice with a pyroptosis-associated gene deficiency when compared with the development of MCMV retinitis in wildtype MAIDS

mice, we investigated the patterns of pyroptosis-associated proteins of the canonical and noncanonical pyroptosis pathways for possible alterations in their pattern of synthesis with particular attention given to cleavage events. Western blot analysis of MCMV-infected eyes collected from caspase-1KO mice with MAIDS**,** GSDMD KO mice with MAIDS, IL-1R1 KO mice with MAIDS, and IL-18 KO mice with MAIDS at 10 days after subretinal MCMV inoculation showed relatively similar patterns of protein production for corresponding proteins associated with the canonical and noncanonical pyroptosis pathways when compared with the patterns of protein production collected from MCMV-infected eyes of wildtype MAIDS mice (Fig. 3.5). Some notable exceptions were observed, however. A deficiency in either capsase-1 production during MAIDS or IL-1R1 production during MAIDS resulted in an absence of cleaved caspase-11 of the noncanonical pyroptosis pathway despite evidence for pro-caspase-11 production (Fig 3.5A and 3.5C). Similarly, a deficiency in IL-1R1 production during MAIDS also resulted in a marked decrease in cleaved GSDMD protein of the canonical pyroptosis pathway (Fig 3.5B).

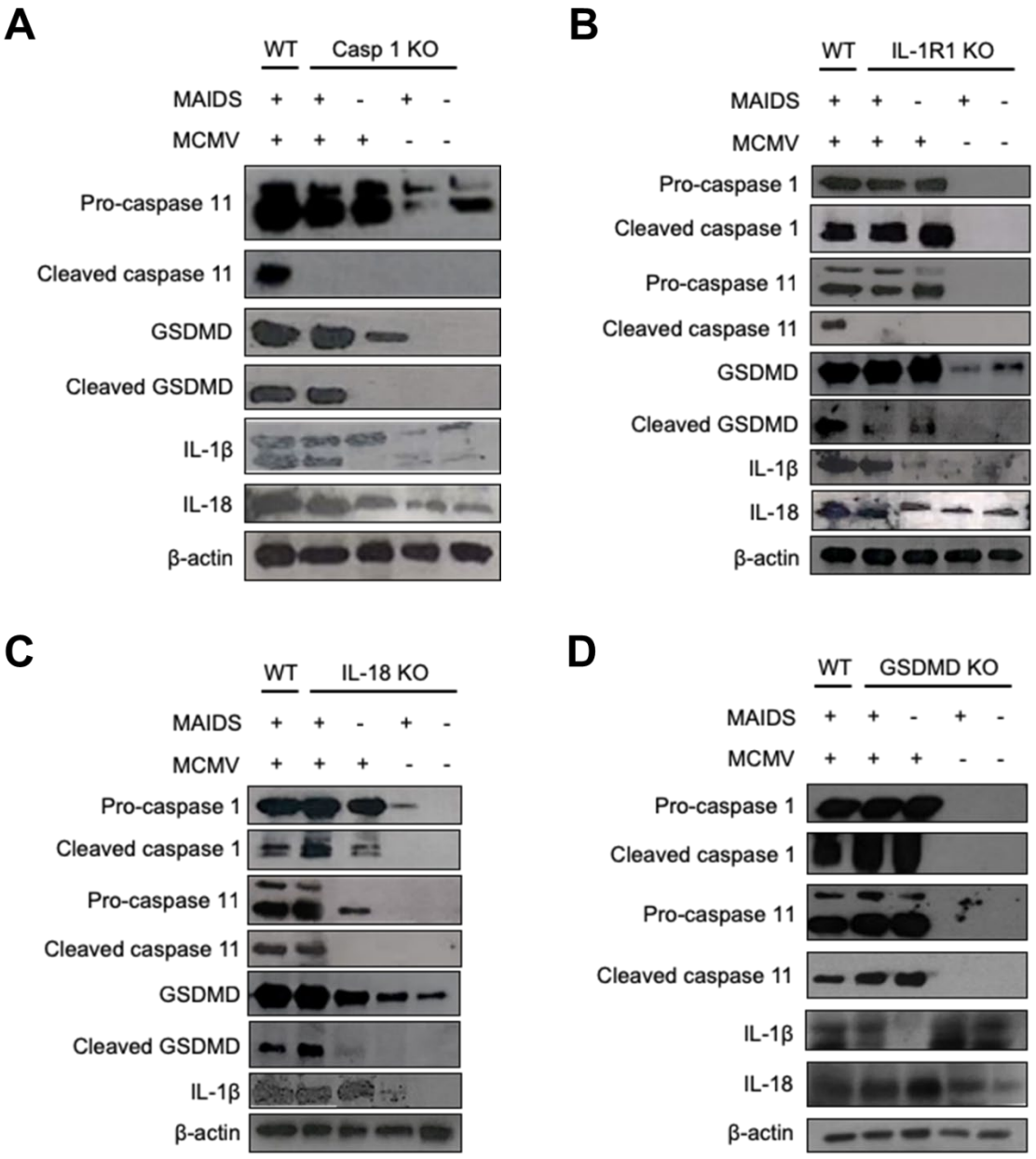

Figure 3.5. Expression of pyroptosis-associated proteins in MCMV infected eyes of wildtype MAIDS mice and caspase-1KO, GSDMD KO, IL-1R1KO, and IL-18KO micewith MAIDS.

WT MAIDS mice and groups of caspase-1 KO (A), GSDMD KO (B), IL-1R1 KO (C), and IL-18 KO (D) mice with MAIDS (n= 4- 6 mice/group) were subretinally infected with 10^4 PFU MCMV. Whole eyes were collected and at 10 dpi and assessed for ocular expression of the known pyroptosis-associated markers by western blot with beta-actin serving as a loading control.

MCMV-infected eyes of wildtype mice with MAIDS and MCMV-infected eyes of mice with MAIDS deficient in the production of a pyroptosis-associated protein harbor equivalent amounts of infectious MCMV. We showed previously that MCMV-infected eyes of retinitis-susceptible wildtype mice with MAIDS harbor significantly high amounts of infectious virus at 10 days after subretinal MCMV inoculation when compared with retinitis-resistant MCMV-infected eyes of healthy mice similarly inoculated with virus [6, 103]. To determine if loss of the canonical pyroptosis pathway (defined as a deficiency in the production of a key pyroptosis-associated protein) resulted in reduced intraocular virus replication during the development of MAIDS-related MCMV retinitis, whole MCMV-infected eyes were collected from groups of wildtype MAIDS mice, caspase-1KO mice with MAIDS**,** GSDMD KO mice with MAIDS, IL-1R1KO mice with MAIDS, and IL-18KO mice with MAIDS at 10 days after subretinal MCMV inoculation (n = 4 – 6 per group) and were individually homogenized and subjected to standard plaque assay to quantify infectious MCMV. Results are shown in Fig 3.6. In agreement with previous findings [6, 103, 226], MCMV-infected eyes of retinitis-susceptible wildtype mice with MAIDS were found to contain high amounts of infectious MCMV (4.3 $x10^4$). In comparison, MCMV-infected eyes of mice with MAIDS with a deficiency in either caspase-1, GSDMD, IL-1R1, or IL-18 also showed high amounts of infectious virus and at levels equivalent to that found within MCMV-infected eyes of wildtype mice with MAIDS with amounts ranging from 4.8 $x10^4$ to 4.4 $x10^4$. While there was a trend for the MCMV-infected eyes collected from pyroptosis-deficient MAIDS mice to exhibit greater amounts of infectious MCMV when compared with wildtype MAIDS mice, this difference was not statistically significant. Thus, loss of the canonical pyroptosis pathway during MAIDS did not affect the

intraocular replication of MCMV when compared with wildtype animals with MAIDS at 10 days following subretinal MCMV inoculation.

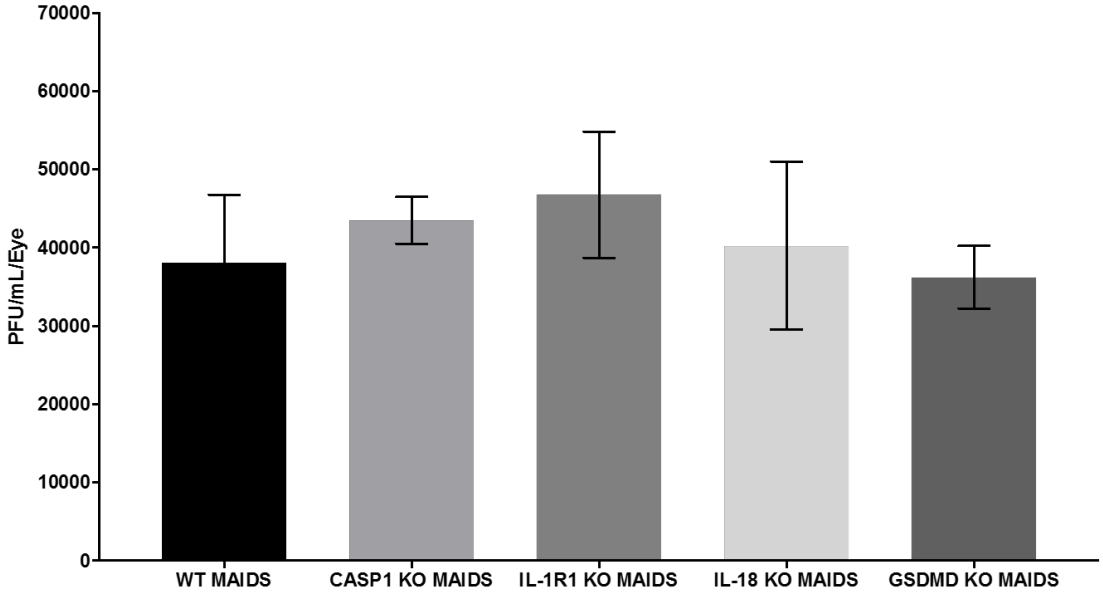

Figure 3.6. WT MAIDS mice and groups of MAIDS mice deficient in the production of a pyroptosis-associated protein harbored equivalent amounts of infectious MCMV.
MCMV-infected eyes were collected 10 dpi following intraocular MCMV injection from wildtype MAIDS mice and MAIDS mice deficient in either caspase-1, IL-1R1, IL-18, and GSDMD. Amount of infectious MCMV were detected in whole eyes by standard plaque assay (n=4-6).

The frequency of full-thickness retinal necrosis is significantly reduced within MCMV-infected eyes of MAIDS mice deficient in the production of a pyroptosis-associated protein when compared with the frequency of full-thickness retinal necrosis MCMV-infected eyes of wildtype MAIDS mice. Our finding that MCMV-infected mice with MAIDS with a deficiency in the pyroptosis pathway harbor high amounts of infectious MCMV led us to suspect that these animals would also develop full-thickness retinal necrosis at a frequency of 80 to 100% as observed by us previously for wildtype mice with MAIDS [6, 103, 226]. To confirm this suspicion, the eyes of groups of mice with MAIDS lacking either caspase-1, GSDMD, IL-

1R1, or IL-18 were inoculated subretinally with MCMV, collected 10 days later, subjected to histopathologic analysis, and scored for the frequency of full-thickness retinal necrosis. The MCMV-infected eyes of groups of wildtype mice with MAIDS included in each experiment served as controls. As reported previously, the frequency of full-thickness retinal necrosis for mice with MAIDS was 100% in each experiment. Surprisingly, however, none (0%) of the MCMV-infected eyes of mice with MAIDS with a deficiency in either caspase-1, GSDMD, IL-1R1, or IL-18 developed full-thickness retinal necrosis. Despite high amounts of intraocular infectious MCMV at levels observed within MCMV-infected eyes of wildtype mice that consistently developed full-thickness retinal necrosis, MCMV-infected eyes of MAIDS mice deficient in a gene essential for pyroptosis consistently failed to develop full-thickness retinal necrosis.

MCMV-infected eyes of MAIDS mice deficient in the production of a pyroptosis-associated protein consistently show prominent RPE proliferation but with relative preservation of the neurosensory retina. In an attempt to resolve the apparent discrepancy of high and equivalent amounts of intraocular infectious virus but without expected full-thickness retinal necrosis development within MCMV-infected eyes of pyroptosis-deficient MAIDS mice when compared MCMV-infected eyes of wildtype MAIDS mice, a detailed histopathologic analysis was performed to define with greater precision the patterns of retinal disease among the different animal groups at 10 days after subretinal MCMV inoculation. Results are shown in Fig 3.7. As expected, histopathologic examination of sections of MCMV-infected eyes collected from wildtype mice with MAIDS showed areas of full-thickness retinal necrosis containing virus-induced inclusions and cytomegalic cells in agreement with several previous publications by us [103]. In sharp contrast, however, histopathologic analysis of MCMV-infected eyes of

groups of caspase-1 KO mice with MAIDS, GSDMD KO mice with MAIDS, IL-1R1 KO mice with MAIDS, and IL-18 KO mice with MAIDS when paired experimentally with MCMV-infected eyes of groups of wildtype mice with MAIDS as controls in separate experiments revealed two major findings. One was an atypical histopathologic feature characterized by widespread RPE proliferation accompanied by detection of virus-induced inclusions. The second was a relative preservation of the neurosensory retina with loss of photoreceptors in some cases but without detection of virus-induced inclusions or cytomegalic cells and without the development of full-thickness retinal necrosis. Moreover, it is noteworthy that this pattern of histopathologic changes was relatively consistent among all groups of animals with MAIDS deficient in the canonical pyroptosis pathway whether loss of caspase-1, GSDMD, IL-1R1, or IL-18 gene activity. Instead, MCMV-infected eyes from caspase-1 KO mice with MAIDS, GSDMD KO mice with MAIDS, IL-1R1 KO mice with MAIDS, and IL-18 KO mice with MAIDS exhibited an unexpected abnormal histopathologic outcome quite different from the of full-thickness retinal necrosis.

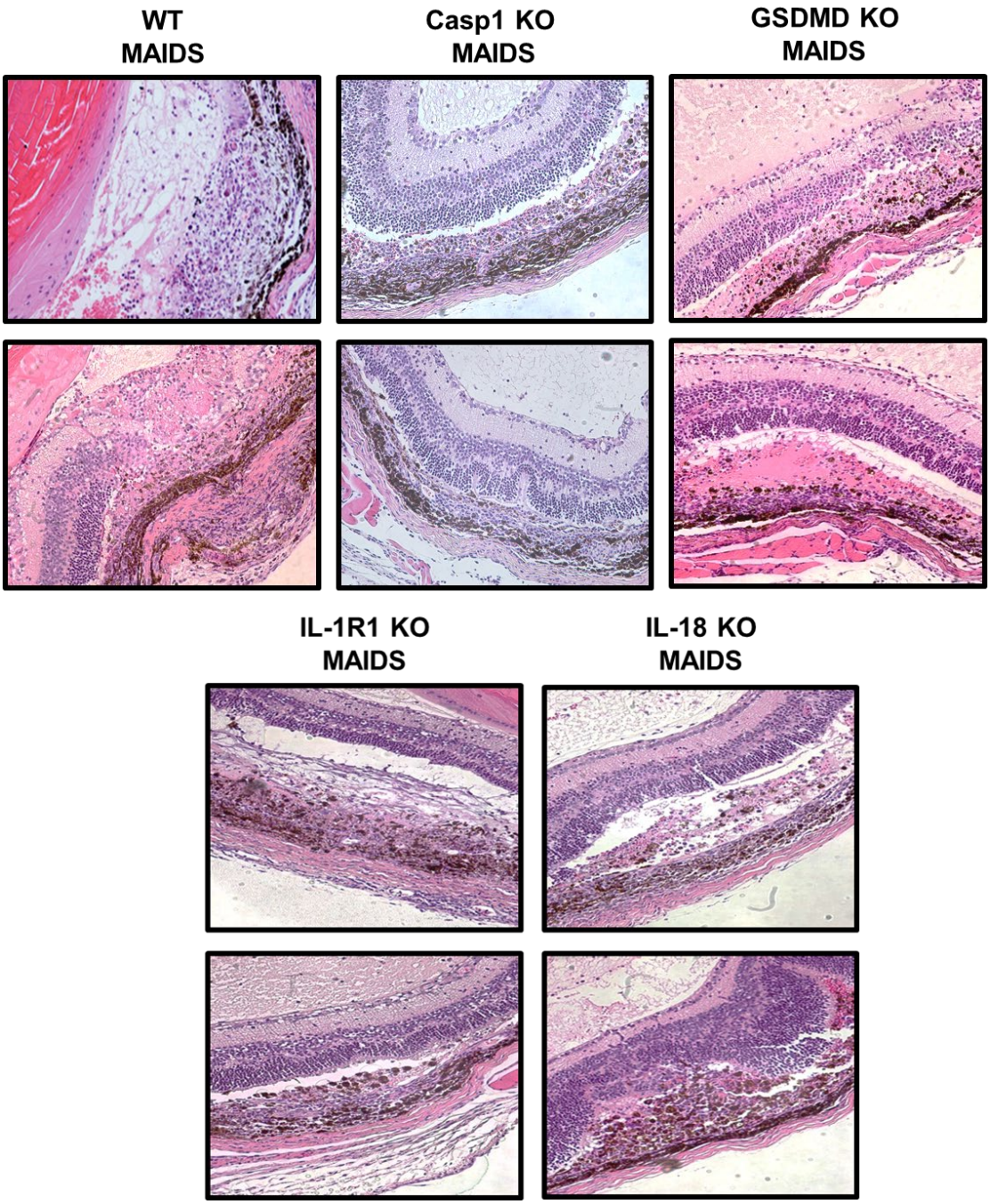

Figure 3.7. MCMV-infected eyes from groups of MAIDS mice deficient in the production of a pyroptosis-associated protein showed prominent RPE proliferation but preservation of the neurosensory retina.

MCMV-infected eyes were collected 10 dpi following intraocular MCMV injection from wildtype MAIDS mice and MAIDS mice deficient in either caspase-1, IL-1R1, IL-18, and GSDMD. H & E staining was done to histopathologically evaluate the presence of retinitis and changes in the retinal architecture.

Loss of pyroptosis-associated genes for caspase-1, GSDMD, IL-1R1, and IL-18 does not entirely abolish the expression of necroptosis-associated proteins in MCMV-infected eyes of MAIDS-10 mice. Necroptosis is another form of programmed cell death pathway that results in a disruption in the membrane integrity, leading to the release of cellular components and resulting in inflammation. During necroptosis, RIPK1 and RIPK3, promoted by TNF-α, are recruited and activated [229-231]. This activation leads to the recruitment and phosphorylation of MLKL, which forms an oligomer complex and migrates to the plasma membrane [230]. Once at the membrane, MLKL forms a pore resulting in the rupture of the cell and subsequent release of DAMPs, triggering a highly pro-inflammatory response [232]. Like inflammasomes and pyroptosis-associated proteins, these necroptosis-related proteins have also been seen stimulated in MAIDS-related MCMV retinitis. To determine if the preservation in the neurosensory retinas in these KO mice had anything to do with the downregulation of necroptosis proteins in the absence of pyroptosis-associated genes, western blot analysis was utilized to detect the presence of necroptosis-associated proteins in caspase-1, GSDMD, IL-1R1, and IL-18 KO MAIDS mice.

Western blot analysis was done on the MCMV-infected eyes of WT MAIDS mice and MAIDS mice deficient in either caspase-1 (Fig. 3.8A), GSDMD (Fig. 3.8B), IL-1R1 (Fig. 3.8C) or IL-18 (Fig. 3.8D) for molecules essential to the necroptosis pathway. For all KO MAIDS mice, RIPK1 and RIPK3 expression in MCMV-infected eyes was relatively similar to that seen in MCMV-infected eyes of WT MAIDS mice. MLKL protein expression and the phosphorylation of MLKL was also expressed in the MCMV-infected eyes of MAIDS mice, either WT or KO. Protein analysis for TNF-α revealed that the unprocessed protein [233] and cleaved form of TNF-α were both expressed in KO MAIDS mice and that this level of expression was the same as the WT MAIDS mice for all KO MAIDS mice except for mice

deficient in GSDMD. This suggests that GSDMD expression may have an influence on the expression of TNF-α in MCMV-infected eyes of MAIDS-10 mice.

The Effect of the Loss of Pyroptosis-associated Proteins on the Expression of Autophagy Proteins in MCMV-infected Eyes of MAIDS-10 Mice. Western blots were also done to determine the level of expression of autophagy-related proteins, beclin-1, and LC3B. Unlike pyroptosis and necroptosis, autophagy is a non-inflammatory form of cell death induced under times of cellular stress [234]. Previously, we have shown that autophagy is not expressed in MAIDS-10 mice with MCMV retinitis. We were then interested in determining if the lack of retinitis in these KO mice was due to the stimulation of autophagy proteins as a means of protecting the retina. Western blots showed that there was no substantial difference seen in both beclin-1 and LC3B between WT MAIDS mice and Casp 1 KO MAIDS mice (Fig. 3.8A), GSDMD KO MAIDS mice (Figure 3.8B), IL-1R1 KO MAIDS mice (Fig. 3.8C), and IL-18 KO MAIDS mice (Fig. 3.8D). This suggests that the loss of these pyroptosis-associated proteins does not result in the upregulation of autophagy markers to preserve the retina from damage following MCMV infection.

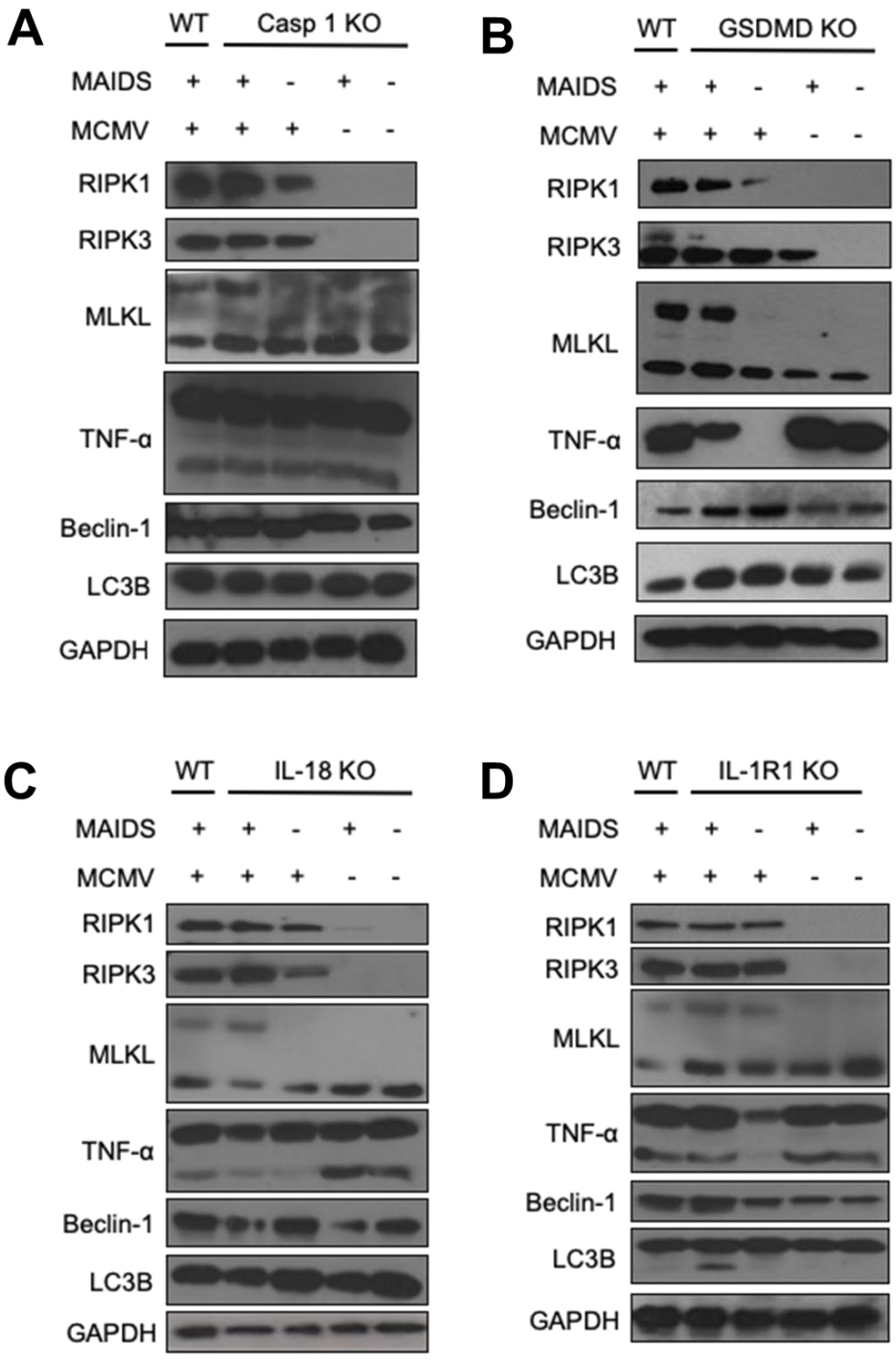

Figure 3.8. Expression of necroptosis- and autophagy-related proteins following ocular MCMV infection in mice deficient in key pyroptosis-associated molecules.

Western blot analysis was performed to visualize ocular expression of necroptosis-associated proteins and autophagy-associated proteins in MCMV infected eyes of WT MAIDS mice and either caspase-1 KO mice (A), GSDMD (B) IL-1R1 KO mice (C), or IL-18 KO mice (D) with the presence or absence of MCMV and/or MAIDS, with GAPDH used as a loading control.

3.3.2 The Loss of Inflammasomes and MAIDS-related MCMV Retinitis

Inflammasomes are high-molecular-weight, multi-protein complexes, that are found in the cytosol of immune cells and regulate the activation of inflammatory responses [171]. There are multiple types of inflammasomes, and each of their distinct assemblies is determined by a unique PPR in response to specific PAMPs or danger signals present in the host's cytosol. Once activated by the inflammatory ligand, the central domain of the inflammasome undergoes oligomerization, resulting in the recruitment of adaptor proteins, such as ASC, to the effector and variable N-terminal domain, which is composed of a PYD and a CARD. The CARD domain, on either the inflammasome or ASC, binds and activates pro-caspase-1 to invoke an inflammatory response [172]. There are several types of inflammasome proteins known to date, including the NLR family members, NLRP1 and NLRP3, as well as AIM2 [161]. The NLRP3 inflammasome [235-250], the NLRP1 inflammasome [251-253] and the AIM2 [214] are well-characterized inflammasomes that have been shown to play a role in several ocular diseases. As we have previously shown that mRNA production of these inflammasomes are highly stimulated in MCMV-infected eyes of MAIDS-10 mice [100], we wanted to define with greater precision the contribution of the NLRP3 inflammasome towards the onset and progression of MCMV retinitis during MAIDS-10.

MCMV-infected eyes of NLRP3KO mice with MAIDS, NLRP1b KO mice with MAIDS, and AIM2 KO mice with MAIDS show patterns of protein synthesis that are relatively similar to those of MCMV-infected eyes of wildtype mice with MAIDS. We continued our comprehensive investigation of MCMV retinitis pathogenesis using mice with MAIDS who were deficient in the production of one of three inflammasomes, either NLRP3, NLRP1b, or AIM2. All groups of KO mice infected with the immunosuppressive murine

retrovirus mixture (LP-BM5 MuLV) developed MAIDS as assessed by their development of a number of MAIDS-related physical and immunologic characteristics (data not shown) described by us previously [100].

Again, we investigated the patterns of pyroptosis-associated proteins of the canonical and noncanonical pyroptosis pathways for possible alterations in their pattern of synthesis. Western blot analysis of MCMV-infected eyes collected from NLRP3KO mice with MAIDS**,** NLRP1b KO mice with MAIDS, and AIM2 KO mice with MAIDS at 10 days after subretinal MCMV inoculation showed relatively similar patterns of protein production for corresponding proteins associated with the canonical and noncanonical pyroptosis pathways when compared with the patterns of protein production collected from MCMV-infected eyes of WT MAIDS mice (Fig. 3.9). Some notable exceptions were observed, however. A deficiency in either NLRP1b production during MAIDS or AIM2 production during MAIDS resulted in an increased in the cleaved caspase-1 protein (Fig 3.9B and 3.9C) but no real changes in the cleaved caspase-11 protein production. Similarly, a deficiency in NLRP1b production during MAIDS also resulted in a slight increase in cleaved GSDMD protein.

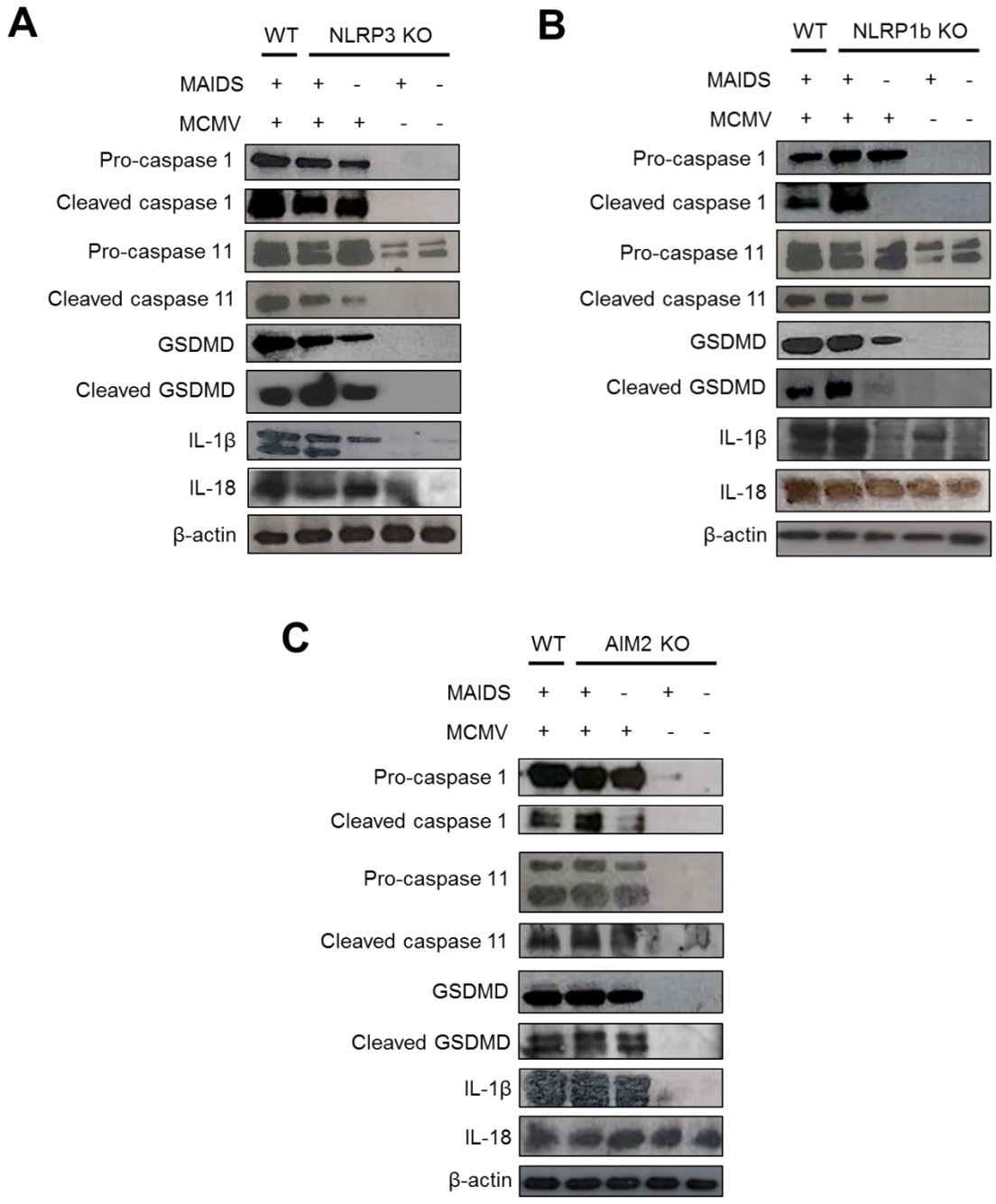

Figure 3.9. Expression of pyroptosis-associated proteins MCMV infected eyes of wildtype MAIDS mice, NLRP3KO, NLRP1b KO, and AIM2KO mice with MAIDS.

WT MAIDS mice and groups of NLRP3KO, NLRP1b KO, and AIM2KO mice with MAIDS (n= 3 - 7 mice/group) were subretinally infected with 10^4 PFU MCMV. Whole eyes were collected and at 10 dpi and assessed for ocular expression of the known pyroptosis-associated markers by western blot with beta-actin serving as a loading control.

MCMV-infected eyes of wildtype mice with MAIDS and MCMV-infected eyes of mice with MAIDS deficient in the production of an inflammasome protein harbor equivalent amounts of infectious MCMV. To determine if loss of any inflammasome resulted in reduced intraocular virus replication during the development of MAIDS-related MCMV retinitis, whole MCMV-infected eyes were collected from groups of WT MAIDS mice, NLPR3 KO mice with MAIDS**,** NLRP1b KO mice with MAIDS, and AIM2 KO mice with MAIDS at 10 days after subretinal MCMV inoculation (n = 4 – 9 per group) are were individually homogenized and subjected to standard plaque assay to quantify infectious MCMV. Results are shown in Fig 3.10. In agreement with previous findings [6, 103, 226], MCMV-infected eyes of retinitis-susceptible wildtype mice with MAIDS were found to contain high amounts of infectious MCMV (2.96×10^4). However, the level of infectious virus was significantly lower in the different group of KO MAIDS mice, with amounts ranging from 1.61×10^4 to 1.75×10^4. Thus, loss of either of these inflammasomes during MAIDS did affect the intraocular replication of MCMV when compared with WT mice with MAIDS at 10 days following subretinal MCMV inoculation.

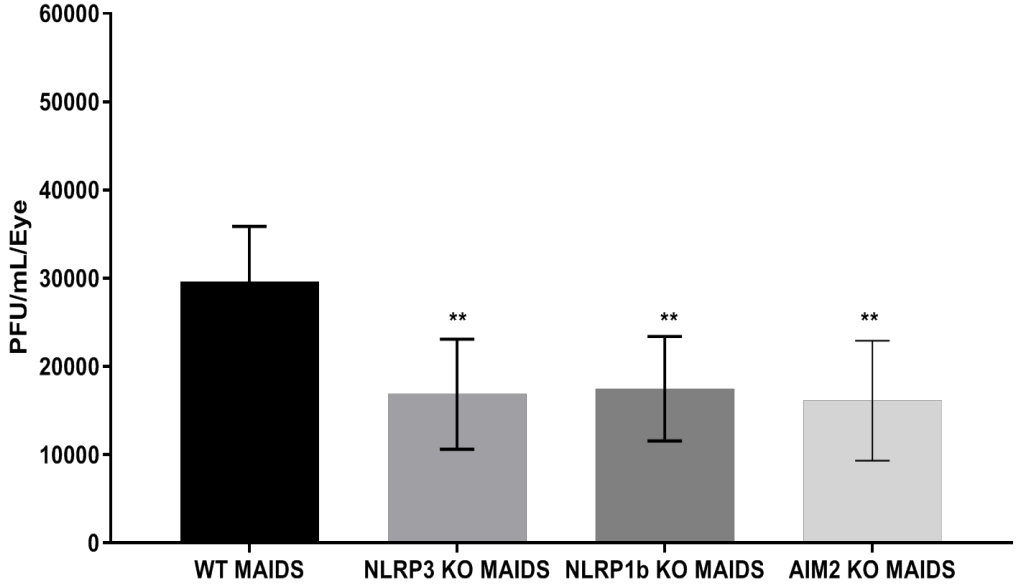

Figure 3.10. WT MAIDS mice and groups of MAIDS mice deficient in the production of an inflammasome-associated protein harbored a decreased amount of infectious MCMV.
MCMV-infected eyes were collected 10 dpi following intraocular MCMV injection from wildtype MAIDS mice and MAIDS mice deficient in either, NLRP3, NLRP1b, or AIM2. Amount of infectious MCMV were detected in whole eyes by standard plaque assay (n=3 - 9).

The frequency of full-thickness retinal necrosis is significantly reduced within MCMV-infected eyes of MAIDS mice deficient in the production of an inflammasome protein when compared with the frequency of full-thickness retinal necrosis MCMV-infected eyes of wildtype MAIDS mice. Our finding that MCMV-infected mice with MAIDS with a deficiency in one of several inflammasomes harbor high amounts of infectious MCMV, despite the significantly lower levels seen in the WT mice with MAIDS, led us to question whether these animals would also develop full-thickness retinal necrosis at a frequency of 80 to 100% like previously seen in WT mice with MAIDS mice or fail to develop this full-thickness retinal necrosis as seen with the MAIDS mice deficient in a key pyroptosis protein. To confirm this, the eyes of groups of mice with MAIDS lacking either NLRP3, NLRP1b, or AIM2 were inoculated subretinally with MCMV, collected 10 days later, subjected to histopathologic

analysis, and scored for the frequency of full-thickness retinal necrosis. The MCMV-infected eyes of groups of WT mice with MAIDS included in each experiment served as controls. As reported previously, the frequency of full-thickness retinal necrosis for mice with MAIDS was between 89-100% in each experiment. Surprisingly, however, none (0%) of the MCMV-infected eyes of mice with MAIDS with a deficiency in either NLRP3 or AIM2 developed full-thickness retinal necrosis, and only 25% of mice (2/8) developed a full-thickness retinal necrosis. Despite high amounts of intraocular infectious MCMV, MCMV-infected eyes of MAIDS mice deficient in an inflammasome gene consistently showed a reduction in its ability to develop full-thickness retinal necrosis.

MCMV-infected eyes of MAIDS mice deficient in the production of an inflammasome-related protein consistently show prominent RPE proliferation but with relative preservation of the neurosensory retina. A detailed histopathologic analysis was performed to define with greater precision the patterns of retinal disease among the different animal groups at 10 days after subretinal MCMV inoculation. Results are shown in Fig 3.11. As expected, histopathologic examination of sections of MCMV-infected eyes collected from wildtype mice with MAIDS showed areas of full-thickness retinal necrosis containing virus-induced inclusions and cytomegalic cells. In sharp contrast, however, histopathologic analysis of MCMV-infected eyes of groups of KO MAIDS mice revealed the same two major findings as seen in the pyroptosis KO MAIDS mice, when paired experimentally with MCMV-infected eyes of groups of WT MAIDS mice. This includes the atypical histopathologic feature characterized by widespread RPE proliferation accompanied by detection of virus-induced inclusions as well as a relative preservation of the neurosensory retina with loss of photoreceptors in some cases but without detection of virus-induced inclusions or cytomegalic cells and without the

development of full-thickness retinal necrosis (the exception being the two NLRP1b KO mice with MAIDS that did show the development of a full-thickness retinal necrosis).

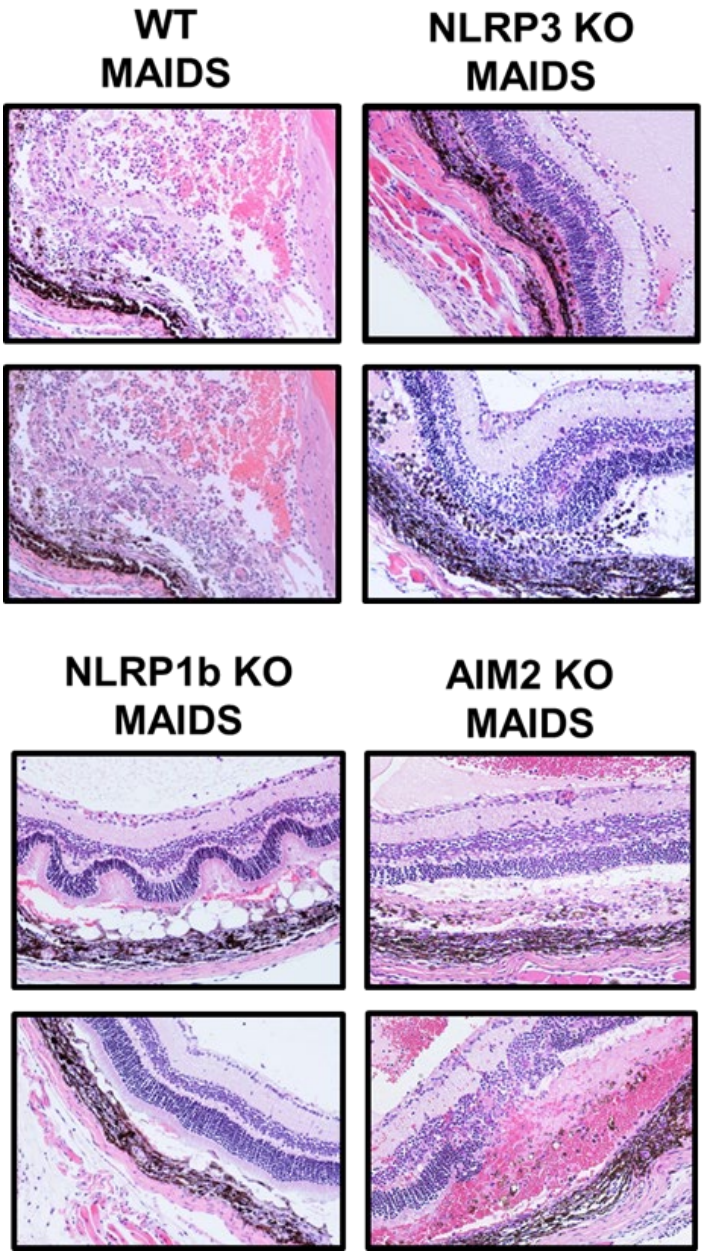

Figure 3.11. MCMV-infected eyes from groups of MAIDS mice deficient in the production of an inflammasome-associated protein showed prominent RPE proliferation but preservation of the neurosensory retina.

MCMV-infected eyes were collected 10 dpi following intraocular MCMV injection from wildtype MAIDS mice and MAIDS mice deficient in either NLRP3, NLRP1b, or AIM2. H & E staining was done to histopathologically evaluate the presence of retinitis and changes in the retinal architecture.

Loss of genes for inflammasomes NLRP3, NLRP1b, and AIM2 does not entirely abolish the expression of necroptosis-associated proteins in MCMV-infected eyes of MAIDS-10 mice. Western blot analysis was done on the MCMV-infected eyes of WT MAIDS mice and MAIDS mice deficient in either NLRP3 (Fig. 3.12A), NLRP1b (Fig. 3.128B), or AIM2 (Fig. 3.12C) for molecules essential to the necroptosis pathway. For all KO MAIDS mice, RIPK1 and RIPK3 expression in MCMV-infected eyes was relatively similar to MCMV-infected eyes of WT MAIDS mice. MLKL protein expression and the phosphorylation of MLKL were also similarly expressed in the MCMV-infected eyes of the groups of KO MAIDS mice when compared to the WT MAIDS mice. Protein analysis for TNF-α revealed that the unprocessed protein and cleaved form of TNF-α were both expressed in KO MAIDS mice and that this level of expression was the same as the WT MAIDS mice for all groups of KO MAIDS mice.

Loss of genes for inflammasomes NLRP3, NLRP1b, and AIM2 does not entirely abolish the expression of autophagy-associated proteins in MCMV-infected eyes of MAIDS-10 mice. Next, we sought to determine if the preservation of the retina during MCMV infection in the eyes of the inflammasome KO MAIDS mice had anything to do with the upregulation of autophagy proteins, LC3B, and beclin-1. Western blots showed that there was no substantial difference seen in both beclin-1 and LC3B among WT MAIDS mice and NLRP3 KO MAIDS mice (Fig. 3.12A), NLRP1b KO MAIDS mice (Fig. 3.12B), and AIM2 KO MAIDS mice (Fig. 3.12C). This suggests that the loss of these pyroptosis-associated proteins does not result in the upregulation of autophagy markers to preserve the retina from damage following MCMV infection.

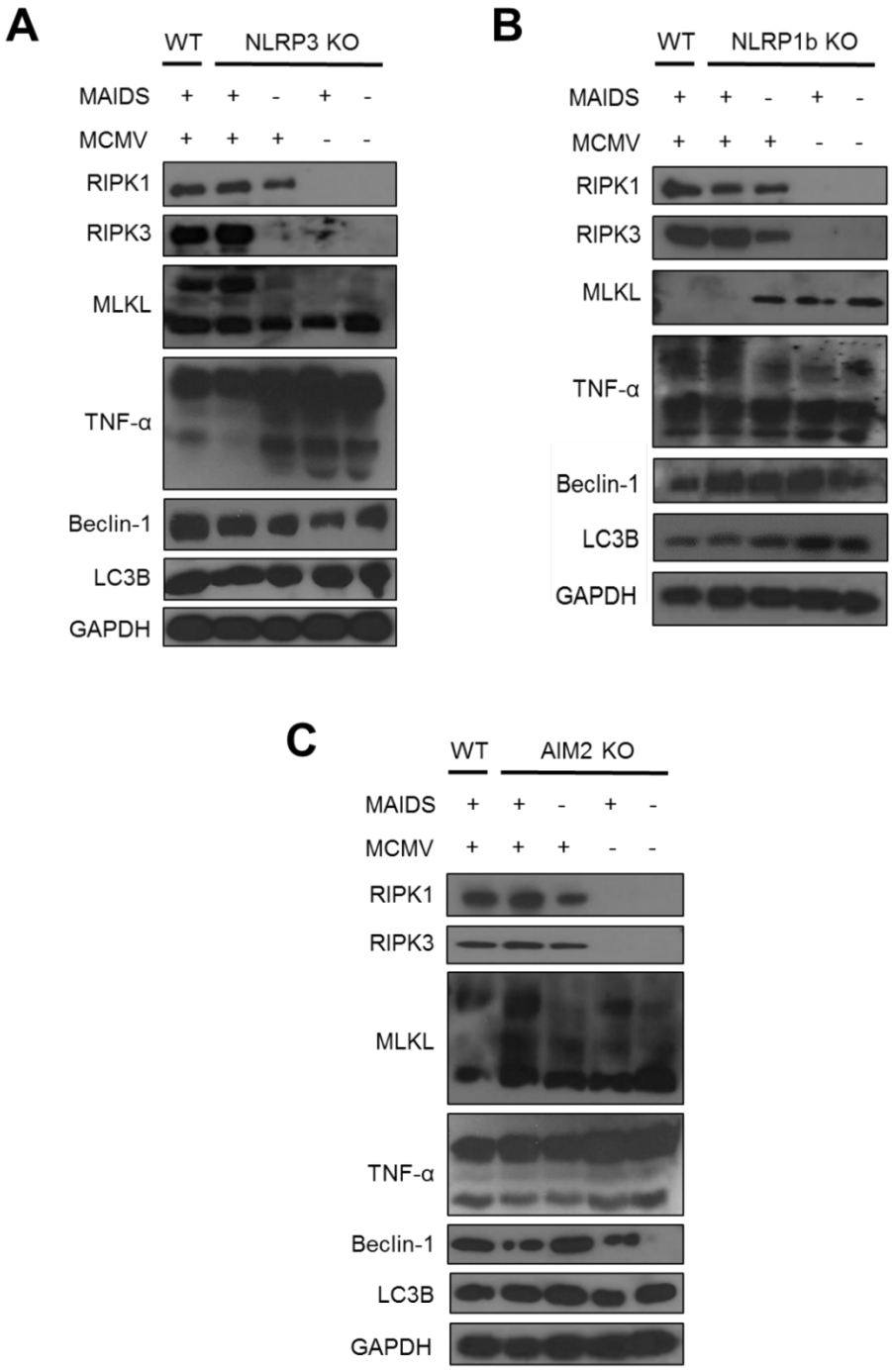

Figure 3.12. Expression of necroptosis- and autophagy-related proteins following ocular MCMV infection in mice deficient in several inflammasomes.

Western blot analysis was performed to visualize ocular expression of necroptosis-associated proteins and autophagy-associated proteins in MCMV infected eyes of WT MAIDS mice and either NLRP3 KO mice (A), NLRP1b KO mice (B), or AIM2 KO mice (C) with the presence or absence of MCMV and/or MAIDS, with GAPDH used as a loading control.

3.4 Ocular MCMV Infection during Corticosteroid-Induced Immunosuppression

The development of MAIDS in C57BL/6 mice shows many immunopathological features like this seen with the maturation of AIDS in HIV-1 infected patients. Additionally, MCMV infection in mice with late stage MAIDS produces retinitis that exhibits histopathologic features that mimic those seen in patients with AIDS-related HCMV retinitis [254]. However, the MAIDS model is not the only model available to study MCMV retinitis. Other researchers have shown that MCMV-infected eyes of C57BL/6 mice immunosuppressed by corticosteroid treatment also results in the development of MCMV retinitis. However, there are several differences between this model of retinitis and the MAIDS model of MCMV retinitis. One significant difference is the development of retinitis in C57BL/6 mice with corticosteroid-induced immunosuppression is at a frequency of only ~50% [109] as opposed to the 80 to 100% frequency seen in MAIDS-related MCMV retinitis. This may be related to the vast difference in the type of immunosuppression between these two models. MAIDS has a slow and progressive development, which goes through distinct phases of immune cell dysfunction over the course of several weeks. Corticosteroid-induced immunosuppression, however, results in a rapid, acute decline in the immune system, which develops over the course of a few days and shows a difference in immune cell populations, particularly macrophages and cytokine response to infection [115, 116]. Recently, our lab has shown that the expression of SOCS1 and SOCS3, which are highly expressed in MAIDS-related MCMV retinitis, are only mildly stimulated in MCMV-infected eyes of corticosteroid-induced immunosuppression [226]. This reduction in SOCS1 and SOCS3 expression is correlated to a less severe retinitis development along with a reduction in ocular viral titer when compared to previously established MAIDS studies [4, 6, 103, 126].

Because of these vast differences in the two immunosuppression models, we were interested in seeing if there were any other differences in molecules known to be stimulated during MAIDS-related MCMV retinitis. As we have repeatedly established that pyroptosis-associated molecules are upregulated in MCMV-infected eyes of MAIDS-10 mice, we sought to determine if these molecules are also stimulated in MCMV-infected eyes of mice with corticosteroid-induced immunosuppression. Theoretically, if these molecules play a role in the pathogenesis of MCMV retinitis, then they should be stimulated in multiple models of this disease.

3.4.1 Pyroptosis Expression during Corticosteroid-induced Immunosuppression

Expression and translation of caspase-1 mRNA in MCMV-infected eyes of mice with corticosteroid-induced immunosuppression. mRNA analysis showed that caspase-1 was significantly stimulated in MCMV-infected eyes of mice with corticosteroid-induced immunosuppression (Fig. 3.13A). Although the level of mRNA stimulation was similar at day 3 post-infection as that seen in MAIDS-10 mice (Fig. 3.13B), there was a slight dip in mRNA expression at day 6 post-infection prior to peak expression seen at day 10 post-infection. Western blot analysis showed that pro-caspase-1 was greatly expressed in MCMV-infected eyes of mice with corticosteroid-induced immunosuppression at all days post-infection with a gradual increase in overall protein levels as the infection progressed. Pro-caspase-1 was also greatly expressed in MCMV-infected eyes of MAIDS-10 mice at all days post-infection, with a slight increase at 6 days post-infection. The appearance of pro-caspase-1 seemed slightly higher in MCMV-infected eyes of MAIDS-10 mice at 3 and 6 days post-infection when compared to the corticosteroid-induced immunosuppressed mice, while the levels of protein expression were reasonably similar at 10 days post-infection between both models of immunosuppression. Although not as greatly

stimulated, the mature caspase-1 protein followed the same trend of stimulation as pro-caspase-1 in MCMV-infected eyes of both MAIDS-10 and corticosteroid-induced immunosuppressed mice (Fig. 3.14).

Expression and translation of caspase-11 mRNA in MCMV-infected eyes of mice with corticosteroid-induced immunosuppression. MCMV-infected eyes of mice with corticosteroid-induced immunosuppression showed substantial stimulation of caspase-11 mRNA at all days post-infection (Fig. 3.13C). The level of expression at 3 days post-infection was only half that seen, at the respective time, in MCMV-infected eye of MAIDS-10 mice (Fig. 3.13D). However, mRNA production for caspase-11 continued to increase in MCMV-infected eyes of mice with corticosteroid-induced immunosuppression from day 6 to day 10 post-infection, where it reached levels not significantly different that that seen in MCMV-infected eyes of MAIDS-10 mice. Protein levels for pro-caspase-11 and cleaved caspase-11 showed similar levels of expression in MCMV-infected eyes between both models of immunosuppression. The main difference seen in caspase-11 protein expression was that MCMV-infected eyes of mice with corticosteroid-induced immunosuppression showed appearance of both pro-caspase-11 and cleaved caspase-11 at day 10 post-infection, whereas the expression of caspase-11 in MCMV-infected eyes of MAIDS-10 was only seen at days 3 and 6 post-infection (Fig. 3.14).

Expression and translation of GSDMD mRNA in MCMV-infected eyes of mice with corticosteroid-induced immunosuppression. Expression of GSDMD mRNA transcripts were significantly stimulated in MCMV-infected eyes of mice with corticosteroid-induced immunosuppression at all days post-infection (Fig 3.13E). Although there was a slight decrease in expression at day 6 post-infection, there was not significant difference in the stimulation of GSDMD mRNA at any day post-infection in mice with corticosteroid-induced

immunosuppression and MAIDS-10 mice (Fig. 3.13F). Protein for the full-length precursor GSDMD was abundant in MCMV-infected eyes of corticosteroid-induced immunosuppressed mice when compared to the mock-treated eyes. The level of expression was greater at days 6 and 10 post-infection. There was a difference in the trend in the expression of GSDMD seen in MCMV-infected eyes of MAIDS-10 mice in which there was greater at days 3 and 6 post-infection. Cleaved GSDMD protein was also higher in MCMV-infected eyes of mice with corticosteroid-induced immunosuppression at 3 and 6 days post-infection with a slight drop in expression at 10 days post-infection. Similar trends were seen for the cleaved form of GSDMD, in MCMV-infected eyes of MAIDS-10 mice (Fig. 3.14).

Expression and translation of IL-1β mRNA in MCMV-infected eyes of mice with corticosteroid-induced immunosuppression IL-1β mRNA expression following MCMV infection of mice with corticosteroid-induced immunosuppression was greatly stimulated at 3 days post-infection. The level of mRNA expression dramatically decreased by 6 days post-infection, and by 10 days post-infection, there was no significant stimulation over the media control eyes (Fig 3.13G). This trend in mRNA expression was similar to that seen in the MCMV-infected eyes of MAIDS-10 mice (Fig. 3.13H), and there was no significance difference in mRNA stimulation between the two groups of mice. Western blot analysis showed that there was a slight appearance of IL-1β protein in MCMV-infected eyes of corticosteroid-induced immunosuppressed mice when compared to the mock injected eyes. This difference was slightly greater at 6 days post-infection. However, there was a greater level of expression in MCMV-infected eyes of MAIDS-10 mice when compared to mock-treated eyes at 3 and 6 days post-infection. There appeared to be no significant differences between the protein levels of MCMV-

infected eyes of mice with either corticosteroid-induced immunosuppression or MAIDS-10 (Fig. 3.14).

Expression and translation of IL-18 mRNA in MCMV-infected eyes of mice with corticosteroid-induced immunosuppression. Although similar levels of IL-18 mRNA stimulation were seen at 3 and 10 days post-infection between mice with corticosteroid-induced immunosuppression (Fig. 3.13I) and MAIDS-10 mice (Fig. 3.13J), the IL-18 mRNA production was slightly greater in MCMV-infected eyes of MAIDS-10 mice at 6 days post-infection. MCMV-infected eyes of corticosteroid-induced immunosuppression mice saw a greater expression of IL-18 protein at all days post-infection when compared to the mock-treated eyes. Not surprisingly, a similar trend was seen in MAIDS-10 mice with possibly a slight increase in protein at 6 days post-infection when compared to mice with corticosteroid-induced immunosuppression (Fig. 3.14), findings that correlated with the trend seen in mRNA production.

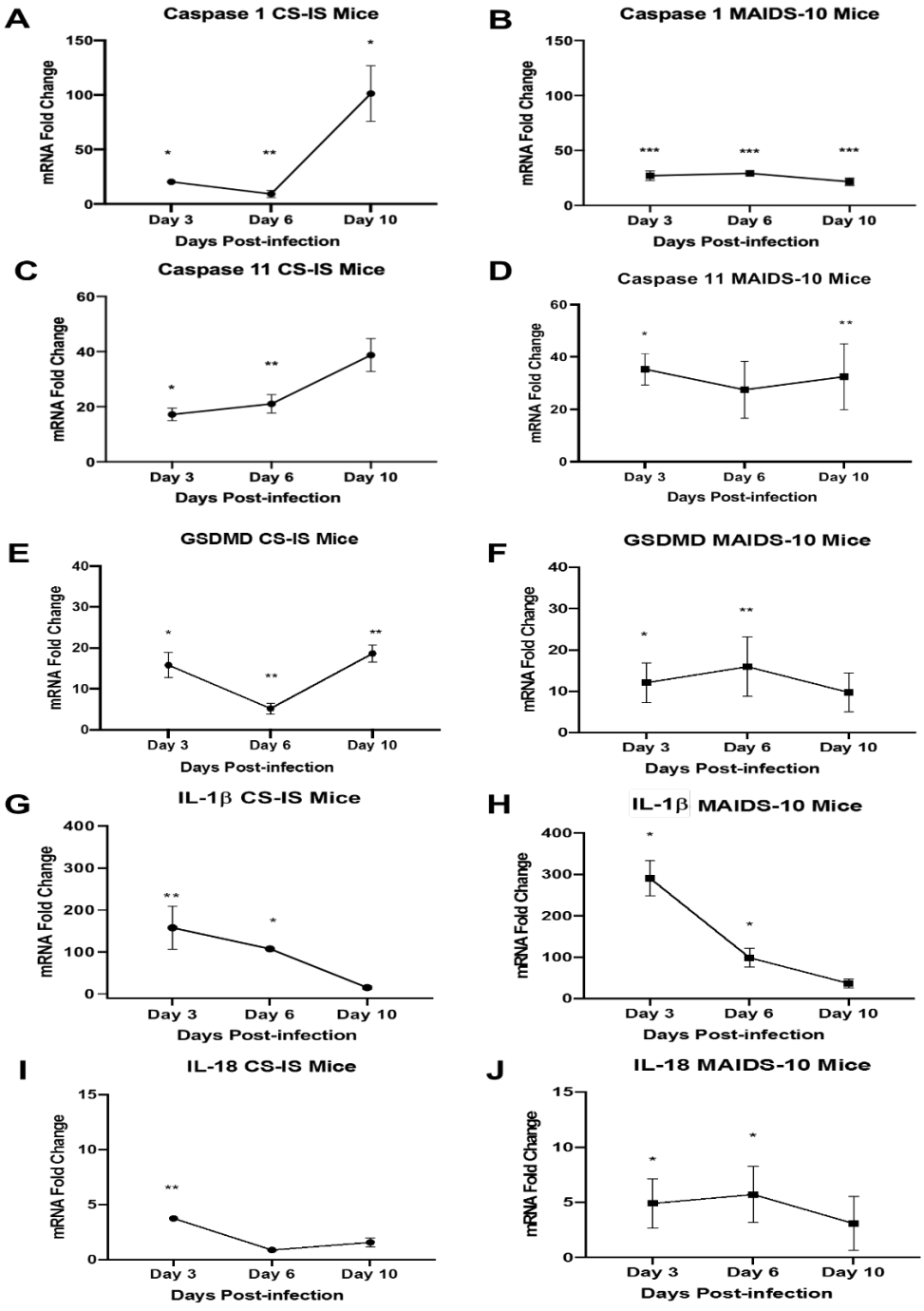

Figure 3.13. Pyroptosis-associated mRNA is stimulated in mice with either corticosteroid-induced immunosuppression (CS-IS) or MAIDS-10.

Homogenized whole eyes of mice with CS-IS and MAIDS-10 were assessed at 3, 6, and 10 dpi for caspase-1 (A and B), caspase-11 (C and D), GSDMD (E and F), IL-1beta (G and H), and IL-18 (I and J) mRNA, with MCMV samples compared back to media controls per day (n=3-5 mice/group). *p<0.05, **p<0.01, and ***p<0.001, MCMV groups compared with media controls at the same time points.

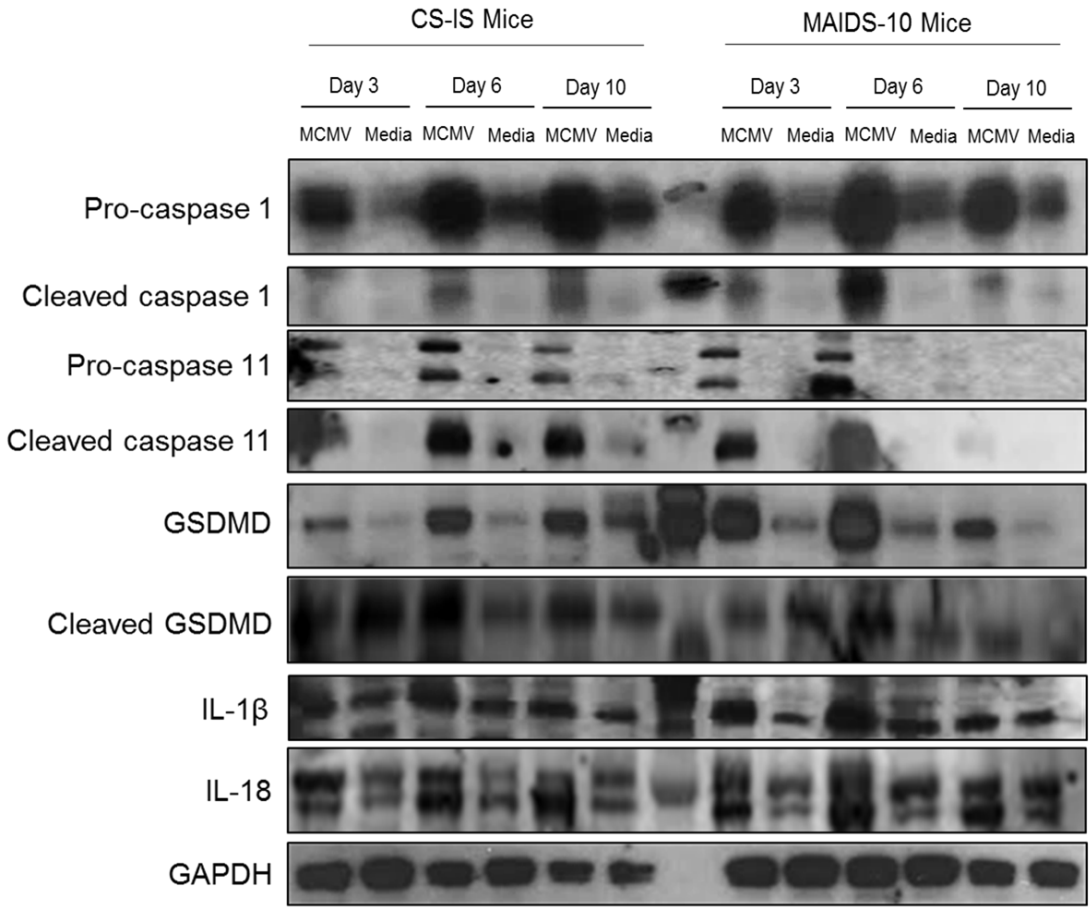

Figure 3.14. Pyroptosis-associated proteins was stimulated in mice with either corticosteroid-induced immunosuppression (CS-IS) or MAIDS-10.

Western blot analysis was performed to assess ocular expression of pyroptosis-associated proteins in groups of mice with corticosteroid-induced immunosuppression (left) or MAIDS-10 mice (right) of both MCMV infected and media control eyes at days 3, 6, and 10 post-infection. GAPDH used as a loading control and a ladder was loaded in the well separating the two groups of mice.

3.4.2 Inflammasome Expression during Corticosteroid-induced Immunosuppression

NLRP1b, but not other inflammasomes, showed a marked reduction in mRNA production of MCMV-infected eyes of mice with corticosteroid-induced immunosuppression when compared to MAIDS-10 mice. Since we have previously shown that the NLRP3, NLRP1b, NLRC4, and AIM2 inflammasomes are stimulated in MCMV-infected eyes of MAIDS-10 mice, we sought to determine if the mRNA of these inflammasomes

were also stimulated in mice immunosuppressed with corticosteroids. mRNA stimulation of NLRP3 in MCMV-infected eyes was highest at 3 days post-infection, dropped off by 6 days post-infection and stayed relatively similar at 10 days post-infection (Fig. 3.15A). No major differences were seen with the level of NLRP3 stimulation in MCMV-infected eyes of MAIDS-10 mice except at 10 days post-infection, when mice with corticosteroid-induced immunosuppression showed a significantly greater level of expression of NLRP3 (Fig. 3.15B). mRNA production for NLRP1b showed a slight significant increase in MCMV-infected eyes over media control eyes that stayed a consistent level at all days post-infection (Fig. 3.15C). This differed from the mRNA production seen in MCMV-infected eyes of MAIDS-10 mice that showed a greater level of stimulation at days 3 and 6 post-infection (Fig. 3.15D). When investigating the NLRC4 inflammasome, it was interesting to see that the levels of stimulations were similar in mice with corticosteroid-induced immunosuppression (Fig. 3.15E) and mice with MAIDS-10 (Fig. 3.15F). However, mice with MAIDS-10 did show a greater stimulation in mRNA expression of NLRC4 at day 3 post-infection when compared to the MCMV-infected eyes of mice with corticosteroid-induced immunosuppression. Although there was a slight difference in the trends of mRNA expression for AIM2 between mice with corticosteroid-induced immunosuppression (Fig. 3.15G) and MAIDS-10 mice (Fig. 3.15H) during the course of infection, no significant difference was seen between the two groups of mice at any days post-infection.

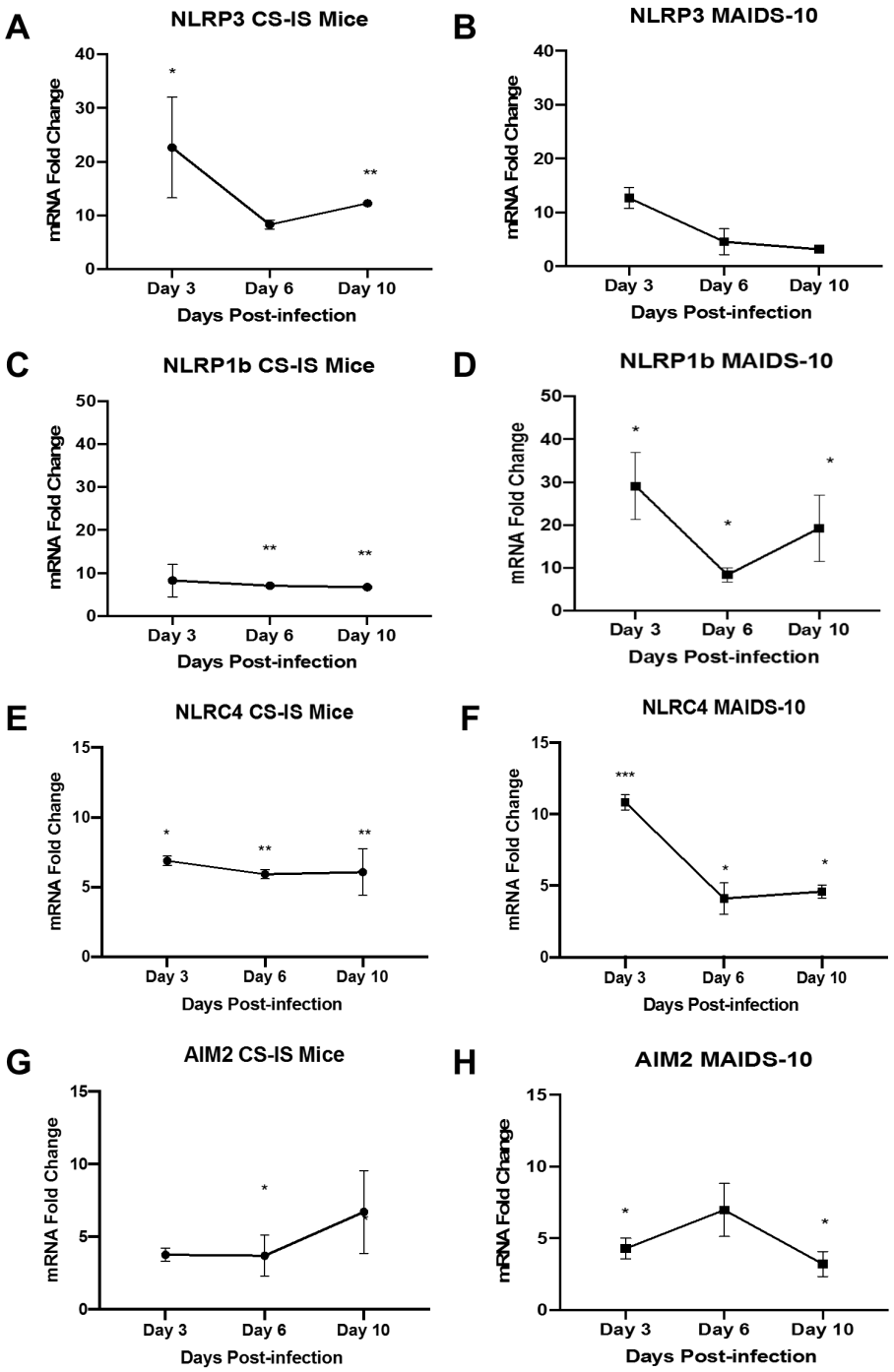

Figure 3.15. Inflammasome mRNA was stimulated in mice with either corticosteroid-induced immunosuppression (CS-IS) or MAIDS-10.

Homogenized whole eyes of mice with corticosteroid-induced immunosuppression and MAIDS-10 were assessed at 3, 6, and 10 dpi for NLRP3 (A and B), NLRP1b (C and D), NLRC4 (E and F), and AIM2 (G and H) mRNA, with MCMV samples compared back to media controls per day (n=3-5 mice/group). *p<0.05, **p<0.01, and ***p<0.001, MCMV groups compared with media controls at the same time points.

3.5 Ocular Expression Following Needle Stick or in Unmanipulated Eyes

Although the expression of our target inflammatory markers is consistently significantly higher in MCMV-infected eyes when compared to the media control eyes, there does seem to be slight stimulation of several of these proteins in eyes injected with media only. To determine the extent that the the needle stick into the subretinal space, or the administration of fluids (void of virus), has on the induction of the inflammatory response, we compared the mRNA expression of the pyroptosis-associated mRNA, caspase-1, caspase-11, GSDMD, IL-1β, and IL-18 (Fig. 3.16A-E), as well as NLRP3, NLRP1b, NLRC4, AIM2 inflammasomes (Fig. 3.17A-D), among groups of mice that received the MCMV infection, the standard media control injection, eyes that were simple poked by the needle without any injection, and eyes that were unmanipulated at all. Six days following the subretinal injections, all eyes were harvested and assessed for target mRNA expression. mRNA analysis of the eyes showed no major stimulation of any target pyroptosis-related and associated inflammasome mRNA in mice without manipulation to their eyes, or with those that received only the needle stick without an injection of fluid. Although a few molecules (caspase-1, GSDMD, IL-18, and NLRP1b) may have seen a slight trend in increased expression in media-injected eyes, these levels were not statistically different from either the unmanipulated eyes or those that were merely poked with the needle. On the contrary, the eyes that received a subretinal injection of MCMV showed a dramatic, statistically significant increases in mRNA expression of all target transcripts when compared to the media treated eyes, the eyes that underwent a simple needle stick into the subretinal space, and the unmanipulated eyes. Therefore, the results suggest that the stimulation of these pyroptosis-associated molecules and associated inflammasomes is substantially enhanced by MCMV, and the needle stick itself is not contributing to this expression.

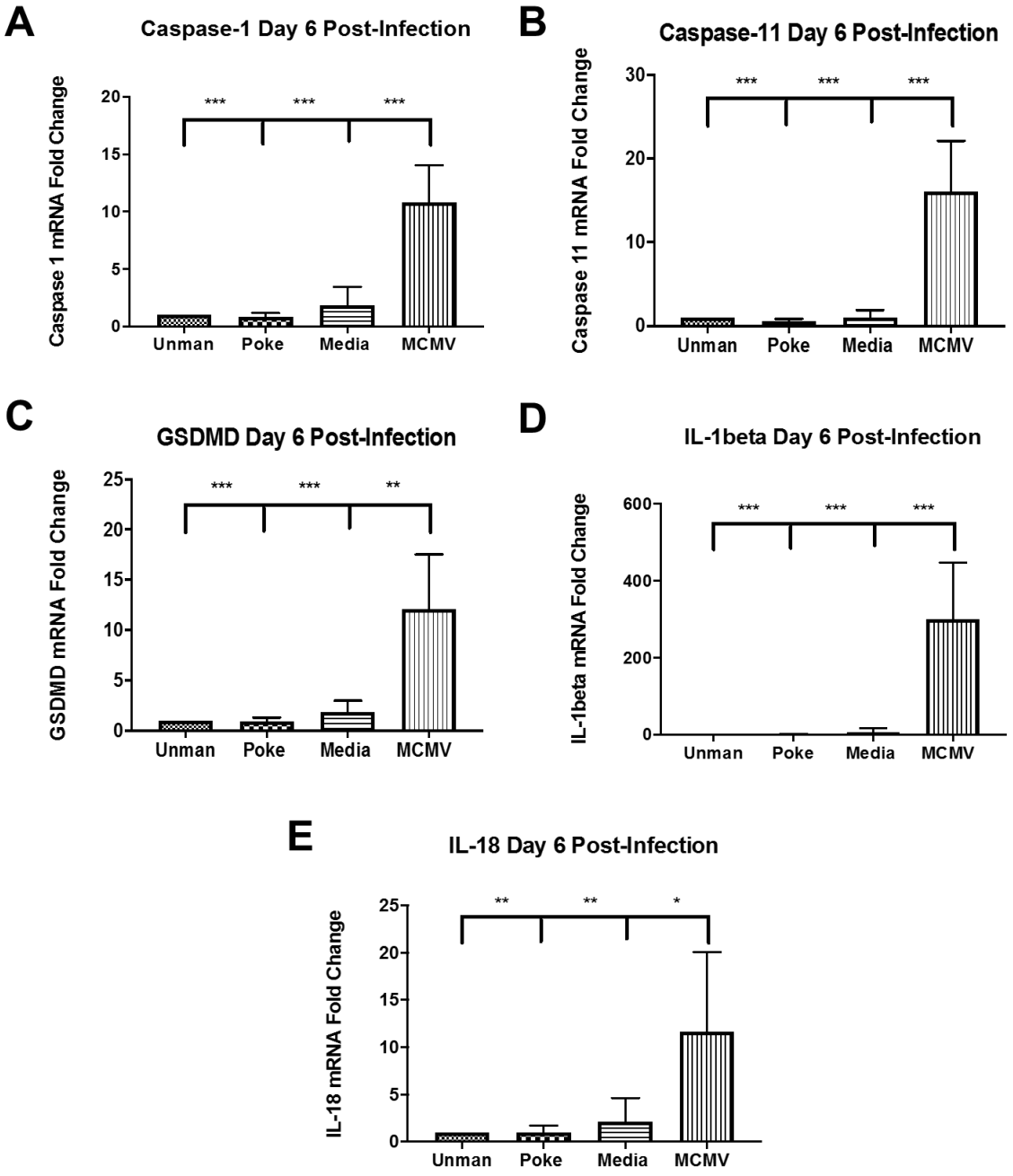

Figure 3.16. Pyroptosis-associated mRNA was not stimulated in unmanipulated eyes, or eyes not infected with MCMV.

MAIDS-10 mice were either injected with MCMV or media, poked with a media without injection of any fluid (poke), or not manipulated with a needle (unman) . At six dpi, whole eyes of each group (n=5) were harvested and assessed for caspase-1 (A), caspase-11 (B), GSDMD (D), IL-1beta (B), and IL-18 (E) mRNA. *p<0.05, **p<0.01, and ***p<0.001, MCMV compared back to other groups as indicated with brackets.

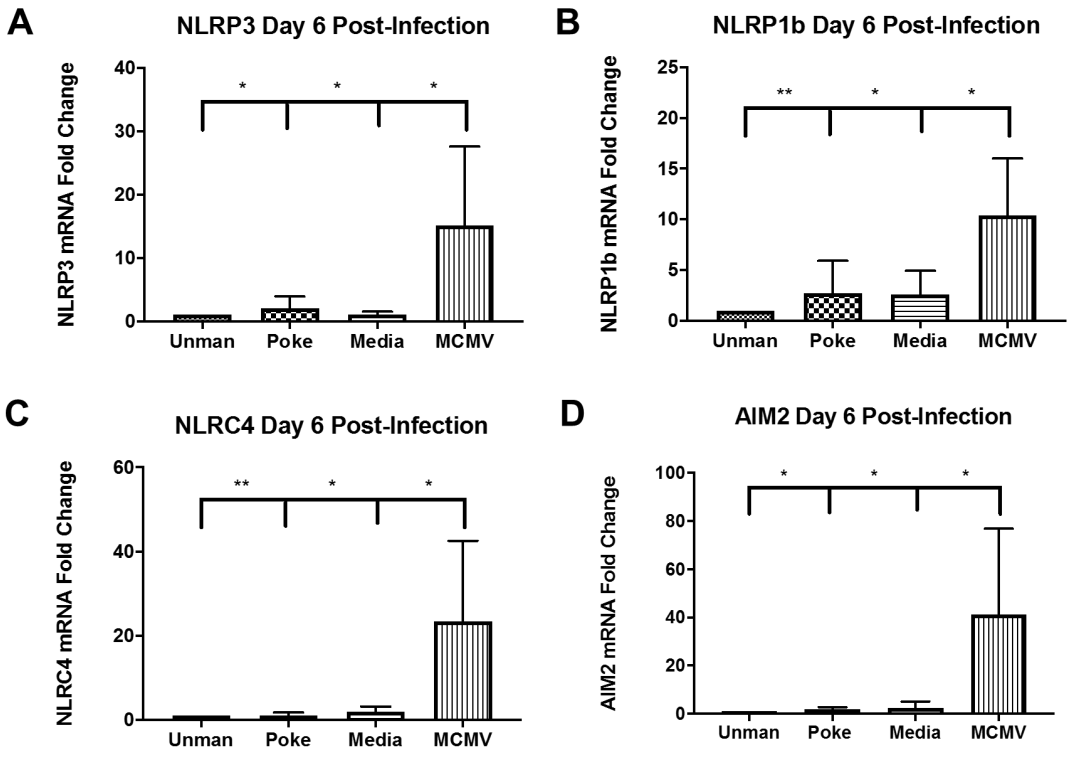

Figure 3.17. Inflammasome mRNA was not stimulated in unmanipulated eyes, or eyes not infected with MCMV.
MAIDS-10 mice were either injected with MCMV or media, poked with a media without injection of any fluid (poke), or not manipulated with a needle (unman) . At six dpi, whole eyes of each group (n=5) were harvested and assessed for NLRP3 (A), NLRP1b (B), NLRC4 (C), and AIM2 (D) mRNA. *$p<0.05$ and **$p<0.01$, MCMV compared back to other groups as indicated with brackets.

4 SPECIFIC AIM 2

Specific Aim 2: Test the Hypothesis that MCMV Replication directly Stimulates Pyroptosis in Infected Cells.

HCMV and MCMV both undergo a temporal, step-wise viral gene expression and replication cascade [12]. The interaction of glycoproteins on the envelope of the virus and host receptors, mediates fusion or endocytosis of the virion into the host cell [25]. Viral tegument proteins are then released into the cell, and some are believed to be transported to the nucleus of the host cell via interactions with the host microtubule machinery. These tegument proteins are bound to capsids, and once in the nucleus, viral transcription, genome replication, and encapsidation occur [26-28]. The transcription and subsequent translation of viral genes follow a specific sequence, starting with IE genes followed by E genes, which results in viral DNA synthesis and expression of L genes. This then allows for the assembly of progeny virions, which egress from the cell. If pyroptosis directly results from CMV infection of the host cell, then at least one of these virologic events may drive the host cell expression of pyroptosis-associated mRNA or protein production.

4.1 Pyroptosis-Associated Expression Kinetics Following MCMV Infection in IC-21 or MEF Cells

Several pyroptosis-associated mRNA transcripts were stimulated in MCMV-infected IC-21 mouse macrophages. We have previously demonstrated that pyroptosis-associated mRNA and protein are stimulated in MCMV-infected eyes during the onset and progression of MCMV retinitis in mice with retroviral-induced immunosuppression [6]. It is unclear, however, if this stimulation of pyroptosis was from direct cellular infection with MCMV

within the retina, or if it was induced by a host response following MCMV infection. Following acute infection, MCMV will establish latency in monocytes and has repeatedly been shown to replicate in macrophages [255, 256]. Therefore, we sought to determine if MCMV infection would stimulate the production of pyroptosis-associated mRNA transcripts in IC-21 mouse macrophages. Monolayers of IC-21 mouse macrophages were infected with MCMV at a moi of 3 and allowed to propagate for up to 72 hpi. MCMV infected IC-21 monolayers showed a statistically significant upregulation of mRNA transcripts for caspase-1 (Fig 4.1A), GSDMD (Fig 4.1B), and IL-1β (Fig 4.1C) at early time-points following infection. Peak expression for these transcripts occurred between 2-4 hpi, which correlates to a relatively early time during productive MCMV infection following viral attachment, adsorption, and release of tegument protein, as well as transcription and translation of MCMV IE gene in macrophages [41]. Interestingly, however, IL-18 mRNA production showed no stimulation in MCMV infected cells when compared to the media treated cells at 1-4 hpi (Fig. 4.1D).

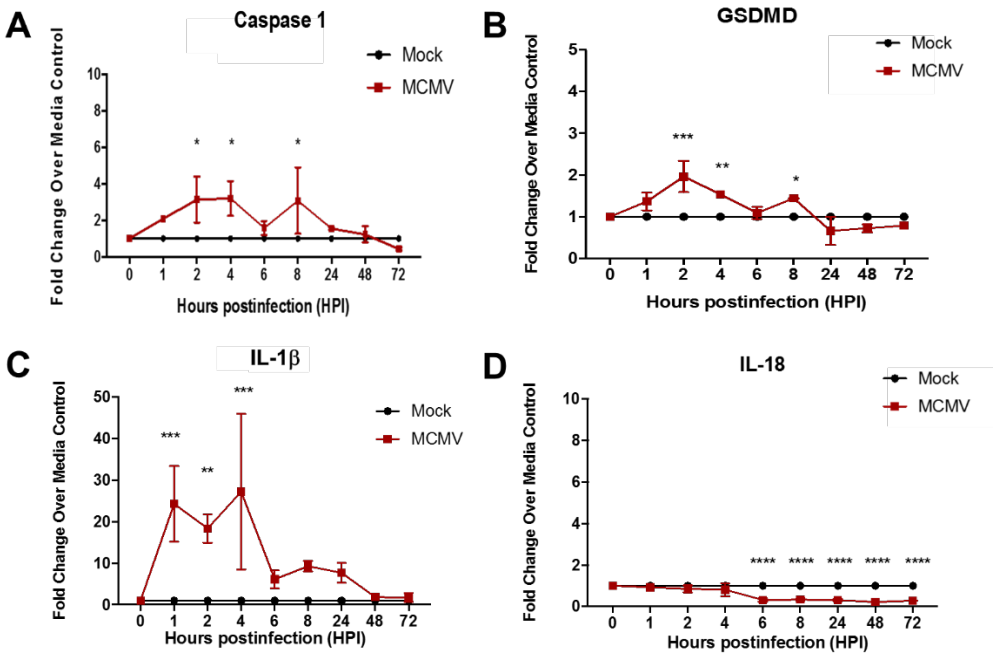

Figure 4.1. MCMV infection stimulated pyroptosis-related mRNA in mouse macrophages. IC-21 mouse macrophages infected with MCMV (moi = 3 PFU/cell) or treated with media control. At indicated time points, cells were harvested and assessed for caspase-1 mRNA (A), GSDMD mRNA (B), IL-1beta mRNA (C) or IL-18 mRNA (D) by real-time RT-PCR assay using the comparative $2^{-\Delta\Delta Ct}$ method, with all samples compared back to the media group at the same time point. Means ±SD of duplicate experimental repeats are shown. * $p<0.05$, ** $p<0.01$, and *** $p<0.001$, compared with respective media controls at the same time points as determined by one-way ANOVA

Most pyroptosis-associated mRNA transcripts were stimulated in MCMV-infected MEF cells. As it has been shown that MCMV replication kinetics differ between macrophages and fibroblasts [257], we sought to determine if the stimulation in pyroptosis-associate mRNA transcripts would also differ between these cell lines following MCMV infection. MEF monolayers were infected with MCMV, at a moi of 3, and allowed to propagate for up to 3 days. Similar to what was seen for IC-21 mouse macrophages, caspase-1 (Fig 4.2A), GSDMD (Fig 4.2B), and IL-1β (Fig 4.2C), but not IL-18 (Fig 4.2D) mRNA transcripts showed significant stimulation in MCMV-infected MEFs. Interestingly, the stimulation seen following MCMV infection in MEFs was more robust than that seen during infection of IC-21 mouse macrophages

and continued for a longer duration. Stimulation of both caspase-1 and IL-1β mRNA expression showed an upregulation starting as early as 30 minutes following MCMV infection and continued to be highly stimulated until approximately 6 hpi. GSDMD mRNA upregulation begins a little later in MEF cells with peak stimulation occurring between 4-8 hpi. This duration of stimulation correlates not only with the viral attachment, adsorption, release of tegument protein, and transcription of MCMV IE gene in macrophages [41], but also the transcription of MCMV E gene. A biphasic upregulation of caspase-1 started to emerge at 24 hpi which could be associated with the transcription and translation of MCMV L gene during productive infection.

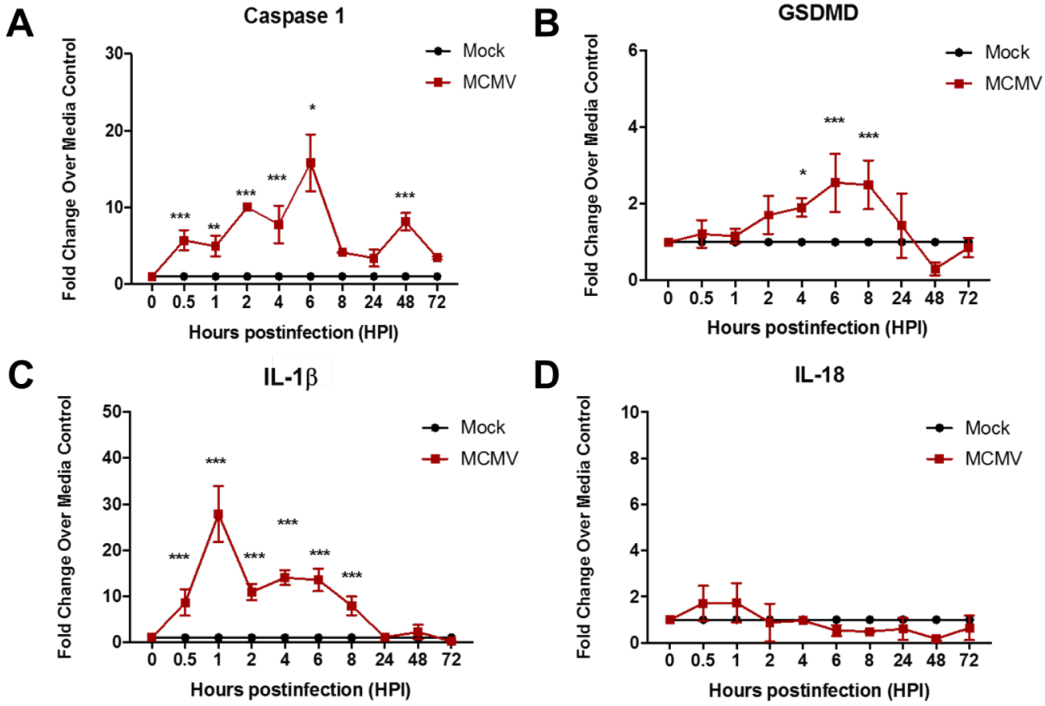

Figure 4.2. Infection of MEFs with MCMV stimulated pyroptosis-associated mRNA transcripts.

MEFs were infected with MCMV (moi = 3 PFU/cell) or treated with media control. At indicated time points, cells were harvested and assessed for caspase-1 mRNA (A), GSDMD mRNA (B), IL-1beta mRNA (C) or IL-18 mRNA (D) by real-time RT-PCR assay using the comparative $2^{-\Delta\Delta Ct}$ method, with all samples compared back to the media group at the same time point. Means ±SD of duplicate experimental repeats are shown. * $p<0.05$, ** $p<0.01$, and *** $p<0.001$, compared with respective media controls at the same time points as determined by one-way ANOVA.

4.2 Pyroptosis-Associated Expression Following Infection with UV-inactivated MCMV in MEF cells

UV-inactivated MCMV does not significantly stimulate pyroptosis-associated mRNA expression in MEF cells. MCMV infection of MEF cells showed the greatest upregulation of the pyroptosis-associated mRNA when compared to the stimulation seen within infected IC-21 mouse macrophages. To determine if the different stages of MCMV gene transcription were responsible for the stimulation of these pyroptosis-related mRNA transcripts, or if early virologic events of attachment, adsorption, and release of tegument proteins were sufficient for this stimulation, we infected monolayers of MEF cells with MCMV inactivated by ultraviolet light (UVi-MCMV). This inactivation leaves glycoproteins and immunologic components of MCMV intact although the virus is unable to undergo viral gene expression and replication in the infected cell [224]. Contrary to the notable upregulation of caspase-1 (Fig 4.3A), GSDMD (Fig 4.3B), IL-1β (Fig 4.3C), and IL-18 (Fig 4.3D) mRNA in MEF cells at early time points following MCMV infection, UVi-MCMV infected cells did not show any upregulation of these mRNA transcripts at any time point.

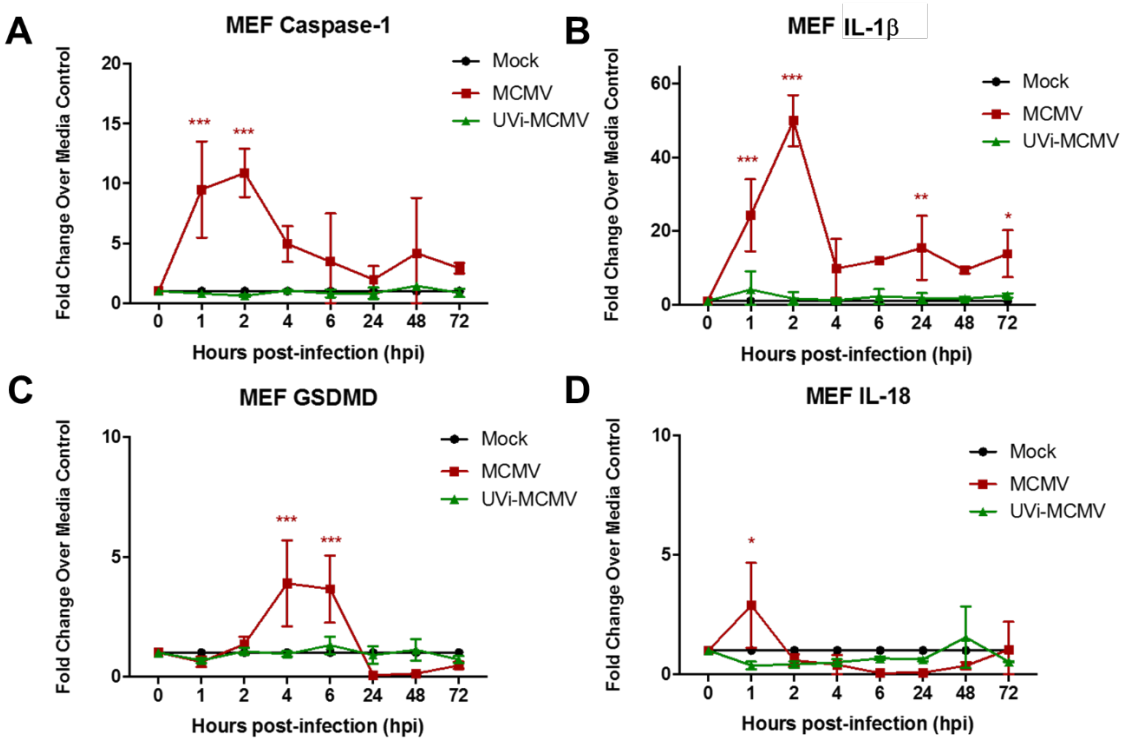

Figure 4.3. UV-inactivation of MCMV abrogated MCMV-related stimulation of pyroptosis mRNA transcripts in MEFs.

MEFs were infected with MCMV (moi = 3 PFU/cell) or treated with either media (control) or equal volume of UVi-MCMV. At indicated time points, cells were harvested and assessed for caspase-1 mRNA (A), GSDMD mRNA (B), IL-1beta mRNA (C) or IL-18 mRNA (D) by real-time RT-PCR assay using the comparative $2^{-\Delta\Delta Ct}$ method, with all samples compared back to the media group at the same time point. Means ±SD of duplicate experimental repeats are shown. * $p<0.05$, ** $p<0.01$, and *** $p<0.001$, compared with respective media controls at the same time points as determined by one-way ANOVA. No statistically significant differences were found between the media controls and the UV-MCMV groups at any time point.

To determine if expression of pyroptosis-associated proteins are substantially stimulated in MEF cells following MCMV infection but not UVi-MCMV infection, immunofluorescence (IF) was done on MCMV-infected and UVi-treated monolayers and assessed for expression of pyroptosis-associated proteins at 6 and 24 hpi. At 6 hpi, caspase-1 (Fig 4.4A) and GSDMD (Fig 4.4B) protein of MCMV-infected cells showed a stark level of protein expression not seen in media treated cells. Although there was some expression of caspase-1 and GSDMD in UVi-

MCMV infected cells, this level was nowhere near the level of expression seen in the MCMV infected cells. IL-1β protein expression was also substantially greater in MCMV-infected cells than seen for media treated cells at 6 hpi (Fig. 4.4C), while no real expression was seen following UVi-MCMV infection. Despite the lack of mRNA upregulation seen during MCMV infection of MEFs at any time point except 1 hpi, IL-18 protein did show a robust level at 6 hpi when compared to the lack of expression seen of IL-18 in the media treated cells (Fig. 4.4D). This expression was ablated in MEF cells treated with UVi-MCMV.

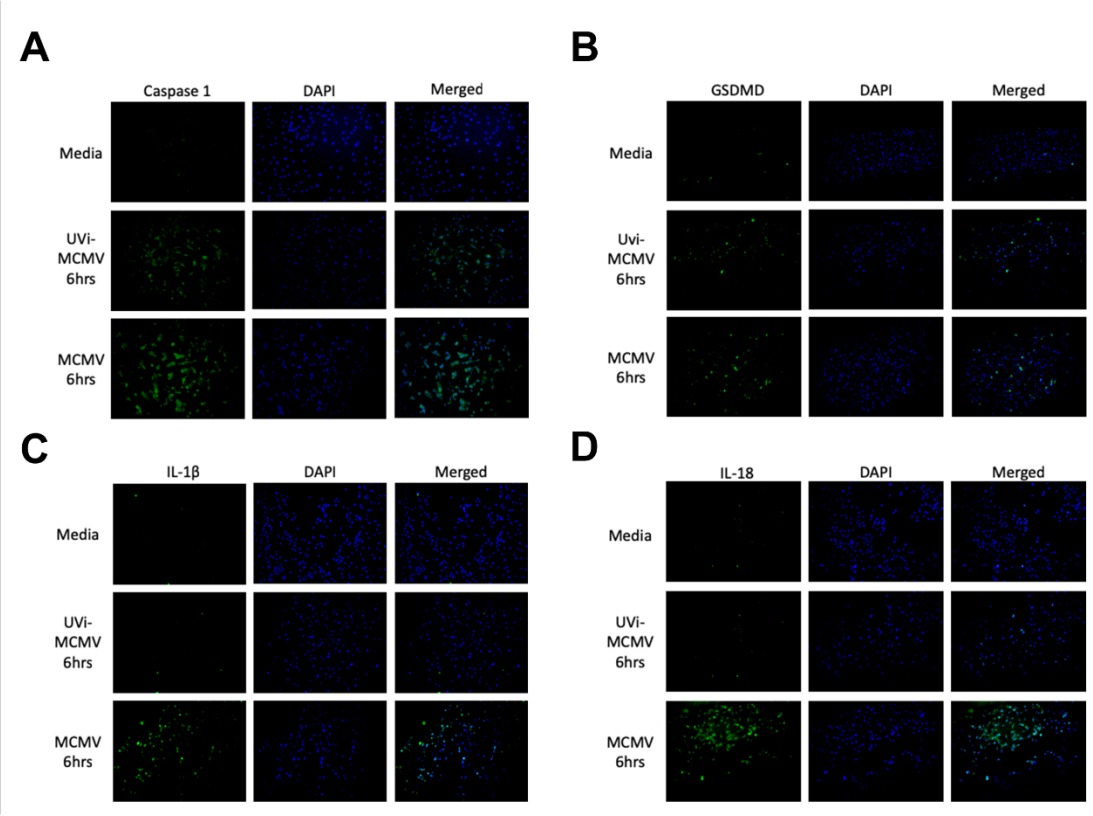

Figure 4.4. UV-inactivation of MCMV reduced MCMV-related stimulation of pyroptosis-related protein in MEFs at 6 hpi.

MEFs MEFs were infected with MCMV (moi = 3 PFU/cell) or treated with either media (control) or equal volume of UVi-MCMV. All 6 hpi all groups were fixed and assessed by immunofluorescent staining for caspase-1 (A), GSDMD (B), IL-1beta (C), or IL-18 (D) protein (green), counterstained with DAPI (blue). Original magnification, 100x.

At 24 hpi, protein expression for caspase-1 (Fig 4.5A), GSDMD (Fig 4.5B), and IL-1β (Fig 4.5C), but not IL-18 (Fig 4.5D) of MCMV-infected cells was greater than that seen at 6 hpi, which were all still remarkably higher than the protein expression seen in the media treated cells. Expression of these proteins were still seen in cells treated with UVi-MCMV when compared to the media treated controls, but the level of stimulation appeared substantially less than that seen in the respective MCMV-infected cells at 24 hpi.

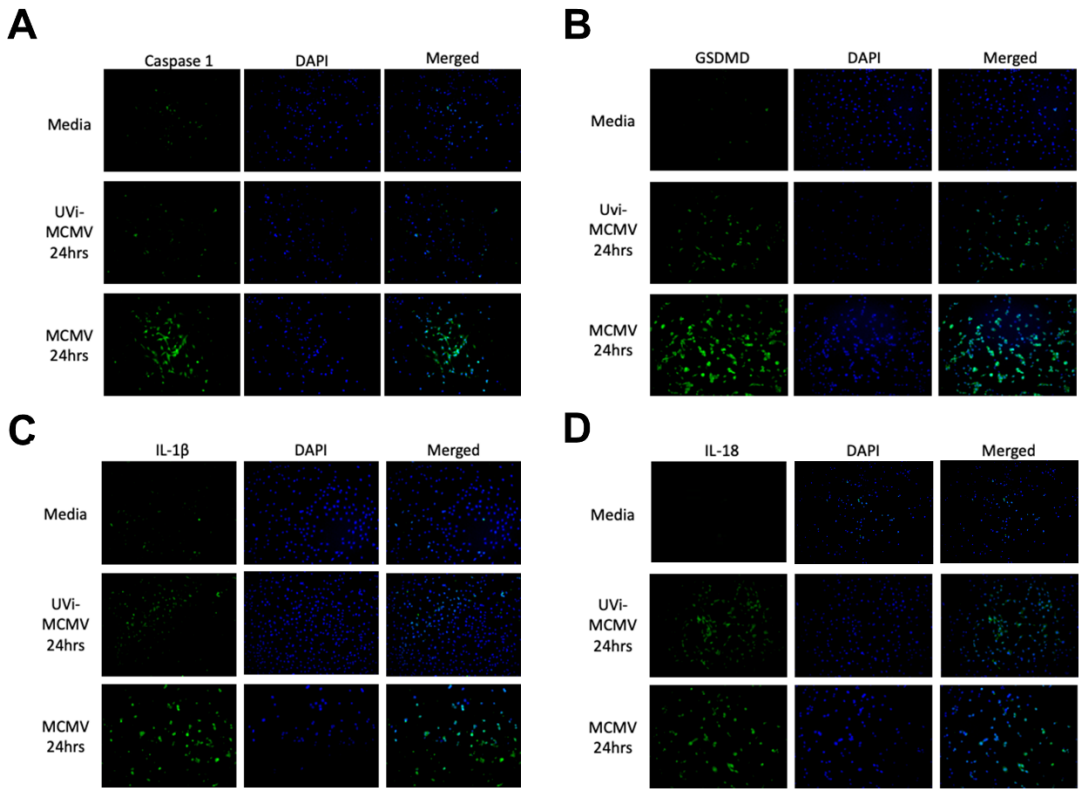

Figure 4.5. UV-inactivation of MCMV reduced MCMV-related stimulation of pyroptosis-related protein in MEFs at 24 hpi.
MEFs MEFs were infected with MCMV (moi = 3 PFU/cell) or treated with either media (control) or equal volume of UVi-MCMV. All 24 hpi all groups were fixed and assessed by immunofluorescent staining for caspase-1 (A), GSDMD (B), IL-1beta (C), or IL-18 (D) protein (green), counterstained with DAPI (blue). Original magnification, 100x.

4.3 Pyroptosis-Associated Expression Kinetics Following HCMV Infection in ARPE-19 or MRC-5 Cells

Pyroptosis-associated mRNA transcripts were not stimulated upon HCMV infection of ARPE-19 or MRC-5 cells. Following our confirmation that MCMV-infected cells can directly stimulate the expression of pyroptosis-related mRNA and/or proteins in an individual cell line, it is feasible to suggest that the stimulation of these mRNA transcripts and proteins seen during our experimental model of MCMV retinitis could be from the direct stimulation of MCMV-infected cells rather than host response to infection. If this is true, then it is likely that the same may be true of HCMV infected cells of individuals with AIDS-related HCMV retinitis as HCMV has been shown to penetrate all layers of the retina and the contiguous RPE where it can actively replicate, as demonstrated by the formation of cytomegalic cells and inclusion bodies throughout necrotic retinal tissue [98, 99]. Therefore, to test our hypothesis that HCMV infection can directly result in the stimulation of pyroptosis-related mRNA transcripts, we infected ARPE-19 cells, a human RPE cell line, with HCMV and measured the production of pyroptosis-associated mRNA transcripts. Monolayers of ARPE-19 cells were infected with HCMV, at a moi of 3, and allowed to propagate for 3 days. At all measured time points, HCMV failed to stimulate mRNA production of caspase-1 (Fig. 4.6A), GSDMD (Fig. 4.6B), IL-1β (Fig. 4.6C), or IL-18 (Fig. 4.6D) at any time post-infection above that seen for the media treated cells.

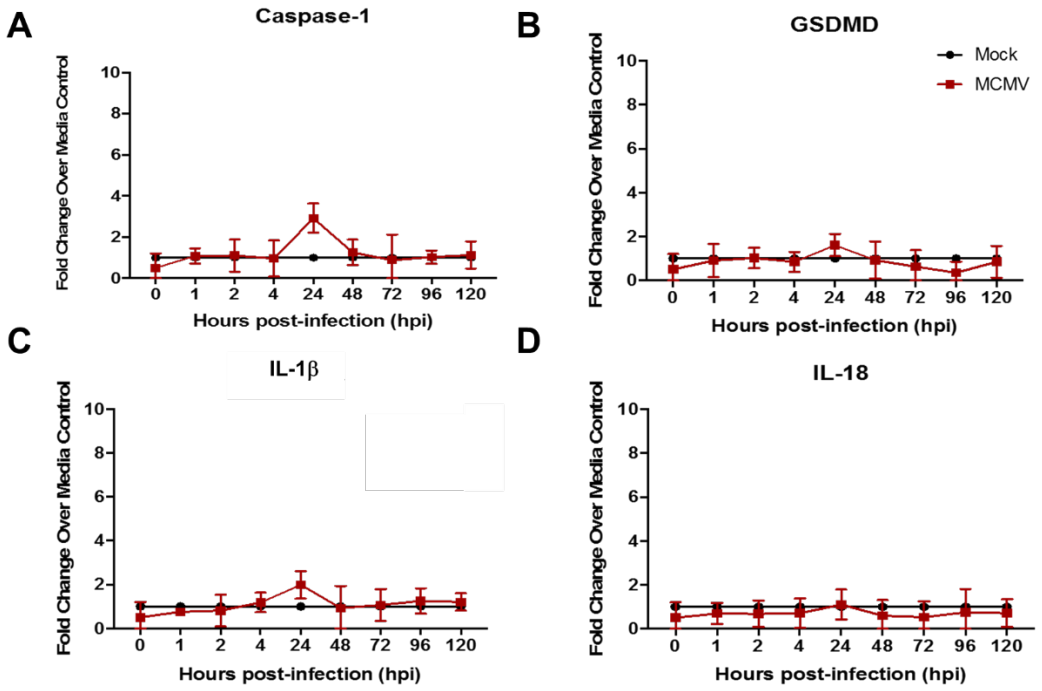

Figure 4.6. Pyroptosis-associated mRNA transcripts were not stimulated in HCMV-infected ARPE-19 cells.

ARPE-19 cells were infected with HCMV (moi = 3 PFU/cell) or treated with media control. At indicated time points, cells were harvested and assessed for caspase-1 mRNA (A), GSDMD mRNA (B), IL-1beta mRNA (C) or IL-18 mRNA (D) by real-time RT-PCR assay using the comparative $2^{-\Delta\Delta Ct}$ method, with all samples compared back to the media group at the same time point. Means ±SD of duplicate experimental repeats are shown. * $p<0.05$, ** $p<0.01$, and *** $p<0.001$, compared with respective media controls at the same time points as determined by one-way ANOVA.

Since RPE cells have so many protective functions aimed at protecting the retina to maintain the visual cycle, we thought it might be possible that this cell type could be actively suppressing this type of programmed cell death or inflammation to avoid provoking an inflammatory response directly adjacent to the retina. Therefore, we wanted to see if cell type made a difference in HCMV stimulation of inflammation and programmed cell death. Since MRC-5 cells are often used to titer HCMV, we knew that HCMV is able to replicate in this cell line. Therefore, MRC-5 fibroblasts were also infected with HCMV at a moi of 3, and infection was allowed to progress for 3 days. Similar to ARPE-19 cells, no mRNA production of caspase-

1 (Fig. 4.7A), GSDMD (Fig. 4.7B), IL-1β (Fig. 4.7C), or IL-18 (Fig. 4.7D) was shown, suggesting that HCMV infection alone may not be enough to stimulate a pro-inflammatory cell death response in these cells.

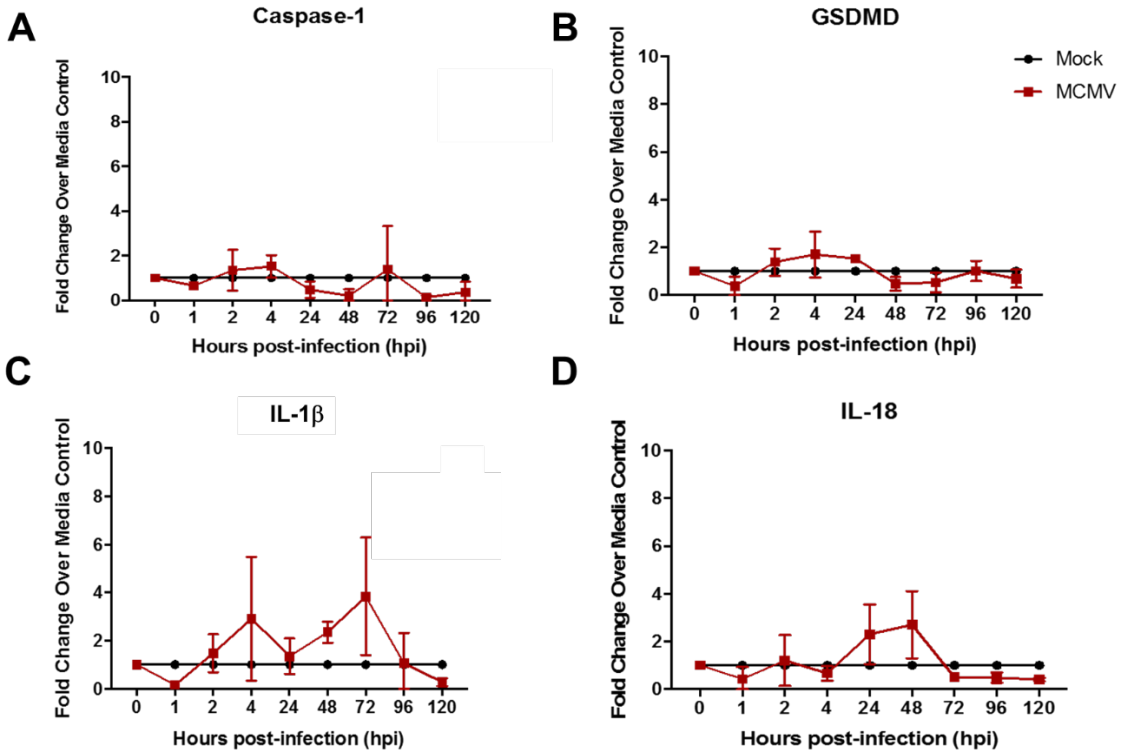

Figure 4.7. MRC-5 cells infected with HCMV did not show stimulation of pyroptosis-associated mRNA transcripts.

MRC-5 cells were infected with HCMV (moi = 3 PFU/cell) or treated with media control. At indicated time points, cells were harvested and assessed for caspase-1 mRNA (A), GSDMD mRNA (B), IL-1beta mRNA (C) or IL-18 mRNA (D) by real-time RT-PCR assay using the comparative $2^{-\Delta\Delta Ct}$ method, with all samples compared back to the media group at the same time point. Means ±SD of duplicate experimental repeats are shown. * $p<0.05$, ** $p<0.01$, and *** $p<0.001$, compared with respective media controls at the same time points as determined by one-way ANOVA.

5 Specific Aim 3

Specific Aim 3: Test the Hypothesis that Other Immune Response Genes or Pathways are Stimulated during the Pathogenesis of MAIDS-related MCMV Retinitis

In addition to the research obtained through the completion of these two specific aims, other experimental endpoints were determined on MAIDS-4 and MAIDS-10 mice to further advance our understanding past these well-known pyroptosis-related molecules and associated inflammasomes. If pertinent, the findings we determined from these studies could help shape the future focus of our investigation on the mechanisms underlying the pathogenesis of MAIDS-related MCMV retinitis.

5.1 Expression of IFI204 during MAIDS-related MCMV Retinitis

Interferon-gamma-inducible protein 16 (IFI16) is a PYD-containing HIN-200 protein that is constitutively expressed in lymphoid cells [258] and acts as a nuclear innate DNA sensor that results in inflammasome activation. Although we have never studied the involvement of the murine homolog of IFI16, IFI204, during MAIDS-related MCMV retinitis, IFI16 has been associated with several human herpesvirus infections [259-264], and the knockdown of IFI204 in corneal epithelium was shown to lead to susceptibility to HSV-1 infection [265]. Therefore, we sought to determine the extent by which IFI204 is stimulated in both MAIDS-4 and MAIDS-10 mice to determine whether IFI204 may also be contributing to MCMV retinitis. mRNA analysis showed that in MAIDS-4 mice (Fig. 5.1A), MCMV-infected eyes saw a slight stimulation of IFI204 that was greater at 3 days post-infection and subsequently decreased by day 10 post-infection when compared to media-injected control eyes. In retinitis susceptible MAIDS-10 mice (Fig. 5.1B), IFI204 mRNA expression showed peak expression at 6 days post-infection that was statistically significant compared to media-injected eyes and was also similar to the highest fold-

change seen in MAIDS-4 mice. Western blot analysis showed a substantial stimulation of IFI204 protein in MCMV-infected eyes of MAIDS-4 mice at both 3 and 6 days post-infection, which had greatly reduced by 10 days post-infection (Fig. 5.1C). MAIDS-10 mice showed an increase in IFI204 protein expression in MCMV-infected eyes when compared to media-injected eyes at all time points, and this trend of expression was similar to that seen during MAIDS-4 (Fig. 5.1D). These results suggest that while IFI204 inflammasomes may be activated in response to MCMV infection, it may not be contributing substantially to the pathogenesis of MCMV retinitis seen in MAIDS-10 mice, possibly due to the stimulation of other inflammasomes that may directly result in the onset of pyroptosis.

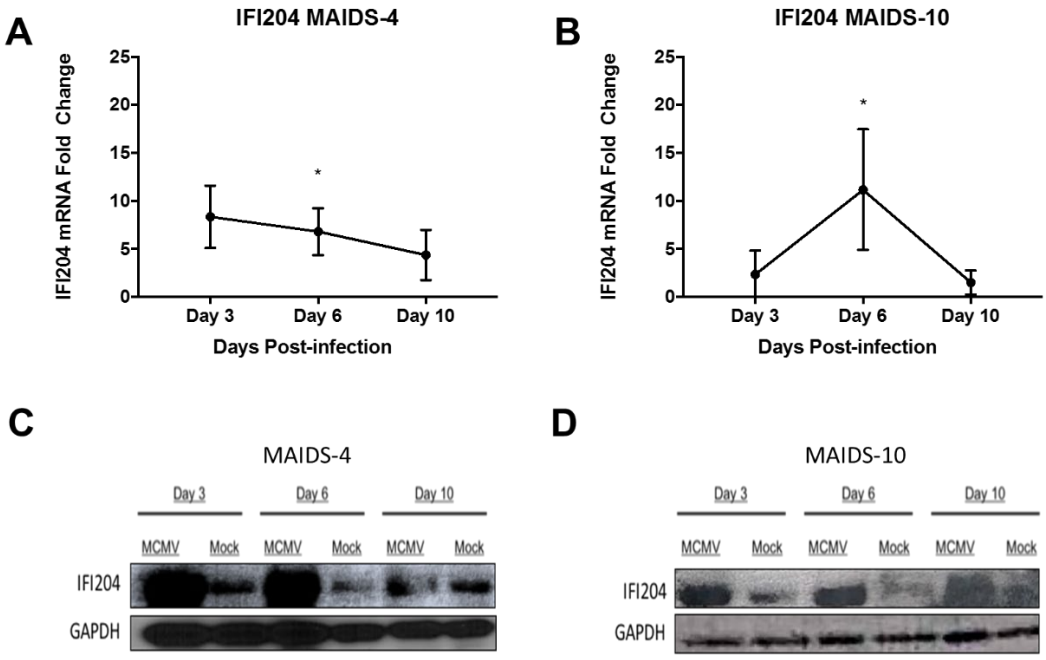

Figure 5.1. Intraocular IFI204 mRNA and protein were moderately stimulated in MCMV infected eyes of both retinitis susceptible MAIDS-10 mice and retinitis-resistant MAIDS-4 mice.

Whole eyes were collected at 3, 6, and 10 days post-infection (dpi) from MCMV infected eyes and media control eyes from groups (n=3-5) of MAIDS-4 and MAIDS-10 mice. Homogenized eyes were assessed for IFI204 mRNA from the MAIDS-4 mice (A) and the MAIDS-10 mice (B). Western blot analysis (C) was performed to assess ocular IFI204 protein expression in MAIDS-4 mice (C) and MAIDS-10 mice (D) with GAPDH used as a loading control. *$p<0.05$, MCMV groups compared with media control at the same time points.

5.2 Role of Autophagy during MAIDS-related MCMV Retinitis

Unlike pyroptosis and necroptosis, autophagy is a non-inflammatory form of cell death that is largely a protective process-induced under stress conditions by which cells engulf damaged organelles or large portions of their cytoplasm [234]. Recently, a link between autophagy and pyroptosis has emerged in which there is thought to be an interplay between the induction of autophagy and the inhibition of pyroptosis. Induction of autophagy in host cells in response to infection may be a means of protecting the cells from cell death [266]. Autophagy is known to play a protective role in the eye, including regulating the homeostasis of the RPE [267]. However, it was recently shown that MCMV might contain a mechanism to inhibit late-stage autophagy in RPE cells [268]. As evidence for multiple cell death pathways has been shown to be stimulated in MAIDS-related MCMV retinitis, it is possible that the induction of cell death may be related to inhibition or downregulation of autophagy. To determine the extent that autophagy was affected in MCMV-infected eyes during the pathogenesis of MCMV retinitis, mRNA analysis for beclin-1 was assessed. Beclin-1 mRNA was not significantly stimulated at 3, 6, and 10 days post-infection in MCMV-infected eyes of both retinitis resistant MAIDS-4 (Fig. 5.2A) mice and retinitis susceptible MAIDS-10 mice (Fig. 5.2B) when compared with uninfected control eyes. Western blot analysis showed that beclin-1 protein was expressed at 3, 6, and 10 days post-infection within MCMV-infected eyes of both MAIDS-4 (Fig. 5.2C) and MAIDS-10 (Fig. 5.2D) mice, however, the protein expression was substantially more in those of MAIDS-4 eyes than MAIDS-10 eyes. To determine the presence of autophagosome formation, a known hallmark of autophagy, LC3B-I, and LC3B-II protein expression was measured. No significant difference was seen for LCB-I protein expression between infected and

uninfected control eyes of both MAIDS-4 and MAIDS-10 mice at days 3, 6, and 10 days post-infection. However, LC3-I protein expression within MCMV-infected MAIDS-4 eyes was substantially increased when compared to LC3B-I protein expression within MCMV-infected MAIDS-10 eyes. Whereas LCB-II formation was detected within both MCMV-infected and media-injected control eyes at days 3, 6, and 10 post-infection, LCB-II formation was not detected within MCMV-infected eyes of MAIDS-10 mice. Taken together, these results suggest that autophagy may play a protective role in the eye that is mitigated during the development of MCMV retinitis in MAIDS-10 mice.

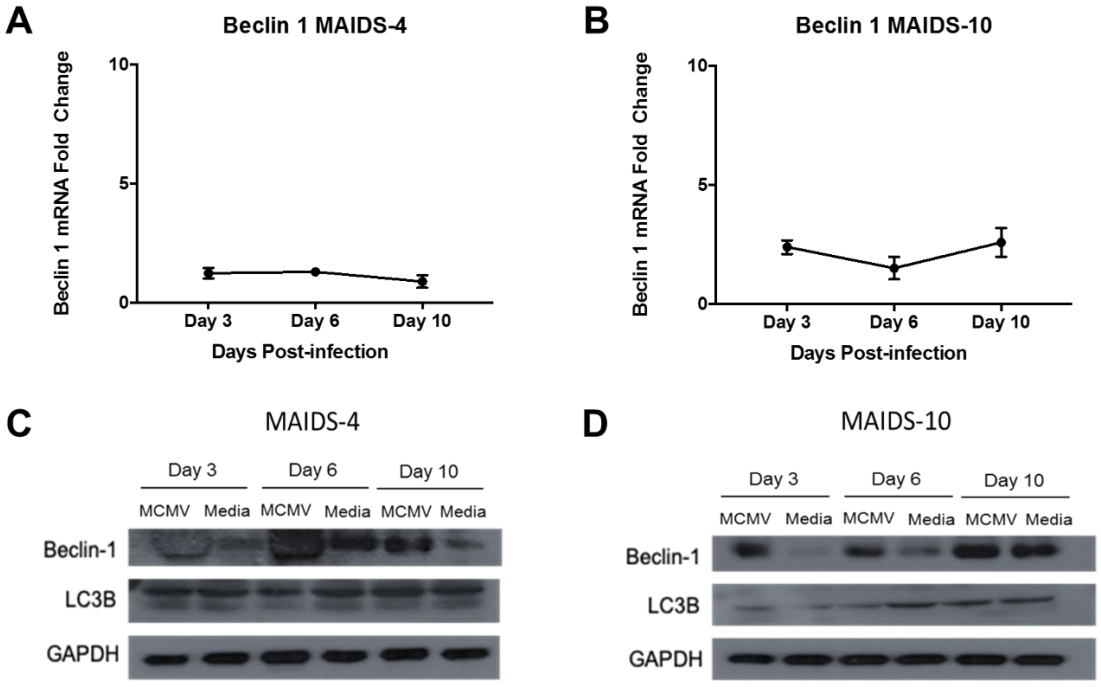

Figure 5.2. Intraocular beclin-1 mRNA and protein were moderately stimulated in MCMV infected eyes of both retinitis susceptible MAIDS-10 mice and retinitis-resistant MAIDS-4 mice.

Whole eyes were collected at 3, 6, and 10 days post-infection (dpi) from MCMV infected eyes and media control eyes from groups (n=3-5) of MAIDS-4 and MAIDS-10 mice. Homogenized eyes were assessed for beclin 1 mRNA from the MAIDS-4 mice (A) and the MAIDS-10 mice (B). Western blot analysis (C) was performed to assess ocular beclin 1 and LC3B protein expression in MAIDS-4 mice (C) and MAIDS-10 mice (D) with GAPDH used as a loading control. *$p<0.05$, MCMV groups compared with media control at the same time points.

5.3 Transcriptional Analysis of Immune Response Genes During Pathogenesis of MAIDS-related MCMV retinitis

It is evident through our previous studies that several factors contribute to the pathogenesis of MAIDS-related MCMV retinitis. Although extensive, our previous work has only scratched the surface of the events employed during this disease progression. Therefore, we opted to use an ultrasensitive technology, NanoString, to investigate hundreds of genes that span several pathways associated with the immune response, following MCMV infection throughout the course of MAIDS development. The goal of this study was to find other potential immunological pathways or targets that could be contributing to the retinal destruction seen during the pathogenesis of experimental MAIDS-related MCMV retinitis.

NanoString technology is a unique technique used to analyze the expression of hundreds of genes simultaneously and has been extensively used to investigate a variety of diseases [269-271]. The multiplexed probe library is made with two probes that are specific to each gene of interest. One probe is the capture probe that contains approximately 50 base pair sequence complementary to a specific target mRNA and is coupled with biotin as an affinity tag. The other probe is the reporter probe that contains approximately 50 base pairs complementary to the target mRNA and is also coupled to a color-coded tag. This color-coded tag is labeled explicitly with specific fluorophores used for detection. The order of the colors on the tag provides a unique barcode for each of the genes of interest, which are scanned by the Nanostring nCounter® system, allowing the system to get a raw count of all the target RNA hybridized to the probes [270]. Utilizing this technology, we were able to get an overview of the involvement of more than 500 genes during the onset and progression of retinitis in MCMV-infected eyes of MAIDS-

10 mice and compare that to the expression of the same genes in both MAIDS-4 and healthy mice, both resistant to retinitis.

Hierarchical Clustering Analysis of 561 Immune Response Gene Transcripts Within MCMV-Infected Eyes of Healthy Mice, MAIDS-4 Mice, and MAIDS-10 Mice. We have previously shown that the upregulation or downregulation of several pathways is involved during the pathogenesis of MAIDS-related MCMV retinitis, yet the knowledge we gained in these past studies have not been at the depth needed to identify and compare the extraordinary number of immune response genes expressed simultaneously within the ocular compartment at critical times during the evolution of MAIDS-related MCMV retinitis Initial studies were performed to determine the overall upregulation or downregulation of 561 immune defense genes during the pathogenesis of MCMV retinitis. This was accomplished using a commercial NanoString nCounter® Murine Immunology Panel that included 15 additional internal reference and housekeeping genes. The left eyes of groups of healthy mice, MAIDS-4 mice, and MAIDS-10 mice (n = 3 – 5) were inoculated with MCMV; the contralateral right eyes of each animal group were mock-infected with maintenance medium only and served as internal controls. At 3, 6, and 10 days after intraocular inoculation, individual MCMV-infected and mock-infected eyes were collected from all animal groups, subjected to total RNA extraction, pooled by groups, and subjected to NanoString nCounter® analysis.

Hierarchical clustering analysis showing the upregulation (blue), downregulation (yellow), or no change (black) in the expression of each of the 561 immune response gene transcripts analyzed for each group of MCMV-infected eyes or mock-infected eyes are shown on Fig 5.3. Inspection of data shows that patterns of gene expression differed greatly when comparing mock-infected and MCMV-infected eyes at each time point examined. More

importantly, the patterns of immune response gene expression were remarkably distinct for each animal group, reflecting resistance or the degree of susceptibility to MCMV retinitis development. The MCMV-infected eyes of healthy mice without MAIDS that show absolute resistance to retinitis development nonetheless exhibited active gene expression (Fig 5.3A). At least some of this transcriptional activity might be attributed to an intraocular trauma created in response to the needle stick that takes place during mock infection. In comparison, MCMV-infected eyes of MAIDS-4 mice and MAIDS-10 mice also showed active gene expression but with increased upregulation of genes when compared with MCMV-infected eyes of healthy mice. Of interest, MCMV-infected eyes of MAIDS-4 mice that fail to develop full-thickness retinal necrosis but nonetheless exhibit RPE proliferation showed an unexpected and extensive upregulation of a majority of the 561 immune response genes investigated at day 6 after virus inoculation (Fig 5.3B) when compared with retinitis-susceptible MCMV-infected eyes of MAIDS-10 mice at day 6 after virus inoculation (Fig 5.3C). This outcome was particularly surprising because of our previous observation that the MCMV-infected eyes of both animal groups harbor high and equivalent amounts of infectious virus. When compared at day 10 when full-thickness retinal necrosis develops within the MCMV-infected eyes of MAIDS-10 mice (but not within MCMV-infected eyes of MAIDS-4 mice), distinctly different patterns of upregulation or downregulation of individual immune response genes were observed.

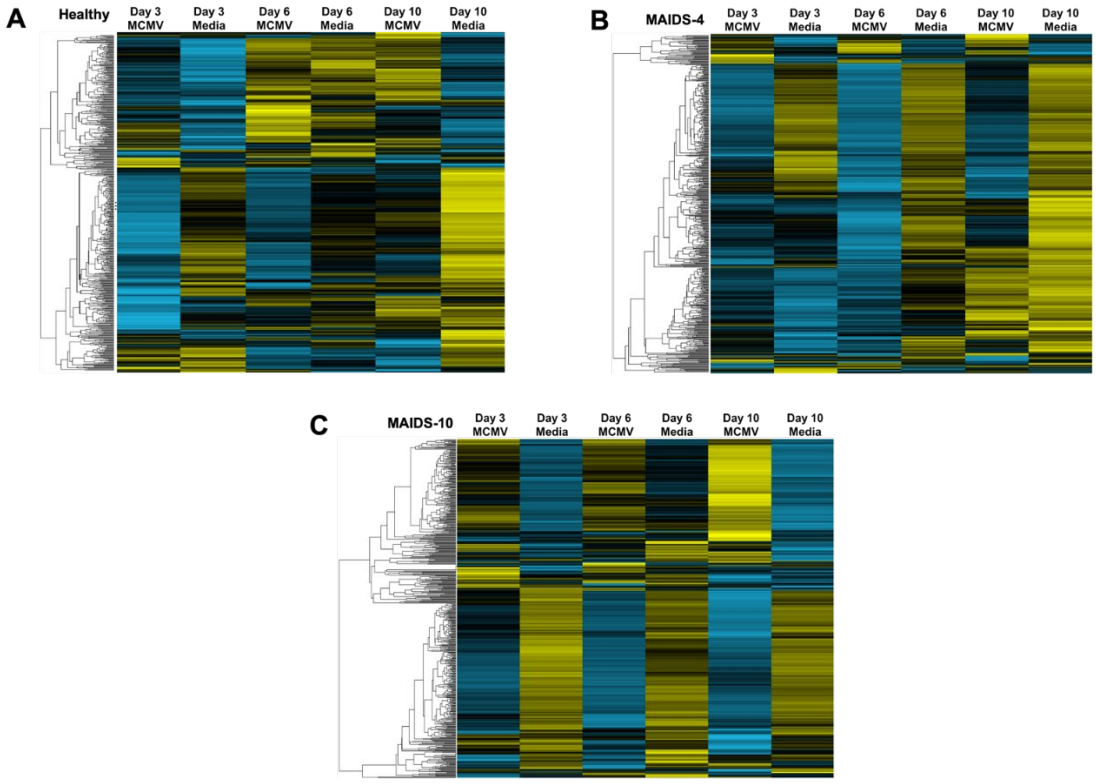

Figure 5.3. Hierarchical clustering analysis of 561 immunology related genes on healthy, MAIDS-4, and MAIDS-10 mice.

MCMV infected eyes and eyes injected with media were collected 3, 6, and 10 dpi from healthy (a), MAIDS-4 (b), and MAIDS-10 (c) mice. RNA was extracted from each eye (n= 3-5 mice/group), and total RNA was pooled for each group. 100ng of RNA from each group was loaded onto the NanoString nCounter® immunology panel. Hierarchical clustering analysis was done using the nSolver software. The columns represent the specified groups, and the lines represent each of the 561 genes on the immunology panel. Yellow color indicates low RNA expression and blue color indicates high RNA expression.

Comparison of MCMV-infected eyes of healthy mice, MAIDS-4 mice, and MAIDS-10 mice for the expression of genes associated with distinct immunologic pathways. We next processed the hierarchical clustering analysis of the 561 immune response gene transcripts from MCMV-infected eyes of healthy mice, MAIDS-4 mice, and MAIDS-10 mice at all time points examined for their involvement in 32 distinct immunologic pathways using the NanoString nSolver software. After determining the fold-change upregulation or downregulation for differentially expressed immune-response genes of MCMV-infected eyes when compared with mock-infected eyes for each animal group, a fold-change of less than two was used to exclude that particular gene from further analysis. This approach revealed 17 genes upregulated and 15 genes downregulated within MCMV-infected eyes of healthy mice, 83 genes upregulated and 4 genes downregulated within MCMV-infected eyes of MAIDS-4 mice, and 92 genes upregulated and 54 genes downregulated within MCMV-infected eyes of MAIDS-10 mice (Fig 5.4). A growing increase in immune response gene activity within MCMV-infected eyes during increased susceptibility to the development of full-thickness retinal necrosis (when analysis proceeded from healthy mice to MAIDS-4 mice to MAIDS-10 mice) was expected as suggested by prior heatmap findings.

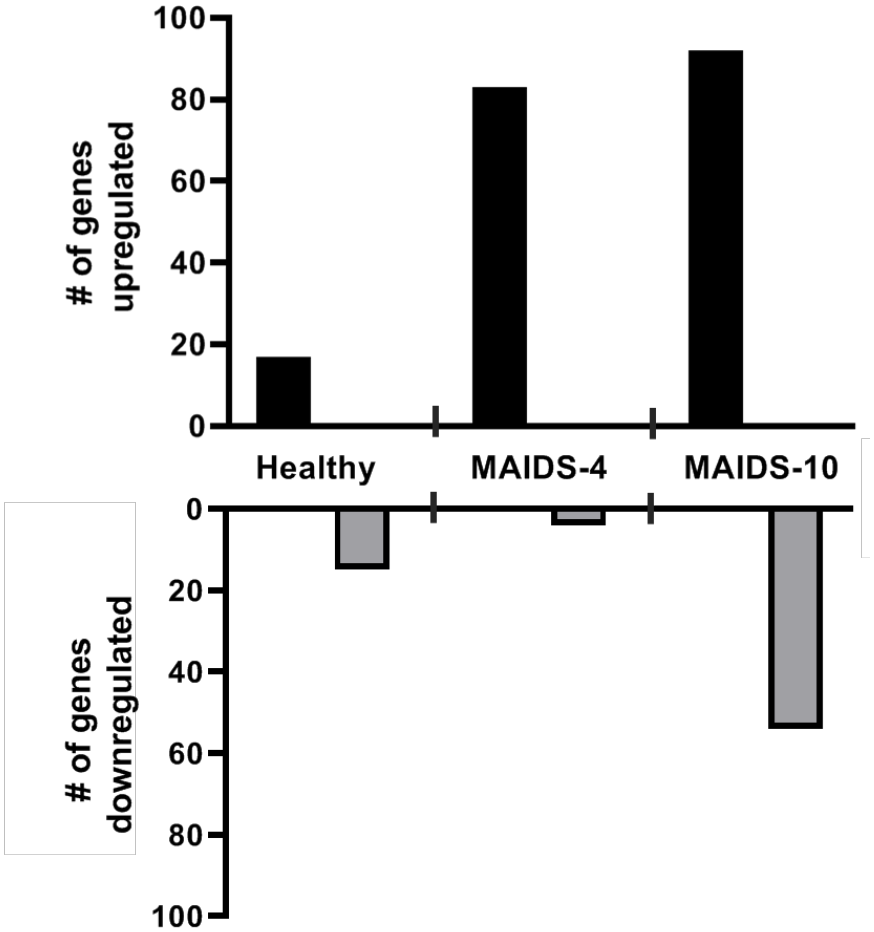

Figure 5.4. Number of upregulated and downregulated genes of MCMV-infected eyes of healthy, MAIDS-4, and MAIDS-10 mice.

Analysis of the differentially expressed genes with a fold-change of higher than two revealed the number of genes that were upregulated and downregulated in groups of healthy, MAIDS-4, and MAIDS-10 mice. Of the 561 genes on the immunology panel 17 genes were upregulated and 15 genes downregulated within MCMV-infected eyes of healthy mice, 83 genes were upregulated and 4 genes were downregulated within MCMV-infected eyes of MAIDS-4 mice, and 92 genes were upregulated and 54 genes were downregulated within MCMV-infected eyes of MAIDS-10 mice.

This trend also continued when the differentially expressed immune response genes showing upregulation of activity were organized into NanoString-defined immunologic pathways for each animal group with the understanding that each gene could be involved with multiple pathways. Categorization into immunologic pathways revealed that five of the 32 NanoString-defined pathways exhibited relatively substantial stimulation of gene activity within MCMV-infected eyes when compared with other pathways of MCMV-infected eyes of healthy mice, MAIDS-4 mice, and MAIDS-10 mice during progressive susceptibility to MCMV retinitis. Those pathways showing the most robust stimulation gene activity included pathways associated with the broad categories of adaptive immunity, innate immunity, host-pathogen interactions, cytokine signaling, and lymphocyte activation (Fig. 5.5A-E). More functionally focused pathways such as those involved with NF-kB signaling, toll-like receptor signaling, NOD-like receptor signaling, chemokine signaling, type 1 interferon signaling, type 2 interferon signaling, tumor necrosis factor (TNF) family signaling, MHC class I antigen presentation, and phagocytosis and degradation also showed less robust but nonetheless heightened gene activity when comparing MCMV-infected eyes of MAIDS-4 and MAIDS-10 mice with MCMV-infected eyes of healthy mice (Fig 5.5F-N). Overall, these findings demonstrated that gene activity associated with immunologic pathways become progressively and dramatically more active in numbers and functions as MCMV-infected eyes become progressively more susceptible to the onset and development of full-thickness retinal necrosis as retrovirus-induced immunosuppression ensues. Moreover, this progressive gene activity is far more complex than originally thought and involved a large number of immune pathways of which several were never considered by us to be involved in the evolution of cytomegalovirus retinitis in retrovirus-immunosuppressed hosts.

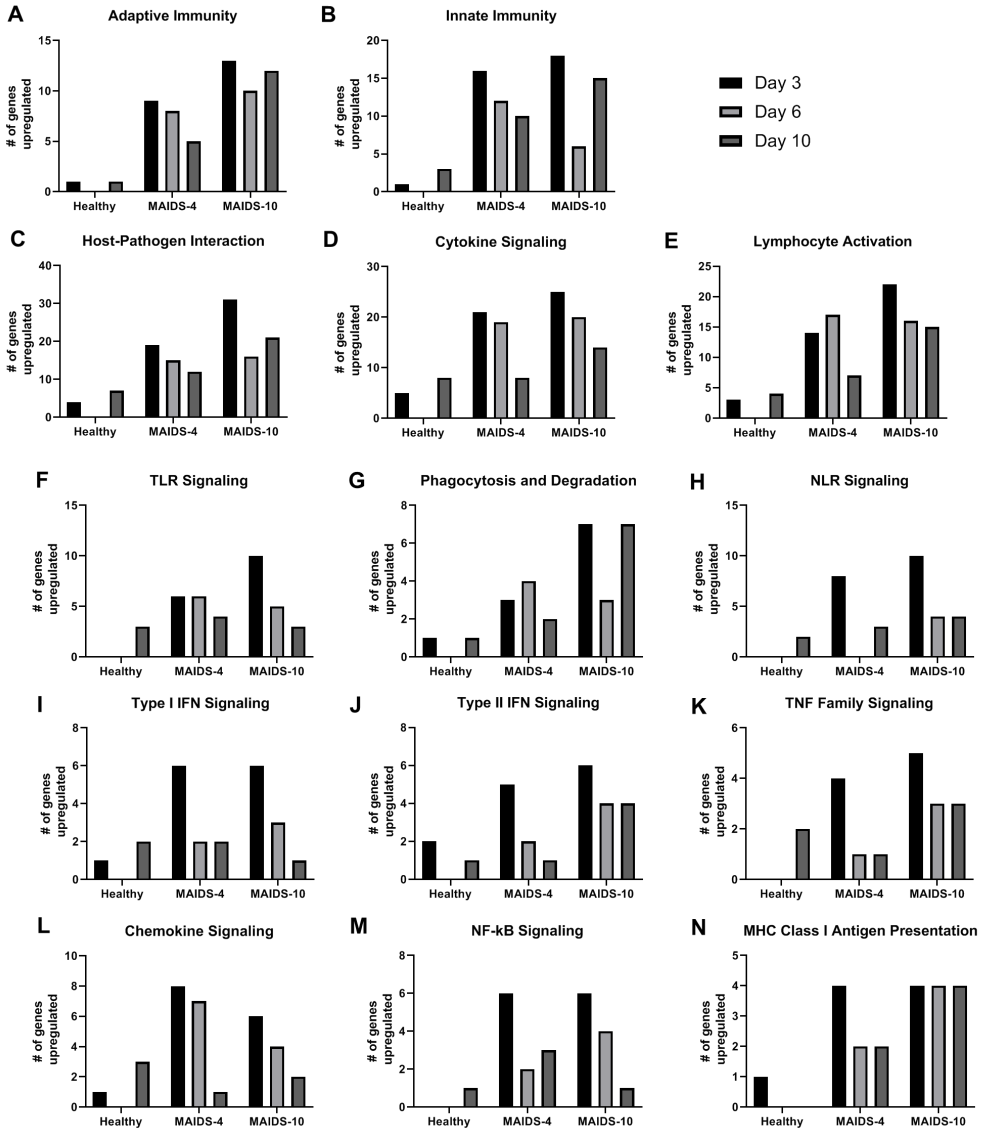

Figure 5.5. Number of upregulated genes associated with different pathways in MCMV-infected eyes of healthy, MAIDS-4, and MAIDS-10 mice.

Analysis of the differentially expressed genes with a fold-change higher than two were classified into the different NanoString-defined pathways. The number of upregulated genes associated with each pathway was graphed for healthy, MAIDS-4, and MAIDS-10 mice at days 3, 6, and 10 postinfection. A-E) Represents the pathways that had the most robust stimulation and included broad pathways associated with adaptive immunity, innate immunity, host-pathogen interactions, cytokine signaling, and lymphocyte activation. F-N) Represents more functionally focused pathways including those involved with NF-kB signaling, toll-like receptor signaling, NOD-like receptor signaling, chemokine signaling, type 1 interferon signaling, type 2 interferon signaling, tumor necrosis factor (TNF) family signaling, MHC class I antigen presentation, and phagocytosis and degradation which also showed a substantial numbers of stimulated genes.

A comparison of the top 15 differentially expressed immunologic-associated genes within MCMV-infected eyes of healthy mice, MAIDS-4 mice, and MAIDS-10 mice. In an attempt to provide a more quantitative analysis of differences in the expression activity of the 561 individual immune response genes analyzed within MCMV-infected eyes of mice showing progressive susceptibility to retinitis development, we focused on 15 differentially expressed genes showing the greatest upregulation at peak levels of expression at 3, 6, or 10 days after intraocular MCMV inoculation and compared them with mock-infected eyes for groups of healthy mice, MAIDS-4 mice, and MAIDS-10 mice. Table 5.1, Table 5.2, and Table 5.3 summarizes our findings for MCMV-infected eyes for each animal group (healthy, MAIDS-4, and MAIDS-10, respectively) with respect to individual genes, their known function(s) [226, 272-313], their overall fold-change at peak expression, and their *p* values when compared with mock-infected eyes. The fold-change for stimulation of the top 15 individual genes within MCMV-infected eyes appeared to increase markedly from healthy mice to MAIDS-4 mice and MAIDS-10 mice as a reflection of increased susceptibility to the onset and development of MCMV retinitis among these animal groups, especially MAIDS-4 animals when compared with MAIDS-10 animals. While the average fold increase for peak expression in activity of these 15 genes was 3.04 for MCMV-infected eyes of healthy mice, the average fold increase for peak expression in activity increased to 20.14 and 20.74 for MCMV-infected eyes of MAIDS-4 mice and MAIDS-10 mice, respectively, suggesting a far more dynamic intraocular gene transcription activity in response to MCMV infection during progressive retrovirus-induced immunosuppression than during immunocompetence. It is also noteworthy that a subset of individual genes exhibited remarkable transcription activity, such as *ccl5,* a gene encoding for a chemokine associated with inflammation which showed an 83.32-fold increase in activity within

MCMV-infected eyes of MAIDS-10 mice susceptible to full-thickness retinal necrosis development.

Table 5.1: Top 15 genes differentially expressed in MCMV-infected eyes of healthy mice.

Top 15 Genes Upregulated in MCMV infected Eyes of Healthy Mice			
Gene	**Function [Ref.]**	**Peak Expression**	**p value**
Bst1	Facilitates pre-B-cell growth and induces cell migration [272]	3.25	0.0298
Casp3	Activation plays a role in the execution -phase of apoptosis [273]	2.36	0.0117
Ccl3	Associated with macrophage recruitment [274]	2.28	0.0324
Ccl9	Induces chemotaxis of CD4+ T cells, CD8+ T cells, and monocytes [275]	3.09	0.0107
Cd2	Regulates natural killer cell lytic activity and proinflammatory cytokine production [276]	2.74	0.0365
Clec5a	Involved in neutrophil extracellular trap formation and proinflammatory cytokine production [277]	3.74	0.0244
Emr1	Murine marker of macrophages (F4/80) [278]	2.48	0.0280
H2-K1	Bind to and present antigens derived from pathogens onto the cell surfaces for T cell recognition [279]	4.37	0.0444
Ifnar2	Part of IFN-α and IFN-β receptor and critical for antiviral immunity [280]	2.10	0.0377
Itgb2	Involved in extravasation into tissues during infection or injury [281]	3.03	0.0016
Jak2	Involved in signal transduction of interferon and cytokine signaling [282]	2.70	0.0131
Ptafr	Involved in proinflammatory signaling [283]	2.53	0.0230
Ptgs2	Involved in the production of prostacyclin, expressed in inflammation [284]	3.80	0.0011
Stat2	Aids in the activation of the transcription of interferon stimulated genes [285]	4.37	0.0350
Tgfb1	Inhibits the actions of T cells and the secretion of IFN-γ, (TNF-α), and interleukins [286, 287, 288]	2.75	0.0091

Table 5.2: Top 15 genes differentially expressed in MCMV-infected eyes of MAIDS-4 mice.

Top 15 Genes Upregulated in MCMV infected Eyes of MAIDS-4 Mice			
Gene	**Function [Ref.]**	**Peak Expression**	**p value**
Ccl12	Attracts eosinophils, monocytes, and lymphocytes to the site of infection [289]	10.88	0.0450
Ccl2	Involved in chemotaxis and regulating inflammation [290]	51.23	0.0353
Ccl7	Promotes the recruitment of monocytes and neutrophils to the site infection [291]	34.39	0.0350
Ccr5	Acts as a receptor for chemokines [292]	11.10	0.0123
Cfb	Regulates the alternative pathway of the complement system [293]	27.79	0.0030
Cxcl10	Attracts CD8+ and CD4+ T cells to the site of inflammation [294]	30.24	0.0374
Cxcl9	Attracts T cells to the site of inflammation [295]	28.12	0.0413
Icos	Involved in the induction and regulation of Th1, Th2, and Th17 immunity [296]	10.01	0.0354
Ifit2	Plays a role in the stimulation of interferons as part of an anti-viral response [297]	17.09	0.0008
Irgm1	Involved in the polarization of M1 (inflammatory driven) macrophages [298]	12.16	0.0450
Itgal	Involved in leukocyte cellular adhesion and costimulatory signaling [299]	11.48	0.0185
Lilrb3	Functions as an inhibitory receptor to help balance the function of innate immune cells [300]	9.59	0.0407
Lilrb4	Transduces a negative signal that inhibits stimulation of the immune response [301]	16.53	0.0209
Ptprc	Suppresses JAK kinases as a negative regulator of cytokine signaling [302]	10.54	0.0490
Slamf7	Induces B cell proliferation [303]	21.03	0.0411

Table 5.3: Top 15 genes differentially expressed in MCMV-infected eyes of MAIDS-10 mice.

Top 15 Genes Upregulated in MCMV infected Eyes of MAIDS-10 Mice			
Gene	**Function [Ref.]**	**Peak Expression**	**p value**
Ccl2	Involved in chemotaxis and regulating inflammation [290]	35.19	0.0323
Ccl5	Promotes the recruitment of leukocytes to the site of infection [304]	83.32	0.0263
Cd274	Plays a major role in suppressing the adaptive arm of the immune system [305]	7.36	0.0145
Ctss	Degrades antigenic proteins for antigen presentation [306]	12.69	0.0443
Cybb	Involved in the formation of reactive oxygen species [307]	9.83	0.0191
Fcgr3	Participates in signal transduction triggering lysis by natural killer cells [308]	6.92	0.0425
Fcgr4	Promotes macrophage-mediated phagocytosis and antigen presentation to T cells [309]	10.03	0.0307
Ifi204	Acts as a nuclear innate DNA sensor resulting in inflammasome activation [310]	15.33	0.0202
Il1rn	Binds non-productively to the interleukin-1 receptor preventing IL-1 from sending a signal [311]	48.31	0.0017
Irgm1	Involved in the polarization of M1 (inflammatory driven) macrophages [298]	8.36	0.0303
Lilrb3	Functions as an inhibitory receptor to help balance the function of innate immune cells [300]	10.74	0.0062
S100a9	Controls macrophage accumulation and cytokine production [312]	17.85	0.0179
Slamf7	Induces B cell proliferation [303]	29.00	0.0425
Socs1	Involved in the negative feedback regulation of cytokine signaling [226]	6.98	0.0208
Tyrobp	Activates signal transduction and plays a role in inflammation [313]	9.42	0.0468

A detailed comparison of the top 15 immune response genes activated within MCMV-infected eyes of healthy mice, MAIDS-4 mice, and MAIDS-10 mice also revealed that some upregulated gene activities were exclusive to each animal group whereas some upregulated gene activities were shared between groups. This is depicted in the Venn diagram shown in Fig 5.6. Whereas the top 15 upregulated genes of the eyes of MCMV-infected mice of healthy mice that are absolutely resistant to MCMV retinitis development were found to be exclusive to this animal group, 4 of the top 15 upregulated genes of the eyes of MCMV-infected mice of MAIDS-4 and MAIDS-10 groups were shared between these animal groups. This observation, however, should not diminish the observation that 11 of the top 15 upregulated genes of the MCMV-infected eyes of these animal groups were exclusive to MAIDS-4 mice and MAIDS-10 mice, animals that exhibit remarkably distinct patterns of MCMV-induced retinal disease.

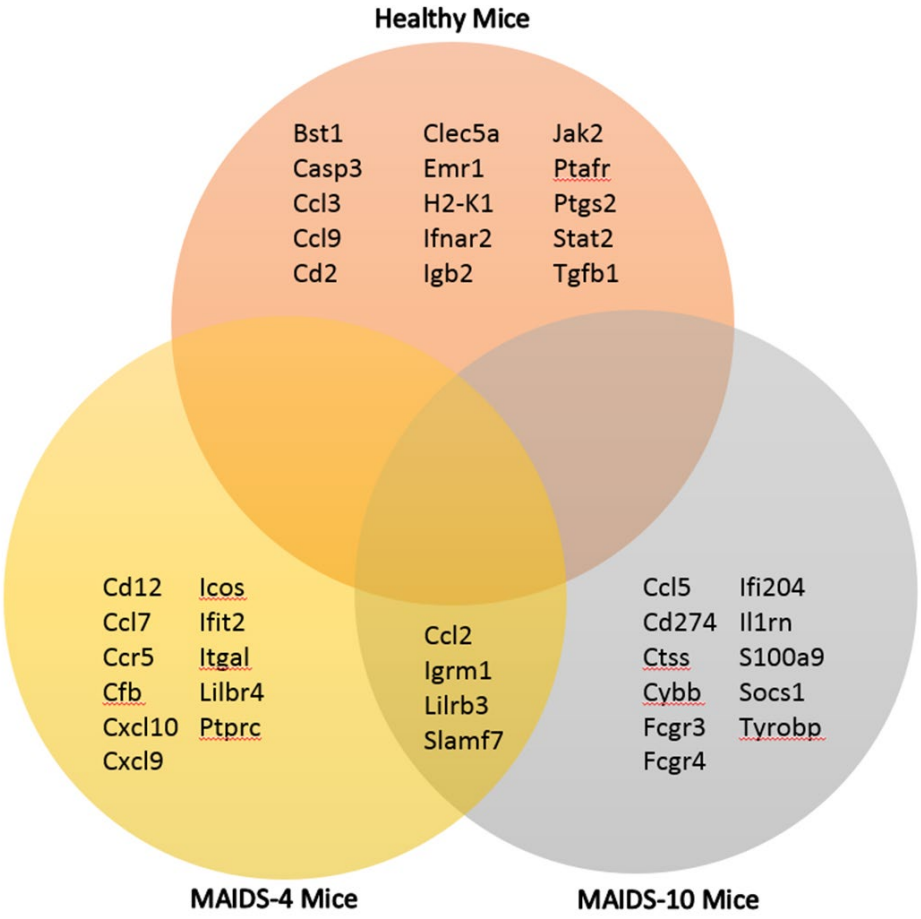

Figure 5.6. Venn diagram comparing the shared expression of the top 15 differentially expressed genes between healthy, MAIDS-4, and MAIDS-10 mice.

The top 15 upregulated genes of MCMV-infected eyes differentially expressed in healthy, MAIDS-4, and MAIDS-10 mice were compared between groups to see if any genes were amongst that highest stimulated in more than one group of mice. Of the 15 genes with the highest RNA fold-changes, only 4 genes are found to be commonly expressed between MAIDS-4 and MAIDS-10 mice.

Analysis of 14 additional immune response gene transcripts of MCMV-infected eyes of healthy mice, MAIDS-4 mice, and MAIDS-10 mice associated with programmed cell death pathways. Use of the commercially available NanoString nCounter® Murine Immunology Panel provided a wealth of new and at times unexpected knowledge on the upregulation or

downregulation of 561 immune response genes during the onset and development of MAIDS-related MCMV retinitis. Given our present interest in programmed cell death pathways and their relative roles in the pathogenesis of MCMV-induced full-thickness retinal necrosis in MAIDS-10 mice, we created a custom panel consisting of 14 genes. These included 3 genes associated with autophagy, 3 genes associated with necroptosis, 2 genes associated with parthanatos, and 6 genes associated with pyroptosis and inflammasomes. Importantly, gene transcription analysis using this custom gene panel for cell death pathways was performed using the same samples collected from MCMV-infected eyes of healthy mice, MAIDS-4 mice, and MAIDS-10 mice that were used above to generate data using the commercially available murine immunology gene panel. Genes associated with apoptosis were excluded from this custom panel because we have already determined previously and with confidence, using mice with MAIDS deficient in key apoptosis-associated genes, that this programmed cell death pathway contributes only minimally to the pathogenesis of MAIDS-related MCMV retinitis.

A summary of the upregulation or downregulation for each of the 14 immune response genes within MCMV-infected eyes of each animal group at 3, 6, and 10 days after intraocular MCMV inoculation, their overall positive (upregulated) or negative (downregulated) fold-change at peak expression, and their *p* values when compared with mock-infected eyes is shown in Table 5.4, Table 5.5, and Table 5.6 for healthy mice, MAIDS-4 mice, and MAIDS-10 mice respectively. Due to the relatively small size of 14 genes being analyzed in this experiment, a two-fold-change in gene activity was not used to exclude some genes for analysis as was done for the 561 immune response genes analyzed above. The MCMV-infected eyes of healthy mice absolutely resistant to the development of MCMV retinitis exhibited a pattern of cell death pathway-associated gene activity that suggested significant quiescence of activity for each

pathway at all days post-infection examined. In fact, downregulation of gene activity was consistently observed for all 3 necroptosis genes and all 6 pyroptosis and associated inflammasome genes at 3, 6, and 10 days post-infection. Gene activities for autopathy and parthanatos were also found to be either downregulated or only minimally upregulated (< 2-fold increase) within MCMV-infected eyes of healthy mice at all days post-infection examined. As MCMV-infected eyes of animals at different stages of MAIDS development became more susceptible to the development of retinal disease, however, genes associated with some but not all cell death pathways under investigation became increasingly active. This was apparent within the MCMV-infected eyes of MAIDS-4 mice and MAIDS-10 mice for necroptosis and pyroptosis and pyroptosis-associated inflammasomes but not for autophagy and parthanatos.

Table 5.4: RNA expression of MCMV-infected eyes of healthy mice for genes on a custom NanoString panel.

Fold Change of MCMV-infected Eyes of Healthy Mice							
Cell Death Pathway	Genes	Day 3		Day 6		Day 10	
		Δ	p value	Δ	p value	Δ	p value
Autophagy	Atg12	1.07	0.3855	1.24	0.0792	1.14	0.1344
Autophagy	Atg5	-1.05	0.0155	-1.13	0.0269	-1.02	0.0047
Autophagy	Becn1	0.05	0.5346	-0.05	0.5090	1.07	0.3855
Necroptosis	Mlkl	-3.53	0.1688	-1.59	0.0012	-4.34	0.0500
Necroptosis	Ripk1	-1.46	0.0491	-1.31	0.0248	-1.63	0.0048
Necroptosis	Ripk3	-2.34	0.0983	-2.01	0.0632	-2.87	0.0016
Parthanatos	Parg	1.07	0.1772	1.24	0.2209	0.02	0.5158
Parthanatos	Parp1	0.07	0.5445	1.33	0.0385	1.11	0.1695
Inflammasome/Pyroptosis	Aim2	-2.27	0.0457	-1.45	0.0013	-2.07	0.0073
Inflammasome/Pyroptosis	Casp11	-6.83	0.2365	-2.86	0.0683	-7.90	0.1394
Inflammasome/Pyroptosis	Gsdmd	-2.64	0.0437	-1.95	0.0636	-2.91	0.0033
Inflammasome/Pyroptosis	Nlrc4	-3.78	0.1043	-1.81	0.1011	-4.14	0.0538
Inflammasome/Pyroptosis	Nlrp1b	-0.01	0.5154	-0.07	0.5284	-1.24	0.0510
Inflammasome/Pyroptosis	Nlrp3	-2.42	0.0483	-0.01	0.5328	-2.25	0.0837

Table 5.5: RNA expression of MCMV-infected eyes of MAIDS-4 mice for genes on a custom NanoString panel.

Fold Change of MCMV-infected Eyes of MAIDS-4 Mice							
Cell Death Pathway	Genes	Day 3		Day 6		Day 10	
		Δ	p value	Δ	p value	Δ	p value
Autophagy	Atg12	0.05	0.5378	-1.13	0.0314	-0.44	0.5109
Autophagy	Atg5	1.52	0.2518	1.19	0.0172	0.10	0.6342
Autophagy	Becn1	1.25	0.3402	1.19	0.0855	0.05	0.5810
Necroptosis	Mlkl	4.73	0.1322	6.69	0.0625	6.01	0.2067
Necroptosis	Ripk1	1.98	0.1282	2.25	0.1306	2.34	0.0547
Necroptosis	Ripk3	3.18	0.2738	4.49	0.2026	5.29	0.0467
Parthanatos	Parg	-0.03	0.5322	-0.13	0.5056	-1.28	0.0612
Parthanatos	Parp1	1.06	0.5000	1.21	0.1669	-1.49	0.1188
Inflammasome/Pyroptosis	Aim2	2.56	0.0470	2.72	0.1099	3.03	0.0995
Inflammasome/Pyroptosis	Casp11	8.74	0.1416	11.25	0.0666	8.81	0.0533
Inflammasome/Pyroptosis	Gsdmd	3.59	0.0783	5.05	0.1068	3.59	0.1095
Inflammasome/Pyroptosis	Nlrc4	7.67	0.1999	7.40	0.0953	4.61	0.0291
Inflammasome/Pyroptosis	Nlrp1b	1.58	0.2863	1.74	0.1732	4.54	0.2836
Inflammasome/Pyroptosis	Nlrp3	4.23	0.1047	3.41	0.0672	3.64	0.1983

Table 5.6: RNA expression of MCMV-infected eyes of MAIDS-10 mice for genes on a custom NanoString panel.

Fold Change of MCMV-infected Eyes of MAIDS-10 Mice							
Cell Death Pathway	Genes	Day 3		Day 6		Day 10	
		Δ	p value	Δ	p value	Δ	p value
Autophagy	Atg12	-0.07	0.5202	1.19	0.3286	1.08	0.0424
Autophagy	Atg5	1.32	0.0101	1.36	0.1665	1.69	0.0092
Autophagy	Becn1	1.41	0.0465	1.28	0.2578	1.59	0.1850
Necroptosis	Mlkl	5.75	0.1482	4.16	0.1853	3.43	0.1166
Necroptosis	Ripk1	2.20	0.0978	1.96	0.0565	2.17	0.0272
Necroptosis	Ripk3	3.80	0.0057	3.93	0.0228	4.14	0.0091
Parthanatos	Parg	-1.14	0.0119	1.21	0.2048	-1.26	0.0085
Parthanatos	Parp1	-0.13	0.5111	1.19	0.1190	-1.63	0.0736
Inflammasome/Pyroptosis	Aim2	2.08	0.1594	2.44	0.0244	2.04	0.1032
Inflammasome/Pyroptosis	Casp11	12.65	0.0358	5.07	0.1811	5.83	0.0631
Inflammasome/Pyroptosis	Gsdmd	4.41	0.0707	2.68	0.1036	3.63	0.0073
Inflammasome/Pyroptosis	Nlrc4	7.20	0.2324	6.05	0.3290	4.23	0.0659
Inflammasome/Pyroptosis	Nlrp1b	-0.10	0.5529	1.80	0.3369	1.12	0.3362
Inflammasome/Pyroptosis	Nlrp3	3.08	0.0882	3.36	0.1534	1.40	0.2788

6 DISCUSSION AND CONCLUSION

6.1 Specific Aim 1: Pyroptosis and Inflammasome Expression during MCMV Infection

Specific Aim 1: Test the Hypothesis that Pyroptosis and Associated Inflammasomes are Stimulated by MCMV during Immunosuppression, Contributing to the Onset and Development of MCMV Retinitis

Our finding that GSDMD was upregulated in MCMV-infected eyes of MAIDS-10 but not MAIDS-4 mice provides further evidence of a role for pyroptosis in MAIDS-related MCMV retinitis. Therefore, we want to determine the role that pyroptosis-related genes and associated inflammasomes have on the development of full-thickness retinal necrosis by inducing MAIDS in mice devoid of one of these molecules and determining the affect ocular MCMV infection has on retinitis development. Further evidence for the involvement of this pathway in the development was assessed by inducing MCMV retinitis in another model of immunosuppression and checking for the stimulation of these pyroptosis-related molecules and associated inflammasomes.

6.1.1 GSDMD and Caspase-11 Expression Following MCMV Infection in MAIDS-4 Mice

Whereas mRNA levels of caspase-1, IL-1β, and IL-18 were not previously shown to be stimulated in the MCMV-infected eyes of MAIDS-4 mice, the mRNA for both GSDMD and caspase-11 showed similar levels of stimulation in MCMV-infected eyes of MAIDS-4 mice as in MAIDS-10 mice when compared to their relative mock infected control eyes. Despite being considered part of the noncanonical pathway, caspase-11 is like caspase-1 in its ability to cleave and activate GSDMD. Therefore, it is not surprising that a consistent pattern of GSDMD mRNA upregulation throughout the course of viral infection in both MAIDS-4 and MAIDS-10 mice

mirrors that seen for caspase-11. While the increase in expression of both caspase-11 and GSDMD at MAIDS-4 suggests the activation of the noncanonical pathway of pyroptosis, MAIDS-4 mice are resistant to retinitis, and it appears that only with the stimulation of the canonical pathway during MAIDS-10 is there resulting retinal damage. This could be attributed to caspase-11 being unable to directly cleave IL-1β and IL-18 [267], thereby preventing the release of the active forms of these cytokines, which may be the driving force behind retinal necrosis. Therefore, the role caspase-11, and its cleavage of GSDMD independent of inflammasomes, plays prior to the onset of retinitis remains to be explored.

6.1.2 The Loss of the Pyroptosis Pathway and MAIDS-related MCMV Retinitis

Inflammasomes and their downstream effector, pyroptosis, are increasingly becoming a topic of interest in ocular disease. Pyroptosis was first described as an alternative cell death pathway involving inflammation [143], a feature that distinguishes it entirely from apoptosis (reviewed in [314]). For this reason, inflammasome driven pyroptosis [315] and its implication in various diseases are of interest. Of note are the recent discoveries centered on the extent to which inflammasomes and/or pyroptosis play a role in several ocular disorders. AMD is a sight-threatening, progressive disorder of the retina that specifically targets and damages the macula, the part of the retina responsible for sharp, central vision. Recently, elevated levels of the NLRP3 inflammasome, IL-1β, and IL-18 expression were found in AMD macular lesions [208]. The destructive effects of AMD can also be seen by resultant RPE thinning or depigmentation, which can lead to RPE atrophy and death of photoreceptors. The NLRP3 inflammasome was found to be upregulated in the RPE during the pathogenesis of advanced AMD following RPE atrophy [209]. Inhibition of the NLRP3 inflammasome components prevented RPE degeneration in a model of AMD [210], providing evidence for NLRP3 driven pyroptosis in the pathophysiology

of AMD. Analysis of photoreceptor cell death in a model of retinal degeneration showed the upregulation of NLRP3, caspase-1, IL-1β, and IL-18 in cone photoreceptors but not rod photoreceptors [211], suggesting that the overall induction of pyroptosis in the retina may be unique to specific cell populations, or influenced by the mechanism leading to cell death. As AIDS-related HCMV-retinitis is also associated with retinal destruction and RPE pathology, it is not surprising that pyroptosis-related molecules, caspase-1, IL-1β, and IL-18, along with several inflammasomes, were previously shown to be stimulated in our mouse model of experimental MAIDS-related MCMV retinitis.

The pyroptosis pathway and several inflammasomes have a profound impact on the development of full-thickness retinal necrosis in MCMV-infected eyes of MAIDS mice. Herein we provide new information showing that pyroptosis and associated inflammasomes indeed play a prominent role in the progression of classic cytomegalovirus retinitis during retrovirus-induced immunosuppression. Our findings provide new evidence: (i) whereas a deficiency in the canonical pyroptosis pathway during MAIDS does not result in a reduction in the amount of infectious virus produced within MCMV-infected eyes when compared with MCMV-infected eyes of wildtype MAIDS animals, the frequency of full-thickness retinal necrosis is significantly reduced to zero within MCMV-infected eyes of pyroptosis-deficient mice with MAIDS when compared with a frequency of 100% within MCMV-infected eyes of wildtype MAIDS mice (ii) a deficiency in several inflammasomes result in a significant reduction in the amount of infectious MCMV produced in infected eyes when compared to wildtype MAIDS mice, but this value is still substantially higher than seen in MCMV-infected eyes of healthy mice; and (iii) the retinas of MCMV-infected eyes of pyroptosis-deficient and inflammasome-deficient mice with MAIDS consistently exhibit abnormal histopathologic

features characterized by RPE proliferation but with relative preservation of the neurosensory retina regardless of which pyroptosis-associated gene of the canonical pyroptosis pathway is compromised.

It is important to note that IL-1R1$^{KO\ mice}$were used for this study instead of mice deficient in IL-1β, as these mice are not commercially available from the vendor used for all previous and concurrent studies. IL-1R1 is a cytokine receptor that binds IL-1 which then initiates intracellular signal transduction resulting in the activation of inflammatory mediators [316]. Although mice lacking the IL-1R1 gene are still capable of producing IL-1β, the receptor is imperative for the biological actions of IL-1β do not respond to the IL-1β produced [317].

The RPE is the likely the source for the high amounts of infectious virus. Because MCMV-infected eyes of all animal groups with MAIDS that were deficient in different genes of the pyroptosis pathway or inflammasomes consistently showed prominent RPE proliferation but without destruction of the neurosensory retina, we postulate that the source for the high amounts of infectious virus production observed within MCMV-infected eyes of KO mice with MAIDS was the RPE rather than cells comprising the neurosensory retina. Whereas virus-induced nuclear inclusions indicative of productive MCMV replication were observed within the RPE of MCMV-infected eyes of KO mice with MAIDS, virus-induced inclusions were not observed within the relatively intact neurosensory retinas of these animals. The neurosensory retina was also devoid of cytomegalic cells that are often prominent within the full-thickness retinal necrosis of MCMV-infected eyes of wildtype MAIDS mice. This support the notion that the RPE are initially infected with virus that originates from the blood and supports rounds of virus replication subsequent to the infection of cells of the neurosensory retina and ultimate development of full-thickness retinal necrosis.

The retinal architecture of all KO mice is like that seen in MAIDS-4 mice. Consistent with other studies that shows a neuroprotective role [318-320] or ocular preservation [243, 246, 252] effects when inhibiting inflammasomes during the course of disease, MAIDS mice deficient in the NLRP3 and the NLRP1b inflammasomes showed a remarkable reduction in the frequency of retinitis, albeit there was still evidence of RPE proliferation and retinal folding. The same resulting architecture was consistent with that seen in all other KO mice utilized throughout this study. It is interesting to note that that loss of the pyroptosis pathway within the MCMV-infected eyes of MAIDS-10 mice converted the pattern of retinal disease to that already observed for MCMV-infected eyes of MAIDS-4 mice. This intriguing observation suggests that pyroptosis is indeed essential for the development of full-thickness retinal necrosis in mice with MAIDS, and, more importantly, suggests that pyroptosis as a key contributor to the pathogenesis of MAIDS-related MCMV retinitis becomes operative later than four weeks after retrovirus infection during the evolution of MAIDS. It is noteworthy that this would be at a time after a shift in cytokine production from a Th1 profile to a Th2 profile that has been shown to commence at 3 to 4 weeks after retrovirus infection during MAIDS development. An identical Th1/Th2 shift in cytokine production has been identified in HIV-infected patients with AIDS.

6.1.3 Ocular MCMV Infection during Corticosteroid-induced Immunosuppression

The results of our study show that MCMV infection highly stimulates both mRNA and protein expression of pyroptosis-related molecules caspase-1, caspase-11, GSDMD, IL-1β, and IL-18, during experimental MCMV retinitis in both retinitis-susceptible MAIDS mice and mice with corticosteroid-induced immunosuppression. This stimulation correlates with the expression of several inflammasomes, NLRP3, NLRP1b, NLRC4, and AIM2 which is also significantly stimulated in both models of immunosuppression. The expression of these proteins in both

models of MCMV retinitis further implicates that these proteins are involved in the pathogenesis of MCMV retinitis. The stimulation of the pyroptosis pathway and associated inflammasomes would invoke large-scale inflammation to the MCMV infection, and this inflammatory response could attribute for the full-thickness retinal necrosis seen during MCMV retinitis.

Although both the retroviral-induced immunosupression and the corticosteroid-induced immunosuppression render C57BL/6 mice susceptible to the development of MCMV retinitis, there are vast differences in the way the immunosuppression develops between these two models. MAIDS have a slow and progressive development, which goes through distinct phases of immune cell dysfunction over the course of several weeks. Corticosteroid-induced immunosuppression, however, results in a rapid, acute decline in the immune system, which develops over the course of several days and shows a difference in immune cell populations, particularly macrophages and cytokine response to infection [115, 116]. However, as both models of immunosuppression results in the development of MCMV retinitis, it is not surprising that the overall stimulation of these inflammatory molecules are similar between corticosteroid-induced immunosuppression and mice with MAIDS-10. These data provide further evidence that pyroptosis-related proteins and associated inflammasomes are involved in the onset and development of experimental MCMV retinitis in susceptible, immunologically suppressed mice.

6.2 Specific Aim 2: Pyroptosis Expression Following MCMV Infection of Cells

Specific Aim 2: Test the Hypothesis That MCMV Replication Directly Stimulates Pyroptosis In Infected Cells

6.2.1 Pyroptosis-Associated Expression Kinetics Following MCMV infection in IC-21 or MEF Cells

Pyroptosis-associated molecules are more highly expressed in MCMV-infected MEFs than in MCMV-infected IC-21 mouse macrophages. We characterized the expression of pyroptosis-related expression during either MCMV or HCMV infection in cell culture models. MCMV infection of IC-21 macrophages and MEF cells resulted in stimulation of several pyroptosis-associated mRNA transcripts. However, despite the early stimulation of caspase-1, GSDMD, and IL-1β of mRNA transcripts in both IC-21 mouse macrophages and MEFs, the level of stimulation was substantially higher in MEFs cell and stayed stimulated for a longer duration. Although, IL-18 mRNA in MEFs showed only a slightly significant stimulation of mRNA transcripts 1 hpi, protein for IL-18 showed robust expression at 6 hpi and 24 hpi suggesting that this pro-inflammatory cytokine is stimulated following MCMV-infection in this cell line. On the contrary, IL-18 mRNA expression was not stimulated following MCMV-infection in IC-21 mouse macrophages and was in fact downregulated at later time-points post-infection. Since IL-18 plays a role in the induction of inflammatory cytokines, TNF-α, IL-6, IL-1β, in addition to being a chemoattractant for neutrophils [321] it is possible that this cytokine is being suppressed by MCMV as an attempt to control inflammation, or prevent destruction by neutrophils. As this downregulation is not seen following ocular MCMV in MAIDS-10 mice developing retinitis [6], it is possible this might be a response specific to macrophages as a means for MCMV to establish latency in these cell types. Further investigation needs to be done to determine which ocular cell types are directly undergoing pyroptosis following MCMV infection during the pathogenesis of MAIDS-related MCMV retinitis.

6.2.2 Pyroptosis-Associated Expression Following Infection with UV-inactivated MCMV in MEF cells

The stimulation of pyroptosis by MCMV may be dependent on viral replication. The substantial reduction of pyroptosis-related mRNA and protein stimulation in MEFs infected with UVi-MCMV suggests that attachment, adsorption, and release of tegument proteins are not sufficient to stimulate this pathway in MCMV-infected MEFs. Therefore, this proposes that MCMV viral gene expression is necessary for triggering the expression of these mRNA transcripts and proteins. The temporal kinetics of MCMV viral replication has previously been characterized in fibroblasts. It has been determined that MCMV IE gene transcription occurs between 1-4 hpi in fibroblasts and is seen as early as 1 hpi in macrophages [32]. E genes for MCMV are detected at about 2 hpi and are seen until about 16 hpi in fibroblasts [33], the point in which MCMV L gene expression begins and can continue for at least 36 hours [30]. The transcription of these L genes encodes for most of the viral tegument and glycoproteins which are involved in capsid assembly, virion maturation, and egress from host cell. Any part of this stepwise viral gene expression and replication has the potential to invoke a response in the host cell that may provoke the induction of pyroptosis. Due to the timing of the mRNA production, it appears as though the induction of caspase-1 and IL-1β mRNA transcription is stimulated immediately following the start of IE transcription. This may mean that the transcription of GSDMD mRNA may result following the transcription of mRNA upstream in the pyroptosis pathway, or it may be that GSDMD mRNA production is directly stimulated by the transcription of viral E genes. Although no mRNA production of pyroptosis-associated molecules is seen as a response to infection with UVi-MCMV, there does appear to be slight expression of these proteins, especially at 24 hpi. Although this expression is nowhere near the level seen for

MCMV infected cells, it could indicate that the presence of foreign viral proteins responsible for either attachment, adsorption, or release from the tegument might stimulate the activation of proteins already expressed by the cell. However, without the stimulation of viral gene expression, there may not be enough danger signals detected by the cell to induce transcription of the mRNA transcripts responsible for carrying out pyroptosis.

6.2.3 Pyroptosis-Associated Expression Kinetics Following HCMV Infection in ARPE-19 or MRC-5 Cells

The lack of stimulation of pyroptosis in HCMV infected ARPE-19 cells may be dependent on the cell type. It was astonishing to observe that HCMV infection of APRE-did not result in the stimulation of mRNA transcripts associated with pyroptosis. RPE cells are polarized epithelial cells that reside between the retina and choroid and provide several functions necessary for the survival of the neurosensory retina. Some of these functions include transportating of nutrients to the retina, regulating homeostasis, scavenging free radicals and reactive oxygen species, and phagocytosis of the rod outer segments following normal circadian shedding [87]. Damage to the RPE could result in the pathogenesis of several retinal diseases, and since the viral proliferation of CMV has been found in the RPE layer in CMV retinitis, it is possible that damage caused by viral infection could lead to the retinitis developed in this model of ocular disease. The use of primary human RPE cultures are often used to study the RPE physiology *in vitro* [322], but this method does not come without limitations. First, primary RPE cells cultured from different donors may display genetic variability and physiological differences between donors. Additionally, it is possible that these cells may also lose their ability to differentiate within a few numbers of passages [323]. Another major disadvantage of primary RPE cells is the difficulty in obtaining human donors. For this reason, the use of an immortalized

cell line of RPE, ARPE-19 [324], has been widely used to study the physiology and characteristics of this tissue. The use of these cells is also not without limitations. A major concern is that ARPE-19 cells may not preserve the specialized characteristics and functions as those seen in RPE *in vivo*. Recently, an RNA-Seq analysis demonstrated that the transcriptome of ARPE-19 cells, appropriately cultured and with a low-passage number, closely resembles those of native human RPE. The study shows that the only differences seen in ARPE cells passaged for 4 months was an increase in genes related to RPE functions, such as visual cycle, phagocytosis, and pigmentation, while there was a decrease in genes regarding cell cycle and proliferation, as well as apoptosis [325]. Since pyroptosis shares a few characteristics with apoptosis, it is feasible that these ARPE-19 cells may also be losing gene transcription that would engage pyroptosis. However, without transcriptome analysis on signaling specific for pyroptosis comparing the cells at different passages, it would be hard to say for sure. Duplication of this study in primary RPE cells obtained from a suitable donor may also help determine if the results of this experiment are related to culture specifications.

The lack of stimulation of pyroptosis in HCMV infected MRC-5 cells may be dependent on virologic replication. Regardless of the lack of stimulation of pyroptosis in ARPE-19 cells, it is rather interesting that infection of MRC-5 cells also did not result in the stimulation of pyroptosis-associated proteins. Contrary to these findings, one study did show that max expression of caspase-1 and IL-1β in CMV infected fibroblasts did show fold-changes over media control cells of 2.4 and 8.9, respectively. However, this study did not specify the kinetics of this stimulation, and therefore it cannot be said with certainty that this expression was during the time points investigated in this present study. Several studies have focused on HCMV's ability to suppress the induction of cell death pathways as a means to prevent inhibition of their

replication. Recently, HCMV was shown to be able to block the induction of necroptosis [326]. Although no substantial evidence has demonstrated that HCMV is capable of inhibiting pyroptosis, one study did suggest that expression of the HCMV gene UL83 was able to reduce the expression of one inflammasome, AIM2, which has been shown to respond to CMV infection, and that this reduced expression inhibited the processing of IL-1β in HEK293T cells [327]. More work needs to be done to investigate if CMV is, in fact, capable of suppressing pyroptosis as a means to promote replication and to determine if this is preventing the stimulation of these mRNA transcripts in MRC-5 fibroblasts.

6.3 Specific Aim 3: Additional Immunological Expression and MCMV Infection

Specific Aim 3: Test the Hypothesis that Other Immune Response Genes or Pathways are Stimulated during the Pathogenesis of MAIDS-related MCMV Retinitis

6.3.1 Expression of IFI204 during MAIDS-related MCMV Retinitis

Inflammasomes are multiprotein complexes that are part of innate immunity and regulate caspase-dependent inflammation and cell death. Inflammasomes, specifically those belonging to the NLR subset, have widely been attributed to ocular diseases [227, 228, 236-238, 328]. The inflammasome-associated protein, IFI16, is a dsDNA sensing protein, and it is well known to be associated with human herpesviruses, all of which contain a dsDNA genome. HSV-1 has been shown to have reduced viral titers in the presence of IFI16 [260]. Additionally, the siRNA mediated knockdown of IFI16 has been shown to result in reactivation of EBV as well as the enhancement of HCMV replication, while overexpression of IFI16 resulted in decreased viral loads for both these herpesviruses [261]. Furthermore, the murine homology, IFI204, has also been shown to be associated with murine models of ocular herpes infection [265]. For this reason, it is not surprising that IFI204 is upregulated in MCMV-infected eyes of both MAIDS-4

and MAIDS-10 mice in response to the dsDNA genome of MCMV. As there appears to be no substantial difference between the stimulation and expression of IFI204 between MCMV-infected eyes of MAIDS-4 mice resistant to retinitis and MAIDS-10 mice susceptible to retinitis, likely, IFI204 is merely responding to the MCMV infection and may not be contributing to the onset and progression of MAIDS-related MCMV retinitis, as might be the case with other previously investigated inflammasomes.

6.3.2 Role of Autophagy during MAIDS-related MCMV Retinitis

Autophagy is a well-conserved pathway that, under normal physiological conditions, regulates cellular homeostasis by eliminating damaged organelles and proteins. Autophagy can also serve adaptive mechanisms during cellular stresses, such as starvation, depletion of growth factor [329], and the removal of intracellular pathogens [329, 330]. Autophagy-related proteins are strongly expressed in several layers of the retinal— the ganglion cell layer, inner nuclear layer, outer nuclear layer—as well as the underlying RPE layer, which depend on autophagy mechanisms to maintain the structure and normal physiological function. Autophagy has been shown to play a protective role against diseases of the retina and RPE, and dysfunction of autophagy has been associated with several ocular disorders such as AMD and a model of photoreceptor degeneration in the rd/rd mouse during light-damage [331]. It can also be activated to prevent Fas-mediated apoptosis, as seen in the photoreceptors following retina-RPE separation [332]. As autophagy plays a role in the ocular clearance of several microorganisms such as *T. gondii* [333]*, Pseudomonas aeruginosa* [334], and HSV-1 [335], we were interested in seeing the response of autophagy-related molecules to MCMV ocular infection. Interestingly, there only appeared to be stimulation of beclin-1 protein in MCMV-infected eyes of both MAIDS-4 and MAIDS-10 mice when compared to the uninfected control eyes. Controversially, beclin-1

mRNA, and LC3B protein expression were similar between infected and uninfected eyes of MAIDS-4 and MAIDS-10 mice, suggesting that autophagy is not induced upon ocular MCMV infection. Surprisingly, the protein levels of beclin-1, LC3B-I, and LC3B-II were all substantially higher in MAIDS-4 mice when compared to MAIDS-10 mice, which suggests that retrovirus-induced immunosuppression impacts the expression of autophagy-associated proteins. This stimulation of autophagy markers within MCMV-infected eyes of MAIDS-4 mice resistant to retinitis suggests that autophagy may play a protective role that is mitigated during the development of MCMV retinitis in MAIDS-10 mice, which as shown, may contribute to the destruction seen from inflammation-related programmed cell death pathways, such as apoptosis and necroptosis. This is in agreement with other studies that suggest that autophagy protects against MCMV retinitis pathogenesis by preventing MCMV infection-induced apoptosis [336], as well as a study that shows that decrease autophagy levels were linked to increased RPE cell susceptibly to apoptosis in response to stress [267].

6.3.3 Transcriptional Analysis of Immune Response Genes During during MAIDS-related MCMV Infection

Herein we confirmed and extended our understanding of some of the immunologic events that take place during the onset and development of cytomegalovirus retinitis in the unique setting of retrovirus-induced immunosuppression. Our findings show (i) the pathogenesis of retinal disease in MCMV-infected eyes of MAIDS-10 mice susceptible to full-thickness retinal necrosis development is associated with the robust upregulation and downregulation of an extensive number of immune response genes that operate in several distinct immune response pathways; (ii) the temporal development of MCMV retinitis within the eyes of MAIDS-10 mice is a dynamic process that involves the upregulation and downregulation of a number of immune

response genes at different times after intraocular MCMV infection; and (iii) the pattern of immune response gene activation differs remarkably within MCMV-infected eyes of healthy mice resistant to retinitis development when compared with MCMV-infected eyes of mice at different stages of MAIDS that exhibit a profound difference in their susceptibility to full-thickness retinitis development. A more focused companion investigation also provided compelling evidence for the stimulation of the transcription of multiple genes associated with the necroptosis and pyroptosis programmed cell death pathways during the development MAIDS-related MCMV retinitis.

For our investigation of immune response gene expression during the pathogenesis of MAIDS-related MCMV retinitis, we used the NanoString nCounter® assay, a recently developed platform capable of making without amplification a direct multiplexed measurement of gene expression within the ocular compartment following intraocular MCMV inoculation of mice for comparisons during immunocompetence and MAIDS. Although it is a powerful tool that allows for the quantification of the expression of hundreds of genes simultaneously and thereby provide a snapshot of gene activity at any one-time during disease pathogenesis, we initiated the investigation mindful of several limitations using this experimental approach. Firstly, the amount of data obtained after the performance of a single experiment is overwhelming and requires thoughtful use of statistical analysis to help provide meaningful conclusions. Secondly, subsequent performance of quantitative RT-PCR and/or western blot assays is essential to confirm the upregulation or downregulation of an individual gene under investigation. Thirdly, the data generated is highly descriptive without providing mechanistic insights into the function of an individual gene during a pathogenic event. Finally, it has not escaped our attention that the NanoString nCounter® assay provides only fold-change differences in transcription activity that

may or may not be biologically significant during disease pathogenesis. The quantitative fold-change activity of an individual gene may not be a true reflection of the unique kinetics of that particular gene's mRNA and consequently its functional ability. For example, a two-fold increase in transcriptional activity may be biologically significant for one gene, but another gene may require a far greater transcriptional increase (and for a greater duration) to be biologically significant.

Despite these limitations, the NanoString nCounter® assay has proven to be a useful tool to point us quickly in new directions of investigation and thereby expand our knowledge base of those immune functions that contribute (or not contribute) to the onset of MCMV-induced retinal disease and progression to full-thickness necrosis during MAIDS. More importantly, however, use of the NanoString nCounter® assay has given us the opportunity to validate previous findings by us and others on the role of various immune responses toward the pathogenesis of experimental MCMV retinitis during immunosuppression. Most of the findings presented herein are in good agreement with findings documented by us in past publications that have focused on various immune-mediated pathways and/or individual molecules associated with innate or adaptive immunity vis-a-vis the pathogenesis of MAIDS-related MCMV retinitis. These include roles for humoral immunity [337], cellular immunity [338, 339] suppressor of cytokine signaling (SOCS) pathways [126, 226], TNF-α [103], interferon-γ [103], and a number of proinflammatory cytokines associated with innate immunity [6, 340] as summarized by us in a recent review [114]. The findings of the present investigation using a custom panel consisting of genes associated with necroptosis and pyroptosis as well as pyroptosis-related inflammasomes also confirm our previous reports that these programmed cell death pathways may be involved in the progression of MCMV retinitis during MAIDS when we used quantitative RT-PCR assays to

show significant intraocular upregulation of many mRNAs involved in the operation of these pathways [6].

In summary, our experience using the NanoString nCounter® assay to provide a novel transcriptional analysis of the 575 immune response genes within MCMV-infected eyes of mice at different stages of MAIDS development compared with MCMV-infected eyes of immunologically normal mice has provided new, and at times, unexpected information on the pathogenesis of MAIDS-related MCMV retinitis. By extension, our findings may also improve our understanding of the pathogenesis AIDS-related HCMV retinitis. While helpful in many ways, we have also identified areas of caution when using this powerful research tool. Future use of this technology by us will be directed toward the identification of host genes expressed by different cell populations of retinal tissues during the onset and progression of MAIDS-related MCMV retinitis. Moreover, because host RNA constitutes an overwhelming portion of the total RNA recovered from infected tissue samples when compared with pathogen RNA that usually comprises a vanishingly small portion of total RNA, this technology will also allow us to investigate with greater precision the pattern of mRNA synthesis for individual MCMV genes that are expressed within retinal tissues and retina-related cell populations during the course of disease development following intraocular MCMV infection of retrovirus-immunosuppressed mice.

6.4 Future Direction

Clinical inhibition of GSDMD with necrosulfonamide could further signify the contribution that the execution of pyroptosis has on the development of experimental MAIDS-related MCMV retinitis. Although mice with systemic knockdown of GSDMD have recently become available, the demand for these mice are still relatively low, and the duration of

time needed to breed and supply these mice can take several months. Additionally, while the use of these mice may demonstrate the necessity for the GSDMD for the development of MAIDS-related MCMV retinitis, it does not directly translate to whether solely ocular inhibition of GSDMD, and not systemic treatment, will prevent further retinal damage in AIDS patients undergoing treatment for AIDS-related HCMV retinitis. Necrosulfonamide (NSA) has recently been identified as a direct chemical inhibitor of GSDMD to inhibit pyroptosis pharmacologically. Systemic administration of this drug was shown to be efficacious in a murine model of sepsis [341], suggesting the potential use of this drug to treat other inflammatory diseases, such as MAIDS-related MCMV retinitis. As many drugs are incapable of crossing the blood-retinal-barrier, it is uncertain if systemic administration of NSA will offer ocular protection against MCMV. Therefore, it would be necessary to establish the effectiveness of systemic or ocular administration of NSA and whether this would need to be given before MCMV infection. Determining the effectiveness of inhibiting GSDMD through NSA would help determine if this could be a pharmacological treatment for AIDS-related HCMV retinitis.

6.5 Clinical Significance

HCMV is an opportunistic infection in individuals with a CD4+ T-cell count below 50 cells/μL and is, therefore, among the most frequent opportunistic infections in individuals with AIDS. AIDS patients are particularly susceptible to sight-threatening retinitis caused by HCMV directly infecting the retinal tissues. Factors that contribute to retinal tissue destruction are virus-induced cytopathology, and inflammation mediated by neutrophils and activated macrophages. Before the availability of cART, 46% of patients with AIDS experienced vision loss and blindness caused by HCMV retinitis [69-71]. Although treatment with cART has lowered the number of new cases of HCMV retinitis, AIDS-related MCMV retinitis remains a significant

ophthalmological problem as access to cART is not readily available worldwide and several individuals who do have access fail to adhere or respond to treatment [71-73]. Although vaccination is one of the more effective methods for controlling problematic infectious diseases, attempts at creating an effective vaccine against HCMV have so far been unsuccessful [74, 75]. HCMV replication can generally be controlled by lifelong administration of antiviral drugs, such as ganciclovir, cidofovir, or foscarnet, yet these drugs may cause harmful side-effects, do not eradicate the virus, and merely slows the progression of ocular damage associated with HCMV infection [76-78]. Although the clinical features of AIDS-related HCMV retinitis are well established, the direct mechanisms by which the HCMV infection of the retina causes the severe retinal damage is still unknown.

To investigate the mechanisms responsible for the onset and progression of the retinal damage seen during AIDS-related HCMV retinitis, our lab uses a clinically relevant mouse model of MAIDS-related MCMV retinitis. The MAIDS model is a suitable model for this study because species-specific retroviruses cause both MAIDS and AIDS, and mice with MAIDS share many immunopathologic features with AIDS patients. This includes a characteristic progressive development of chronic generalized lymphadenopathy, a polyclonal B-cell activation, and a shift in the levels of Th1 and Th2 CD4+ T-cells with an eventual diminishment in CD4+ T-cell and CD8+ T-cell counts and functions [112, 119, 121-123]. Retinitis susceptible MAIDS mice will then develop retinitis ten days post subretinal MCMV injection, exhibiting histopathological features similar to those seen in AIDS-related HCMV retinitis, which include full-thickness retinal necrosis, the presence of cytomegalic cells, and transition zones between areas of the normal and diseased retina [4, 125].

By using this model, the work contributing to this study also contributed to the advancement of ocular research by furthering our fundamental understandings of the pathogenesis of AIDS-related HCMV retinitis, as well as the potential contribution to the stimulation of pyroptosis-associated proteins may have on the onset of retinal destruction in general. If pyroptosis does contribute to the pathogenesis of retinal destruction, prevention of this pathway may be a target to help improve the treatment and prevention of further damage to affected eyes and/or offer protection to the contralateral eye from undergoing vision loss. As several caspases may induce pyroptosis, a pan-caspase-inhibitor, if clinically available, may be offered as a locally administered treatment option. As other cell death pathways may be caspase-dependent, this form of treatment could be a way to mitigate retinal destruction resulting from multiple cell death pathways. As the activation of GSDMD is ultimately responsible for the formation of pores in the cells and mass release of inflammatory cytokines, inhibition of GSDMD by ocular administration of necrosulfonamide, if proven effective, may be another form of treatment option to combat the retinal destruction seen with AIDS-related HCMV retinitis.

6.6 Summary

Specific Aim 1. The pyroptosis pathway and associated inflammasomes are stimulated within the ocular compartment of MCMV-infected eyes of retinitis susceptible MAIDS-10 mice. There is a marked reduction in the activity of the pyroptosis pathway and associated inflammasomes in MCMV-infected eyes of MAIDS-4 mice resistant to the development of full-thickness retinal necrosis. The presence of viral inclusion bodies in the RPE but not the neurosensory retina of all KO MAIDS mice suggests that the RPE is the source of the high amounts of infectious virus in MCMV-infected eyes. The loss of the pyroptosis pathway and inflammasomes convert the pattern of retinal disease to that seen for MAIDS-4 mice. This

suggests that pyroptosis is essential for the development of full-thickness retinal necrosis in MAIDS mice, which becomes operative at least four weeks following retrovirus infection. The simulation of pyroptosis associated molecules and associated inflammasomes in MCMV-infected eyes of mice immune suppressed with corticosteroids suggests that the pyroptosis pathway and associated inflammasomes play a role in the development of MCMV retinitis in different models of immunosuppressed mice.

Specific Aim 2. In summary, pyroptosis-associated expression following MCMV infection of murine cells lines suggests that pyroptosis-associated molecules are stimulated directly by MCMV infection. The failure of UVi-MCMV to stimulate pyroptosis-associated molecules to the same extent as seen following MCMV infection suggests that this stimulation is largely independent of the attachment, adsorption, or release of viral tegument proteins. CMV stimulation of pyroptosis-associated mRNA is both species-specific and cell-type dependent

Specific Aim 3. All in all, our additional results suggest that other inflammasomes, such as IFI204, stimulated following MCMV infection, but may not be directly responsible for the development of MCMV retinitis. However, the autophagy form of cell death does not appear to be playing a role in the pathogenesis of this disease. Transcriptional analysis revealed that MCMV-infected eyes of MAIDS-10 mice susceptible to full-thickness retinal necrosis development is associated with a robust upregulation and downregulation of an extensive number of immune response genes that operate in several distinct immune response pathways. The temporal development of MCMV retinitis within the eyes of MAIDS-10 mice is a dynamic process that involves the upregulation and downregulation of a number of immune response genes at different times after intraocular MCMV infection. The pattern of immune response gene

activation differs remarkably within MCMV-infected eyes of healthy mice resistant to retinitis development when compared with MCMV-infected eyes of mice at different stages of MAIDS

6.7 Conclusions

The pursuit of these specific aims was to test the central hypothesis that pyroptosis and associated inflammasomes contribute to the onset and progression of retinal damage during MAIDS-related MCMV retinitis. Several inflammasomes and pyroptosis-associated molecules have already been shown to be stimulated during MAIDS-related MCMV retinitis, and the stimulation of GSDMD during the pathogenesis of MAIDS-related MCMV retinitis further supports the notion that pyroptosis is stimulated during MCMV retinitis in susceptible mice. The absence of full-thickness retinal necrosis in mice deficient in pyroptosis-related or inflammasomes genes suggest the pyroptosis pathway and associated inflammasomes are essential for the onset and progression of MCMV retinitis in susceptible MAIDS-10 mice. The simulation of pyroptosis-associated molecules and associated inflammasomes in MCMV-infected eyes of mice immune suppressed with corticosteroids suggests that the pyroptosis pathway and associated inflammasomes play a role in the development of MCMV retinitis in different models of immunosuppressed mice. The stimulation of the pyroptosis-associated molecules appears to be a direct result of infection by MCMV, and the magnitude of stimulation may be specific to the cell type infected.

REFERENCES

1. Dix RD, Cousins SW. AIDS-related cytomegalovirus retinitis: lessons from the laboratory. Curr Eye Res. 2004;29(2-3):91-101. doi: 10.1080/02713680490504641. PubMed PMID: 15512956.
2. Holland GN. AIDS and ophthalmology: the first quarter century. Am J Ophthalmol. 2008;145(3):397-408. Epub 2008/02/20. doi: 10.1016/j.ajo.2007.12.001. PubMed PMID: 18282490.
3. Jabs DA. Cytomegalovirus retinitis and the acquired immunodeficiency syndrome--bench to bedside: LXVII Edward Jackson Memorial Lecture. Am J Ophthalmol. 2011;151(2):198-216.e1. Epub 2010/12/21. doi: 10.1016/j.ajo.2010.10.018. PubMed PMID: 21168815; PubMed Central PMCID: PMCPMC3057105.
4. Dix RD, Cray C, Cousins SW. Mice immunosuppressed by murine retrovirus infection (MAIDS) are susceptible to cytomegalovirus retinitis. Curr Eye Res. 1994;13(8):587-95. PubMed PMID: 7956311.
5. Jolicoeur P. Murine acquired immunodeficiency syndrome (MAIDS): an animal model to study the AIDS pathogenesis. FASEB journal : official publication of the Federation of American Societies for Experimental Biology. 1991;5(10):2398-405. Epub 1991/07/01. doi: 10.1096/fasebj.5.10.2065888. PubMed PMID: 2065888.
6. Chien H, Dix RD. Evidence for multiple cell death pathways during development of experimental cytomegalovirus retinitis in mice with retrovirus-induced immunosuppression: apoptosis, necroptosis, and pyroptosis. J Virol. 2012;86(20):10961-78. doi: 10.1128/JVI.01275-12. PubMed PMID: 22837196; PubMed Central PMCID: PMCPMC3457157.
7. Pellet PaR, B. The family herpesviridae: a brief introduction. Howley DMKaPM, editor. Philadelphia, Pa, USA: Lippincott Williams & Wilkins; 2007. 2479–99 p.
8. Davison AJ, Eberle R, Ehlers B, Hayward GS, McGeoch DJ, Minson AC, et al. The order Herpesvirales. Archives of virology. 2009;154(1):171-7. Epub 2008/12/11. doi: 10.1007/s00705-008-0278-4. PubMed PMID: 19066710; PubMed Central PMCID: PMCPMC3552636.
9. Alejandro S-P, Cordeiro MNDS. Application of Bioinformatics for the Search of Novel Anti-Viral Therapies: Rational Design of Anti-Herpes Agents. Current Bioinformatics. 2011;6(1):81-93. doi: http://dx.doi.org/10.2174/157489311795222392.
10. Yamanishi K, Okuno T, Shiraki K, Takahashi M, Kondo T, Asano Y, et al. Identification of human herpesvirus-6 as a causal agent for exanthem subitum. Lancet (London, England). 1988;1(8594):1065-7. Epub 1988/05/14. doi: 10.1016/s0140-6736(88)91893-4. PubMed PMID: 2896909.
11. Tanaka K, Kondo T, Torigoe S, Okada S, Mukai T, Yamanishi K. Human herpesvirus 7: another causal agent for roseola (exanthem subitum). The Journal of pediatrics. 1994;125(1):1-5. Epub 1994/07/01. doi: 10.1016/s0022-3476(94)70113-x. PubMed PMID: 8021757.
12. Mocarski ES, Jr., Shenk, T., Pass, R.F. Cytomegalovirus. In: D.M. Knipe H, P.M.,, editor. Fields virology. Philadelphia: Lippincott Williams& Cilkins; 2007. p. 2702-72.
13. Britt B. Maturation and egress. In: Arvin A, Campadelli-Fiume G, Mocarski E, Moore PS, Roizman B, Whitley R, et al., editors. Human Herpesviruses: Biology, Therapy, and Immunoprophylaxis. Cambridge: Cambridge University Press

14. Tandon R, Mocarski ES. Viral and host control of cytomegalovirus maturation. Trends in microbiology. 2012;20(8):392-401. Epub 2012/05/29. doi: 10.1016/j.tim.2012.04.008. PubMed PMID: 22633075; PubMed Central PMCID: PMCPMC3408842.
15. Wang H, Huang C, Dong J, Yao Y, Xie Z, Liu X, et al. Complete protection of mice against lethal murine cytomegalovirus challenge by immunization with DNA vaccines encoding envelope glycoprotein complex III antigens gH, gL and gO. PloS one. 2015;10(3):e0119964. Epub 2015/03/25. doi: 10.1371/journal.pone.0119964. PubMed PMID: 25803721; PubMed Central PMCID: PMCPMC4372543.
16. Varnum SM, Streblow DN, Monroe ME, Smith P, Auberry KJ, Pasa-Tolic L, et al. Identification of proteins in human cytomegalovirus (HCMV) particles: the HCMV proteome. J Virol. 2004;78(20):10960-6. Epub 2004/09/29. doi: 10.1128/jvi.78.20.10960-10966.2004. PubMed PMID: 15452216; PubMed Central PMCID: PMCPMC521840.
17. Terhune SS, Schroer J, Shenk T. RNAs are packaged into human cytomegalovirus virions in proportion to their intracellular concentration. J Virol. 2004;78(19):10390-8. Epub 2004/09/16. doi: 10.1128/jvi.78.19.10390-10398.2004. PubMed PMID: 15367605; PubMed Central PMCID: PMCPMC516422.
18. Gandhi MK, Khanna R. Human cytomegalovirus: clinical aspects, immune regulation, and emerging treatments. The Lancet Infectious diseases. 2004;4(12):725-38. Epub 2004/11/30. doi: 10.1016/s1473-3099(04)01202-2. PubMed PMID: 15567122.
19. Cunningham C, Gatherer D, Hilfrich B, Baluchova K, Dargan DJ, Thomson M, et al. Sequences of complete human cytomegalovirus genomes from infected cell cultures and clinical specimens. J Gen Virol. 2010;91(Pt 3):605-15. Epub 2009/11/13. doi: 10.1099/vir.0.015891-0. PubMed PMID: 19906940; PubMed Central PMCID: PMCPMC2885759.
20. Ebeling A, Keil GM, Knust E, Koszinowski UH. Molecular cloning and physical mapping of murine cytomegalovirus DNA. J Virol. 1983;47(3):421-33. Epub 1983/09/01. PubMed PMID: 6312075; PubMed Central PMCID: PMCPMC255283.
21. Mercer JA, Marks JR, Spector DH. Molecular cloning and restriction endonuclease mapping of the murine cytomegalovirus genome (Smith Strain). Virology. 1983;129(1):94-106. Epub 1983/08/01. doi: 10.1016/0042-6822(83)90398-7. PubMed PMID: 6310888.
22. Rawlinson WD, Farrell HE, Barrell BG. Analysis of the complete DNA sequence of murine cytomegalovirus. J Virol. 1996;70(12):8833-49. Epub 1996/12/01. PubMed PMID: 8971012; PubMed Central PMCID: PMCPMC190980.
23. Davison AJ, Bhella D. Comparative genome and virion structure. In: Arvin A, Campadelli-Fiume G, Mocarski E, Moore PS, Roizman B, Whitley R, et al., editors. Human Herpesviruses: Biology, Therapy, and Immunoprophylaxis. Cambridge: Cambridge University Press
Copyright (c) Cambridge University Press 2007.; 2007.
24. McGregor A, Choi KY. Cytomegalovirus antivirals and development of improved animal models. Expert opinion on drug metabolism & toxicology. 2011;7(10):1245-65. Epub 2011/09/03. doi: 10.1517/17425255.2011.613824. PubMed PMID: 21883024; PubMed Central PMCID: PMCPMC4545654.
25. Isaacson MK, Juckem LK, Compton T. Virus entry and innate immune activation. Curr Top Microbiol Immunol. 2008;325:85-100. Epub 2008/07/22. doi: 10.1007/978-3-540-77349-8_5. PubMed PMID: 18637501.

26. Gibson W. Structure and formation of the cytomegalovirus virion. Curr Top Microbiol Immunol. 2008;325:187-204. Epub 2008/07/22. doi: 10.1007/978-3-540-77349-8_11. PubMed PMID: 18637507.
27. Kalejta RF. Functions of human cytomegalovirus tegument proteins prior to immediate early gene expression. Curr Top Microbiol Immunol. 2008;325:101-15. Epub 2008/07/22. doi: 10.1007/978-3-540-77349-8_6. PubMed PMID: 18637502.
28. Ogawa-Goto K, Tanaka K, Gibson W, Moriishi E, Miura Y, Kurata T, et al. Microtubule network facilitates nuclear targeting of human cytomegalovirus capsid. J Virol. 2003;77(15):8541-7. Epub 2003/07/15. doi: 10.1128/jvi.77.15.8541-8547.2003. PubMed PMID: 12857923; PubMed Central PMCID: PMCPMC165267.
29. Hermiston TW, Malone CL, Witte PR, Stinski MF. Identification and characterization of the human cytomegalovirus immediate-early region 2 gene that stimulates gene expression from an inducible promoter. J Virol. 1987;61(10):3214-21. Epub 1987/10/01. PubMed PMID: 3041043; PubMed Central PMCID: PMCPMC255900.
30. Pari GS. Nuts and bolts of human cytomegalovirus lytic DNA replication. Curr Top Microbiol Immunol. 2008;325:153-66. Epub 2008/07/22. doi: 10.1007/978-3-540-77349-8_9. PubMed PMID: 18637505.
31. Chantler JK, Hudson JB. Proteins of murine cytomegalovirus: identification of structural and nonstructural antigens in infected cells. Virology. 1978;86(1):22-36. Epub 1978/05/01. doi: 10.1016/0042-6822(78)90004-1. PubMed PMID: 208248.
32. Pinto AK, Munks MW, Koszinowski UH, Hill AB. Coordinated function of murine cytomegalovirus genes completely inhibits CTL lysis. J Immunol. 2006;177(5):3225-34. Epub 2006/08/22. doi: 10.4049/jimmunol.177.5.3225. PubMed PMID: 16920962.
33. Keil GM, Ebeling-Keil A, Koszinowski UH. Temporal regulation of murine cytomegalovirus transcription and mapping of viral RNA synthesized at immediate early times after infection. J Virol. 1984;50(3):784-95. Epub 1984/06/01. PubMed PMID: 6328008; PubMed Central PMCID: PMCPMC255738.
34. Patrick Murray KR, Michael Pfaller. Medical Microbiology2005.
35. Kaariainen L, Klemola E, Paloheimo J. Rise of cytomegalovirus antibodies in an infectious-mononucleosis-like syndrome after transfusion. British medical journal. 1966;1(5498):1270-2. Epub 1966/05/21. doi: 10.1136/bmj.1.5498.1270. PubMed PMID: 4287282; PubMed Central PMCID: PMCPMC1844561.
36. Roubille C, Brunel AS, Gahide G, Vernhet Kovacsik H, Le Quellec A. Cytomegalovirus (CMV) and acute myocarditis in an immunocompetent patient. Internal medicine (Tokyo, Japan). 2010;49(2):131-3. Epub 2010/01/16. doi: 10.2169/internalmedicine.49.2313. PubMed PMID: 20075576.
37. Vanstechelman F, Vandekerckhove H. Cytomegalovirus myocarditis in an immunocompetent patient. Acta cardiologica. 2012;67(2):257-60. Epub 2012/05/31. doi: 10.1080/ac.67.2.2154221. PubMed PMID: 22641988.
38. Manian FA, Smith T. Ganciclovir for the treatment of cytomegalovirus pneumonia in an immunocompetent host. Clinical infectious diseases : an official publication of the Infectious Diseases Society of America. 1993;17(1):137-8. Epub 1993/07/01. doi: 10.1093/clinids/17.1.137-a. PubMed PMID: 8394747.
39. Karakelides H, Aubry MC, Ryu JH. Cytomegalovirus pneumonia mimicking lung cancer in an immunocompetent host. Mayo Clinic proceedings. 2003;78(4):488-90. Epub 2003/04/10. doi: 10.4065/78.4.488. PubMed PMID: 12683701.

40. Grilli E, Galati V, Bordi L, Taglietti F, Petrosillo N. Cytomegalovirus pneumonia in immunocompetent host: case report and literature review. Journal of clinical virology : the official publication of the Pan American Society for Clinical Virology. 2012;55(4):356-9. Epub 2012/09/15. doi: 10.1016/j.jcv.2012.08.010. PubMed PMID: 22975082.
41. Tajiri H, Kozaiwa K, Tanaka-Taya K, Tada K, Takeshima T, Yamanishi K, et al. Cytomegalovirus hepatitis confirmed by in situ hybridization in 3 immunocompetent infants. Scandinavian journal of infectious diseases. 2001;33(10):790-3. Epub 2001/12/01. doi: 10.1080/003655401317074707. PubMed PMID: 11728056.
42. Colgan R, Michocki R, Greisman L, Moore TA. Antiviral drugs in the immunocompetent host: part I. Treatment of hepatitis, cytomegalovirus, and herpes infections. American family physician. 2003;67(4):757-62, 675. Epub 2003/03/05. PubMed PMID: 12613729.
43. Gupta P, Suryadevara M, Das A. Cytomegalovirus-induced hepatitis in an immunocompetent patient. The American journal of case reports. 2014;15:447-9. Epub 2014/10/19. doi: 10.12659/ajcr.890945. PubMed PMID: 25325934; PubMed Central PMCID: PMCPMC4206484.
44. Saliba WR, Raz R, Keness Y, Goldstein LH, Reshef A, Elias M. Cytomegalovirus encephalitis in an immunocompetent pregnant woman. European journal of clinical microbiology & infectious diseases : official publication of the European Society of Clinical Microbiology. 2004;23(7):563-6. Epub 2004/06/29. doi: 10.1007/s10096-004-1166-9. PubMed PMID: 15221616.
45. Salamano R, Gervaz E, Manana G, Pena S, Panuncio A, Puppo C, et al. [Cytomegalovirus encephalitis in an immunocompetent patient: clinical, neuropathological and ultrastructural analysis]. Arquivos de neuro-psiquiatria. 2001;59(4):954-8. Epub 2001/12/06. doi: 10.1590/s0004-282x2001000600022. PubMed PMID: 11733845.
46. Donnet A, Gouirand R, Zandotti C, Grisoli F. [Cytomegalovirus encephalitis in an immunocompetent adult]. Revue neurologique. 1996;152(10):640-1. Epub 1996/10/01. PubMed PMID: 9033959.
47. Belo F, Mendes I, Calha M, Mendonca C. Cytomegalovirus encephalitis in an immunocompetent child: a sceptic diagnosis. BMJ case reports. 2012;2012. Epub 2012/11/29. doi: 10.1136/bcr-2012-006796. PubMed PMID: 23188841; PubMed Central PMCID: PMCPMC4544757.
48. Radwan A, Metzinger JL, Hinkle DM, Foster CS. Cytomegalovirus retinitis in immunocompetent patients: case reports and literature review. Ocular immunology and inflammation. 2013;21(4):324-8. Epub 2013/05/15. doi: 10.3109/09273948.2013.786095. PubMed PMID: 23662740.
49. Dollard SC, Grosse SD, Ross DS. New estimates of the prevalence of neurological and sensory sequelae and mortality associated with congenital cytomegalovirus infection. Reviews in medical virology. 2007;17(5):355-63. Epub 2007/06/02. doi: 10.1002/rmv.544. PubMed PMID: 17542052.
50. Cannon MJ, Davis KF. Washing our hands of the congenital cytomegalovirus disease epidemic. BMC public health. 2005;5:70. Epub 2005/06/22. doi: 10.1186/1471-2458-5-70. PubMed PMID: 15967030; PubMed Central PMCID: PMCPMC1182379.
51. Britt W. Manifestations of human cytomegalovirus infection: proposed mechanisms of acute and chronic disease. Curr Top Microbiol Immunol. 2008;325:417-70. Epub 2008/07/22. doi: 10.1007/978-3-540-77349-8_23. PubMed PMID: 18637519.

52. Freed EO. HIV-1 replication. Somatic cell and molecular genetics. 2001;26(1-6):13-33. Epub 2002/12/06. doi: 10.1023/a:1021070512287. PubMed PMID: 12465460.
53. Freed EOaMAM. Human Immunodeficiency Viruses: Replication. In: Howley DMKaPM, editor. Fields Virology. Philadelphia, PA, USA: Lippencott Williams & Wilkins; 2013.
54. Robinson HL. New hope for an aids vaccine. Nature Reviews Immunology. 2002;2(4):239-50. doi: 10.1038/nri776.
55. Gelderblom HR. Assembly and morphology of HIV: potential effect of structure on viral function. AIDS (London, England). 1991;5(6):617-37. Epub 1991/06/01. PubMed PMID: 1652977.
56. Zhang C, Zhou S, Groppelli E, Pellegrino P, Williams I, Borrow P, et al. Hybrid spreading mechanisms and T cell activation shape the dynamics of HIV-1 infection. PLoS computational biology. 2015;11(4):e1004179. Epub 2015/04/04. doi: 10.1371/journal.pcbi.1004179. PubMed PMID: 25837979; PubMed Central PMCID: PMCPMC4383537.
57. Churchill J, Hosie MJ. Lentiviruses and Macrophages.
58. Jolly C, Kashefi K, Hollinshead M, Sattentau QJ. HIV-1 cell to cell transfer across an Env-induced, actin-dependent synapse. J Exp Med. 2004;199(2):283-93. Epub 2004/01/22. doi: 10.1084/jem.20030648. PubMed PMID: 14734528; PubMed Central PMCID: PMCPMC2211771.
59. Sattentau Q. Avoiding the void: cell-to-cell spread of human viruses. Nat Rev Microbiol. 2008;6(11):815-26. Epub 2008/10/17. doi: 10.1038/nrmicro1972. PubMed PMID: 18923409.
60. Duncan CJ, Russell RA, Sattentau QJ. High multiplicity HIV-1 cell-to-cell transmission from macrophages to CD4+ T cells limits antiretroviral efficacy. AIDS (London, England). 2013;27(14):2201-6. Epub 2013/09/06. doi: 10.1097/QAD.0b013e3283632ec4. PubMed PMID: 24005480; PubMed Central PMCID: PMCPMC4714465.
61. Yavuz B, Morgan J, Showalter L, Crakes K, Dandekar S, Herrera C, et al. Pharmaceutical Approaches to HIV Treatment and Prevention. Advanced Therapeutics. 2018:1800054. doi: 10.1002/adtp.201800054.
62. Goodrich DW, Duesberg PH. Retroviral recombination during reverse transcription. Proc Natl Acad Sci U S A. 1990;87(6):2052-6. Epub 1990/03/01. doi: 10.1073/pnas.87.6.2052. PubMed PMID: 1690424; PubMed Central PMCID: PMCPMC53624.
63. Charpentier C, Nora T, Tenaillon O, Clavel F, Hance AJ. Extensive recombination among human immunodeficiency virus type 1 quasispecies makes an important contribution to viral diversity in individual patients. J Virol. 2006;80(5):2472-82. Epub 2006/02/14. doi: 10.1128/jvi.80.5.2472-2482.2006. PubMed PMID: 16474154; PubMed Central PMCID: PMCPMC1395372.
64. Bonhoeffer S, Chappey C, Parkin NT, Whitcomb JM, Petropoulos CJ. Evidence for positive epistasis in HIV-1. Science (New York, NY). 2004;306(5701):1547-50. Epub 2004/11/30. doi: 10.1126/science.1101786. PubMed PMID: 15567861.
65. Nora T, Charpentier C, Tenaillon O, Hoede C, Clavel F, Hance AJ. Contribution of recombination to the evolution of human immunodeficiency viruses expressing resistance to antiretroviral treatment. J Virol. 2007;81(14):7620-8. Epub 2007/05/12. doi: 10.1128/jvi.00083-07. PubMed PMID: 17494080; PubMed Central PMCID: PMCPMC1933369.
66. Vogel M, Schwarze-Zander C, Wasmuth JC, Spengler U, Sauerbruch T, Rockstroh JK. The treatment of patients with HIV. Deutsches Arzteblatt international. 2010;107(28-29):507-15;

quiz 16. Epub 2010/08/13. doi: 10.3238/arztebl.2010.0507. PubMed PMID: 20703338; PubMed Central PMCID: PMCPMC2915483.
67. Volberding PA, Deeks SG. Antiretroviral therapy and management of HIV infection. Lancet (London, England). 2010;376(9734):49-62. Epub 2010/07/09. doi: 10.1016/s0140-6736(10)60676-9. PubMed PMID: 20609987.
68. Levy JA. HIV and the Pathogenesis of AIDS. 2007;3rd Edition.
69. Holland GN, Gottlieb MS, Yee RD, Schanker HM, Pettit TH. Ocular disorders associated with a new severe acquired cellular immunodeficiency syndrome. Am J Ophthalmol. 1982;93(4):393-402. PubMed PMID: 6280503.
70. Jabs DA, Bartlett JG. AIDS and ophthalmology: a period of transition. Am J Ophthalmol. 1997;124(2):227-33. PubMed PMID: 9262548.
71. Jabs DA, Enger C, Bartlett JG. Cytomegalovirus retinitis and acquired immunodeficiency syndrome. Arch Ophthalmol. 1989;107(1):75-80. PubMed PMID: 2535932.
72. Stewart MW. Optimal management of cytomegalovirus retinitis in patients with AIDS. Clin Ophthalmol. 2010;4:285-99. PubMed PMID: 20463796; PubMed Central PMCID: PMCPMC2861935.
73. Heiden D, Ford N, Wilson D, Rodriguez WR, Margolis T, Janssens B, et al. Cytomegalovirus retinitis: the neglected disease of the AIDS pandemic. PLoS Med. 2007;4(12):e334. doi: 10.1371/journal.pmed.0040334. PubMed PMID: 18052600; PubMed Central PMCID: PMCPMC2100142.
74. Schleiss MR. Cytomegalovirus vaccine development. Curr Top Microbiol Immunol. 2008;325:361-82. PubMed PMID: 18637516; PubMed Central PMCID: PMCPMC2831992.
75. Schleiss M. Progress in cytomegalovirus vaccine development. Herpes. 2005;12(3):66-75. PubMed PMID: 16393522.
76. Ahmed A. Antiviral treatment of cytomegalovirus infection. Infect Disord Drug Targets. 2011;11(5):475-503. PubMed PMID: 21827432.
77. Harter G, Michel D. Antiviral treatment of cytomegalovirus infection: an update. Expert Opin Pharmacother. 2012;13(5):623-7. doi: 10.1517/14656566.2012.658775. PubMed PMID: 22299626.
78. Lurain NS, Chou S. Antiviral drug resistance of human cytomegalovirus. Clin Microbiol Rev. 2010;23(4):689-712. doi: 10.1128/CMR.00009-10. PubMed PMID: 20930070; PubMed Central PMCID: PMCPMC2952978.
79. Miller SJH. Ophthalmology: Principles and Concepts. Br J Ophthalmol. 1980;64(11):876-. PubMed PMID: PMC1043840.
80. Kolb H. Gross Anatomy of the Eye. H. Kolb EF, and R. Nelson, editor. University of Utah Health Sciences Center: Salt Lake City (UT)1995.
81. Scott JE. The chemical morphology of the vitreous. Eye (London, England). 1992;6 (Pt 6):553-5. Epub 1992/01/01. doi: 10.1038/eye.1992.120. PubMed PMID: 1289129.
82. Kolb H. Anatomy of the Eye. H. Kolb EF, and R. Nelson, editor. University of Utah Health Sciences Center: Salt Lake City (UT).1995.
83. Kolb H. Simple Anatomy of the Retina. H. Kolb EF, and R. Nelson, editor. University of Utah Health Sciences Center: Salt Lake City (UT)1995.
84. Grossniklaus HE, E.E. Geisert, and J.M. Nickerson. Chapter Twenty-Two -Introduction to the Retina. John JFHaMN, editor: Academic Press; 2015.
85. Do MTH, Yau K-W. Intrinsically photosensitive retinal ganglion cells. Physiological reviews. 2010;90(4):1547-81. doi: 10.1152/physrev.00013.2010. PubMed PMID: 20959623.

86. Simo R, Villarroel M, Corraliza L, Hernandez C, Garcia-Ramirez M. The retinal pigment epithelium: something more than a constituent of the blood-retinal barrier--implications for the pathogenesis of diabetic retinopathy. Journal of biomedicine & biotechnology. 2010;2010:190724. Epub 2010/02/26. doi: 10.1155/2010/190724. PubMed PMID: 20182540; PubMed Central PMCID: PMCPMC2825554.
87. Strauss O. The retinal pigment epithelium in visual function. Physiological reviews. 2005;85(3):845-81. Epub 2005/07/01. doi: 10.1152/physrev.00021.2004. PubMed PMID: 15987797.
88. Smith RS, Rudt LA. Ocular vascular and epithelial barriers to microperoxidase. Investigative ophthalmology. 1975;14(7):556-60. Epub 1975/07/01. PubMed PMID: 806549.
89. Bellhorn RW. Permeability of blood-ocular barriers of neonatal and adult cat to sodium fluorescein. Investigative ophthalmology & visual science. 1980;19(8):870-7. Epub 1980/08/01. PubMed PMID: 7409982.
90. Kolb H. Simply Anatomy of the Retina. University of
Utah Health Sciences Center: Salt Lake City (UT)1995.
91. Hazlett LD, Hendricks RL. Reviews for immune privilege in the year 2010: immune privilege and infection. Ocular immunology and inflammation. 2010;18(4):237-43. Epub 2010/07/29. doi: 10.3109/09273948.2010.501946. PubMed PMID: 20662654.
92. Medawar PB. Immunity to homologous grafted skin; the fate of skin homografts transplanted to the brain, to subcutaneous tissue, and to the anterior chamber of the eye. British journal of experimental pathology. 1948;29(1):58-69. Epub 1948/02/01. PubMed PMID: 18865105; PubMed Central PMCID: PMCPMC2073079.
93. Kaplan HJ, Streilein JW. Immune response to immunization via the anterior chamber of the eye. I. F. lymphocyte-induced immune deviation. J Immunol. 1977;118(3):809-14. Epub 1977/03/01. PubMed PMID: 321682.
94. Streilein JW. Ocular immune privilege: therapeutic opportunities from an experiment of nature. Nature reviews Immunology. 2003;3(11):879-89. Epub 2003/12/12. doi: 10.1038/nri1224. PubMed PMID: 14668804.
95. Boycott BB, Hopkins JM. Microglia in the retina of monkey and other mammals: its distinction from other types of glia and horizontal cells. Neuroscience. 1981;6(4):679-88. Epub 1981/01/01. doi: 10.1016/0306-4522(81)90151-2. PubMed PMID: 6165924.
96. Chen L, Yang P, Kijlstra A. Distribution, markers, and functions of retinal microglia. Ocular immunology and inflammation. 2002;10(1):27-39. Epub 2002/12/04. doi: 10.1076/ocii.10.1.27.10328. PubMed PMID: 12461701.
97. Bringmann A, Pannicke T, Grosche J, Francke M, Wiedemann P, Skatchkov SN, et al. Muller cells in the healthy and diseased retina. Progress in retinal and eye research. 2006;25(4):397-424. Epub 2006/07/15. doi: 10.1016/j.preteyeres.2006.05.003. PubMed PMID: 16839797.
98. Hofman FM, Hinton DR. Tumor necrosis factor-alpha in the retina in acquired immune deficiency syndrome. Investigative ophthalmology & visual science. 1992;33(6):1829-35. Epub 1992/05/01. PubMed PMID: 1582785.
99. Pepose JS, Holland GN, Nestor MS, Cochran AJ, Foos RY. Acquired immune deficiency syndrome. Pathogenic mechanisms of ocular disease. Ophthalmology. 1985;92(4):472-84. Epub 1985/04/01. doi: 10.1016/s0161-6420(85)34008-3. PubMed PMID: 2987769.
100. Alston CI, Carter, J.J., Dix, R.D. Cytomegalovirus and the-Eye: AIDS-Related Retinitis and Beyond. Herpesviridae. 2017:42.

101. Dudgeon JA. Cytomegalovirus infection. Archives of disease in childhood. 1971;46(249):581-3. Epub 1971/10/01. doi: 10.1136/adc.46.249.581. PubMed PMID: 4336019; PubMed Central PMCID: PMCPMC1647851.
102. Dix R, Cousins S. Murine cytomegalovirus retinitis during MAIDS: Susceptibility correlates with elevated intraocular levels of interleukin-4 mRNA. Curr Eye Res. 2003;26(3-4):211-7. Epub 2003/06/20. doi: 10.1076/ceyr.26.3.211.14902. PubMed PMID: 12815549.
103. Dix RD, Cousins SW. Susceptibility to murine cytomegalovirus retinitis during progression of MAIDS: correlation with intraocular levels of tumor necrosis factor-alpha and interferon-gamma. Curr Eye Res. 2004;29(2-3):173-80. Epub 2004/10/30. doi: 10.1080/02713680490504876. PubMed PMID: 15512964.
104. Holland GN, Fang EN, Glasgow BJ, Zaragoza AM, Siegel LM, Graves MC, et al. Necrotizing retinopathy after intraocular inoculation of murine cytomegalovirus in immunosuppressed adult mice. Investigative ophthalmology & visual science. 1990;31(11):2326-34. Epub 1990/11/01. PubMed PMID: 2173685.
105. Atherton SS, Newell CK, Kanter MY, Cousins SW. T cell depletion increases susceptibility to murine cytomegalovirus retinitis. Investigative ophthalmology & visual science. 1992;33(12):3353-60. Epub 1992/11/01. PubMed PMID: 1330968.
106. Atherton SS, Newell CK, Kanter MY, Cousins SW. Retinitis in euthymic mice following inoculation of murine cytomegalovirus (MCMV) via the supraciliary route. Curr Eye Res. 1991;10(7):667-77. PubMed PMID: 1655355.
107. Selgrade MK, Nedrud JG, Collier AM, Gardner DE. Effects of cell source, mouse strain, and immunosuppressive treatment on production of virulent and attenuated murine cytomegalovirus. Infection and immunity. 1981;33(3):840-7. Epub 1981/09/01. PubMed PMID: 6270000; PubMed Central PMCID: PMCPMC350788.
108. Chalmer JE, Mackenzie JS, Stanley NF. Resistance to murine cytomegalovirus linked to the major histocompatibility complex of the mouse. J Gen Virol. 1977;37(1):107-14. Epub 1977/10/01. doi: 10.1099/0022-1317-37-1-107. PubMed PMID: 199700.
109. Zhang M, Zhou J, Marshall B, Xin H, Atherton SS. Lack of iNOS facilitates MCMV spread in the retina. Investigative ophthalmology & visual science. 2007;48(1):285-92. Epub 2007/01/02. doi: 10.1167/iovs.06-0792. PubMed PMID: 17197545.
110. Mosier DE, Yetter RA, Morse HC, 3rd. Retroviral induction of acute lymphoproliferative disease and profound immunosuppression in adult C57BL/6 mice. J Exp Med. 1985;161(4):766-84. PubMed PMID: 2984305; PubMed Central PMCID: PMCPMC2189053.
111. Haas M, Meshorer A. Reticulum cell neoplasms induced in C57BL/6 mice by cultured virus grown in stromal hematopoietic cell lines. Journal of the National Cancer Institute. 1979;63(2):427-39. Epub 1979/08/01. PubMed PMID: 222931.
112. Watson RR. Murine models for acquired immune deficiency syndrome. Life sciences. 1989;44(3):iii-xv. Epub 1989/01/01. doi: 10.1016/0024-3205(89)90592-4. PubMed PMID: 2536876.
113. Cunnigham RK, Thacore HR, Zhou P, Terzian R, Nakeeb S, Zaleski MB. Murine AIDS: a model for the human disease or a distinct entity? Immunologic research. 1994;13(1):21-8. Epub 1994/01/01. doi: 10.1007/bf02918221. PubMed PMID: 7897259.
114. Carter J, Alston CI, Oh J, Duncan L-A, Esquibel Nemeno JG, Byfield SN, et al. Mechanisms of AIDS-related cytomegalovirus retinitis. Future Virology. 2019;14(8):545-60. doi: 10.2217/fvl-2019-0033.

115. Zhang M, Covar J, Marshall B, Dong Z, Atherton SS. Lack of TNF-alpha promotes caspase-3-independent apoptosis during murine cytomegalovirus retinitis. Investigative ophthalmology & visual science. 2011;52(3):1800-8. Epub 2011/02/12. doi: 10.1167/iovs.10-6904. PubMed PMID: 21310911; PubMed Central PMCID: PMCPMC3101684.
116. Sloka JS, Stefanelli M. The mechanism of action of methylprednisolone in the treatment of multiple sclerosis. Multiple sclerosis (Houndmills, Basingstoke, England). 2005;11(4):425-32. Epub 2005/07/27. doi: 10.1191/1352458505ms1190oa. PubMed PMID: 16042225.
117. Hamelin-Bourassa D, Skamene E, Gervais F. Susceptibility to a mouse acquired immunodeficiency syndrome is influenced by theH-2. Immunogenetics. 1989;30(4):266-72. doi: 10.1007/BF02421330.
118. Chen Y, Mendoza S, Davis-Gorman G, Cohen Z, Gonzales R, Tuttle H, et al. Neutrophil activation by murine retroviral infection during chronic ethanol consumption. Alcohol and alcoholism (Oxford, Oxfordshire). 2003;38(2):109-14. Epub 2003/03/14. doi: 10.1093/alcalc/agg049. PubMed PMID: 12634256.
119. Morse HC, 3rd, Yetter RA, Via CS, Hardy RR, Cerny A, Hayakawa K, et al. Functional and phenotypic alterations in T cell subsets during the course of MAIDS, a murine retrovirus-induced immunodeficiency syndrome. J Immunol. 1989;143(3):844-50. Epub 1989/08/01. PubMed PMID: 2545779.
120. Makino M, Winkler DF, Wunderlich J, Hartley JW, Morse HC, Holmes KL. High expression of NK-1.1 antigen is induced by infection with murine AIDS virus. Immunology. 1993;80(2):319-25. Epub 1993/10/01. PubMed PMID: 8262561; PubMed Central PMCID: PMCPMC1422179.
121. Mosier DE, Yetter RA, Morse HC, 3rd. Functional T lymphocytes are required for a murine retrovirus-induced immunodeficiency disease (MAIDS). The Journal of experimental medicine. 1987;165(6):1737-42. Epub 1987/06/01. PubMed PMID: 3035057; PubMed Central PMCID: PMCPMC2188367.
122. Gazzinelli RT, Makino M, Chattopadhyay SK, Snapper CM, Sher A, Hugin AW, et al. CD4+ subset regulation in viral infection. Preferential activation of Th2 cells during progression of retrovirus-induced immunodeficiency in mice. J Immunol. 1992;148(1):182-8. Epub 1992/01/01. PubMed PMID: 1345785.
123. Hartley JW, Fredrickson TN, Yetter RA, Makino M, Morse HC, 3rd. Retrovirus-induced murine acquired immunodeficiency syndrome: natural history of infection and differing susceptibility of inbred mouse strains. J Virol. 1989;63(3):1223-31. PubMed PMID: 2536830; PubMed Central PMCID: PMCPMC247818.
124. Rosenberg AS, Maniero TG, Morse HC, 3rd. In vivo immunologic deficits in mice with murine acquired immunodeficiency syndrome and the effect of LP-BM5 infection on rejection of skin from infected mice. Transplant Proc. 1991;23(1 Pt 1):167-9. PubMed PMID: 1990505.
125. Crough T, Khanna R. Immunobiology of human cytomegalovirus: from bench to bedside. Clin Microbiol Rev. 2009;22(1):76-98, Table of Contents. Epub 2009/01/13. doi: 10.1128/cmr.00034-08. PubMed PMID: 19136435; PubMed Central PMCID: PMCPMC2620639.
126. Blalock EL, Chien H, Dix RD. Systemic reduction of interleukin-4 or interleukin-10 fails to reduce the frequency or severity of experimental cytomegalovirus retinitis in mice with retrovirus-induced immunosuppression. Ophthalmology and eye diseases. 2012;4:79-90. Epub 2012/01/01. doi: 10.4137/oed.s10294. PubMed PMID: 23650460; PubMed Central PMCID: PMCPMC3619657.

127. Blalock EL, Chien H, Dix RD. Murine cytomegalovirus downregulates interleukin-17 in mice with retrovirus-induced immunosuppression that are susceptible to experimental cytomegalovirus retinitis. Cytokine. 2013;61(3):862-75. Epub 2013/02/19. doi: 10.1016/j.cyto.2013.01.009. PubMed PMID: 23415673; PubMed Central PMCID: PMCPMC3595332.
128. Bigger JE, Tanigawa M, Zhang M, Atherton SS. Murine cytomegalovirus infection causes apoptosis of uninfected retinal cells. Investigative ophthalmology & visual science. 2000;41(8):2248-54. Epub 2000/07/13. PubMed PMID: 10892869.
129. Bradley JR. TNF-mediated inflammatory disease. The Journal of pathology. 2008;214(2):149-60. Epub 2007/12/29. doi: 10.1002/path.2287. PubMed PMID: 18161752.
130. Rahman MM, McFadden G. Modulation of tumor necrosis factor by microbial pathogens. PLoS pathogens. 2006;2(2):e4. Epub 2006/03/07. doi: 10.1371/journal.ppat.0020004. PubMed PMID: 16518473; PubMed Central PMCID: PMCPMC1383482.
131. Mondino BJ, Sidikaro Y, Mayer FJ, Sumner HL. Inflammatory mediators in the vitreous humor of AIDS patients with retinitis. Investigative ophthalmology & visual science. 1990;31(5):798-804. Epub 1990/05/01. PubMed PMID: 2110558.
132. Elmore S. Apoptosis: a review of programmed cell death. Toxicologic pathology. 2007;35(4):495-516. Epub 2007/06/15. doi: 10.1080/01926230701320337. PubMed PMID: 17562483; PubMed Central PMCID: PMCPMC2117903.
133. Ferguson TA, Griffith TS. The role of Fas ligand and TNF-related apoptosis-inducing ligand (TRAIL) in the ocular immune response. Chemical immunology and allergy. 2007;92:140-54. Epub 2007/02/01. doi: 10.1159/000099265. PubMed PMID: 17264490.
134. Golstein P. Cell death: TRAIL and its receptors. Current biology : CB. 1997;7(12):R750-3. Epub 1998/02/21. PubMed PMID: 9382834.
135. Brunner T, Wasem C, Torgler R, Cima I, Jakob S, Corazza N. Fas (CD95/Apo-1) ligand regulation in T cell homeostasis, cell-mediated cytotoxicity and immune pathology. Seminars in immunology. 2003;15(3):167-76. Epub 2003/10/18. PubMed PMID: 14563115.
136. Ehrenschwender M, Wajant H. The role of FasL and Fas in health and disease. Advances in experimental medicine and biology. 2009;647:64-93. Epub 2009/09/18. doi: 10.1007/978-0-387-89520-8_5. PubMed PMID: 19760067.
137. Wallach D, Varfolomeev EE, Malinin NL, Goltsev YV, Kovalenko AV, Boldin MP. Tumor necrosis factor receptor and Fas signaling mechanisms. Annual review of immunology. 1999;17:331-67. Epub 1999/06/08. doi: 10.1146/annurev.immunol.17.1.331. PubMed PMID: 10358762.
138. Chinnaiyan AM. The apoptosome: heart and soul of the cell death machine. Neoplasia (New York, NY). 1999;1(1):5-15. Epub 2000/08/10. PubMed PMID: 10935465; PubMed Central PMCID: PMCPMC1716059.
139. Hill MM, Adrain C, Duriez PJ, Creagh EM, Martin SJ. Analysis of the composition, assembly kinetics and activity of native Apaf-1 apoptosomes. The EMBO journal. 2004;23(10):2134-45. Epub 2004/04/23. doi: 10.1038/sj.emboj.7600210. PubMed PMID: 15103327; PubMed Central PMCID: PMCPMC424369.
140. Brune W. Inhibition of programmed cell death by cytomegaloviruses. Virus research. 2011;157(2):144-50. Epub 2010/10/26. doi: 10.1016/j.virusres.2010.10.012. PubMed PMID: 20969904.

141. Halonen SK. Modulation of host programmed cell death pathways by the intracellular protozoan parasite, Toxoplasma gondii—implications for maintenance of chronic infection and potential therapeutic applications. Cell Death-Autophagy, Apoptosis and Necrosis. 2015:373-93.
142. Zhou W, Yuan J. Necroptosis in health and diseases. Seminars in cell & developmental biology. 2014;35:14-23. Epub 2014/08/05. doi: 10.1016/j.semcdb.2014.07.013. PubMed PMID: 25087983.
143. Cookson BT, Brennan MA. Pro-inflammatory programmed cell death. Trends in microbiology. 2001;9(3):113-4. Epub 2001/04/17. PubMed PMID: 11303500.
144. Bergsbaken T, Fink SL, Cookson BT. Pyroptosis: host cell death and inflammation. Nat Rev Microbiol. 2009;7(2):99-109. doi: 10.1038/nrmicro2070. PubMed PMID: 19148178; PubMed Central PMCID: PMCPMC2910423.
145. Aglietti RA, Estevez A, Gupta A, Ramirez MG, Liu PS, Kayagaki N, et al. GsdmD p30 elicited by caspase-11 during pyroptosis forms pores in membranes. Proc Natl Acad Sci U S A. 2016;113(28):7858-63. Epub 2016/06/25. doi: 10.1073/pnas.1607769113. PubMed PMID: 27339137; PubMed Central PMCID: PMCPMC4948338.
146. Sharma D, Kanneganti TD. The cell biology of inflammasomes: Mechanisms of inflammasome activation and regulation. The Journal of cell biology. 2016;213(6):617-29. Epub 2016/06/22. doi: 10.1083/jcb.201602089. PubMed PMID: 27325789; PubMed Central PMCID: PMCPMC4915194.
147. Shi J, Gao W, Shao F. Pyroptosis: Gasdermin-Mediated Programmed Necrotic Cell Death. Trends in biochemical sciences. 2017;42(4):245-54. Epub 2016/12/10. doi: 10.1016/j.tibs.2016.10.004. PubMed PMID: 27932073.
148. Shalini S, Dorstyn L, Dawar S, Kumar S. Old, new and emerging functions of caspases. Cell death and differentiation. 2015;22(4):526-39. Epub 2014/12/20. doi: 10.1038/cdd.2014.216. PubMed PMID: 25526085; PubMed Central PMCID: PMCPMC4356345.
149. Wilson KP, Black JA, Thomson JA, Kim EE, Griffith JP, Navia MA, et al. Structure and mechanism of interleukin-1 beta converting enzyme. Nature. 1994;370(6487):270-5. doi: 10.1038/370270a0. PubMed PMID: 8035875.
150. Mariathasan S, Newton K, Monack DM, Vucic D, French DM, Lee WP, et al. Differential activation of the inflammasome by caspase-1 adaptors ASC and Ipaf. Nature. 2004;430(6996):213-8. Epub 06/09. doi: 10.1038/nature02664. PubMed PMID: 15190255.
151. Lu A, Li Y, Schmidt FI, Yin Q, Chen S, Fu T-M, et al. Molecular basis of caspase-1 polymerization and its inhibition by a new capping mechanism. Nat Struct Mol Biol. 2016;23(5):416-25. Epub 04/04. doi: 10.1038/nsmb.3199. PubMed PMID: 27043298.
152. Vince JE, Silke J. The intersection of cell death and inflammasome activation. Cellular and molecular life sciences : CMLS. 2016;73(11-12):2349-67. Epub 04/11. doi: 10.1007/s00018-016-2205-2. PubMed PMID: 27066895.
153. Garlanda C, Dinarello Charles A, Mantovani A. The Interleukin-1 Family: Back to the Future. Immunity. 2013;39(6):1003-18. doi: https://doi.org/10.1016/j.immuni.2013.11.010.
154. Joosten LA, Netea MG, Fantuzzi G, Koenders MI, Helsen MM, Sparrer H, et al. Inflammatory arthritis in caspase-1 gene–deficient mice: Contribution of proteinase 3 to caspase-1–independent production of bioactive interleukin-1β. Arthritis & Rheumatism: Official Journal of the American College of Rheumatology. 2009;60(12):3651-62.
155. Guma M, Ronacher L, Liu-Bryan R, Takai S, Karin M, Corr M. Caspase-1–independent activation of interleukin-1β in neutrophil-predominant inflammation. Arthritis & Rheumatism: Official Journal of the American College of Rheumatology. 2009;60(12):3642-50.

156. Nakanishi K, Yoshimoto T, Tsutsui H, Okamura H. Interleukin-18 regulates both Th1 and Th2 responses. Annual review of immunology. 2001;19:423-74. Epub 2001/03/13. doi: 10.1146/annurev.immunol.19.1.423. PubMed PMID: 11244043.
157. Okamura H, Tsutsi H, Komatsu T, Yutsudo M, Hakura A, Tanimoto T, et al. Cloning of a new cytokine that induces IFN-gamma production by T cells. Nature. 1995;378(6552):88-91. Epub 1995/11/02. doi: 10.1038/378088a0. PubMed PMID: 7477296.
158. Ushio S, Namba M, Okura T, Hattori K, Nukada Y, Akita K, et al. Cloning of the cDNA for human IFN-gamma-inducing factor, expression in Escherichia coli, and studies on the biologic activities of the protein. J Immunol. 1996;156(11):4274-9. Epub 1996/06/01. PubMed PMID: 8666798.
159. Gu Y, Kuida K, Tsutsui H, Ku G, Hsiao K, Fleming MA, et al. Activation of interferon-gamma inducing factor mediated by interleukin-1beta converting enzyme. Science (New York, NY). 1997;275(5297):206-9. Epub 1997/01/10. doi: 10.1126/science.275.5297.206. PubMed PMID: 8999548.
160. Lacey CA, Mitchell WJ, Dadelahi AS, Skyberg JA. Caspase-1 and Caspase-11 Mediate Pyroptosis, Inflammation, and Control of Brucella Joint Infection. Infection and immunity. 2018;86(9). Epub 2018/06/27. doi: 10.1128/iai.00361-18. PubMed PMID: 29941463; PubMed Central PMCID: PMCPMC6105886.
161. Broz P, Dixit VM. Inflammasomes: mechanism of assembly, regulation and signalling. Nature reviews Immunology. 2016;16(7):407-20. Epub 2016/06/14. doi: 10.1038/nri.2016.58. PubMed PMID: 27291964.
162. Ramirez MLG, Poreba M, Snipas SJ, Groborz K, Drag M, Salvesen GS. Extensive peptide and natural protein substrate screens reveal that mouse caspase-11 has much narrower substrate specificity than caspase-1. The Journal of biological chemistry. 2018;293(18):7058-67. Epub 2018/02/08. doi: 10.1074/jbc.RA117.001329. PubMed PMID: 29414788; PubMed Central PMCID: PMCPMC5936834.
163. Kambara H, Liu F, Zhang X, Liu P, Bajrami B, Teng Y, et al. Gasdermin D Exerts Anti-inflammatory Effects by Promoting Neutrophil Death. Cell reports. 2018;22(11):2924-36. Epub 2018/03/15. doi: 10.1016/j.celrep.2018.02.067. PubMed PMID: 29539421; PubMed Central PMCID: PMCPMC5878047.
164. Burgener SS, Leborgne NGF, Snipas SJ, Salvesen GS, Bird PI, Benarafa C. Cathepsin G Inhibition by Serpinb1 and Serpinb6 Prevents Programmed Necrosis in Neutrophils and Monocytes and Reduces GSDMD-Driven Inflammation. Cell reports. 2019;27(12):3646-56.e5. Epub 2019/06/20. doi: 10.1016/j.celrep.2019.05.065. PubMed PMID: 31216481.
165. Kayagaki N, Stowe IB, Lee BL, O'Rourke K, Anderson K, Warming S, et al. Caspase-11 cleaves gasdermin D for non-canonical inflammasome signalling. Nature. 2015;526(7575):666-71. Epub 2015/09/17. doi: 10.1038/nature15541. PubMed PMID: 26375259.
166. Shi J, Zhao Y, Wang K, Shi X, Wang Y, Huang H, et al. Cleavage of GSDMD by inflammatory caspases determines pyroptotic cell death. Nature. 2015;526(7575):660-5. Epub 2015/09/17. doi: 10.1038/nature15514. PubMed PMID: 26375003.
167. Liu X, Zhang Z, Ruan J, Pan Y, Magupalli VG, Wu H, et al. Inflammasome-activated gasdermin D causes pyroptosis by forming membrane pores. Nature. 2016;535(7610):153-8. Epub 2016/07/08. doi: 10.1038/nature18629. PubMed PMID: 27383986; PubMed Central PMCID: PMCPMC5539988.

168. Ding J, Wang K, Liu W, She Y, Sun Q, Shi J, et al. Pore-forming activity and structural autoinhibition of the gasdermin family. Nature. 2016;535(7610):111-6. Epub 2016/06/10. doi: 10.1038/nature18590. PubMed PMID: 27281216.
169. Taabazuing CY, Okondo MC, Bachovchin DA. Pyroptosis and Apoptosis Pathways Engage in Bidirectional Crosstalk in Monocytes and Macrophages. Cell chemical biology. 2017;24(4):507-14.e4. Epub 2017/04/11. doi: 10.1016/j.chembiol.2017.03.009. PubMed PMID: 28392147; PubMed Central PMCID: PMCPMC5467448.
170. Chen KW, Demarco B, Heilig R, Shkarina K, Boettcher A, Farady CJ, et al. Extrinsic and intrinsic apoptosis activate pannexin-1 to drive NLRP 3 inflammasome assembly. 2019;38(10):e101638.
171. Martinon F, Burns K, Tschopp J. The inflammasome: a molecular platform triggering activation of inflammatory caspases and processing of proIL-beta. Molecular cell. 2002;10(2):417-26. Epub 2002/08/23. PubMed PMID: 12191486.
172. Broz P. Recognition of Intracellular Bacteria by Inflammasomes. Microbiology spectrum. 2019;7(2). Epub 2019/03/09. doi: 10.1128/microbiolspec.BAI-0003-2019. PubMed PMID: 30848231.
173. Martinon F, Petrilli V, Mayor A, Tardivel A, Tschopp J. Gout-associated uric acid crystals activate the NALP3 inflammasome. Nature. 2006;440(7081):237-41. Epub 2006/01/13. doi: 10.1038/nature04516. PubMed PMID: 16407889.
174. Dostert C, Petrilli V, Van Bruggen R, Steele C, Mossman BT, Tschopp J. Innate immune activation through Nalp3 inflammasome sensing of asbestos and silica. Science (New York, NY). 2008;320(5876):674-7. Epub 2008/04/12. doi: 10.1126/science.1156995. PubMed PMID: 18403674; PubMed Central PMCID: PMCPMC2396588.
175. Mariathasan S, Weiss DS, Newton K, McBride J, O'Rourke K, Roose-Girma M, et al. Cryopyrin activates the inflammasome in response to toxins and ATP. Nature. 2006;440(7081):228-32. Epub 2006/01/13. doi: 10.1038/nature04515. PubMed PMID: 16407890.
176. Ng J, Hirota SA, Gross O, Li Y, Ulke-Lemee A, Potentier MS, et al. Clostridium difficile toxin-induced inflammation and intestinal injury are mediated by the inflammasome. Gastroenterology. 2010;139(2):542-52, 52.e1-3. Epub 2010/04/20. doi: 10.1053/j.gastro.2010.04.005. PubMed PMID: 20398664.
177. Allen IC, Scull MA, Moore CB, Holl EK, McElvania-TeKippe E, Taxman DJ, et al. The NLRP3 inflammasome mediates in vivo innate immunity to influenza A virus through recognition of viral RNA. Immunity. 2009;30(4):556-65. Epub 2009/04/14. doi: 10.1016/j.immuni.2009.02.005. PubMed PMID: 19362020; PubMed Central PMCID: PMCPMC2803103.
178. Kim S, Bauernfeind F, Ablasser A, Hartmann G, Fitzgerald KA, Latz E, et al. Listeria monocytogenes is sensed by the NLRP3 and AIM2 inflammasome. European journal of immunology. 2010;40(6):1545-51. Epub 2010/03/25. doi: 10.1002/eji.201040425. PubMed PMID: 20333626; PubMed Central PMCID: PMCPMC3128919.
179. McElvania Tekippe E, Allen IC, Hulseberg PD, Sullivan JT, McCann JR, Sandor M, et al. Granuloma formation and host defense in chronic Mycobacterium tuberculosis infection requires PYCARD/ASC but not NLRP3 or caspase-1. PloS one. 2010;5(8):e12320. Epub 2010/09/03. doi: 10.1371/journal.pone.0012320. PubMed PMID: 20808838; PubMed Central PMCID: PMCPMC2924896.

180. Gross O, Poeck H, Bscheider M, Dostert C, Hannesschlager N, Endres S, et al. Syk kinase signalling couples to the Nlrp3 inflammasome for anti-fungal host defence. Nature. 2009;459(7245):433-6. Epub 2009/04/03. doi: 10.1038/nature07965. PubMed PMID: 19339971.
181. Wang X, Gong P, Zhang X, Li S, Lu X, Zhao C, et al. NLRP3 Inflammasome Participates in Host Response to Neospora caninum Infection. Frontiers in immunology. 2018;9:1791. Epub 2018/08/15. doi: 10.3389/fimmu.2018.01791. PubMed PMID: 30105037; PubMed Central PMCID: PMCPMC6077289.
182. Petrilli V, Papin S, Dostert C, Mayor A, Martinon F, Tschopp J. Activation of the NALP3 inflammasome is triggered by low intracellular potassium concentration. Cell death and differentiation. 2007;14(9):1583-9. Epub 2007/06/30. doi: 10.1038/sj.cdd.4402195. PubMed PMID: 17599094.
183. Zhou R, Yazdi AS, Menu P, Tschopp J. A role for mitochondria in NLRP3 inflammasome activation. Nature. 2011;469(7329):221-5. Epub 2010/12/03. doi: 10.1038/nature09663. PubMed PMID: 21124315.
184. Bauernfeind F, Bartok E, Rieger A, Franchi L, Nunez G, Hornung V. Cutting edge: reactive oxygen species inhibitors block priming, but not activation, of the NLRP3 inflammasome. J Immunol. 2011;187(2):613-7. Epub 2011/06/17. doi: 10.4049/jimmunol.1100613. PubMed PMID: 21677136; PubMed Central PMCID: PMCPMC3131480.
185. Boyden ED, Dietrich WF. Nalp1b controls mouse macrophage susceptibility to anthrax lethal toxin. Nature genetics. 2006;38(2):240-4. Epub 2006/01/24. doi: 10.1038/ng1724. PubMed PMID: 16429160.
186. Duncan JA, Canna SW. The NLRC4 Inflammasome. Immunological reviews. 2018;281(1):115-23. Epub 2017/12/17. doi: 10.1111/imr.12607. PubMed PMID: 29247997; PubMed Central PMCID: PMCPMC5897049.
187. Kofoed EM, Vance RE. Innate immune recognition of bacterial ligands by NAIPs determines inflammasome specificity. Nature. 2011;477(7366):592-5. Epub 2011/08/30. doi: 10.1038/nature10394. PubMed PMID: 21874021; PubMed Central PMCID: PMCPMC3184209.
188. Mariathasan S, Newton K, Monack DM, Vucic D, French DM, Lee WP, et al. Differential activation of the inflammasome by caspase-1 adaptors ASC and Ipaf. Nature. 2004;430(6996):213-8. Epub 2004/06/11. doi: 10.1038/nature02664. PubMed PMID: 15190255.
189. Sutterwala FS, Mijares LA, Li L, Ogura Y, Kazmierczak BI, Flavell RA. Immune recognition of Pseudomonas aeruginosa mediated by the IPAF/NLRC4 inflammasome. J Exp Med. 2007;204(13):3235-45. Epub 2007/12/12. doi: 10.1084/jem.20071239. PubMed PMID: 18070936; PubMed Central PMCID: PMCPMC2150987.
190. Zamboni DS, Kobayashi KS, Kohlsdorf T, Ogura Y, Long EM, Vance RE, et al. The Birc1e cytosolic pattern-recognition receptor contributes to the detection and control of Legionella pneumophila infection. Nature immunology. 2006;7(3):318-25. Epub 2006/01/31. doi: 10.1038/ni1305. PubMed PMID: 16444259.
191. Miao EA, Ernst RK, Dors M, Mao DP, Aderem A. Pseudomonas aeruginosa activates caspase-1 through Ipaf. Proc Natl Acad Sci U S A. 2008;105(7):2562-7. Epub 2008/02/08. doi: 10.1073/pnas.0712183105. PubMed PMID: 18256184; PubMed Central PMCID: PMCPMC2268176.
192. Brodsky IE, Palm NW, Sadanand S, Ryndak MB, Sutterwala FS, Flavell RA, et al. A Yersinia effector protein promotes virulence by preventing inflammasome recognition of the type III secretion system. Cell host & microbe. 2010;7(5):376-87. Epub 2010/05/19. doi:

10.1016/j.chom.2010.04.009. PubMed PMID: 20478539; PubMed Central PMCID: PMCPMC2883865.
193. Luo X, Yang Y, Shen T, Tang X, Xiao Y, Zou T, et al. Docosahexaenoic acid ameliorates palmitate-induced lipid accumulation and inflammation through repressing NLRC4 inflammasome activation in HepG2 cells. Nutrition & metabolism. 2012;9(1):34. Epub 2012/04/21. doi: 10.1186/1743-7075-9-34. PubMed PMID: 22515414; PubMed Central PMCID: PMCPMC3428681.
194. Muruve DA, Petrilli V, Zaiss AK, White LR, Clark SA, Ross PJ, et al. The inflammasome recognizes cytosolic microbial and host DNA and triggers an innate immune response. Nature. 2008;452(7183):103-7. Epub 2008/02/22. doi: 10.1038/nature06664. PubMed PMID: 18288107.
195. Rathinam VA, Jiang Z, Waggoner SN, Sharma S, Cole LE, Waggoner L, et al. The AIM2 inflammasome is essential for host defense against cytosolic bacteria and DNA viruses. Nature immunology. 2010;11(5):395-402. Epub 2010/03/31. doi: 10.1038/ni.1864. PubMed PMID: 20351692; PubMed Central PMCID: PMCPMC2887480.
196. Burckstummer T, Baumann C, Bluml S, Dixit E, Durnberger G, Jahn H, et al. An orthogonal proteomic-genomic screen identifies AIM2 as a cytoplasmic DNA sensor for the inflammasome. Nature immunology. 2009;10(3):266-72. Epub 2009/01/23. doi: 10.1038/ni.1702. PubMed PMID: 19158679.
197. Hornung V, Ablasser A, Charrel-Dennis M, Bauernfeind F, Horvath G, Caffrey DR, et al. AIM2 recognizes cytosolic dsDNA and forms a caspase-1-activating inflammasome with ASC. Nature. 2009;458(7237):514-8. Epub 2009/01/23. doi: 10.1038/nature07725. PubMed PMID: 19158675; PubMed Central PMCID: PMCPMC2726264.
198. Martinon F, Mayor A, Tschopp J. The inflammasomes: guardians of the body. Annual review of immunology. 2009;27:229-65. Epub 2009/03/24. doi: 10.1146/annurev.immunol.021908.132715. PubMed PMID: 19302040.
199. de Torre-Minguela C, Mesa Del Castillo P, Pelegrín P. The NLRP3 and Pyrin Inflammasomes: Implications in the Pathophysiology of Autoinflammatory Diseases. Frontiers in immunology. 2017;8:43. Epub 2017/02/14. doi: 10.3389/fimmu.2017.00043. PubMed PMID: 28191008; PubMed Central PMCID: PMCPMC5271383.
200. Kayagaki N, Warming S, Lamkanfi M, Vande Walle L, Louie S, Dong J, et al. Non-canonical inflammasome activation targets caspase-11. Nature. 2011;479(7371):117-21. Epub 2011/10/18. doi: 10.1038/nature10558. PubMed PMID: 22002608.
201. Baker PJ, Boucher D, Bierschenk D, Tebartz C, Whitney PG, D'Silva DB, et al. NLRP3 inflammasome activation downstream of cytoplasmic LPS recognition by both caspase-4 and caspase-5. European journal of immunology. 2015;45(10):2918-26. Epub 2015/07/16. doi: 10.1002/eji.201545655. PubMed PMID: 26173988.
202. Pillon NJ, Chan KL, Zhang S, Mejdani M, Jacobson MR, Ducos A, et al. Saturated fatty acids activate caspase-4/5 in human monocytes, triggering IL-1beta and IL-18 release. American journal of physiology Endocrinology and metabolism. 2016;311(5):E825-e35. Epub 2016/11/03. doi: 10.1152/ajpendo.00296.2016. PubMed PMID: 27624102.
203. Chen R, Zhu S, Zeng L, Wang Q, Sheng Y, Zhou B, et al. AGER-Mediated Lipid Peroxidation Drives Caspase-11 Inflammasome Activation in Sepsis. Frontiers in immunology. 2019;10:1904. Epub 2019/08/24. doi: 10.3389/fimmu.2019.01904. PubMed PMID: 31440260; PubMed Central PMCID: PMCPMC6694796.

204. Karki R, Man SM, Malireddi RKS, Gurung P, Vogel P, Lamkanfi M, et al. Concerted activation of the AIM2 and NLRP3 inflammasomes orchestrates host protection against Aspergillus infection. Cell host & microbe. 2015;17(3):357-68. Epub 2015/02/24. doi: 10.1016/j.chom.2015.01.006. PubMed PMID: 25704009; PubMed Central PMCID: PMCPMC4359672.
205. Ichinohe T, Lee HK, Ogura Y, Flavell R, Iwasaki A. Inflammasome recognition of influenza virus is essential for adaptive immune responses. J Exp Med. 2009;206(1):79-87. Epub 2009/01/14. doi: 10.1084/jem.20081667. PubMed PMID: 19139171; PubMed Central PMCID: PMCPMC2626661.
206. Thomas PG, Dash P, Aldridge JR, Jr., Ellebedy AH, Reynolds C, Funk AJ, et al. The intracellular sensor NLRP3 mediates key innate and healing responses to influenza A virus via the regulation of caspase-1. Immunity. 2009;30(4):566-75. Epub 2009/04/14. doi: 10.1016/j.immuni.2009.02.006. PubMed PMID: 19362023; PubMed Central PMCID: PMCPMC2765464.
207. Kip E, Naze F, Suin V, Vanden Berghe T, Francart A, Lamoral S, et al. Impact of caspase-1/11, -3, -7, or IL-1beta/IL-18 deficiency on rabies virus-induced macrophage cell death and onset of disease. Cell death discovery. 2017;3:17012. Epub 2017/03/11. doi: 10.1038/cddiscovery.2017.12. PubMed PMID: 28280602; PubMed Central PMCID: PMCPMC5339016.
208. Wang Y, Hanus JW, Abu-Asab MS, Shen D, Ogilvy A, Ou J, et al. NLRP3 Upregulation in Retinal Pigment Epithelium in Age-Related Macular Degeneration. International journal of molecular sciences. 2016;17(1). doi: 10.3390/ijms17010073. PubMed PMID: 26760997; PubMed Central PMCID: PMCPMC4730317.
209. Tseng WA, Thein T, Kinnunen K, Lashkari K, Gregory MS, D'Amore PA, et al. NLRP3 inflammasome activation in retinal pigment epithelial cells by lysosomal destabilization: implications for age-related macular degeneration. Investigative ophthalmology & visual science. 2013;54(1):110-20. Epub 2012/12/12. doi: 10.1167/iovs.12-10655. PubMed PMID: 23221073; PubMed Central PMCID: PMCPMC3544415.
210. Tarallo V, Hirano Y, Gelfand BD, Dridi S, Kerur N, Kim Y, et al. DICER1 loss and Alu RNA Induce Age-Related Macular Degeneration via the NLRP3 Inflammasome and MyD88. Cell. 2012;149(4):847-59. doi: 10.1016/j.cell.2012.03.036. PubMed PMID: 22541070; PubMed Central PMCID: PMCPMC3351582.
211. Viringipurampeer IA, Metcalfe AL, Bashar AE, Sivak O, Yanai A, Mohammadi Z, et al. NLRP3 inflammasome activation drives bystander cone photoreceptor cell death in a P23H rhodopsin model of retinal degeneration. Human molecular genetics. 2016;25(8):1501-16. Epub 2016/03/25. doi: 10.1093/hmg/ddw029. PubMed PMID: 27008885; PubMed Central PMCID: PMCPMC4805309.
212. Jin X, Jin H, Shi Y, Guo Y, Zhang H. Pyroptosis, a novel mechanism implicated in cataracts. Molecular medicine reports. 2018;18(2):2277-85. Epub 2018/06/30. doi: 10.3892/mmr.2018.9188. PubMed PMID: 29956729.
213. Sun N, Zhang H. Pyroptosis in pterygium pathogenesis. Bioscience reports. 2018;38(3). Epub 2018/05/05. doi: 10.1042/bsr20180282. PubMed PMID: 29724886; PubMed Central PMCID: PMCPMC6048216.
214. Pronin A, Pham D, An W, Dvoriantchikova G, Reshetnikova G, Qiao J, et al. Inflammasome Activation Induces Pyroptosis in the Retina Exposed to Ocular Hypertension Injury. Frontiers in molecular neuroscience. 2019;12:36. Epub 2019/04/02. doi:

10.3389/fnmol.2019.00036. PubMed PMID: 30930743; PubMed Central PMCID: PMCPMC6425693.
215. Gu C, Draga D, Zhou C, Su T, Zou C, Gu Q, et al. miR-590-3p Inhibits Pyroptosis in Diabetic Retinopathy by Targeting NLRP1 and Inactivating the NOX4 Signaling Pathway. Investigative ophthalmology & visual science. 2019;60(13):4215-23. Epub 2019/10/17. doi: 10.1167/iovs.19-27825. PubMed PMID: 31618425.
216. Zhang Y, Song Z, Li X, Xu S, Zhou S, Jin X, et al. Long noncoding RNA KCNQ1OT1 induces pyroptosis in diabetic corneal endothelial keratopathy. American journal of physiology Cell physiology. 2019. Epub 2019/11/07. doi: 10.1152/ajpcell.00053.2019. PubMed PMID: 31693400.
217. Mauel J, Defendi V. Infection and transformation of mouse peritoneal macrophages by simian virus 40. J Exp Med. 1971;134(2):335-50. Epub 1971/08/01. doi: 10.1084/jem.134.2.335. PubMed PMID: 4326994; PubMed Central PMCID: PMCPMC2139048.
218. Heise MT, Pollock JL, O'Guin A, Barkon ML, Bormley S, Virgin HWt. Murine cytomegalovirus infection inhibits IFN gamma-induced MHC class II expression on macrophages: the role of type I interferon. Virology. 1998;241(2):331-44. Epub 1998/03/21. doi: 10.1006/viro.1997.8969. PubMed PMID: 9499808.
219. Menard C, Wagner M, Ruzsics Z, Holak K, Brune W, Campbell AE, et al. Role of murine cytomegalovirus US22 gene family members in replication in macrophages. J Virol. 2003;77(10):5557-70. Epub 2003/04/30. doi: 10.1128/jvi.77.10.5557-5570.2003. PubMed PMID: 12719548; PubMed Central PMCID: PMCPMC154053.
220. Presti RM, Popkin DL, Connick M, Paetzold S, Virgin HWt. Novel cell type-specific antiviral mechanism of interferon gamma action in macrophages. J Exp Med. 2001;193(4):483-96. Epub 2001/02/22. doi: 10.1084/jem.193.4.483. PubMed PMID: 11181700; PubMed Central PMCID: PMCPMC2195910.
221. Strobl B, Bubic I, Bruns U, Steinborn R, Lajko R, Kolbe T, et al. Novel functions of tyrosine kinase 2 in the antiviral defense against murine cytomegalovirus. J Immunol. 2005;175(6):4000-8. Epub 2005/09/09. doi: 10.4049/jimmunol.175.6.4000. PubMed PMID: 16148148.
222. Kelsey DK, Kern ER, Overall JC, Jr., Glasgow LA. Effect of cytosine arabinoside and 5-iodo-2'-deoxyuridine on a cytomegalovirus infection in newborn mice. Antimicrob Agents Chemother. 1976;9(3):458-64. PubMed PMID: 176935; PubMed Central PMCID: PMCPMC429552.
223. Sinickas VG, Ashman RB, Blanden RV. The cytotoxic response to murine cytomegalovirus. I. Parameters in vivo. J Gen Virol. 1985;66 (Pt 4):747-55. doi: 10.1099/0022-1317-66-4-747. PubMed PMID: 2984317.
224. Loh L, Hudson JB. Immunosuppressive effect of murine cytomegalovirus. Infection and immunity. 1980;27(1):54-60. Epub 1980/01/01. PubMed PMID: 6244228; PubMed Central PMCID: PMCPMC550721.
225. Duan Y, Ji Z, Atherton SS. Dissemination and replication of MCMV after supraciliary inoculation in immunosuppressed BALB/c mice. Investigative ophthalmology & visual science. 1994;35(3):1124-31. Epub 1994/03/01. PubMed PMID: 8125723.
226. Alston CI, Dix RD. Reduced frequency of murine cytomegalovirus retinitis in C57BL/6 mice correlates with low levels of suppressor of cytokine signaling (SOCS)1 and SOCS3 expression within the eye during corticosteroid-induced immunosuppression. Cytokine.

2017;97:38-41. Epub 2017/05/31. doi: 10.1016/j.cyto.2017.05.021. PubMed PMID: 28558309; PubMed Central PMCID: PMCPMC5517024.
227. Wang S, Miura M, Jung Y, Zhu H, Gagliardini V, Shi L, et al. Identification and characterization of Ich-3, a member of the interleukin-1beta converting enzyme (ICE)/Ced-3 family and an upstream regulator of ICE. The Journal of biological chemistry. 1996;271(34):20580-7. Epub 1996/08/23. PubMed PMID: 8702803.
228. Kang SJ, Wang S, Hara H, Peterson EP, Namura S, Amin-Hanjani S, et al. Dual role of caspase-11 in mediating activation of caspase-1 and caspase-3 under pathological conditions. The Journal of cell biology. 2000;149(3):613-22. Epub 2000/05/03. PubMed PMID: 10791975; PubMed Central PMCID: PMCPMC2174843.
229. Brune W, Andoniou CE. Die Another Day: Inhibition of Cell Death Pathways by Cytomegalovirus. Viruses. 2017;9(9). Epub 2017/09/05. doi: 10.3390/v9090249. PubMed PMID: 28869497; PubMed Central PMCID: PMCPMC5618015.
230. Cho YS, Challa S, Moquin D, Genga R, Ray TD, Guildford M, et al. Phosphorylation-driven assembly of the RIP1-RIP3 complex regulates programmed necrosis and virus-induced inflammation. Cell. 2009;137(6):1112-23. Epub 2009/06/16. doi: 10.1016/j.cell.2009.05.037. PubMed PMID: 19524513; PubMed Central PMCID: PMCPMC2727676.
231. Lotzerich M, Roulin PS, Boucke K, Witte R, Georgiev O, Greber UF. Rhinovirus 3C protease suppresses apoptosis and triggers caspase-independent cell death. Cell death & disease. 2018;9(3):272. Epub 2018/02/17. doi: 10.1038/s41419-018-0306-6. PubMed PMID: 29449668; PubMed Central PMCID: PMCPMC5833640.
232. Cho YS. The role of necroptosis in the treatment of diseases. BMB reports. 2018;51(5):219-24. Epub 2018/04/11. doi: 10.5483/bmbrep.2018.51.5.074. PubMed PMID: 29636122; PubMed Central PMCID: PMCPMC5988575.
233. Idriss HT, Naismith JH. TNF alpha and the TNF receptor superfamily: structure-function relationship(s). Microscopy research and technique. 2000;50(3):184-95. Epub 2000/07/13. doi: 10.1002/1097-0029(20000801)50:3<184::aid-jemt2>3.0.co;2-h. PubMed PMID: 10891884.
234. Deter RL, De Duve C. Influence of glucagon, an inducer of cellular autophagy, on some physical properties of rat liver lysosomes. The Journal of cell biology. 1967;33(2):437-49. Epub 1967/05/01. doi: 10.1083/jcb.33.2.437. PubMed PMID: 4292315; PubMed Central PMCID: PMCPMC2108350.
235. Kumar B, Cashman SM, Kumar-Singh R. Complement-Mediated Activation of the NLRP3 Inflammasome and Its Inhibition by AAV-Mediated Delivery of CD59 in a Model of Uveitis. Molecular therapy : the journal of the American Society of Gene Therapy. 2018. Epub 2018/04/22. doi: 10.1016/j.ymthe.2018.03.012. PubMed PMID: 29678656.
236. Jin X, Wang C, Wu W, Liu T, Ji B, Zhou F. Cyanidin-3-glucoside Alleviates 4-Hydroxyhexenal-Induced NLRP3 Inflammasome Activation via JNK-c-Jun/AP-1 Pathway in Human Retinal Pigment Epithelial Cells. Journal of immunology research. 2018;2018:5604610. Epub 2018/06/02. doi: 10.1155/2018/5604610. PubMed PMID: 29854843; PubMed Central PMCID: PMCPMC5952446.
237. Liu Q, Zhang F, Zhang X, Cheng R, Ma JX, Yi J, et al. Fenofibrate ameliorates diabetic retinopathy by modulating Nrf2 signaling and NLRP3 inflammasome activation. Molecular and cellular biochemistry. 2017. Epub 2017/12/22. doi: 10.1007/s11010-017-3256-x. PubMed PMID: 29264825.
238. Kosmidou C, Efstathiou NE, Hoang MV, Notomi S, Konstantinou EK, Hirano M, et al. Issues with the Specificity of Immunological Reagents for NLRP3: Implications for Age-related

Macular Degeneration. Scientific reports. 2018;8(1):461. Epub 2018/01/13. doi: 10.1038/s41598-017-17634-1. PubMed PMID: 29323137; PubMed Central PMCID: PMCPMC5764999.
239. Basu S, Fowler BJ, Kerur N, Arnvig KB, Rao NA. NLRP3 inflammasome activation by mycobacterial ESAT-6 and dsRNA in intraocular tuberculosis. Microbial pathogenesis. 2018;114:219-24. Epub 2017/11/29. doi: 10.1016/j.micpath.2017.11.044. PubMed PMID: 29180292.
240. Chaurasia SS, Lim RR, Parikh BH, Wey YS, Tun BB, Wong TY, et al. The NLRP3 Inflammasome May Contribute to Pathologic Neovascularization in the Advanced Stages of Diabetic Retinopathy. Scientific reports. 2018;8(1):2847. Epub 2018/02/13. doi: 10.1038/s41598-018-21198-z. PubMed PMID: 29434227; PubMed Central PMCID: PMCPMC5809448.
241. Gao J, Cui JZ, To E, Cao S, Matsubara JA. Evidence for the activation of pyroptotic and apoptotic pathways in RPE cells associated with NLRP3 inflammasome in the rodent eye. Journal of neuroinflammation. 2018;15(1):15. Epub 2018/01/14. doi: 10.1186/s12974-018-1062-3. PubMed PMID: 29329580; PubMed Central PMCID: PMCPMC5766992.
242. Anderson OA, Finkelstein A, Shima DT. A2E induces IL-1ss production in retinal pigment epithelial cells via the NLRP3 inflammasome. PloS one. 2013;8(6):e67263. Epub 2013/07/11. doi: 10.1371/journal.pone.0067263. PubMed PMID: 23840644; PubMed Central PMCID: PMCPMC3696103.
243. Lei C, Lin R, Wang J, Tao L, Fu X, Qiu Y, et al. Amelioration of amyloid beta-induced retinal inflammatory responses by a LXR agonist TO901317 is associated with inhibition of the NF-kappaB signaling and NLRP3 inflammasome. Neuroscience. 2017;360:48-60. Epub 2017/08/02. doi: 10.1016/j.neuroscience.2017.07.053. PubMed PMID: 28760679.
244. Liang L, Tan X, Zhou Q, Zhu Y, Tian Y, Yu H, et al. IL-1beta triggered by peptidoglycan and lipopolysaccharide through TLR2/4 and ROS-NLRP3 inflammasome-dependent pathways is involved in ocular Behcet's disease. Investigative ophthalmology & visual science. 2013;54(1):402-14. Epub 2012/12/06. doi: 10.1167/iovs.12-11047. PubMed PMID: 23211828.
245. Gimenez F, Bhela S, Dogra P, Harvey L, Varanasi SK, Jaggi U, et al. The inflammasome NLRP3 plays a protective role against a viral immunopathological lesion. Journal of leukocyte biology. 2016;99(5):647-57. Epub 2015/10/31. doi: 10.1189/jlb.3HI0715-321R. PubMed PMID: 26516184; PubMed Central PMCID: PMCPMC4831481.
246. Bian F, Xiao Y, Zaheer M, Volpe EA, Pflugfelder SC, Li DQ, et al. Inhibition of NLRP3 Inflammasome Pathway by Butyrate Improves Corneal Wound Healing in Corneal Alkali Burn. International journal of molecular sciences. 2017;18(3). Epub 2017/03/10. doi: 10.3390/ijms18030562. PubMed PMID: 28273882; PubMed Central PMCID: PMCPMC5372578.
247. Rosenzweig HL, Woods A, Clowers JS, Planck SR, Rosenbaum JT. The NLRP3 inflammasome is active but not essential in endotoxin-induced uveitis. Inflammation research : official journal of the European Histamine Research Society [et al]. 2012;61(3):225-31. Epub 2011/11/29. doi: 10.1007/s00011-011-0404-8. PubMed PMID: 22119862; PubMed Central PMCID: PMCPMC3335428.
248. Zheng Q, Ren Y, Reinach PS, Xiao B, Lu H, Zhu Y, et al. Reactive oxygen species activated NLRP3 inflammasomes initiate inflammation in hyperosmolarity stressed human corneal epithelial cells and environment-induced dry eye patients. Experimental eye research.

2015;134:133-40. Epub 2015/02/24. doi: 10.1016/j.exer.2015.02.013. PubMed PMID: 25701684.
249. Zheng Q, Ren Y, Reinach PS, She Y, Xiao B, Hua S, et al. Reactive oxygen species activated NLRP3 inflammasomes prime environment-induced murine dry eye. Experimental eye research. 2014;125:1-8. Epub 2014/05/20. doi: 10.1016/j.exer.2014.05.001. PubMed PMID: 24836981.
250. Niu L, Zhang S, Wu J, Chen L, Wang Y. Upregulation of NLRP3 Inflammasome in the Tears and Ocular Surface of Dry Eye Patients. PloS one. 2015;10(5):e0126277. Epub 2015/05/12. doi: 10.1371/journal.pone.0126277. PubMed PMID: 25962072; PubMed Central PMCID: PMCPMC4427105.
251. Chi W, Li F, Chen H, Wang Y, Zhu Y, Yang X, et al. Caspase-8 promotes NLRP1/NLRP3 inflammasome activation and IL-1beta production in acute glaucoma. Proc Natl Acad Sci U S A. 2014;111(30):11181-6. Epub 2014/07/16. doi: 10.1073/pnas.1402819111. PubMed PMID: 25024200; PubMed Central PMCID: PMCPMC4121847.
252. Li Y, Liu C, Wan XS, Li SW. NLRP1 deficiency attenuates diabetic retinopathy (DR) in mice through suppressing inflammation response. Biochemical and biophysical research communications. 2018;501(2):351-7. Epub 2018/03/25. doi: 10.1016/j.bbrc.2018.03.148. PubMed PMID: 29571734.
253. Prager P, Hollborn M, Steffen A, Wiedemann P, Kohen L, Bringmann A. P2Y1 Receptor Signaling Contributes to High Salt-Induced Priming of the NLRP3 Inflammasome in Retinal Pigment Epithelial Cells. PloS one. 2016;11(10):e0165653. Epub 2016/10/28. doi: 10.1371/journal.pone.0165653. PubMed PMID: 27788256; PubMed Central PMCID: PMCPMC5082949.
254. Chidrawar S, Khan N, Wei W, McLarnon A, Smith N, Nayak L, et al. Cytomegalovirus-seropositivity has a profound influence on the magnitude of major lymphoid subsets within healthy individuals. Clin Exp Immunol. 2009;155(3):423-32. doi: 10.1111/j.1365-2249.2008.03785.x. PubMed PMID: 19220832; PubMed Central PMCID: PMCPMC2669518.
255. Hanson LK, Slater JS, Karabekian Z, Virgin HWt, Biron CA, Ruzek MC, et al. Replication of murine cytomegalovirus in differentiated macrophages as a determinant of viral pathogenesis. J Virol. 1999;73(7):5970-80. Epub 1999/06/11. PubMed PMID: 10364349; PubMed Central PMCID: PMCPMC112658.
256. Jordan MC, Mar VL. Spontaneous activation of latent cytomegalovirus from murine spleen explants. Role of lymphocytes and macrophages in release and replication of virus. The Journal of clinical investigation. 1982;70(4):762-8. Epub 1982/10/01. doi: 10.1172/jci110672. PubMed PMID: 6288769; PubMed Central PMCID: PMCPMC370284.
257. Alston CI, Dix RD. Murine cytomegalovirus infection of mouse macrophages stimulates early expression of suppressor of cytokine signaling (SOCS)1 and SOCS3. PloS one. 2017;12(2):e0171812-e. doi: 10.1371/journal.pone.0171812. PubMed PMID: 28182772.
258. Trapani JA, Browne KA, Dawson MJ, Ramsay RG, Eddy RL, Show TB, et al. A novel gene constitutively expressed in human lymphoid cells is inducible with interferon-gamma in myeloid cells. Immunogenetics. 1992;36(6):369-76. Epub 1992/01/01. PubMed PMID: 1526658.
259. Roy A, Dutta D, Iqbal J, Pisano G, Gjyshi O, Ansari MA, et al. Nuclear Innate Immune DNA Sensor IFI16 Is Degraded during Lytic Reactivation of Kaposi's Sarcoma-Associated Herpesvirus (KSHV): Role of IFI16 in Maintenance of KSHV Latency. J Virol. 2016;90(19):8822-41. Epub 2016/07/29. doi: 10.1128/jvi.01003-16. PubMed PMID: 27466416; PubMed Central PMCID: PMCPMC5021400.

260. Johnson KE, Bottero V, Flaherty S, Dutta S, Singh VV, Chandran B. IFI16 restricts HSV-1 replication by accumulating on the hsv-1 genome, repressing HSV-1 gene expression, and directly or indirectly modulating histone modifications. PLoS pathogens. 2014;10(11):e1004503. Epub 2014/11/07. doi: 10.1371/journal.ppat.1004503. PubMed PMID: 25375629; PubMed Central PMCID: PMCPMC4223080.
261. Gariano GR, Dell'Oste V, Bronzini M, Gatti D, Luganini A, De Andrea M, et al. The intracellular DNA sensor IFI16 gene acts as restriction factor for human cytomegalovirus replication. PLoS pathogens. 2012;8(1):e1002498. Epub 2012/02/01. doi: 10.1371/journal.ppat.1002498. PubMed PMID: 22291595; PubMed Central PMCID: PMCPMC3266931.
262. Lo Cigno I, De Andrea M, Borgogna C, Albertini S, Landini MM, Peretti A, et al. The Nuclear DNA Sensor IFI16 Acts as a Restriction Factor for Human Papillomavirus Replication through Epigenetic Modifications of the Viral Promoters. J Virol. 2015;89(15):7506-20. Epub 2015/05/15. doi: 10.1128/jvi.00013-15. PubMed PMID: 25972554; PubMed Central PMCID: PMCPMC4505635.
263. Ansari MA, Singh VV, Dutta S, Veettil MV, Dutta D, Chikoti L, et al. Constitutive interferon-inducible protein 16-inflammasome activation during Epstein-Barr virus latency I, II, and III in B and epithelial cells. J Virol. 2013;87(15):8606-23. Epub 2013/05/31. doi: 10.1128/jvi.00805-13. PubMed PMID: 23720728; PubMed Central PMCID: PMCPMC3719826.
264. Singh VV, Kerur N, Bottero V, Dutta S, Chakraborty S, Ansari MA, et al. Kaposi's sarcoma-associated herpesvirus latency in endothelial and B cells activates gamma interferon-inducible protein 16-mediated inflammasomes. J Virol. 2013;87(8):4417-31. Epub 2013/02/08. doi: 10.1128/jvi.03282-12. PubMed PMID: 23388709; PubMed Central PMCID: PMCPMC3624349.
265. Conrady CD, Zheng M, Fitzgerald KA, Liu C, Carr DJ. Resistance to HSV-1 infection in the epithelium resides with the novel innate sensor, IFI-16. Mucosal immunology. 2012;5(2):173-83. Epub 2012/01/13. doi: 10.1038/mi.2011.63. PubMed PMID: 22236996; PubMed Central PMCID: PMCPMC3288395.
266. Abdelaziz DH, Khalil H, Cormet-Boyaka E, Amer AO. The cooperation between the autophagy machinery and the inflammasome to implement an appropriate innate immune response: do they regulate each other? Immunological reviews. 2015;265(1):194-204. Epub 2015/04/17. doi: 10.1111/imr.12288. PubMed PMID: 25879294; PubMed Central PMCID: PMCPMC4747236.
267. Kaarniranta K, Tokarz P, Koskela A, Paterno J, Blasiak J. Autophagy regulates death of retinal pigment epithelium cells in age-related macular degeneration. Cell biology and toxicology. 2017;33(2):113-28. Epub 2016/12/03. doi: 10.1007/s10565-016-9371-8. PubMed PMID: 27900566; PubMed Central PMCID: PMCPMC5325845.
268. Mo J, Zhang M, Marshall B, Smith S, Covar J, Atherton S. Interplay of autophagy and apoptosis during murine cytomegalovirus infection of RPE cells. Molecular vision. 2014;20:1161-73. Epub 2014/10/18. PubMed PMID: 25324684; PubMed Central PMCID: PMCPMC4145064.
269. Veldman-Jones MH, Lai Z, Wappett M, Harbron CG, Barrett JC, Harrington EA, et al. Reproducible, Quantitative, and Flexible Molecular Subtyping of Clinical DLBCL Samples Using the NanoString nCounter System. Clinical cancer research : an official journal of the American Association for Cancer Research. 2015;21(10):2367-78. Epub 2014/10/11. doi: 10.1158/1078-0432.ccr-14-0357. PubMed PMID: 25301847.

270. Geiss GK, Bumgarner RE, Birditt B, Dahl T, Dowidar N, Dunaway DL, et al. Direct multiplexed measurement of gene expression with color-coded probe pairs. Nature biotechnology. 2008;26(3):317-25. Epub 2008/02/19. doi: 10.1038/nbt1385. PubMed PMID: 18278033.
271. Veldman-Jones MH, Brant R, Rooney C, Geh C, Emery H, Harbron CG, et al. Evaluating Robustness and Sensitivity of the NanoString Technologies nCounter Platform to Enable Multiplexed Gene Expression Analysis of Clinical Samples. Cancer research. 2015;75(13):2587-93. Epub 2015/06/13. doi: 10.1158/0008-5472.can-15-0262. PubMed PMID: 26069246.
272. Funaro A, Ortolan E, Bovino P, Lo Buono N, Nacci G, Parrotta R, et al. Ectoenzymes and innate immunity: the role of human CD157 in leukocyte trafficking. Frontiers in bioscience (Landmark edition). 2009;14:929-43. Epub 2009/03/11. doi: 10.2741/3287. PubMed PMID: 19273109.
273. Choudhary GS, Al-harbi S, Almasan A. Caspase-3 Activation Is a Critical Determinant of Genotoxic Stress-Induced Apoptosis. In: Mor G, Alvero AB, editors. Apoptosis and Cancer: Methods and Protocols. New York, NY: Springer New York; 2015. p. 1-9.
274. Gibaldi D, Vilar-Pereira G, Pereira IR, Silva AA, Barrios LC, Ramos IP, et al. CCL3/Macrophage Inflammatory Protein-1α Is Dually Involved in Parasite Persistence and Induction of a TNF- and IFNγ-Enriched Inflammatory Milieu in Trypanosoma cruzi-Induced Chronic Cardiomyopathy. Frontiers in immunology. 2020;11:306. Epub 2020/03/21. doi: 10.3389/fimmu.2020.00306. PubMed PMID: 32194558; PubMed Central PMCID: PMCPMC7063958.
275. Hara T, Bacon KB, Cho LC, Yoshimura A, Morikawa Y, Copeland NG, et al. Molecular cloning and functional characterization of a novel member of the C-C chemokine family. The Journal of Immunology. 1995;155(11):5352.
276. McNerney ME, Kumar V. The CD2 Family of Natural Killer Cell Receptors. In: Compans RW, Cooper MD, Honjo T, Koprowski H, Melchers F, Oldstone MBA, et al., editors. Immunobiology of Natural Killer Cell Receptors. Berlin, Heidelberg: Springer Berlin Heidelberg; 2006. p. 91-120.
277. Sung PS, Hsieh SL. CLEC2 and CLEC5A: Pathogenic Host Factors in Acute Viral Infections. Frontiers in immunology. 2019;10:2867. Epub 2019/12/24. doi: 10.3389/fimmu.2019.02867. PubMed PMID: 31867016; PubMed Central PMCID: PMCPMC6909378.
278. Hamann J, Koning N, Pouwels W, Ulfman LH, van Eijk M, Stacey M, et al. EMR1, the human homolog of F4/80, is an eosinophil-specific receptor. 2007;37(10):2797-802. doi: 10.1002/eji.200737553.
279. Shiina T, Blancher A, Inoko H, Kulski JK. Comparative genomics of the human, macaque and mouse major histocompatibility complex. Immunology. 2017;150(2):127-38. Epub 2016/07/11. doi: 10.1111/imm.12624. PubMed PMID: 27395034; PubMed Central PMCID: PMCPMC5214800.
280. Shepardson KM, Larson K, Johns LL, Stanek K, Cho H, Wellham J, et al. IFNAR2 Is Required for Anti-influenza Immunity and Alters Susceptibility to Post-influenza Bacterial Superinfections. Frontiers in immunology. 2018;9:2589-. doi: 10.3389/fimmu.2018.02589. PubMed PMID: 30473701.
281. Shukla AK, McIntyre LL, Marsh SE, Schneider CA, Hoover EM, Walsh CM, et al. CD11a expression distinguishes infiltrating myeloid cells from plaque-associated microglia in Alzheimer's disease. 2019;67(5):844-56. doi: 10.1002/glia.23575.

282. Bole-Feysot C, Goffin V, Edery M, Binart N, Kelly PA. Prolactin (PRL) and its receptor: actions, signal transduction pathways and phenotypes observed in PRL receptor knockout mice. Endocrine reviews. 1998;19(3):225-68. Epub 1998/06/17. doi: 10.1210/edrv.19.3.0334. PubMed PMID: 9626554.
283. Bhosle VK, Rivera JC, Zhou TE, Omri S, Sanchez M, Hamel D, et al. Nuclear localization of platelet-activating factor receptor controls retinal neovascularization. Cell discovery. 2016;2:16017. Epub 2016/07/28. doi: 10.1038/celldisc.2016.17. PubMed PMID: 27462464; PubMed Central PMCID: PMCPMC4941644.
284. Kunzmann AT, Murray LJ, Cardwell CR, McShane CM, McMenamin ÚC, Cantwell MM. PTGS2 (Cyclooxygenase-2) Expression and Survival among Colorectal Cancer Patients: A Systematic Review. Cancer Epidemiology Biomarkers & Prevention. 2013;22(9):1490. doi: 10.1158/1055-9965.EPI-13-0263.
285. Blaszczyk K, Nowicka H, Kostyrko K, Antonczyk A, Wesoly J, Bluyssen HAR. The unique role of STAT2 in constitutive and IFN-induced transcription and antiviral responses. Cytokine & Growth Factor Reviews. 2016;29:71-81. doi: https://doi.org/10.1016/j.cytogfr.2016.02.010.
286. Wahl SM, Hunt DA, Wong HL, Dougherty S, McCartney-Francis N, Wahl LM, et al. Transforming growth factor-beta is a potent immunosuppressive agent that inhibits IL-1-dependent lymphocyte proliferation. J Immunol. 1988;140(9):3026-32. Epub 1988/05/01. PubMed PMID: 3129508.
287. Letterio JJ, Roberts AB. Regulation of immune responses by TGF-beta. Annual review of immunology. 1998;16:137-61. Epub 1998/05/23. doi: 10.1146/annurev.immunol.16.1.137. PubMed PMID: 9597127.
288. Gilbert KM, Thoman M, Bauche K, Pham T, Weigle WO. Transforming growth factor-beta 1 induces antigen-specific unresponsiveness in naive T cells. Immunological investigations. 1997;26(4):459-72. Epub 1997/06/01. doi: 10.3109/08820139709022702. PubMed PMID: 9246566.
289. Jia GQ, Gonzalo JA, Lloyd C, Kremer L, Lu L, Martinez-A C, et al. Distinct expression and function of the novel mouse chemokine monocyte chemotactic protein-5 in lung allergic inflammation. The Journal of experimental medicine. 1996;184(5):1939-51. doi: 10.1084/jem.184.5.1939. PubMed PMID: 8920881.
290. Lim SY, Yuzhalin AE, Gordon-Weeks AN, Muschel RJ. Targeting the CCL2-CCR2 signaling axis in cancer metastasis. Oncotarget. 2016;7(19):28697-710. doi: 10.18632/oncotarget.7376. PubMed PMID: 26885690.
291. Ford J, Hughson A, Lim K, Bardina SV, Lu W, Charo IF, et al. CCL7 Is a Negative Regulator of Cutaneous Inflammation Following Leishmania major Infection. Frontiers in immunology. 2018;9:3063. Epub 2019/01/24. doi: 10.3389/fimmu.2018.03063. PubMed PMID: 30671055; PubMed Central PMCID: PMCPMC6331479.
292. Berger EA, Murphy PM, Farber JM. Chemokine receptors as HIV-1 coreceptors: roles in viral entry, tropism, and disease. Annual review of immunology. 1999;17:657-700. Epub 1999/06/08. doi: 10.1146/annurev.immunol.17.1.657. PubMed PMID: 10358771.
293. Yang M, Fan J-j, Wang J, Zhao Y, Teng Y, Liu P. Association of the C2–CFB locus with non-infectious uveitis, specifically predisposed to Vogt–Koyanagi–Harada disease. Immunologic Research. 2016;64(2):610-8. doi: 10.1007/s12026-015-8762-x.

294. Karin N, Razon H. Chemokines beyond chemo-attraction: CXCL10 and its significant role in cancer and autoimmunity. Cytokine. 2018;109:24-8. doi: https://doi.org/10.1016/j.cyto.2018.02.012.
295. Tokunaga R, Zhang W, Naseem M, Puccini A, Berger MD, Soni S, et al. CXCL9, CXCL10, CXCL11/CXCR3 axis for immune activation - A target for novel cancer therapy. Cancer Treat Rev. 2018;63:40-7. Epub 2017/11/26. doi: 10.1016/j.ctrv.2017.11.007. PubMed PMID: 29207310.
296. Wikenheiser DJ, Stumhofer JS. ICOS Co-Stimulation: Friend or Foe? Frontiers in immunology. 2016;7:304. Epub 2016/08/26. doi: 10.3389/fimmu.2016.00304. PubMed PMID: 27559335; PubMed Central PMCID: PMCPMC4979228.
297. Su W, Xiao W, Chen L, Zhou Q, Zheng X, Ju J, et al. Decreased IFIT2 Expression In Human Non-Small-Cell Lung Cancer Tissues Is Associated With Cancer Progression And Poor Survival Of The Patients. OncoTargets and therapy. 2019;12:8139-49. Epub 2019/10/22. doi: 10.2147/ott.S220698. PubMed PMID: 31632065; PubMed Central PMCID: PMCPMC6781603.
298. Zhang Y-H, He M, Wang Y, Liao A-H. Modulators of the Balance between M1 and M2 Macrophages during Pregnancy. 2017;8(120). doi: 10.3389/fimmu.2017.00120.
299. Naeim F. Chapter 2 - Principles of Immunophenotyping. In: Naeim F, Rao PN, Grody WW, editors. Hematopathology. Oxford: Academic Press; 2008. p. 27-55.
300. Jones DC, Hewitt CRA, López-Álvarez MR, Jahnke M, Russell AI, Radjabova V, et al. Allele-specific recognition by LILRB3 and LILRA6 of a cytokeratin 8-associated ligand on necrotic glandular epithelial cells. Oncotarget. 2016;7(13):15618-31. doi: 10.18632/oncotarget.6905. PubMed PMID: 26769854.
301. John S, Chen H, Deng M, Gui X, Wu G, Chen W, et al. A Novel Anti-LILRB4 CAR-T Cell for the Treatment of Monocytic AML. Molecular therapy : the journal of the American Society of Gene Therapy. 2018;26(10):2487-95. Epub 2018/08/07. doi: 10.1016/j.ymthe.2018.08.001. PubMed PMID: 30131301.
302. Rheinländer A, Schraven B, Bommhardt U. CD45 in human physiology and clinical medicine. Immunology Letters. 2018;196:22-32. doi: https://doi.org/10.1016/j.imlet.2018.01.009.
303. Kim JR, Mathew SO, Patel RK, Pertusi RM, Mathew PA. Altered expression of signalling lymphocyte activation molecule (SLAM) family receptors CS1 (CD319) and 2B4 (CD244) in patients with systemic lupus erythematosus. Clinical and experimental immunology. 2010;160(3):348-58. Epub 2010/03/16. doi: 10.1111/j.1365-2249.2010.04116.x. PubMed PMID: 20345977.
304. Aldinucci D, Colombatti A. The inflammatory chemokine CCL5 and cancer progression. Mediators of inflammation. 2014;2014:292376. Epub 2014/02/14. doi: 10.1155/2014/292376. PubMed PMID: 24523569; PubMed Central PMCID: PMCPMC3910068.
305. Yang L, Cai Y, Zhang D, Sun J, Xu C, Zhao W, et al. miR-195/miR-497 Regulate CD274 Expression of Immune Regulatory Ligands in Triple-Negative Breast Cancer. J Breast Cancer. 2018;21(4):371-81. Epub 2018/12/26. doi: 10.4048/jbc.2018.21.e60. PubMed PMID: 30607158.
306. Zhao P, Lieu T, Barlow N, Metcalf M, Veldhuis NA, Jensen DD, et al. Cathepsin S causes inflammatory pain via biased agonism of PAR2 and TRPV4. The Journal of biological chemistry. 2014;289(39):27215-34. Epub 2014/08/15. doi: 10.1074/jbc.M114.599712. PubMed PMID: 25118282; PubMed Central PMCID: PMCPMC4175355.

307. Gul-Kahraman K, Yilmaz-Bozoglan M, Sahna E. Physiological and pharmacological effects of melatonin on remote ischemic perconditioning after myocardial ischemia-reperfusion injury in rats: Role of Cybb, Fas, NfκB, Irisin signaling pathway. 2019;67(2):e12589. doi: 10.1111/jpi.12589.
308. Vivier E, Morin P, O'Brien C, Druker B, Schlossman SF, Anderson P. Tyrosine phosphorylation of the Fc gamma RIII(CD16): zeta complex in human natural killer cells. Induction by antibody-dependent cytotoxicity but not by natural killing. J Immunol. 1991;146(1):206-10. Epub 1991/01/01. PubMed PMID: 1701792.
309. Jakus Z, Németh T, Verbeek JS, Mócsai A. Critical but overlapping role of FcgammaRIII and FcgammaRIV in activation of murine neutrophils by immobilized immune complexes. J Immunol. 2008;180(1):618-29. Epub 2007/12/22. doi: 10.4049/jimmunol.180.1.618. PubMed PMID: 18097064; PubMed Central PMCID: PMCPMC2647079.
310. Kerur N, Veettil MV, Sharma-Walia N, Bottero V, Sadagopan S, Otageri P, et al. IFI16 acts as a nuclear pathogen sensor to induce the inflammasome in response to Kaposi Sarcoma-associated herpesvirus infection. Cell host & microbe. 2011;9(5):363-75. doi: 10.1016/j.chom.2011.04.008. PubMed PMID: 21575908.
311. Perrier S, Darakhshan F, Hajduch E. IL-1 receptor antagonist in metabolic diseases: Dr Jekyll or Mr Hyde? FEBS letters. 2006;580(27):6289-94. Epub 2006/11/14. doi: 10.1016/j.febslet.2006.10.061. PubMed PMID: 17097645.
312. Shabani F, Farasat A, Mahdavi M, Gheibi N. Calprotectin (S100A8/S100A9): a key protein between inflammation and cancer. Inflammation Research. 2018;67(10):801-12. doi: 10.1007/s00011-018-1173-4.
313. Haure-Mirande J-V, Audrain M, Fanutza T, Kim SH, Klein WL, Glabe C, et al. Deficiency of TYROBP, an adapter protein for TREM2 and CR3 receptors, is neuroprotective in a mouse model of early Alzheimer's pathology. Acta Neuropathol. 2017;134(5):769-88. Epub 2017/06/13. doi: 10.1007/s00401-017-1737-3. PubMed PMID: 28612290.
314. Poon IK, Lucas CD, Rossi AG, Ravichandran KS. Apoptotic cell clearance: basic biology and therapeutic potential. Nature reviews Immunology. 2014;14(3):166-80. Epub 2014/02/01. doi: 10.1038/nri3607. PubMed PMID: 24481336; PubMed Central PMCID: PMCPMC4040260.
315. Miao EA, Leaf IA, Treuting PM, Mao DP, Dors M, Sarkar A, et al. Caspase-1-induced pyroptosis is an innate immune effector mechanism against intracellular bacteria. Nature immunology. 2010;11(12):1136-42. Epub 2010/11/09. doi: 10.1038/ni.1960. PubMed PMID: 21057511; PubMed Central PMCID: PMCPMC3058225.
316. McMahan CJ, Slack JL, Mosley B, Cosman D, Lupton SD, Brunton LL, et al. A novel IL-1 receptor, cloned from B cells by mammalian expression, is expressed in many cell types. The EMBO journal. 1991;10(10):2821-32. Epub 1991/10/01. PubMed PMID: 1833184; PubMed Central PMCID: PMCPMC452992.
317. Labow M, Shuster D, Zetterstrom M, Nunes P, Terry R, Cullinan EB, et al. Absence of IL-1 signaling and reduced inflammatory response in IL-1 type I receptor-deficient mice. The Journal of Immunology. 1997;159(5):2452.
318. Meng XF, Tan L, Tan MS, Jiang T, Tan CC, Li MM, et al. Inhibition of the NLRP3 inflammasome provides neuroprotection in rats following amygdala kindling-induced status epilepticus. Journal of neuroinflammation. 2014;11:212. Epub 2014/12/18. doi: 10.1186/s12974-014-0212-5. PubMed PMID: 25516224; PubMed Central PMCID: PMCPMC4275944.
319. Feng J, Wang J, Du Y, Liu Y, Zhang W, Chen J, et al. Dihydromyricetin inhibits microglial activation and neuroinflammation by suppressing NLRP3 inflammasome activation in

APP/PS1 transgenic mice. CNS neuroscience & therapeutics. 2018. Epub 2018/06/06. doi: 10.1111/cns.12983. PubMed PMID: 29869390.
320. Xu X, Yin D, Ren H, Gao W, Li F, Sun D, et al. Selective NLRP3 inflammasome inhibitor reduces neuroinflammation and improves long-term neurological outcomes in a murine model of traumatic brain injury. Neurobiology of disease. 2018;117:15-27. Epub 2018/06/03. doi: 10.1016/j.nbd.2018.05.016. PubMed PMID: 29859317.
321. Netea MG, Fantuzzi G, Kullberg BJ, Stuyt RJ, Pulido EJ, McIntyre RC, Jr., et al. Neutralization of IL-18 reduces neutrophil tissue accumulation and protects mice against lethal Escherichia coli and Salmonella typhimurium endotoxemia. J Immunol. 2000;164(5):2644-9. Epub 2000/02/29. doi: 10.4049/jimmunol.164.5.2644. PubMed PMID: 10679104.
322. Stern JH, Temple S. Stem cells for retinal replacement therapy. Neurotherapeutics : the journal of the American Society for Experimental NeuroTherapeutics. 2011;8(4):736-43. Epub 2011/09/29. doi: 10.1007/s13311-011-0077-6. PubMed PMID: 21948217; PubMed Central PMCID: PMCPMC3250303.
323. Adijanto J, Philp NJ. Cultured primary human fetal retinal pigment epithelium (hfRPE) as a model for evaluating RPE metabolism. Experimental eye research. 2014;126:77-84. Epub 2014/02/04. doi: 10.1016/j.exer.2014.01.015. PubMed PMID: 24485945; PubMed Central PMCID: PMCPMC4345411.
324. Dunn KC, Aotaki-Keen AE, Putkey FR, Hjelmeland LM. ARPE-19, a human retinal pigment epithelial cell line with differentiated properties. Experimental eye research. 1996;62(2):155-69. Epub 1996/02/01. doi: 10.1006/exer.1996.0020. PubMed PMID: 8698076.
325. Samuel W, Jaworski C, Postnikova OA, Kutty RK, Duncan T, Tan LX, et al. Appropriately differentiated ARPE-19 cells regain phenotype and gene expression profiles similar to those of native RPE cells. Molecular vision. 2017;23:60-89. Epub 2017/03/31. PubMed PMID: 28356702; PubMed Central PMCID: PMCPMC5360456.
326. Omoto S, Guo H, Talekar GR, Roback L, Kaiser WJ, Mocarski ES. Suppression of RIP3-dependent necroptosis by human cytomegalovirus. The Journal of biological chemistry. 2015;290(18):11635-48. Epub 2015/03/18. doi: 10.1074/jbc.M115.646042. PubMed PMID: 25778401; PubMed Central PMCID: PMCPMC4416866.
327. Huang Y, Ma D, Huang H, Lu Y, Liao Y, Liu L, et al. Interaction between HCMV pUL83 and human AIM2 disrupts the activation of the AIM2 inflammasome. Virology journal. 2017;14(1):34. Epub 2017/02/22. doi: 10.1186/s12985-016-0673-5. PubMed PMID: 28219398; PubMed Central PMCID: PMCPMC5319029.
328. Kuang S, Zheng J, Yang H, Li S, Duan S, Shen Y, et al. Structure insight of GSDMD reveals the basis of GSDMD autoinhibition in cell pyroptosis. Proc Natl Acad Sci U S A. 2017;114(40):10642-7. Epub 2017/09/21. doi: 10.1073/pnas.1708194114. PubMed PMID: 28928145; PubMed Central PMCID: PMCPMC5635896.
329. Mizushima N, Klionsky DJ. Protein turnover via autophagy: implications for metabolism. Annual review of nutrition. 2007;27:19-40. Epub 2007/02/22. doi: 10.1146/annurev.nutr.27.061406.093749. PubMed PMID: 17311494.
330. Pankiv S, Clausen TH, Lamark T, Brech A, Bruun JA, Outzen H, et al. p62/SQSTM1 binds directly to Atg8/LC3 to facilitate degradation of ubiquitinated protein aggregates by autophagy. The Journal of biological chemistry. 2007;282(33):24131-45. Epub 2007/06/21. doi: 10.1074/jbc.M702824200. PubMed PMID: 17580304.

331. Mellen MA, de la Rosa EJ, Boya P. The autophagic machinery is necessary for removal of cell corpses from the developing retinal neuroepithelium. Cell death and differentiation. 2008;15(8):1279-90. Epub 2008/03/29. doi: 10.1038/cdd.2008.40. PubMed PMID: 18369370.
332. Besirli CG, Chinskey ND, Zheng QD, Zacks DN. Autophagy activation in the injured photoreceptor inhibits fas-mediated apoptosis. Investigative ophthalmology & visual science. 2011;52(7):4193-9. Epub 2011/03/23. doi: 10.1167/iovs.10-7090. PubMed PMID: 21421874; PubMed Central PMCID: PMCPMC3175961.
333. Subauste CS, Wessendarp M. CD40 restrains in vivo growth of Toxoplasma gondii independently of gamma interferon. Infection and immunity. 2006;74(3):1573-9. Epub 2006/02/24. doi: 10.1128/iai.74.3.1573-1579.2006. PubMed PMID: 16495528; PubMed Central PMCID: PMCPMC1418638.
334. Mohankumar V, Ramalingam S, Chidambaranathan GP, Prajna L. Autophagy induced by type III secretion system toxins enhances clearance of Pseudomonas aeruginosa from human corneal epithelial cells. Biochemical and biophysical research communications. 2018;503(3):1510-5. Epub 2018/07/23. doi: 10.1016/j.bbrc.2018.07.071. PubMed PMID: 30031608.
335. Leib DA, Alexander DE, Cox D, Yin J, Ferguson TA. Interaction of ICP34.5 with Beclin 1 modulates herpes simplex virus type 1 pathogenesis through control of CD4+ T-cell responses. J Virol. 2009;83(23):12164-71. Epub 2009/09/18. doi: 10.1128/jvi.01676-09. PubMed PMID: 19759141; PubMed Central PMCID: PMCPMC2786728.
336. Mo J, Atherton SS, Wang L, Liu S. Autophagy protects against retinal cell death in mouse model of cytomegalovirus retinitis. BMC ophthalmology. 2019;19(1):146. Epub 2019/07/12. doi: 10.1186/s12886-019-1141-y. PubMed PMID: 31291924.
337. Dix RD, Cray C, Cousins SW. Antibody Alone Does Not Prevent Experimental Cytomegalovirus Retinitis in Mice with Retrovirus-lnduced Immunodeficiency (MAIDS). Ophthalmic Research. 1997;29(6):381-92. doi: 10.1159/000268039.
338. Dix RD, Giedlin M, Cousins SW. Systemic cytokine immunotherapy for experimental cytomegalovirus retinitis in mice with retrovirus-induced immunodeficiency. Investigative ophthalmology & visual science. 1997;38(7):1411-7.
339. Dix RD, Cousins SW. Interleukin-2 immunotherapy of murine cytomegalovirus retinitis during MAIDS correlates with increased intraocular CD8+ T-cell infiltration. Ophthalmic Res. 2003;35(3):154-9. Epub 2003/04/25. doi: 10.1159/000070051. PubMed PMID: 12711843.
340. Chien H, Alston CI, Dix RD. Suppressor of Cytokine Signaling 1 (SOCS1) and SOCS3 Are Stimulated within the Eye during Experimental Murine Cytomegalovirus Retinitis in Mice with Retrovirus-Induced Immunosuppression. Journal of Virology. 2018;92(18):e00526-18. doi: 10.1128/JVI.00526-18.
341. Rathkey JK, Zhao J, Liu Z, Chen Y, Yang J, Kondolf HC, et al. Chemical disruption of the pyroptotic pore-forming protein gasdermin D inhibits inflammatory cell death and sepsis. Science immunology. 2018;3(26). Epub 2018/08/26. doi: 10.1126/sciimmunol.aat2738. PubMed PMID: 30143556; PubMed Central PMCID: PMCPMC6462819.